

THESIS ON NATURAL AND EXACT SCIENCES B186

**Petrophysical Models of the CO₂ Plume
at Prospective Storage Sites
in the Baltic Basin**

KAZBULAT SHOGENOV

TUT
PRESS

TALLINN UNIVERSITY OF TECHNOLOGY
Institute of Geology

This dissertation was accepted for the defence of the degree of Doctor of Philosophy in Earth Sciences on 22.05.2015

Supervisor: Dr Alla Shogenova
Institute of Geology at Tallinn University of Technology

Advisors:

Dr Olga Vizika-Kavvadias, IFP Energies nouvelles (French Petroleum Institute, Paris)
Davide Gei, National Institute of Oceanography and Experimental Geophysics (OGS), Italy

Opponents:

Associate Prof Krzysztof Labus, Institute for Applied Geology, Silesian University of Technology, Poland

Dr Argo Jõelett, Institute of Ecology and Earth Sciences, Tartu University, Estonia

Defence of the thesis: June 30, 2015 at Tallinn University of Technology, Ehitajate tee 5, Tallinn, 19086, Estonia

Declaration:

Hereby I declare that this doctoral thesis, my original investigation and achievement, submitted for the doctoral degree at Tallinn University of Technology, has not been submitted for a doctoral or an equivalent academic degree.

Kazbulat Shogenov



Copyright: Kazbulat Shogenov, 2015
ISSN 1406-4723
ISBN 978-9949-23-794-4 (publication)
ISBN 978-9949-23-795-1 (PDF)

LOODUS- JA TÄPPISTEADUSED B186

**CO₂ voo petrofüüsikalised mudelid
Balti basseini perspektiivsetes
ladustamiskohtades**

KAZBULAT ŠOGENOV

CONTENTS

LIST OF ORIGINAL PUBLICATIONS.....	7
Closely related publications.....	8
Terms and Abbreviations.....	9
1. INTRODUCTION.....	11
1.1 Motivation for CCS in the Baltic States.....	13
1.1.1 CO ₂ emissions.....	13
1.1.2 CCS regulations.....	14
1.2 Requirements for the storage site.....	15
1.2.1 Reservoir rocks.....	15
1.2.2 Cap rocks.....	16
1.3 CO ₂ -reservoir rock interaction.....	16
1.4 Geological background.....	17
1.4.1 Baltic Basin.....	17
1.4.2 Cambrian Deimena Formation.....	19
1.4.3 Diagenetic alterations.....	19
1.4.4 Storage sites.....	20
1.5 CO ₂ storage capacity.....	21
1.5.1 Global capacity.....	21
1.5.2 Estonian capacity.....	21
1.5.3 Regional capacity.....	21
2. DATA AND METHODS.....	23
2.1 Selection and characterization of the storage site.....	23
2.1.1 Geochemical and mineralogical composition.....	23
2.1.2 Petrophysical measurements.....	25
2.1.3 Experimental and interpretation uncertainties.....	25
2.1.4 Assessment of the quality of reservoir rocks.....	25
2.2 Estimation of the CO ₂ storage capacity.....	26
2.3 Alteration experiment.....	27
2.4 3D geological modelling.....	27
2.4.1 3D structural model.....	27
2.4.2 Facies and petrophysical modelling.....	28
2.5 Numerical seismic modelling.....	30
2.5.1 2D uniform modelling.....	30
2.5.2 CO ₂ plume modelling.....	32
2.5.3 Seismic and poro-viscoelastic properties.....	32
2.6 The software applied.....	33
3. RESULTS.....	34
3.1. Reservoir quality of sandstones before alteration.....	34
3.2 CO ₂ storage capacity of the studied structures.....	37
3.2.2 The E7 structure.....	39
3.2.3 The South Kandava structure.....	39
3.2.4 The Dobeles structure.....	39
3.3 Reservoir quality of sandstones after alteration.....	39

3.3.1 The E6 structure.....	39
3.3.2 The E7 structure.....	40
3.3.3 The South Kandava structure.....	41
3.4 3D geological and petrophysical models of the E6 structure	44
3.5 Numerical seismic models of the E6 structure	46
3.5.1 Seismic properties of the reservoir formations	46
3.5.2 Synthetic seismic sections	46
3.5.2.1 Plane-wave datasets	46
4. DISCUSSION.....	48
4.1 Storage site selection, characterization and risk assessment	48
4.2 3D geological models	50
4.3 CO ₂ storage capacity.....	50
4.4 Assessment of reservoir quality.....	51
4.5 Alteration experiment	52
4.6 Numerical seismic models.....	55
5. CONCLUSIONS	58
ACKNOWLEDGEMENTS.....	60
REFERENCES	61
ABSTRACT	71
KOKKUVÕTE	73
ELULOOKIRJELDUS	75
CURRICULUM VITAE.....	78
ORIGINAL PUBLICATIONS	81

LIST OF ORIGINAL PUBLICATIONS

This thesis is based on the following papers, referred to in the text by Roman numerals as listed below.

I SHOGENOV, K., SHOGENOVA, A. & VIZIKA-KAVVADIAS, O. 2013. Petrophysical properties and capacity of prospective structures for geological storage of CO₂ onshore and offshore Baltic. Elsevier, Energy Procedia, 37, 5036–5045.

II SHOGENOV, K., SHOGENOVA, A. & VIZIKA-KAVVADIAS, O. 2013. Potential structures for CO₂ geological storage in the Baltic Sea: case study offshore Latvia. Bulletin of the Geological Society of Finland, 85(1), 65–81.

III SHOGENOV, K. & GEI, D. 2013. Seismic numerical modelling to monitor CO₂ storage in the Baltic Sea offshore structure. 10-13 June 2013, London, UK, Extended Abstract. EAGE, ID 16848, Tu-P08-13, 1–4.

IV SHOGENOV, K., SHOGENOVA, A., VIZIKA-KAVVADIAS, O. & NAUROY, J. F. 2015. Experimental modeling of CO₂-fluid-rock interaction: evolution of the composition and properties of host rocks in the Baltic Region. Earth and Space Science, AGU (accepted).

V SHOGENOV, K., SHOGENOVA, A., VIZIKA-KAVVADIAS, O. & NAUROY, J. F. 2015. Reservoir quality and petrophysical properties of Cambrian sandstones and their changes during the experimental modelling of CO₂ storage in the Baltic Basin. Estonian Journal of Earth Science, 64(3), (accepted).

VI SHOGENOV, K., GEI, D., FORLIN, E. & SHOGENOVA, A. Petrophysical and numerical seismic modelling of CO₂ geological storage in the E6 structure, Baltic Sea, offshore Latvia. Petroleum Geoscience (submitted).

Closely related publications

Shogenova, A., Piessens, K., Holloway, S., Bentham, M., Martínez, R., Kristin, M., Flornes, K.M., Poulsen, N.E., Wójcicki, A., Šliaupa, S., Kucharič, L., Dudu, A., Persoglia, S., Hladik, V., Saftic, B., Kvassnes, A., **Shogenov, K.**, Ivask, J., Suárez, I., Sava, C., Sorin, A. & Chikkatur, A. 2014. Implementation of the EU CCS Directive in Europe: results and development in 2013. *Energy Procedia*, 63, 6662–6670.

Shogenova, A., Piessens, K., Ivask, J., **Shogenov, K.**, Martínez, R., Suárez, I., Flornes, K.M., Poulsen, N.E., Wójcicki, A., Šliaupa, S., Kucharic, L., Dudu, A., Persoglia, S., Holloway, S. & Saftic, B. 2013. CCS Directive transposition into national laws in Europe: progress and problems by the end of 2011. *Energy Procedia*, 37, 7723–7731.

Šliaupa, S., Lojka, R., Tasáryová, Z., Kolejka, V., Hladík, V., Kotulová, J., Kucharič, L., Fejdi, V., Wojcicki, A., Tarkowski, R., Uliasz-Misiak, B., Šliaupienė, R., Nulle, I., Pomeranceva, R., Ivanova, O., Shogenova, A. & **Shogenov, K.** 2013. CO₂ storage potential of sedimentary basins of Slovakia, The Czech Republic, Poland, and Baltic States. *Geological Quarterly*, 57(2), 219–232.

Shogenova, A., **Shogenov, K.**, Vaher, R., Ivask, J., Šliaupa, S., Vangkilde-Pedersen, T., Uibu, M. & Kuusik, R. 2011. CO₂ geological storage capacity analysis in Estonia and neighbouring regions. *Energy Procedia*, 4, 2785–2792.

Shogenova, A., **Shogenov, K.**, Pomeranceva, R., Nulle, I., Neele, F. & Hendriks, C. 2011. Economic modelling of the capture–transport–sink scenario of industrial CO₂ emissions: the Estonian–Latvian cross-border case study. *Energy Procedia*, 4, 2385–2392.

Shogenova, A., **Shogenov, K.**, Schleifer, N. & Kallaste, T. 2010. Chemical composition and physical properties of the rocks. (Pöldvere, A., ed.) *Estonian Geological Sections, Viki Drill Core*, 10, 30–35.

Shogenova, A., Šliaupa, S., Vaher, R., **Shogenov, K.** & Pomeranceva, R. 2009. The Baltic Basin: structure, properties of reservoir rocks and capacity for geological storage of CO₂. *Estonian Journal of Earth Sciences*, 58(4), 259–267.

Shogenova, A., Šliaupa, S., **Shogenov, K.**, Šliaupiene, R., Pomeranceva, R., Uibu, M. & Kuusik, R. 2009. Possibilities for geological storage and mineral trapping of industrial CO₂ emissions in the Baltic region. *Energy Procedia*, 1, 2753–2760.

Šliaupa, S., Shogenova, A., **Shogenov, K.**, Šliaupiene, R., Zabele, A. & Vaher, R. 2008. Industrial carbon dioxide emissions and potential geological sinks in the Baltic States. *Oil Shale*, 25(4), 465–484.

Terms and Abbreviations

1D – 1-dimensional

2D – 2-dimensional

3D – 3-dimensional

4D – 4-dimensional

Aquifer – layer, formation, or group of formations of permeable rocks, saturated with water and with a degree of permeability that allows water withdrawal through wells (Marsily, 1986; Bachu et al., 2007)

API – American Petroleum Institute

Baltic Region – Baltic States (Estonia, Latvia and Lithuania)

Baltic Sea Region – Denmark, Estonia, Latvia, Finland, Germany, Lithuania, Poland, Russia, Sweden, Norway and Belarus (EU Baltic Sea Region Strategy)

Baltic Basin, or Baltic Syncline – a Late Ediacaran–Phanerozoic polygenetic sedimentary basin, a 700 km x 500 km synclinal structure located in the western part of the East European Craton.

Bsl – below sea level

Cambrian Series 3 – earlier Middle Cambrian (Sundberg et al., 2011; Peng et al., 2012)

Cap rock – a low-permeability (< 0.01 mD) rock (aquitard or aquiclude) overlying a reservoir and retaining hydrocarbons and/or other gases (Bachu et al., 2007)

CO₂ – carbone dioxide

CCS – CO₂ capture and storage

CGS – CO₂ geological storage

Db91/Db92 – wells 91 and 92, respectively, in the Dobeles onshore structure in Latvia

IG TUT – Institute of Geology at Tallinn University of Technology

IFPEN – IFP Energies nouvelles (French Petroleum Institute, Paris)

IR – insoluble residue

κ – gas permeability (mD)

Kn24/Kn27 – wells 24 and 27, respectively, in the South Kandava onshore structure in Latvia

LEGMC – Latvian Environmental, Geological and Meteorological Centre

M_{CO_2} – CO₂ storage capacity (kg)

mD – millidarcy

Mt – million tonnes

NG – net to gross ratio of the aquifer in the trap (%)

NRMS – Normalized Root Mean Square, a 4D time-lapse seismic specific repeatability metrics, a method to qualitatively estimate changes in seismic reflection

OGS – National Institute of Oceanography and Experimental Geophysics

P_{atm} – atmospheric pressure (bar)

Q – flow rate, the volume of fluid which passes per unit time (m^3/s)

Q_P – P-wave quality factor (see Q)

Q_S – S-wave quality factor (see Q)

Quality factor – dimensionless value. It is a ratio of a peak energy of a wave to the dissipated energy. As waves travel, they lose energy with distance and time due to spherical divergence and absorption. Such energy loss must be accounted for when restoring seismic amplitudes to perform fluid and lithologic interpretations, such as amplitude versus offset (AVO) analysis (Schlumberger Oilfield Glossary, <http://www.glossary.oilfield.slb.com>)

S_{ef} – storage efficiency factor (for the trap volume, %)

SEM – scanning electron microscope

ν – Poisson’s ratio, the negative ratio of transverse to axial strain

V_{Pdry} – P-wave velocity in dry rock.

V_{Pwet} – P-wave velocity in water-saturated rock or under in situ conditions

V_{Sdry} – S-wave or shear wave velocity in dry rock

V_{Swet} – S-wave velocity in water-saturated rock or under in situ conditions

V_{pore} – volume of pores in the rock

V_{solid} – volume of solid matrix in the rock

V_{total} – total volume of the rock sample

XRD analysis – X-ray diffraction analysis. A technique for the semiquantitative mineralogical analysis of a sample of rock by measuring the diffraction peaks in X-rays diffracted by the sample

XRF analysis – X-ray fluorescence analysis. A technique for elemental analysis of samples based on the characteristic fluorescence given off by different elements subjected to X-rays

ρ_{CO2t} – density of CO_2 in reservoir conditions (kg/m^3)

ρ_{dry} – density of dry samples (kg/m^3)

ρ_{fluid} – density of gas–brine mixture (kg/m^3)

ρ_{solid} – grain or matrix density (kg/m^3)

ρ_{wet} – density of the partially saturated rock (kg/m^3)

μ_{gas} – viscosity of gas (mPa·s)

φ – porosity (%)

φ_{ef} – open or effective porosity (%)

1. INTRODUCTION

The **aim** of this PhD research was to compose petrophysical models of the CO₂ plume during possible CO₂ geological storage (CGS) in prospective on- and offshore deep subsurface structures in the Baltic sedimentary basin. The modelling results will support the implementation of CO₂ Capture and Geological Storage (CCS) technology in the Baltic States as one of the effective measures to mitigate climate change.

The knowledge about deep subsurface structures in the region is limited due to scarcity of geophysical and drill core data mostly obtained during geological explorations in the 1970s–1980s. Carbon dioxide geological storage projects have not yet started in the Baltic Basin and it is thus not possible to study in situ CO₂ plume behaviour. Therefore, a number of experimental, laboratory and modern stochastic and numerical modelling methods using previously available and new experimental data were applied in this study.

The following **objectives** were included in the research in order to reach its main target:

- Selection of storage sites and data collection, including:
 - Selection of CO₂ geological storage sites, rock sampling and measurement of geochemical and petrophysical properties;
- Characterization of the selected structures:
 - Reservoir characterization and risk assessment; 3D geological static modelling of the storage sites;
 - Estimation of CO₂ storage capacity;
- Estimation of the influence of CGS on the properties of rocks:
 - Laboratory CO₂ injection-like alteration experiment with reservoir rocks;
 - Estimation of petrophysical alterations in rocks caused by geochemical and mineralogical CO₂–fluid–rock interactions;
- Numerical seismic modelling to support the monitoring of CGS, including:
 - 4D time-lapse rock physics and numerical seismic modelling;
 - Coupling of the chemically induced petrophysical alteration effect of CO₂ – hosting rocks measured in the laboratory with time-lapse numerical seismic modelling;
 - Modelling of the possible shape of CO₂ plume migration in the storage site.

The **novelties** of the multidisciplinary geoscientific results obtained in this PhD research are the following:

1. Four geological structures prospective for CGS in the Baltic Region, located onshore (South Kandava and Dobeļe) and offshore in Latvia (E6) and Lithuania (E7), were characterized using available geological and geophysical data and new laboratory measurements of 24 reservoir

and cap rock samples from five boreholes. The petrophysical properties, chemical and mineralogical composition and surface morphology of these samples were interpreted together with previously obtained data (PAPER I, PAPER II).

2. 3D static models of the reservoir sandstone of the top of the Deimena Formation of Cambrian Series 3 (earlier Middle Cambrian; Sundberg et al., 2011; Peng et al., 2012) and cross sections of the reservoir and primary Lower Ordovician cap rocks for the four studied structures were constructed using geological, gamma-ray logging and laboratory data. For the first time optimistic and conservative CO₂ storage capacity of these four structures was estimated with different levels of reliability (PAPER I, PAPER II).
3. A new classification of the reservoir quality of rocks for CGS in terms of gas permeability and porosity was proposed for the Deimena Formation sandstones in the Baltic Basin based on the previously available data and those measured by the author. The quality of the reservoir rocks in the four studied structures and their appropriateness for CGS were characterized according to the new classification (PAPER V).
4. Analytical quantitative estimation of the influence of possible CGS in the Baltic Region on the properties of the host rocks of the Deimena Formation was done to support more reliable petrophysical and geophysical models of the CO₂ plume. The petrophysical, geochemical and mineralogical parameters of 12 sandstone samples from the South Kandava, E6 and E7 structures were measured and analysed before and after the CO₂ injection-like alteration experiment (PAPER IV, PAPER V).
5. Our results showed the relationship between diagenetic alterations of Cambrian Deimena Formation reservoir sandstones and their changes caused by the CO₂ injection-like experiment (PAPER IV, PAPER V).
6. A more detailed 3D geological, lithological and petrophysical numerical model of the largest E6 structure offshore Latvia was built for the first time using the advanced modelling software Petrel.
7. 4D time-lapse numerical seismic modelling based on rock physics studies was applied to analyse the feasibility of CGS monitoring in the E6 structure in the Baltic Sea. The possible shape of CO₂ plume migration was modelled (PAPER III, PAPER VI).
8. For the first time the petrophysical alteration effect induced by CO₂ was incorporated into the numerical seismic modelling methodology. The petrophysical properties of the host rocks measured before and after the alteration experiment were applied in the modelling. The alteration approach indicated the importance of implementing this effect in such a modelling routine for CGS monitoring and filled the gap in previous seismic models (PAPER VI).

The obtained results and their novelty have a **practical value** for the demonstration of CGS and its monitoring in the Baltic Sea Region. The monitoring, verification and accounting for CO₂ is critical for the widespread application of CO₂ storage. The methods applied in this research to separate structures and results of the CO₂ injection-like experiment can be useful for the basin-scale modelling of CGS in the Baltic Basin and in sandstone reservoirs in other basins.

Different parts of this study were presented on scientific conferences and workshops during 2012–2014: 11th Greenhouse Gas Control Technologies conference – GHGT-11 in Kyoto, 7th and 8th CO₂ GeoNet Open Forum in Venice, 11th Colloquium on Baltic Sea Marine Geology in Helsinki, 75th EAGE Conference & Exhibition incorporating SPE EUROPEC 2013 in London, 54th International Scientific Conference 'Environmental and Climate Technologies' in Riga in 2013 and 11th Middle East Geosciences Conference and Exhibition in Bahrain.

1.1 Motivation for CCS in the Baltic States

The reduction of the greenhouse effect of the Earth's atmosphere is a major concern for researchers and everyone who cares about the future of our planet. Carbon dioxide (CO₂) is an important greenhouse gas responsible for the recent global climate change. It is capable of absorbing heat radiation from the Earth's surface and contributes to the increase in the temperature of the atmosphere. Nevertheless, if the level of CO₂ in the atmosphere changes drastically, the greenhouse effect can alter the conditions on the Earth (National Research Council, 2010). The Intergovernmental Panel on Climate Change (IPCC, 2005), U.S. Environmental Protection Agency (USEPA, 2013), etc. have stated that fossil fuel combustion is a major source of CO₂ emissions to the atmosphere (USGS CSRA Team, 2013).

This research is related to CCS, one of the most promising technologies and fields of study, which is considered to be an effective measure for mitigating the climate change induced by greenhouse gases (Holloway, 2002; IEA, 2004; Metz et al., 2005; Bachu et al., 2007; Arts et al., 2008; IEA, 2013; IPCC, 2014). The overall reduction of CO₂ emissions will likely involve some combination of technologies. However, for the immediate future, industrial CO₂ storage in geological reservoirs is a reliable option, because the knowledge derived from the oil and gas production industries has helped to solve some of the major engineering challenges. The scientific community agrees on the importance of reducing industrial CO₂ emissions in the atmosphere using CGS in, for example, (1) deep saline aquifers, (2) depleted oil and gas fields, (3) unmineable coal seams and (4) porous basalt formations.

1.1.1 CO₂ emissions

Estonia is the largest CO₂ emitter among the Baltic States. According to the European Research Centre EDGAR (<http://edgar.jrc.ec.europa.eu/>, Olivier et al., 2014), total CO₂ emissions produced in Estonia in 2013 were 20.3 Mt,

which is higher than in the other Baltic States (Latvia – 7.9 Mt and Lithuania – 17.9 Mt). Estonian CO₂ emissions per capita are one of the highest in Europe (15.8 tonnes per capita in 2013, the second in Europe after Luxemburg with 20.4 tonnes) due to the use of local oil shale for energy production. Carbon dioxide emissions per capita in 2013 in the Baltic States and other European countries using other energy sources were much lower (5.9 tonnes in Lithuania and 3.8 tonnes in Latvia). The total European CO₂ emission data and per capita data for 2012 are available in Shogenova et al. (2014).

1.1.2 CCS regulations

Directive 2009/31/EC of the European Parliament and of the Council of 23 April 2009 on the geological storage of carbon dioxide was published on 5 June 2009, and entered into force on 25 June 2009. This directive established a legal framework for the environmentally safe geological storage of CO₂ to contribute to the fight against climate change. By the end of 2013 the CCS Directive was fully transposed to national law of Estonia, Latvia and Lithuania. While CO₂ storage is permitted in a number of European countries including Lithuania, it is prohibited (except for research and development) in Estonia, due to its geological conditions, and also in Latvia.

The main reasons for taking the decision to prohibit storage in Latvia include: (1) lack of experience in using CCS technology on an industrial scale and dealing with its environmental impact; (2) opposition from experts in the environmental authorities and from environmental organisations; (3) the absence of demand for CCS from Latvia's energy and industrial operators, as natural gas is used as a fuel almost exclusively, and the capacity of combustion plants is small compared to the rest of the EU and (4) Latvian structures are intended to be used primarily for natural gas storage and for obtaining geothermal energy. The duration of the ban is dependent on information to be provided by the Ministry of Environmental Protection and Regional Development to the Latvian Parliament. The Parliament will then use this information to determine whether to lift or maintain the ban.

As industrial-scale CO₂ storage is not permitted in Estonia and Latvia, the regulations include a requirement for new large power plants (with a capacity of 300 MW or more) to be capture-ready, with assessed possibilities for transboundary CO₂ transportation and storage (Shogenova et al., 2013, 2014).

In such a situation the most probable scenarios for the storage of Estonian CO₂ emissions depend on regional decisions and cooperation with other Baltic Sea countries (Denmark, Finland, Germany, Iceland, Latvia, Lithuania, Norway, Poland, the Russian Federation and Sweden). Before the implementation of the CO₂ storage technology in the region it is necessary to demonstrate its long-term safety for both humans and the environment. The ministers of the Baltic Sea Region states, responsible for energy, and the European Commissioner for Energy convened in May 2012 and signed a communique expressing their commitment to further develop and strengthen the

energy cooperation in the period 2012–2015. The demonstration of the transportation and storage of CO₂ was among cooperation activities.

1.2 Requirements for the storage site

Our study is focused on the CO₂ storage in deep saline aquifers (>800 m depth, >35 g/l salinity), composed of reservoir rocks overlain by the cap rock (seal). This is the most widespread worldwide option currently under consideration for CCS/CGS.

1.2.1 Reservoir rocks

A typical reservoir for CGS is a geological formation consisting of sandstone or carbonate rock characterized by ‘good’ effective porosity and permeability. Effective (open) porosity is the porosity that is available for free fluids; it excludes all non-connected porosity, including the space occupied by clay-bound water (Schön, 1996). The ranges of ‘good’ reservoir porosity and permeability for oil and gas reservoirs are 15–20% and 50–250 millidarcy (mD), respectively (Tiab & Donaldson, 2012).

Until now there is no unified classification specifying requirements for ‘high-’, ‘good-’ or ‘low-quality’ reservoirs for CO₂ storage. As a general rule the formation permeability must exceed 200 mD for a specific reservoir to provide sufficient injectivity (Van Der Meer, 1993). However, the values greater than 300 mD are preferred and considered as positive indicators to start the screening process of the possible storage site (Chadwick et al., 2006; Vangkilde-Pedersen & Kirk, 2009). The porosities should be larger than 20%, while those below 10% and permeability below 200 mD are considered ‘cautionary’ by these authors (Table 1). The cumulative thickness of reservoirs should be greater than 50 m. The reservoirs less than 20 m thick are considered unsuitable for the storage of large amounts of CO₂. According to Halland et al. (2013), a homogeneous 50 m thick reservoir with a permeability >500 mD and porosity >25% is estimated as a ‘high-quality’ reservoir, while a heterogeneous 15 m thick reservoir with a permeability <10 mD and porosity <15% is considered as a ‘low-quality’ reservoir for CGS.

The classification of hydrocarbon reservoirs proposed by Ханин (1965, 1969) was used during exploration for hydrocarbon deposits on the territory of the Baltic States and later for the characterization of petroleum geology in the region (Zdanavičiute & Sakalauskas, 2001). Based on porosity and permeability, Ханин divided hydrocarbon reservoirs into six classes without any overlapping of these parameters in reservoir quality classes (Table 1). In his classification the hydrocarbon reservoirs of ‘high’ and ‘very high’ quality have a permeability more than 500 and 1000 mD, respectively, while requirements for porosity (18–20 and >20%) are close to the positive indicators for CO₂ storage reservoirs (>20%) given by Chadwick et al. (2006) and Vangkilde-Pedersen & Kirk (2009).

1.2.2 Cap rocks

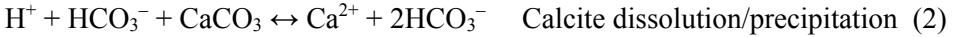
Cap rock is defined as a low-permeability (<0.01 mD) rock (aquitard or aquiclude) that overlies a reservoir and retains hydrocarbons and/or other gases (Bachu et al., 2007). However, its porosity can be relatively high, in the range 15–30% (Armitage et al., 2011). A cap rock less than 20 m thick is cautionary, whereas thicknesses greater than 100 m are preferable (Chadwick et al., 2006).

1.3 CO₂–reservoir rock interaction

When injected into the aquifer or water-flooded oil reservoir, CO₂ has an impact on the pH level of in situ brine, modifying it into a more acidic state. Isotope studies of natural analogues of CO₂ reservoirs suggest that the dissolution of CO₂ in formation brine is the main phenomenon in the long term, causing the acidification of native brine to a pH of approximately 3–5 (Gilfillan et al., 2009; Liu et al., 2011, 2012). Chemically, this simple acid reaction is illustrated by equation (1), showing the formation and dissociation of carbonic acid (H₂CO₃⁰) from dissolved CO₂ in formation brine:

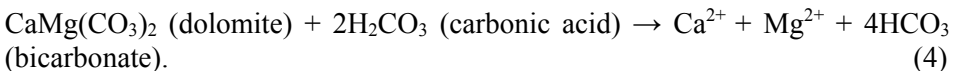


Acidic brine then reacts with the solid matrix of reservoir sediments (i.e. calcite, dolomite and anhydrite):



This exact phenomenon, induced by CO₂ injection into the aquifer, was applied as the main factor of the experiment and is a basis for further research.

A number of recent papers have been dedicated to CO₂–brine–host reservoir rock interactions, both for sandstones and carbonate rocks (Ross et al., 1982; Svec & Grigg, 2001; Grigg & Svec, 2003; Rochelle et al., 2004; Bertier et al., 2006; Czernichowski-Lauriol et al., 2006; Egermann et al., 2006; Pawar et al., 2006; Izgec et al., 2008; Bemmer & Lombard, 2010; Carroll et al., 2011, 2013; Nguyen et al., 2013). The CGS-related laboratory experiments, numerical modelling and field monitoring of CO₂ storage sites have shown both partial dissolution and precipitation of various minerals. The reaction of carbonic acid with aluminosilicate or carbonate minerals produces significant alkalinity (Kaszuba & Janecky, 2009):



The alkalinity of in situ brine cannot overcome the acidity within the repository that was produced by the dissolution of supercritical CO₂ fluid.

However, due to the separation of brine from supercritical CO₂ and the prevailing chemical potential of carbonic acid, alkalinity in brine can neutralize the acidity, yielding near-neutral pH (Kaszuba & Janecky, 2009).

1.4 Geological background

1.4.1 Baltic Basin

The main target for the CGS study in Estonia, Latvia and Lithuania is the Baltic Basin (700 km × 500 km synclinal structure), a Late Ediacaran–Phanerozoic polygenetic sedimentary basin that developed in a peri-cratonic setting in the western part of the East European Platform.

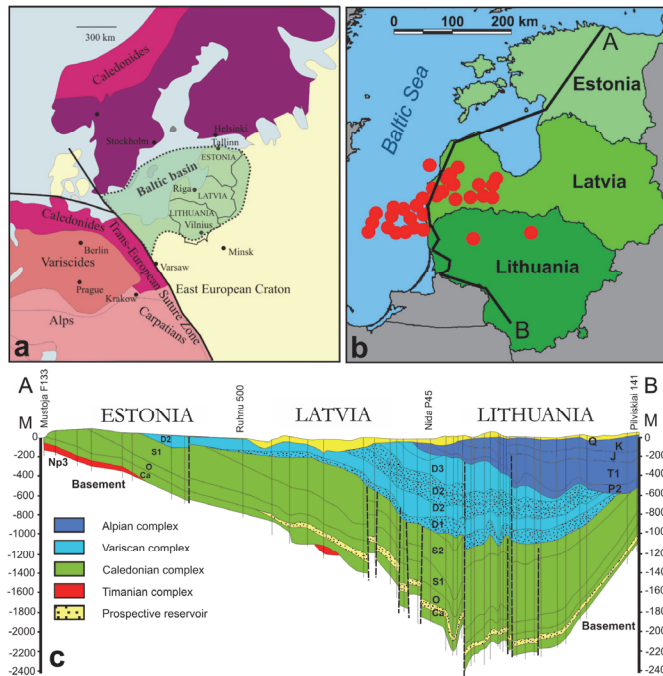


Figure 1. (a) Structure map of the Baltic Basin. (b) Approximate location of onshore and offshore Latvian and Lithuanian structures in the Cambrian aquifer prospective for CGS (CO₂ storage potential exceeding 2 Mt), shown by red circles. The black line A–B represents the geological cross section shown in Fig. 1c. (c) Geological cross section across Estonia, Latvia and Lithuania. The cross section line A–B is shown in Fig. 1b. Major aquifers are indicated by dots. Dotted vertical lines mark faults. The cross section clearly indicates that Estonia is out of the recommended depth frames for CGS (minimum recommended depth for CGS is 800 m). Np3 – Ediacaran; Ca – Cambrian; O – Ordovician; S1 – Lower Silurian (Llandovery and Wenlock series); S2 – Upper Silurian (Ludlow and Pridoli series); D1, D2 and D3 – Lower, Middle and Upper Devonian, respectively; P2 – Middle Permian; T1 – Lower Triassic; J – Jurassic; K – Cretaceous; Q – Quaternary (PAPER II).

It overlies the Palaeoproterozoic crystalline basement of the East European Craton, specifically the West Lithuanian Granulite Domain, flanked by terranes

of the Svecofennian Orogen southeast of the Baltic Sea (Gorbatshev & Bogdanova, 1993). Basin fill consists of Ediacaran–Lower Palaeozoic, Devonian–Carboniferous and Permian–Mesozoic successions, coinciding with what are referred to as the Caledonian, Variscan and Alpine stages of the tectonic development of the basin, respectively. These are separated by regional unconformities and overlain by a thin cover of Cenozoic deposits (Poprawa et al., 1999).

Freimanis and colleagues stated that several structures have been singled out in the Latvian part of the Baltic Syneclise (Figs 1, 2). The Estonian–Latvian and Lithuanian monoclines are the marginal structures of the Baltic syneclise. The Liepaja depression is a distinctly asymmetrical depression (length 200 km, width up to 70 km, trough amplitude 800 m) with a gentle northern and a steep near-fault southern edge. The Liepaja–Saldus zone of highs crosses the Baltic syneclise, stretching from the Swedish offshore towards the northeast for about 400 km. The width of the zone is 25–80 km. From northeast to southwest, the basement submerges from 500 to 1900 m. The Liepaja–Saldus zone is a complex system of disjunctive-plicative dislocations, the intensity of which exceeds that in other areas of the Baltic syneclise. The amplitude of uplift in the anticline structures reaches 600 m. The Gdansk–Kura depression is only represented by its northern peripheral part. The South Latvian step, about 100 km long, is a sublatitudinal tectonic block in southern Latvia. The amplitudes of boundary faults reach 400–500 m (Freimanis et al., 1993).

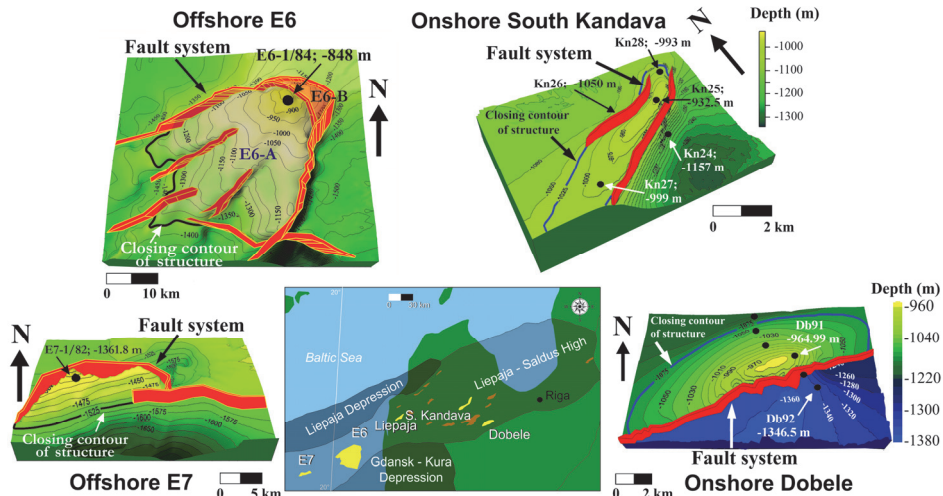


Figure 2. Location of Latvian onshore structures prospective for CGS in the Cambrian aquifer and the studied South Kandava and Dobele structures onshore Latvia, E6 structure offshore Latvia and E7 structure offshore Lithuania. Large regional structures complicating the Baltic Syneclise in the study area are shown according to Freimanis et al. (1993). The 3D geological models of the top of the Cambrian Deimena Formation of the four studied structures are shown (PAPER I, PAPER II, PAPER IV).

1.4.2 Cambrian Deimena Formation

The Cambrian stratigraphy is similar both on- and offshore Latvia (Grigelis, 2011). The lithofacies implies the deepening of the sedimentation environment and maximum transgression at the beginning of Kybartai time. Rocks of the Deimena Formation of Cambrian Series 3 (earlier Middle Cambrian) deposited in a shallow regressing marine basin subjected to tides and storms and are dominated by quartz sandstones with subordinate claystone layers (mud shelf). The poorly sorted sandstones of various grain size, containing gravel fraction, were deposited at the end of Deimena time. The major Deimena reservoir lies regressively on the Kybartai Formation. The regression was associated with the more sandy composition of deposits. Numerous faults dissect the Cambrian reservoir body. They form important pathways for fluid migration, while high-amplitude faults provide a blockage for fluid migration in the uplifted structures.

Cambrian Series 3 saline aquifer (depth 700–1700 m) located in the central–western part of the Baltic Basin suits best for the CO₂ storage in the Baltic Region. It is composed of 25–80 m thick Deimena Formation sandstone covered by up to 46 m thick shales and clayey carbonates of primary cap rocks of the Lower Ordovician Zebre Formation. Shale rocks are dark, thin-layered (0.5–2 mm) and highly fissile. A 0.5 m layer of greenish-grey glauconite-bearing sandy marlstones with minor limestone lenses is observed at the base of the onshore Zebre Formation. The reservoir rocks are also covered by 130–230 m thick Ordovician and 100–225 m thick Silurian impermeable clayey carbonate secondary cap rocks (Fig. 1b, c). The Cambrian Deimena Formation is clearly indicated by low natural radioactivity on gamma-ray log readings. Clayey interbeds and marlstone layers in the reservoir are easily determined by increased gamma-ray readings. Cap rocks, represented by clayey sediments of Ordovician and Silurian formations, correspond to the highest readings (Fig. 3; PAPER I, PAPER V).

The Cambrian aquifer includes potable water in the northern shallow part of the Baltic Basin, mineral water (salinity 10 g/l) in southern Estonia and saline water in the Deimena Formation at more than 800 m depths, with salinity up to 120 g/l in the central and 150–180 g/l in the southern and western parts of the basin, where fluid temperature reaches 88 °C (Zdanavičiute & Sakalauskas, 2001). The last mentioned geochemical and pressure–temperature conditions of formation fluids allow the use of the Deimena Formation reservoir for CGS at depths of 800–2500 m, where CO₂ can be stored in a supercritical state (>31°C and >73 atm).

1.4.3 Diagenetic alterations

The studied Cambrian rocks were subjected to different diagenetic conditions across the basin, with a wide spectrum of rock modification under shallow to deep burial conditions reflected in growing clay mineral maturity with increasing depth, variations in the composition of sandstone cement, with authigenic quartz prevailing in the deep part of the basin and carbonate cements

prevailing in the basin periphery, changes in the pore water composition, grading from Ca–CO₃ type in the east to Na–Cl type in the west, etc. The carbonate cement of sandstones changes in mineralogy from common ferroan dolomite and ankerite to less common calcite and siderite (Sliupa et al., 2008b).

Quartz cementation that formed during the late diagenetic stage (Лашкова, 1979; Sikorska & Paczesna, 1997) and increases with depth is the main factor influencing the reservoir properties of rocks both in onshore and offshore structures. Quartz is the main cement mineral, occurring in the form of authigenic overgrowths on detrital quartz grains. According to Čyžienė et al. (2006), quartz cement is regionally widespread, but mainly confined to areas where present-day temperatures in the Cambrian are 50–90 °C. Sliupa et al. (2008b) stated that quartz cementation started at 1 km depth. The amount of quartz cement increases towards the deeper buried parts of the basin in West Lithuania, but is highly variable on a local scale and even within individual structures. Quartz cement contents show a negative correlation with porosity (Čyžienė et al., 2006) and carbonate cement (Sliupa et al., 2008b).

Another diagenetic process negatively influencing the reservoir properties is compaction. The importance of mechanical compaction in reducing porosity and causing lithification is stressed by Čyžienė et al. (2006). Compaction comprised the mechanical rearrangement of grains throughout the sandstones as well as the chemical compaction along shale–sandstone contacts and within shales. Grain breakage is rare, and no intergranular pressure solution in clay-free clean sandstones has been observed. In sandstones detrital quartz grains mainly have point contacts. Differences in the degree of mechanical compaction are probably related to both maximum burial depth and variations in the depositional texture and susceptibility of sand to mechanical compaction (Лашкова, 1979; Kilda & Friis, 2002).

1.4.4 Storage sites

Four geological structures, located onshore (South Kandava and Dobeļe) and offshore Latvia (E6) and Lithuania (E7) and serving as prospective CGS sites in the Baltic Region, were studied in this research. All the studied structures are situated within the tectonically dislocated Liepāja–Saldus zone of highs (Fig. 2). The deepest Deimena Formation rocks occur in the offshore E7 structure. This structure is also characterized by the highest temperature of 46 °C and water salinity of 125 g/l. The shallowest offshore structure E6 shows a lower temperature (36 °C) and the lowest salinity of Cambrian fluids (99 g/l). The onshore structures exhibit the average depth of the Deimena Formation (933–950 m) but a lower temperature than rocks in the offshore structures (18–24.5 °C). The salinity of the Cambrian fluids is also average, 113–114 g/l compared to the offshore structures. Sandstones at the top of the Deimena Formation in the South Kandava uplift and in its lowered wing have undergone diagenetic carbonate cementation represented by calcite, dolomite and ankerite (PAPER I).

Based on exploration reports (Бабыке et al., 1983), we have treated E7 as a Latvian offshore structure (PAPER I. PAPER II). However, according to the new Latvian–Lithuanian territorial agreement in the Baltic Sea, signed by Prime Ministers of Latvia and Lithuania in 1999, the E7 structure belongs now to Lithuania (Šteinerts, 2012). Location of the E7 structure at the Latvian–Lithuanian border and the conflict of interest in its ownership could also cause problems during its use for CGS. Storage in this structure could be considered as transboundary and will need bilateral agreements.

1.5 CO₂ storage capacity

1.5.1 Global capacity

The global economic potential of CCS amounts to 220–2200 GtCO₂ cumulatively, which means that CCS contributes 15–55% of the total mitigation effort worldwide until 2100, averaged over a range of baseline scenarios (Metz et al., 2005). Worldwide, a number of known pilot storage and large-scale CCS demonstration projects are ongoing on and/or monitored, the first of which, Sleipner (Norway), started in 1996. Nevertheless, there are gaps in the knowledge of short- and long-term (10–100 and 100–10000 years, respectively) phenomena accompanying the process of the storage of CO₂ in deep geological formations. A detailed estimate of the national geological CO₂ storage resources is required to make informed decisions about the implementation of CGS in the study area (USGS CSRA Team, 2013).

1.5.2 Estonian capacity

Geological conditions in Estonia are unsuitable for CGS because of the shallow sedimentary basin (thickness lower than 800 m, Fig. 1b, c) and potable water available in all known aquifers. The most prospective structures for CGS in the East Baltic Region (Estonia, Latvia and Lithuania) are available in Latvia, represented by a number of anticline onshore and offshore structures (Figs 1b, 2; Šliaupa et al., 2008a; Shogenova et al., 2009a, 2009b, 2011a, 2011b; Šliaupa et al., 2013; PAPER I, PAPER II, PAPER IV). The economic modelling of the possible capture–transport–sink scenario of Estonian CO₂ emissions, produced by the two largest Estonian power plants (Estonian and Baltic) and stored in two Latvian onshore structures Luku-Duku and South Kandava, was carried out with participation of the author of this thesis in the frame of EU GeoCapacity project (Shogenova et al., 2011b).

1.5.3 Regional capacity

The regional theoretical storage potential of the Cambrian sandstone saline aquifers below 800 m in the Baltic Sea Region has been estimated as 16 Gt (Vernon et al., 2013). The average storage capacity of the Cambrian reservoir in the western part of the Baltic Basin in the S41/Dalders structure of the Swedish offshore sector is 145 Mt, while the average capacity of the regional Cambrian Faludden stratigraphic trap is 5.58 Gt (Sopher et al., 2014). For comparison, the

total estimated storage capacity of the Jurassic sandstone formations in the Norwegian Sea is 5.5 Gt (Halland et al., 2013). The storage capacity of the Utsira sandstone formation, a stratigraphic trap of the first in the world Sleipner storage site in the North Sea, is estimated approximately as 15 Gt (Halland et al., 2011).

More than 30 anticlinal deep geological structures onshore and offshore Latvia, with different sizes and a storage capacity exceeding 2 Mt of CO₂, have been estimated as prospective for CGS. The total capacity of 16 onshore and 14 offshore structural traps in Latvia was estimated as 400 and 300 Mt, respectively. The structural capacity of Lithuania is only 29 Mt. The potential for Enhanced Hydrocarbon Recovery in the Baltic onshore and offshore structures is 5.7 Mt in Lithuanian onshore, 26 Mt onshore and 7 Mt offshore Kaliningrad District of Russia, and 7 Mt in oil- and 16 Mt in gas-fields offshore Poland (Šliaupa et al., 2013). In the EU Geocapacity project the CO₂ storage capacity of the Dobele structure was estimated as 56 Mt and of South Kandava as 44 Mt (Shogenova et al., 2009a; PAPER I). In this study the storage capacity of these structures was updated with different levels of reliability (PAPER I).

1.6 Numerical seismic modelling

The time-lapse seismic method is known as highly suitable technique for monitoring the CO₂ injection into a saline aquifer. The effects of CO₂ on seismic data are large both in terms of seismic amplitudes and observed velocity push-down (Arts et al., 2000). A 4D time-lapse rock physics and numerical seismic modelling methodology (Carcione, 2007) permits prediction of the seismic response of CO₂ in the storage site, planning the monitoring of plume migration, estimation of reservoir integrity and supporting possible leakage notification. This method also allows optimizing the seismic surveys, which should be repeated over time to monitor the evolution of injected CO₂ (Rossi et al., 2008; Picotti et al., 2012).

A large number of cognate studies have been carried out during last several years in operating CO₂ storage sites, e.g. Sleipner in Norway (Arts et al., 2003, 2004a, 2004b; Carcione et al., 2006; Chadwick et al., 2006) and prospective for CGS sites, such as Atzbach-Schwanenstadt in Austria (Rossi et al., 2008; Picotti et al., 2012) and Calgary in Canada (Vera, 2012). These studies have given similar results (see PAPER VI).

2. DATA AND METHODS

2.1 Selection and characterization of the storage site

The onshore structures of South Kandava and Dobele, estimated as prospective for CGS in Latvia (Shogenova et al., 2009a), were selected for research. Due to lack of experimental data from offshore structures in the area, the E6 and E7 structures in the Baltic Sea were also studied.

Four onshore wells from the South Kandava (Kn24 and Kn27) and Dobele structures (Db91 and Db92), as well as wells E6-1/84 and E7-1/82 from offshore structures E6 and E7, respectively, were studied using four unpublished exploration reports. In addition, 24 samples, including 15 samples from the Deimena Formation sandstone reservoir and 9 samples from the Zebre Formation cap rock, were taken from five drill cores stored in the LEGMC (Fig. 3). Cross sections were constructed and correlated (Fig. 3) based on gamma-ray logging data (Силантьев et al., 1970; Дмитриев et al., 1973; Бабуке et al., 1983; Андриющенко et al., 1985).

Three-dimensional structural models were constructed in Golden Software Surfer 8 using structure maps of the top reservoir and cross sections of wells (Figs 2, 3; PAPER I, PAPER II, PAPER IV).

The available seismic section of the E6 structure was interpreted and, using structural maps of the E6 reservoir and cap rock top and cross section of well E6-1/84, the geological cross section of the E6 structure was constructed (Fig. 4 in PAPER II).

2.1.1 Geochemical and mineralogical composition

The total chemical composition of 24 samples was determined by X-ray fluorescence (XRF) analysis. The total carbon (C) and total sulphur (S) contents were measured via the Leco method by Acme Analytical Laboratories Ltd. before and after the alteration experiment. CaO, MgO and insoluble residue (IR) were analysed by the titration geochemical method in the Institute of Geology at Tallinn University of Technology and the qualitative mineral composition was estimated by X-ray diffraction (XRD) by Acme Analytical Laboratories Ltd. only before the alteration experiment. Thin sections of the rock samples were studied in the IG TUT using a Scanning Electron Microscope (SEM) equipped with an energy dispersive spectrometer (EDS). Only the chemical composition of the original shales from the Zebre Formation cap rock (from the Dobele and South Kandava structures) was analysed. Due to their weak consolidation these samples were not used for petrophysical measurements or in the laboratory alteration experiment.

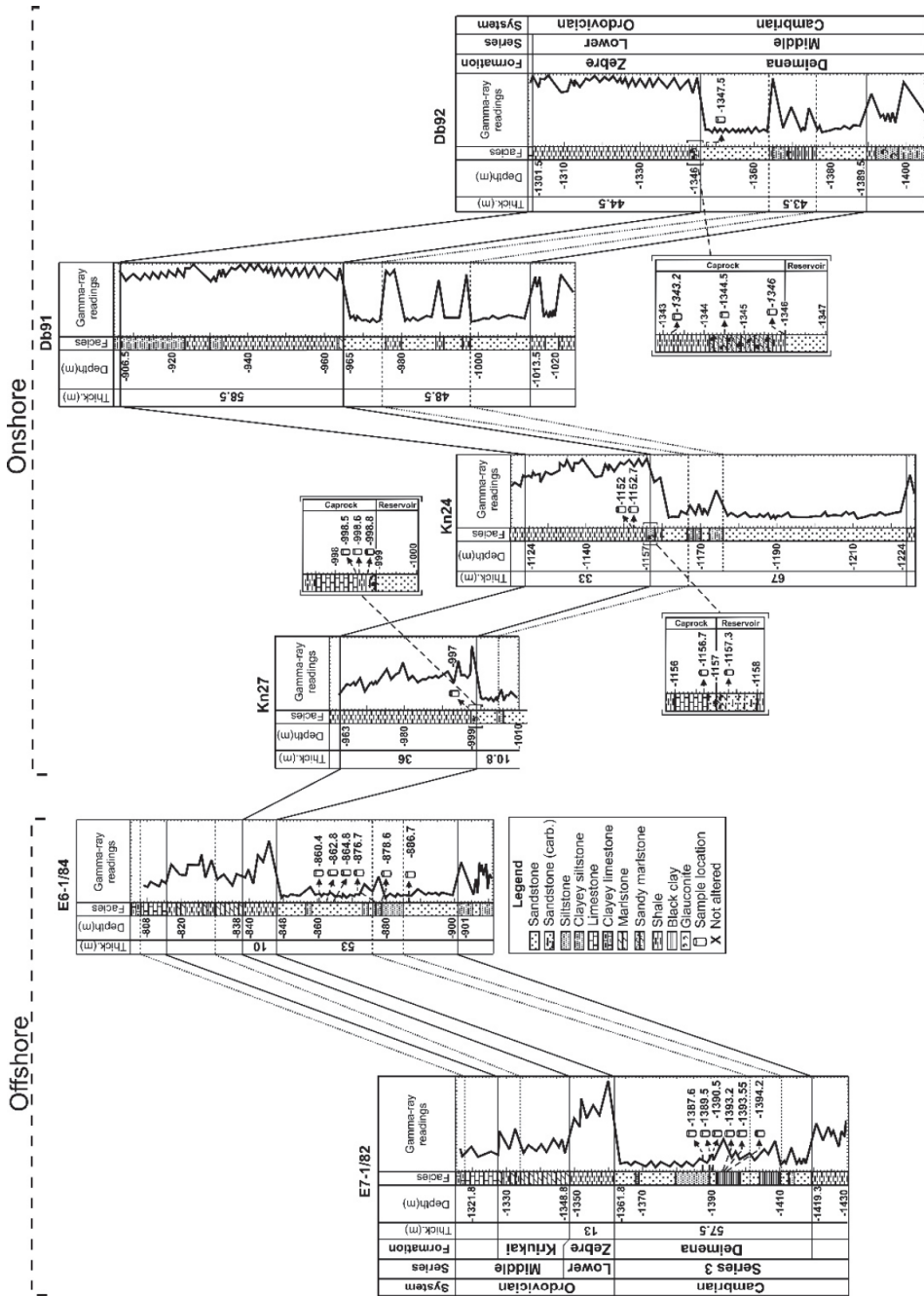


Figure 3. Cross section of the studied wells showing the correlation of the Deimena Formation reservoir and Zebre Formation primary cap rock by logging and drill core data. Location of the 24 sampled rocks is shown by cylinders (modified after PAPER IV and PAPER V).

2.1.2 Petrophysical measurements

According to exploration reports, open or effective porosity (φ_{ef}) in the studied samples was estimated by the saturation method (Жданов, 1981). Gas permeability (κ) was determined when passing gas through the samples using the 'GK-5' apparatus. A more detailed description of κ measurements is given in Shogenova et al. (2009a). P-wave acoustic velocities of dry and wet rock samples were measured with the 'DUK-20' equipment (100 KHz) in two directions (X and Y) to take anisotropy into account.

Helium density and porosity, gas permeability and acoustic wave velocities in the thesis were measured in the petrophysical laboratory of IFP Energies nouvelles following the recommendations of the American Petroleum Institute (API, 1998). A more detailed description of these methods is given in PAPER II. The results are available in PAPER I and PAPER II.

2.1.3 Experimental and interpretation uncertainties

Experimental uncertainties include the quality control of petrophysical measurements and uncertainties related to geochemical and mineralogical interactions. To distinguish between a real trend in a data set and variation due to the experimental uncertainty, the American Petroleum Institute (API, 1998) has recommended reporting core analyses data together with a statement of the uncertainty with which these data were recorded.

Variation in the permeability and acoustic velocity measurements was quite high in this study due to sample sizes that differed from the standard ones at the IFPEN petrophysical and petro-acoustic laboratories. The standard samples were 40 mm in diameter and 80 mm in length, thus the length/diameter ratio should be higher or equal to two (Egermann et al., 2006). The studied samples, however, were 25 mm in diameter and 11–27 mm in length. The experimentally established accuracy and related uncertainty for different parameters is described in PAPER IV and PAPER V.

Uncertainties in the interpretation of results are caused by the limited number of samples available for measurements, limitations of the laboratory experiment, the wide range of minerals that can be used to describe major element chemistry obtained by XRF analysis and semi-quantitative results provided by SEM-EDS.

2.1.4 Assessment of the quality of reservoir rocks

The effective porosity and permeability data of 115 samples from six drill cores (E6-1/84, E7-1/82, Kn24 and Kn27, Db91 and Db92) described in old exploration reports (Силантьев et al., 1970; Дмитриев et al., 1973; Бабуке et al., 1983; Андриященко et al., 1985), from the Liepaja-San borehole (GEOBALTICA project, Shogenova et al. 2009a) and those recently measured in IFPEN (PAPER I, PAPER II) were used for the classification of the reservoir quality of sandstones.

Gas permeability κ , calculated as an average value of permeability measured in horizontal and vertical directions, was applied in this study. A more

detailed description of the permeability measurements from the Liepaja structure (Liepaja-San borehole) is given in Shogenova et al. (2009a).

Physical properties of a total of 139 samples from seven boreholes (offshore E6-1/84 and E7-1/82 and onshore Kn24 and Kn27, Db91 and Db92, and Liepaja-San), measured recently and reported earlier, were used for the development of a new classification of the reservoir quality of rocks for CGS in terms of gas permeability and porosity for sandstones of the Deimena Formation. The data set employed comprises the κ values of 127 samples, φ_{ef} values of 128 samples, grain density of 102 samples, bulk density of 129 dry samples, V_{Pdry} in 60 dry samples and V_{Sdry} in 10 dry samples measured recently or published and reported earlier (Shogenova et al., 2001b; PAPER I, PAPER II).

2.2 Estimation of the CO₂ storage capacity

The theoretical storage capacity of the structures was assumed using a well-known formula for the estimation of the capacity of a structural trap (Bachu et al., 2007):

$$M_{CO_2t} = A \times h \times NG \times \varphi \times \rho_{CO_2} \times S_{ef}, \quad (5)$$

where M_{CO_2t} is storage capacity (kg), A is the area of an aquifer in the trap (m²), h is the average thickness of the aquifer in the trap (m), NG is an average net to gross ratio of the aquifer in the trap (%), φ is the average porosity of the aquifer in the trap (%), ρ_{CO_2t} is the in situ CO₂ density in reservoir conditions (kg/m³), S_{ef} is the storage efficiency factor (for the trap volume, %). The CO₂ storage efficiency factor is the volume of CO₂ that could be stored in the reservoir per unit volume of original fluids in place. A different S_{ef} is used for each structure based on its reservoir properties and different methods are employed to estimate these factors (PAPER I, PAPER II). According to Bachu et al. (2007) and Vangkilde-Pedersen et al. (2009), S_{ef} of a high-quality reservoir with faults on two sides is 20%, with faults on three sides 10% and with faults on all sides 3–5%. The S_{ef} value of 40% could be implemented for an open reservoir structure without faults. The South Kandava onshore structure has faults on two sides and only partially a fault limits its third side. Therefore, the S_{ef} value of 15% was selected for this structure. This approach was termed as ‘optimistic’ (PAPER I) due to the higher values of the factors in comparison with subsequent results obtained by another method. In addition, S_{ef} for E6-A and E6-B compartments of the E6 offshore structure were estimated. The S_{ef} values of 10% and 4% in the optimistic approach were determined for E6-A and E6-B, respectively. The E6-A compartment is limited by faults on three sides and E6-B on four sides. Based on the US Department of Energy report (US DOE, 2008), we decided to lower and round the values of S_{ef} for the so-called ‘conservative’ estimation approach (PAPER I). The S_{ef} values obtained by US DOE using Monte Carlo simulation are between 1% and 4% for deep saline aquifers for a 15% to 85% confidence range. The efficiency factor of 4% was selected for all the structures and the E6-A compartment, and 2% for E6-B in

this simplified estimation model, which did not consider pressure change and compressibility within the reservoir due to CO₂ injection (Van der Meer & Egberts, 2008). Optimistic and conservative M_{CO_2t} were calculated with minimum, maximum and average values (min-max/mean) of porosity, determined using recently measured and earlier reported data (PAPER I, PAPER II). The ‘min-max/mean’ approach was chosen due to uncertainties related to lack of experimental data.

The ρ_{CO_2t} value depends on in situ reservoir pressure and temperature. These were estimated using a plot of the supercritical state of CO₂ under in situ conditions (Bachu, 2003).

2.3 Alteration experiment

The homogeneous alteration method or retarded acid approach was conducted at IFPEN. It constitutes in the placement of samples into the Hastelloy cell maintained under vacuum conditions and injection of an acid solution. Acid treatment was performed at 10 bar pressure and temperature of 60 °C (for at least one day), simulating CO₂-rich brine in an aquifer characterized by lowered pH (approximately three units). The day after, each sample was placed in a 25-mm-diameter cell and flooded by three pore volumes of 20 g L⁻¹ NaCl brine at 20 °C to stop the weathering. After this flooding the samples were dried in an oven for three days. The procedure was repeated three times. This method has been developed and described in detail in Egermann et al. (2006), Bemmer & Lombard (2010), Bemmer et al. (2011), PAPER IV and PAPER V.

In the present thesis, 12 reservoir rock samples from four wells (offshore E6-1/84 and E7-1/82, and onshore South Kandava 24 and 27, Fig. 3) treated with acid brine are discussed. Bulk and grain helium density, helium porosity, gas permeability and acoustic P- and S-wave velocities in dry samples, the chemical and mineralogical composition and surface morphology were studied in all samples both before and after the alteration experiment.

Additionally three transitional cap rock samples taken part in the experiment were described in PAPER IV. The experimental protocol did not support chemical measurements of the acid solution composition during the experiment. The alteration experiment involved all 15 samples together in one solution under the same conditions. The changes in sample weights were caused by partial destruction of some samples.

2.4 3D geological modelling

2.4.1 3D structural model

Three main surfaces were considered in the model, corresponding to stratigraphic boundaries interpreted using well logs and seismic data: (1) top of the Ordovician Formation (part of the secondary cap rock), (2) top of the reservoir – the Cambrian Series 3 Deimena Formation and (3) bottom of the

reservoir. Two main zones have been defined in the model representing, respectively, (1) cap rock and (2) reservoir units. More precise internal layering within the reservoir and the primary cap rock were integrated into the model using log data from the E6-1/84 well. The layering was set up in order to increase the vertical resolution of the grid and to take the lithological and petrophysical partitioning of the reservoir into account. Thus, we could accurately populate our geological model with both lithological and petrophysical parameters (porosity and permeability). We defined five layers within the cap rock and also five layers within the 53 m thick reservoir. The proportional layering method was employed in stratigraphic modelling, resulting in the grid proportional to the corresponding top and base surfaces.

2.4.2 Facies and petrophysical modelling

Geological lithofacies were modelled first in order to constrain the distribution of porosity and permeability in the geological model. These petrophysical properties depend both on the primary sedimentation environment and following diagenetic processes. Because of the relatively low degree of diagenetic alterations of the reservoir rocks in the E6 structure (PAPER I, PAPER II, PAPER V), these alterations were not considered in the model.

Stochastic modelling was applied to populate the volumetric grid with data obtained from composite log analysis, core measurements and bibliography (Андрющенко et al., 1985; Shogenova et al., 2010; PAPER I, PAPER II, PAPER III, PAPER V). This type of approach was applied due to lack of analytical data for this study: only one well was drilled in the structure and only one 2D seismic profile was available from the vintage oil exploration survey.

Eight facies with a specific range of petrophysical properties (porosity and permeability) were identified within the model (limestone, oil-bearing limestone, shale, marlstone, sandstone-1, sandstone-2, siltstone and silty sandstone) by analysing core data (four facies for both the cap rock and reservoir) and assigned to the model (Fig. 4; Table 1). Layers 1–5 of the cap rock are mainly represented by oil-bearing limestone, shale, limestone, marlstone and shale, respectively. Reservoir layers 6–10 consist mainly of sandstone, siltstone, sandstone, silty sandstone and sandstone-2, respectively (Fig. 4).

In order to populate the model with facies and petrophysical properties, three modelling algorithms of Geostatistical Software Library were applied (Deutsch & Journel, 1998): (1) *Truncated Gaussian Simulation*, (2) *Sequential Indicator Simulation* and (3) *Gaussian Random Function*. For facies distribution within the cap rock and reservoir layers the *Truncated Gaussian Simulation* and *Sequential Indicator Simulation* methods were used, respectively. The *Gaussian Random Function* simulation was applied to the porosity distribution in all formations. Constant average values reported for all cap rock facies, except for oil-bearing limestone were assigned to permeability distribution. The *Gaussian Random Function* simulation was used for permeability distribution in the reservoir facies and oil-bearing limestone of the cap rock.

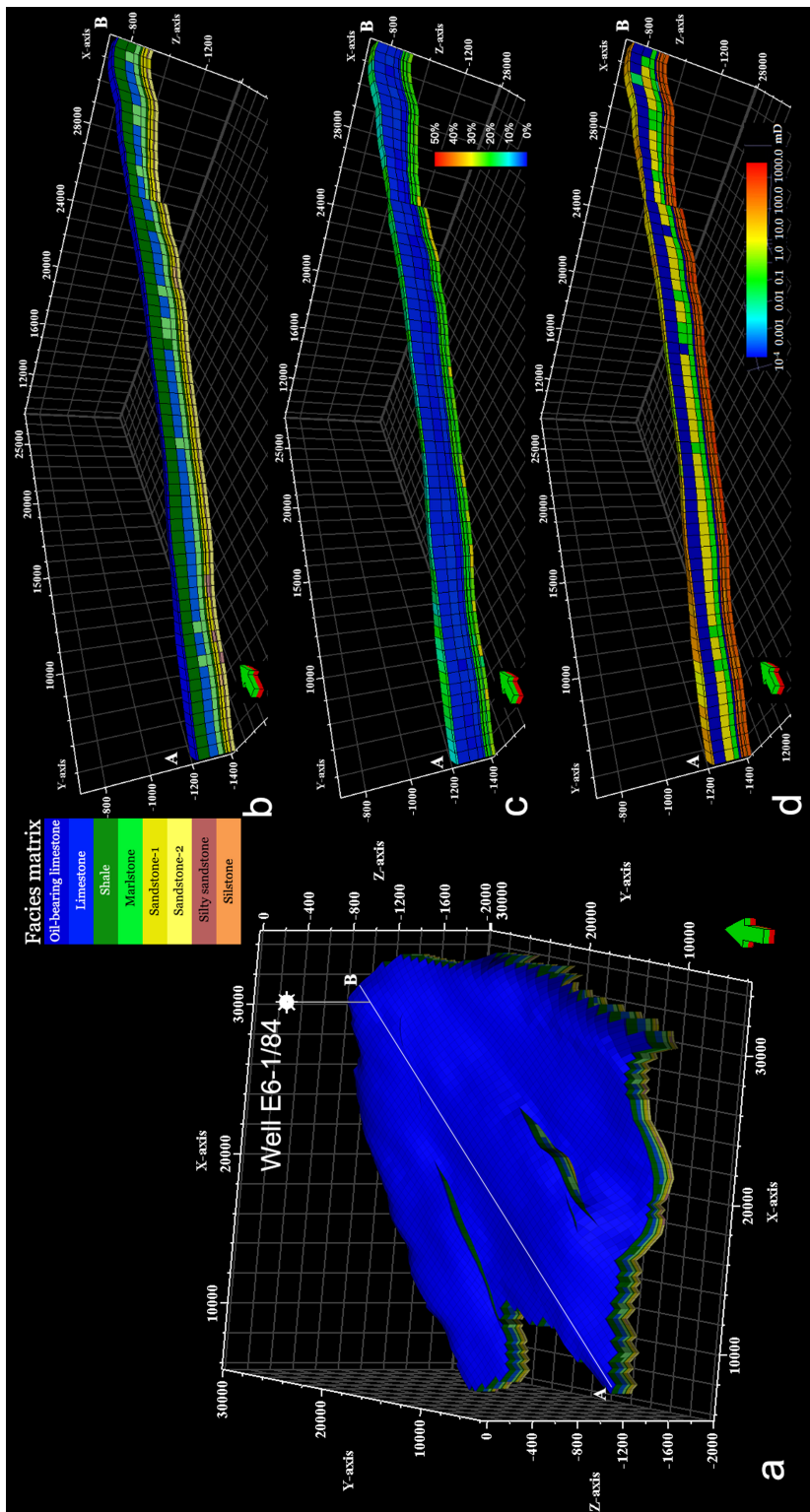


Figure 4. (a) 3D geological static facies model of the E6-A compartment of the E6 offshore structure with location of the well E6-1/84. All layers of the 3D model are shown. The white line A–B represents the geological cross section shown in Fig. 4b–d. Cross sections of (b) facies, (c) porosity and (d) permeability distribution along the line A–B.

Table 1. The facies and the range of petrophysical properties used to populate the 3D geological static model

Facies		Porosity (mD)			Permeability (mD)		
		min	max	mean	min	max	mean
Cap rock	Limestone	2	4	3	-	-	6*
	Oil-bearing limestone	10.8	23.6	18.3	0.2	24	5
	Shale	3.2	3.9	3.6	-	-	0.0001*
	Marlstone	2	4	3	-	-	0.15*
Reservoir	Sandstone-1	16.5	23.9	21	45	334	140
	Sandstone-2	21.9	33.5	25	141	400	230
	Siltstone	14.5	21.5	19	30	440	230
	Silty sandstone	13.6	21.5	17	10	104	56

* Constant data were implemented in the algorithm

2.5 Numerical seismic modelling

Two different approaches to CO₂ distribution in the hosting rock were applied to numerical seismic modelling (PAPER VI): (i) homogeneous CO₂ saturation of the reservoir (uniform model) and (ii) CO₂ plume accumulation (plume model). Therefore we produced synthetic data sets for four scenarios: (1) uniform model without the alteration effect, (2) uniform model with the alteration effect, (3) plume model without the alteration effect and (4) plume model with the alteration effect. Synthetic seismic sections were produced, analysed and compared with the baseline data set (before the injection of CO₂). We considered the first two scenarios to explore the effectiveness of the seismic technique for CGS monitoring in the long term, when CO₂ has homogeneously spread within the storage reservoir. The third and fourth scenarios present more realistic approaches in the short term and involve more complex study (plume shape and inhomogeneous CO₂ saturation).

2.5.1 2D uniform modelling

Figure 5a shows the 2D geological model implemented for numerical seismic modelling and extrapolated for the interpretation of the E6 seismic section. Well E6-1/84 is located approximately in the middle of the model. According to specific physical properties of rock the Deimena reservoir was split into three parts: Reservoir-1, Reservoir-2, and Reservoir-3 (Fig. 5a). Due to shortage of experimental data (only one well drilled in the structure), the three sub reservoirs were approximated to be homogeneous without vertical or lateral heterogeneity. The Saldus Formation of the Upper Ordovician oil reservoir is shown by a 10 m thick black layer between the Ordovician and Silurian (Fig. 5a).

All layers in the geological model were characterized and populated with specific lithology, and the measured or computed petrophysical properties recalculated under in situ conditions before and after the alteration experiment (Tables 2, 3).

Table 2. Characteristics and physical properties of the main rock formations shown in the seismic model (Fig. 5)

Formation	Lithology	Depth* (m)	T (°C)	P (MPa)	ρ_{wet} (kg/m ³)	φ_{ef} (%)	κ (mD)	V_P (m/s)	V_S (m/s)	Q_P	Q_S	μ (Gpa)	K_{dry} (Gpa)
Sea water	-	0	10	0.1	1030	-	-	1480	-	-	-	-	-
Devonian	Sandstone	36.5	7	0.8	2226	15	2	2474	1133	66	8	2.86	-
Silurian	Carbonate shales	580	31	6.3	2244	6-16	<01	2570	1043	71	16	2.44	-
Ordovician Saldus Fm. (Oil reservoir)	Limestone	702	5	8.4	2342	18	6	2970	1395	95	28	4.56	-
Ordovician (Cap rock)	Carbonate shales	712.5	35	8.6	2540	3	<0.01	2628	1093	74	17	3.04	-
Deimena (Reservoir-1)	Sandstone	848	37	9.3	2341	21	160	2836	1400	250	94	4.59	4.21
Deimena (Reservoir-2)	Sandstone	876	37	9.7	2400	17	60	2873	1349	761	255	4.37	4.00
Deimena (Reservoir-3)	Sandstone	885	37	9.8	2306	25	230	2872	1510	211	87	5.26	4.82
Cambrian	Siltstone	901	38	10	2324	3-18	0.2-23	2746	1675	81	0	6.52	-
Basement	Granite	1018	41	11.2	2675	-	-	5800	3454	362	171	31.9	-

* Depth of the top of the formation in well E6-1/84

All formations except for the Oil reservoir are saturated with brine. Temperature (T) and pressure (P) of the formations top; ρ_{wet} – the bulk density of brine-saturated rock samples; φ_{ef} – effective porosity; κ – permeability; V_P and V_S – compressional (P) and shear (S) waves velocities, respectively; Q_P and Q_S – quality factors of P- and S-waves, respectively; μ and K_{dry} – shear and bulk modulus of dry rocks, respectively (K_{dry} estimated only for reservoir formations).

Table 3. Estimated seismic (poro-viscoelastic) properties of the reservoir rock formations after the alteration experiment shown in the seismic model (Fig. 5)

Formation	Lithology	ρ_{wet} (kg/m ³)	φ_{ef} (%)	κ (mD)	V_P (m/s)	V_S (m/s)	Q_S	μ (Gpa)	K_{dry} (Gpa)
Reservoir-1	Sandstone	2270	23	140	2743	1319	189	68	3.95
Reservoir-2	Sandstone	2388	16	90	2856	1283	1163	360	3.93
Reservoir-3	Sandstone	2188	30	280	2735	1415	202	81	4.38

All reservoir formations are saturated with brine

2.5.2 CO₂ plume modelling

A simplified CO₂ plume accumulation model was based on studies of gravity flows within a permeable medium for an axisymmetric geometry (Huppert & Woods, 1995; Lyle et al., 2005; Bickle et al., 2007) and it took field monitoring and numerical modelling studies of the existing offshore storage site (Sleipner, North Sea, e.g. Fornel & Estublier, 2013; Zhang & Agarwal, 2014) into account. The possible evolution and migration of the CO₂ plume within the reservoir layers in the E6 potential storage site was described at a specific time and with a given amount of injected CO₂. The fluid saturation has been assumed according to the structural, stratigraphic, lithological and petrophysical properties of different reservoir layers (Scenario-3 and Scenario-4; Fig. 5b).

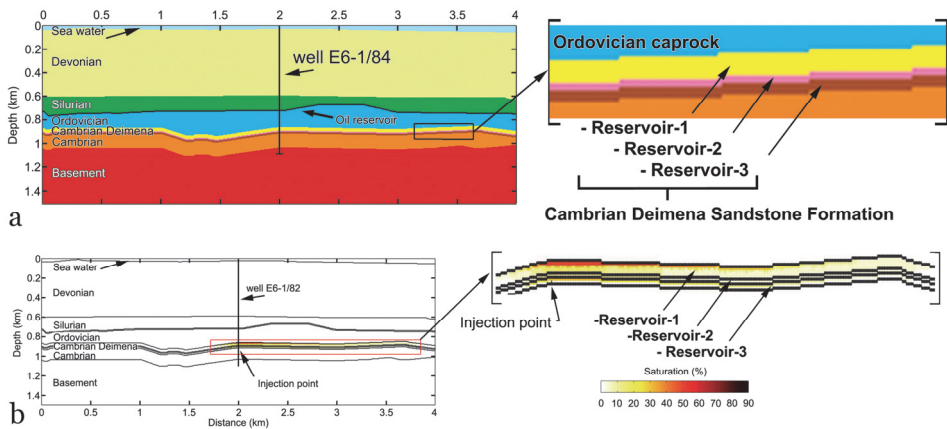


Figure 5. (a) 2D geological model of the E6 offshore structure implemented for seismic modelling and a magnification of the three reservoirs; (b) plume saturation model of CO₂ injected into the reservoir formation in the E6 structure. Different CO₂ saturation of reservoir formation fluids is indicated. Black lines within the structure are formations borders.

2.5.3 Seismic and poro-viscoelastic properties

Seismic parameters of the reservoir layers were computed using the properties of rocks (ρ_{solid} , ρ_{dry} , ϕ_{ef} , κ and V_{Pdry}) measured on dry-rock samples before and after the alteration experiments at the IFPEN rock physics laboratories (PAPER I, PAPER II, PAPER III, PAPER IV and PAPER V). The measured parameters were coupled with data available in the exploration report for the E6 structure (Андрющенко et al., 1985). The measured, reported or estimated data (average from measured and reported for different parts of the reservoir layer) were applied in modelling. The estimated ρ_{solid} value was used for Reservoir-1, reported value for Reservoir-2 and measured value for Reservoir-3. Estimated ρ_{dry} , ϕ_{ef} and κ were employed for Reservoir-1 and Reservoir-3, and reported values for Reservoir-2. Estimated V_{Pdry} was used for Reservoir-1 and reported V_{Pdry} for Reservoir-2 and Reservoir-3.

The results of the petrophysical alteration of the E6 structure for Reservoir-1 and Reservoir-3 were considered as reservoir rock properties after the alteration experiment (PAPER IV, PAPER V). Due to lack of samples characterizing change in the rock properties of Reservoir-2 and V_{Pdry} change in Reservoir-1 and Reservoir-3, alteration results of the identical reservoir samples (with similar properties before alteration) from the Lithuanian offshore structure E7 structure were used (Fig. 2; PAPER II; PAPER IV, PAPER V).

The layers above and below the storage formation were assigned the experimental P-wave velocities (V_{Pwet}) obtained from unpublished results of active seismic surveys, laboratory measurements of dry and wet samples of the oil reservoir of the Upper Ordovician Saldus Formation from well E6-1/84 (Андрющенко et al., 1985) and reported measurements of more than 1000 rock samples of the northern part of the Baltic sedimentary basin (Shogenova et al., 2010).

Seismic properties of different formations (PAPER III; PAPER IV) were computed considering rock physics theories described in detail in the PAPER VI.

2.6 The software applied

The following software packages were used for different tasks in this PhD research: ArcGIS (mapping the CO₂ storage sites), Corel Draw 12 (construction of the cross sections), Adobe Photoshop 8 (presentation of the SEM images of rocks and construction of the 2D seismic model), Golden Software Surfer 8 (digitizing structural maps and building 3D geological models), Statistica for Windows (statistical analyses and 2D graphs of the relationships of the studied parameters), Jewel Suite and Petrel from Schlumberger (detailed 3D geological and petrophysical static modelling), MatLab 7 (computing numerical seismic equations and CO₂ plume geometry), Absoft Fortran Compiler and Seismic Unix software (compilation of the seismic modelling code and computing seismograms and snapshots).

3. RESULTS

3.1. Reservoir quality of sandstones before alteration

Considering permeability and porosity requirements for CO₂ geological storage (Van Der Meer, 1993; Chadwick et al., 2006; Vangkilde-Pedersen & Kirk, 2009; Tiab & Donaldson, 2012; Halland et al., 2013), hydrocarbon reservoir classification by these parameters proposed by Ханин (1965, 1969) and data of 115 sandstone samples reported earlier and measured recently (Shogenova et al., 2009a; PAPER I, PAPER II), the studied reservoir sandstones from the Deimena Formation were subdivided into four groups and eight classes based on reservoir quality (Table 4; Fig. 6a; Table 2 in PAPER V). The groups were distinguished using permeability limits of 300, 100, 10 and 1 mD. Each group was subdivided into two porosity classes.

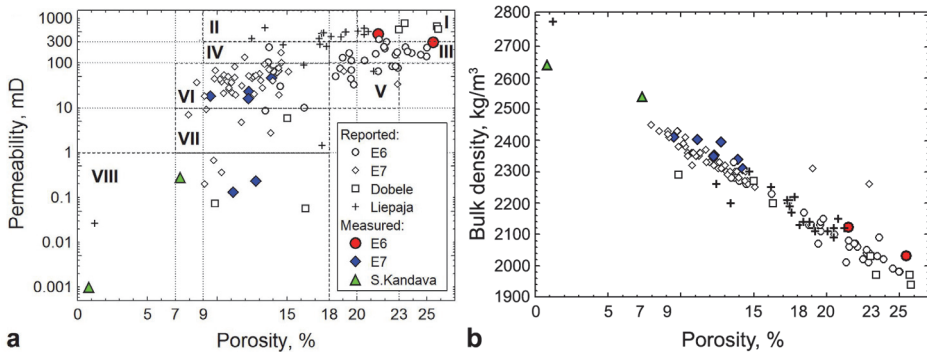


Figure 6. (a) Gas permeability versus porosity of the reported and measured sandstones in eight reservoir quality classes I–VIII (PAPER V). (b) Bulk density measured on dry samples versus porosity. Data are based on 115 sandstone samples from the Deimena Formation of two offshore and three onshore structures from seven boreholes, reported and measured before the alteration experiment.

The first group, ‘very appropriate’ for CGS (classes I and II) includes samples from the offshore E6, onshore Dobele-92 and Liepaja-San boreholes.

The second group, ‘appropriate’ for CGS, class III, is composed of rocks from the E6-1/84 borehole, while class IV also includes rocks from the E7-1/82 and Liepaja-San boreholes.

The third group, ‘cautionary’ for CGS, ‘cautionary-1’ class V includes samples mainly from the E6-1/84 borehole, while ‘cautionary-2’ class VI contains mostly rocks from the E7-1/82 borehole.

The last, ‘very low’ reservoir quality class VIII from the fourth group, ‘not appropriate’ for CGS, includes clay-cemented samples from the E7 structure and carbonate-cemented samples from South Kandava, supplemented by three samples from the Dobele and Liepaja structures (Fig. 6a, 6b; PAPER V). Class VII includes only earlier reported samples (E6, E7, Liepaja and Dobele

Table 4. Classification of the reservoir rocks by permeability and porosity

Hydrocarbon reservoirs (Ханин 1965, 1969)				CO ₂ storage standards*				Classification of the studied rocks for CO ₂ storage**							
Group	Class	Reservoir quality	κ (mD)	φ_{ef} (%)	Group	Class	Reservoir quality	κ (mD)	φ_{ef} (%)	Group	Application for CGS	Class	Reservoir quality	κ (mD)	φ_{ef} (%)
1	I	Very high	≥ 1000	≥ 20	I	I	High Preferred	>500 >300	>25 >20	1	Very appropriate	I	High-1	>300	≥ 20
	II	High	500–1000	18–20	1	II	Good	50–250	15–20	2	Appropriate	III	Good	100–300	>18
	III	Average	100–500	14–18	III	III	Moderate	50–250	10–15			IV	Moderate	9–18	
2	IV	Reduced	10–100	8–14	2	IV	Cautionary	<200 <50	<10	3	Cautionary	V	Cautionary-1	10–100	18–23
	V	Low	1–10	2–8	V	V	Low	<10	<15	4	Not appropriate	VI	Cautionary-2	7–18	
	VI	Very low	<1	<2	VI	VI	Very low	<10	<15			VII	Low	1–10	7–18
												VIII	Very low	<1	<18

*CO₂ storage standards modified after Van Der Meer (1993), Chadwick et al. (2006), Vangkilde-Pedersen & Kirk (2009), Tiab & Donaldson (2012), Halland et al. (2013): group 1, acceptable for CGS; group 2, cautionary.

** New classification based on the studied data (reported and measured in laboratory before the alteration experiment) proposed by authors for the studied region and geological structures. κ : gas permeability; φ_{ef} : effective porosity.

structures), which had higher permeability and porosity, lower grain and bulk density and P-wave velocity than rocks of class VIII.

According to the chemical and lithological classification proposed by Kleesment & Shogenova (2005) and Shogenova et al. (2005), Kn27-4 is a mixed carbonate-siliciclastic sandstone ($50 < IR < 70\%$), while the other studied samples (E6-1–E6-3, E7-1–E7-7 and Kn24-4) are siliciclastic sandstones ($IR > 70\%$) of different quality, and clay and carbonate cement content (Table 3 in PAPER V).

According to our classification based on permeability and porosity (Table 4), offshore sandstones from the E6 structure are mainly of ‘good’ and ‘high-1’ reservoir quality (classes III and I, respectively), with a small number of samples of ‘cautionary-1’ V class and rare samples of classes IV, VI and VII.

Offshore sandstones from the E7 structure are mainly of ‘cautionary-2’ reservoir quality class VI. Few samples belong to classes IV–VII. Clay-cemented samples from the downward part of the E7 reservoir ($70 < SiO_2 < 90\%$ and $Al_2O_3 > 5\%$, Table 3 in PAPER V) and carbonate-cemented samples ($65 < SiO_2 < 85\%$ and $CaO > 5\%$, Table 3 in PAPER V) from the upward part of the onshore South Kandava structure are in ‘very low’ quality class VIII.

The ‘high-1’ and ‘good’ reservoir quality (classes I and III, respectively) quartz sandstones from the E6 structure are composed mainly of quartz, with minor amounts of clay (illite and/or kaolinite) and carbonate cement forming minerals, admixture of feldspar and accessory minerals represented by pyrite, barite, anatase and/or brookite, and zircon (PAPER I, PAPER II).

The sandstones from the E7 offshore structure are also composed mainly of quartz. Compared to sandstones of the E6 structure, sandstones of the E7 structure in some parts of the Deimena Formation contain more clay and carbonate minerals, including ankerite, dolomite, admixture of feldspar and clay fraction represented by kaolinite and illite. In the upper part of the Deimena Formation the sandstones are mostly cemented by quartz-generated cement. Rocks in the lower part are characterized by conformation of quartz grains due to dissolution under the pressure (PAPER I, PAPER II).

The transitional reservoir (trans-res) sandstones from the South Kandava onshore structure (located 0.2–0.3 m below the Lower Ordovician cap rock formation) are characterized by a higher carbonate cement content than the other studied pure reservoir sandstones. Trans-res sandstone Kn24-4 (0.3 m below the cap rock formation, Figs 3, 7; PAPER V) was estimated by the XRD and XRF analyses as ankerite-cemented almost pure quartz sandstone of ‘very low’ reservoir quality (class VIII).

Trans-res rock sample Kn27-4 (0.2 m below the cap rock formation) was estimated by XRD analysis as sandstone with abundant quartz and minor calcite (mixed carbonate–siliciclastic rock by geochemical interpretation) and was assigned ‘low’ reservoir quality (class VII).

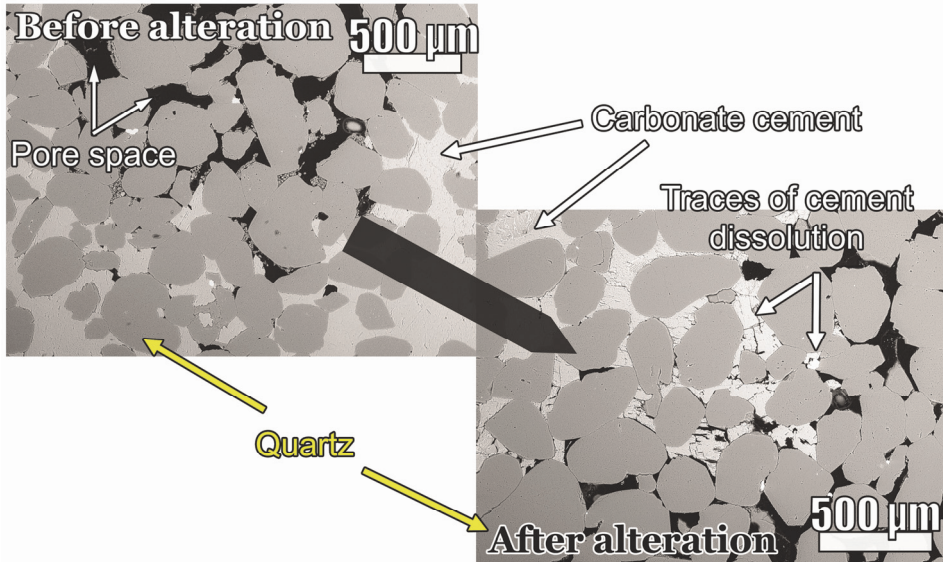


Figure 7. SEM microphotographs of thin sections of trans-reservoir carbonate-cemented medium-grained poorly-sorted Deimena sandstone sample Kn24-4 (Table 3 in PAPER V) before (left) and after (right) the alteration experiment (PAPER V). The sample was of ‘very low’ reservoir quality before the alteration experiment and became of ‘moderate’ reservoir quality (class IV) after the experiment.

3.2 CO₂ storage capacity of the studied structures

The estimated CO₂ storage capacity of each structure, total capacity of the onshore and offshore structures and four structures together according to ‘optimistic’ and ‘conservative’ approaches with different levels of reliability (min/max/mean) are in Table 5 (PAPER I, PAPER II).

3.2.1 The E6 structure

The closing contour of the E6 structure was determined by the top depth contour of 1350 m (Fig. 2; PAPER I, PAPER II). The closing contour, reported by the LEGMC, was at 950 m (http://mapx.map.vgd.gov.lv/geo3/VGD_OIL_PAGE). Line 76033 of the cross section, based on seismic data, crosses the Deimena Formation at a depth of 950 m. The propagation of a slope within the Deimena Formation could be clearly detected between lines 76033 and Line1 (Fig. 4 in PAPER II). We took account of the depth range of the Deimena Formation and structural uplift within E6 and the fault system that separates the E6 structure from the enviroing deposit surfaces. The total area of the structure is 600 km². With the 1350 m closing contour of the reservoir top, an approximate area of the larger part of the structure, E6-A, is 553 km², while the smaller part E6-B takes up 47 km². The thickness of the reservoir in the well is 53 m. The value of ρ_{CO_2r} was 658 kg/m³, corresponding to a depth of 848 m and temperature 36 °C. The estimated minimum, maximum and average porosities

Table 5. Physical parameters of the Baltic structural traps

Reservoir parameters										CO ₂ storage capacity (Mt)				
Structure	Depth of top (m)	Thickness (m)	Trap area (km ²)	Salinit y(g/l)	Pressure (mPa)	T (°C)	CO ₂ density (kg/m ³)	S _{eff} Opt./Cons. (%)	Optimistic estimates			Conservative estimates		
									Min	Max	Mean	Min	Max	Mean
E6-A	848	53	553	99	9.3	36	658	10/4	243	582	365	97	233	146
E6-B	848	53	47	99	9.3	36	658	4/2	8	20	12	4	10	6
E6 total	848	53	600	99	9.3	36	658	10; 4/4; 2	251	602	377	101	243	152
E7	1362	58	43	125	14.7	46	727	20/4	14	66	34	3	13	7
Total CO₂ storage capacity of the studied offshore structures (Mt)									265	668	411	104	256	159
S. Kandava	933	42	97	113	10.5	24.5	820	15/4	5	122	95	1	32	25
Dobeles	950	52	70	114	13	18	900	20/4	56	145	106	11	29	21
Total CO₂ storage capacity of the studied onshore structures (Mt)									61	267	201	12	61	46
Total CO₂ storage capacity of four structures (Mt)									326	935	612	116	317	205

S_{eff}Opt./Cons. is a storage efficiency factor for the optimistic/conservative estimates. The NG in E6 was estimated by logging data as 90%, in E7 as 80%, in Kandava as 90%, in Dobeles as 85%, Fig. 3.

of 14–33.5% (mean 21%) were used for calculation (Table 1 in PAPER II). The estimated theoretical CO₂ storage capacity of the E6 structure was 264–631 Mt (mean 396 Mt) based on the optimistic approach, and 106–252 Mt (mean 158 Mt) based on the conservative approach in PAPER I. Then the optimistic storage capacity of the entire structure was reduced to 251–602 Mt (mean 377 Mt) (Table 5; PAPER II). The theoretical optimistic and conservative CO₂ storage capacities of two split parts of the reservoir were estimated separately. Based on the optimistic approach, the CO₂ storage capacity of the E6-A part was 243–582 Mt (mean 365 Mt) and of the E6-B part 8–20 Mt (mean 12 Mt). The conservative capacity of E6-A was 97–233 Mt (mean 146 Mt) and of the E6-B part 4–10 Mt (mean 6 Mt).

3.2.2 The E7 structure

The closing contour of the E7 structure reported by the LEGMC is 1450 m (http://mapx.map.vgd.gov.lv/geo3/VGD_OIL_PAGE). Based on the depth range of the Deimena Formation, the fault system bounding the structure and structural uplift within the structure, a depth of 1525 m was considered as the closing contour of the reservoir top. In case of the 1525 m level, an approximate area of the E7 structure (43 km²) is 14 times smaller than that of E6 (PAPER I).

The thickness of the reservoir in the well is 58 m. The value of ρ_{CO_2} 727 kg/m³ was taken as corresponding to a depth of 1362 m and temperature 46 °C. The estimated minimum, maximum and average porosities of 5–23% (mean 12%) were used for calculation. The CO₂ storage capacity of the E7 structure assessed by the optimistic approach was 14–66 Mt (mean 34 Mt) and 3–13 Mt (mean 7 Mt) by the conservative approach (Table 5; PAPER II).

3.2.3 The South Kandava structure

The CO₂ storage capacity, estimated using the optimistic approach, was 5–122/95 Mt, and based on the conservative approach, 1–32/25 Mt (Table 5; PAPER I). The CO₂ storage capacity, estimated earlier within the EU Geocapacity project (44 Mt; Shogenova et al., 2009a), is in the same range with our optimistic capacities.

3.2.4 The Dobele structure

The estimated CO₂ storage potential in the Dobele structure is 56–145/106 Mt according to the optimistic approach and 11–29/21 Mt according to the conservative approach (Table 5; PAPER I). The CO₂ storage capacity estimated earlier within the EU Geocapacity project (56 Mt, Shogenova et al., 2009a), corresponds to our minimum optimistic estimate.

3.3 Reservoir quality of sandstones after alteration

3.3.1 The E6 structure

An increase in φ_{ef} , supported by a decrease in ρ_{dry} and ρ_{solid} , and a slight decrease in sample weight, due to the dissolution of minor carbonate cement,

displacement of clay cement after the experiment and minor increase in microfractures in grains, were determined after the alteration experiment in the studied samples from the E6 offshore structure (Table 6; Table 3 in PAPER V). However, the changes in their κ and ϕ_{ef} did not cause a significant change in reservoir quality and after the experiment samples from the E6 structure remained in the same ‘high-1’ and ‘good’ reservoir quality classes (Table 6; Figs 6a, 8, 9; PAPER V).

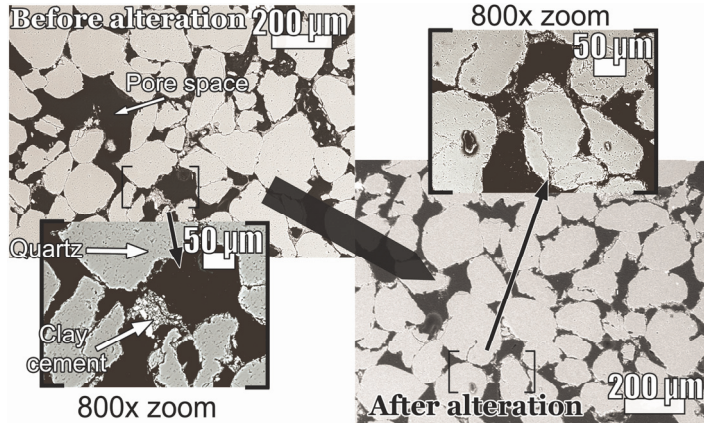


Figure 8. SEM microphotographs of thin sections of reservoir fine-grained poorly sorted Deimena Formation sandstone sample E6-3 (Table 3 in PAPER V) before (left) and after (right) the alteration experiment. The sample is of ‘high-1’ (class I) reservoir quality sandstone, very appropriate for CGS with no changes in the reservoir quality after the experiment.

3.3.2 The E7 structure

Reliable changes in the physical properties of rock were detected in the nearly pure (estimated by XRD) quartz sandstones E7-2–E7-5 sampled from the depth interval 1389.5–1393.2 in the E7 offshore structure (Table 6; Fig. 10; PAPER V). A decrease in ρ_{solid} in these samples and a decrease in ϕ_{ef} in samples E7-2 and E7-3 were recorded. A reliable decrease in the sample weight and a significant increase in κ were detected in sample E7-3 (Figs 10, 11; PAPER V). Additionally, a reliable decrease in V_{Pdry} and V_{Sdry} was determined in sample E7-3. A reliable decrease in ρ_{dry} was registered only in sample E7-4 (Table 6). However, the only sample E7-3 from class VI (‘cautionary-2’) improved its reservoir quality up to class IV (‘moderate’) owing to its permeability increase, while the quality of the other samples did not improve after the experiment.

Only a slight decrease in sample weight, ρ_{solid} , a significant reduction in the V_{Pdry} supported by some insignificant variations in κ and ϕ_{ef} were determined in clay-cemented sandstones E7-6 and E7-7 of initially ‘very low’ quality class VIII. After alteration both samples remained in the same reservoir quality class (Table 6; PAPER V).

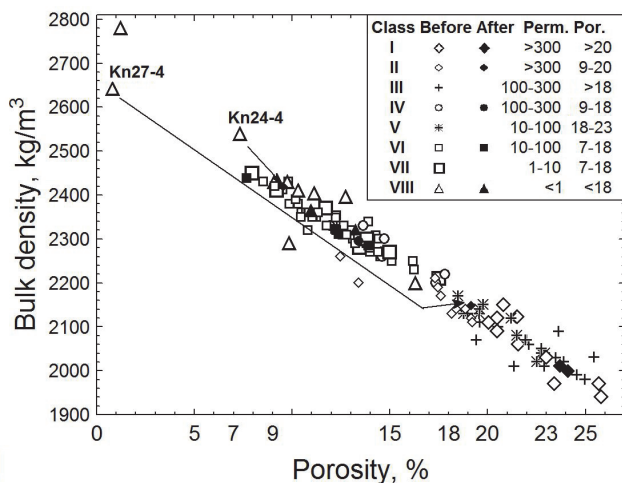


Figure 9. Bulk density measured on dry samples versus porosity of the sandstones of the Deimena Formation from two offshore and three onshore structures for 115 samples reported and measured before alteration (empty symbols) and 12 samples measured after alteration (black symbols) in terms of reservoir quality classes I–VIII (Table 4, Table 2 in PAPER V). Perm. – gas permeability; Por. – porosity.

3.3.3 The South Kandava structure

The weight of trans-res sandstone sample Kn24-4 from the South Kandava onshore structure had decreased during the alteration experiment. This is explained by the dissolution of cement (expressed by a decrease in CaO content from 5.61% before to 3.95% after alteration, Table 3 in PAPER V), a decrease in ρ_{dry} and ρ_{solid} and in V_{Pdry} associated with a significant rise in ϕ_{ef} and accompanied by drastically increased κ (Table 6; Figs 7, 9 10; PAPER V).

Thin section study confirmed the results of the rock physical measurements, showing the dissolution and microfracturing of carbonate cement and displacement of clay cement, which previously blocked pores, after the alteration (Fig. 7; PAPER V). Owing to drastic changes in porosity and permeability, the reservoir quality of this rock sample improved up to ‘moderate’ reservoir quality class IV, ‘appropriate’ for CGS (group 2, Table 6; PAPER V).

The trans-res rock sample Kn27-4 (0.2 m below the cap rock formation, Figs 3, 12) was estimated by XRD analysis as sandstone with abundant quartz and minor calcite (mixed carbonate-siliciclastic rock by geochemical interpretation) and was assigned to the ‘low’ reservoir quality (class VII). The sample weight decreased due to partial dissolution of carbonate cement (expressed by a decrease in CaO content from 15.69% before to 12.23% after alteration, Table 3 in PAPER V), accompanied by reduction in V_{Pdry} , V_{Sdry} and the ρ_{dry} and drastic increase in ϕ_{ef} and κ induced by chemical alteration (Table 6; Figs 9, 10, 12). This improved the reservoir quality of this sample up to ‘high-2’ reservoir quality class II, ‘very appropriate’ for CGS (group 1).

Table 6. Reservoir quality classes and petrophysical properties of the Deimena Formation studied in the alteration experiment

Sample	Depth (m)		Reservoir quality class		Weight ($\text{kg} \cdot 10^{-3}$)		Bulk density (kg/m^3)		Grain density (kg/m^3)		Porosity (%)		Permeability (mD)		V_p (m/s)		V_s (m/s)	
	Before	After	Before	After	Before	After	Before	After	Before	After	Before	After	Before	After	Before	After	Before	After
E6-1	860.4	I	17.6	17.5	2123	2011	2705	2635	21.5	23.7	440	380	-	2310	-	-	-	-
E6-2	886.7	III	12.0	6.4*	2031	1863	2725	2661	25.5	30.0	290	-	-	-	-	-	-	-
E6-3	886.7	I	10.2	10.0	-	1999	2718	2633	-	24.1	400	490	-	-	-	-	-	-
E7-1	1387.6	VI	16.8	16.7	2354	2310	2683	2636	12.3	12.4	23	26	3583	3300	-	-	-	-
E7-2	1389.5	VI	26.5	26.5	2412	2439	2666	2641	9.5	7.7	18	16	2457	2280	1725	-	-	-
E7-3	1390.5	VI	24.8	24.6	2309	2295	2693	2650	14.3	13.4	66	130	3096	2750	2194	1850	-	-
E7-4	1390.5	VI	15.6	15.5	2339	2284	2716	2653	13.9	13.9	46	78	-	-	-	-	-	-
E7-5	1393.2	VI	24.9	24.8	2349	2323	2676	2646	12.2	12.2	16	19	3097	3100	2230	2020	-	-
E7-6*	1394.2	VIII	24.7	24.3	2403	2367	2704	2659	11.1	11.0	0.13	0.18	2524	1230	-	-	-	-
E7-7*	1394.2	VIII	24.8	16.1*	2395	2322	2746	2676	12.8	13.3	0.23	0.23	2130	2130	-	-	-	-
Kn24-4**	1157.3	VIII	35.3	31.6	2642	2148	2741	2675	7.3	9.6	0.28	300	4556	4030	3225	-	-	-
Kn27-4**	998.8	VIII	35.0	27.1	2539	2419	2664	2658	0.8	19.1	0.001	550	5400	4380	3600	2540	-	-

Before, samples measured before the alteration experiment; after, samples measured after the alteration experiment; V_p , P-wave velocity; V_s , S-wave velocity; * clay-cemented; ** carbonate-cemented sandstones from the South Kandava structure;

Bold and *italic* numbers in the table correspond, respectively to 'reliable' and 'not reliable' changes in petrophysical parameters after the alteration experiment according to measurement errors. 'Not reliable' values also correspond to the parameters not subjected to alteration.

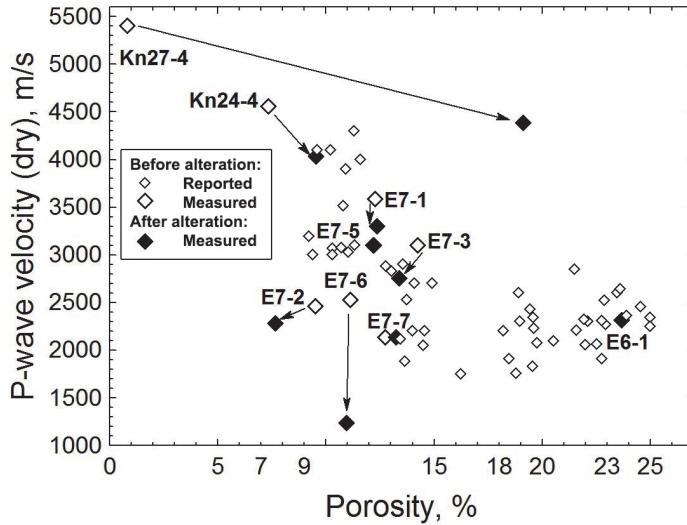


Figure 10. P-wave velocity versus porosity in dry sandstones reported (52 samples) and measured before (8 samples) and after the alteration experiment (9 samples). A decrease in the grain density in all the samples and a decrease in velocity in most of the rocks were determined after the experiment.

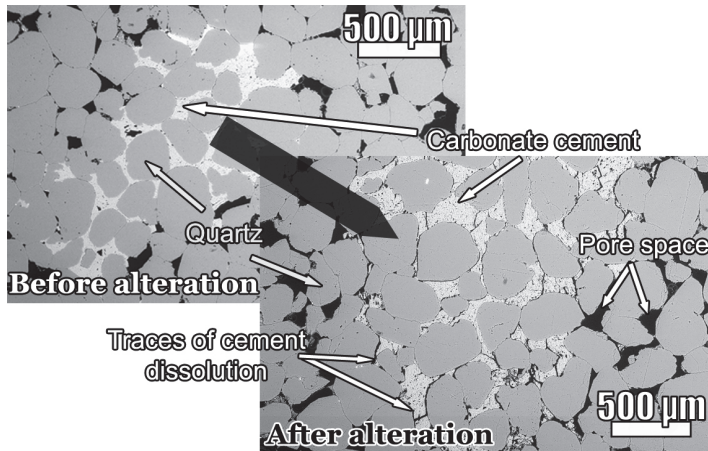


Figure 11. SEM microphotographs of thin sections of reservoir carbonate-cemented medium- to fine-grained well-sorted Deimena Formation sandstone sample E7-3 (Table 3 in PAPER V) before (left) and after (right) the alteration experiment. The sample is of 'cautionary-2' reservoir quality (class VI), with improved quality up to 'moderate' (class IV) after alteration.

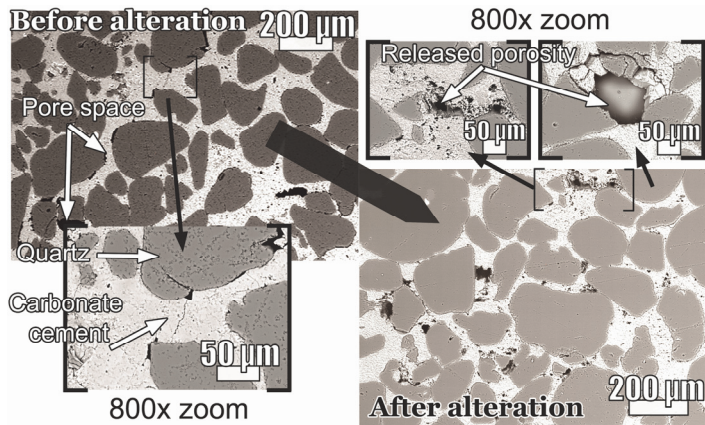


Figure 12. SEM microphotographs of thin sections of trans-reservoir carbonate-cemented sample Kn27-4 from medium- to very fine-grained (fine-grained in general) unsorted Deimena sandstone from the South Kandava structure (Table 3 in PAPER V) before (left) and after (right) the alteration experiment (PAPER V). The sandstone was of ‘very low’ reservoir quality. During the alteration experiment its reservoir quality improved up to ‘high-2’ (class II), ‘very appropriate’ for CGS (Table 4).

3.4 3D geological and petrophysical models of the E6 structure

A 3D geological static model was built for the E6 structure (Figs 4, 13) with a cell size of 500 m x 500 m (see Table 5). The Cambrian Deimena Formation reservoir and the Ordovician primary cap rock in E6-A were modelled and populated with both lithological and petrophysical parameters (porosity and permeability). A summary of meshing data and statistics of petrophysical properties in the cap and reservoir rock implemented in the model is shown in Tables 7 and 8, respectively.

Table 7. Volumetric grid parameters implemented in the 3D geological modelling

Size (X-Y-Z) (m)	29371.5–26534–826
Depth range (m)	693–1519
Cell size (m)	500 x 500
Grid cells (nI x nJ x nKGridLayers)	67 x 59 x 10
Total number of 3D grid cells:	39530
Number of faults:	8

Table 8. Porosity and permeability statistics of the model of the E6 structure

Porosity (%)							
	Min	Max	Delta	Mean (μ)	Std (σ)	Var (σ^2)	Sum
Cap rock	2	23.6	21.6	5.9	5.9	34.7	69 256
Reservoir	13.6	33.5	19.9	20.8	3.9	15.1	245 905
Permeability [mD]							
	Min	Max	Delta	Mean (μ)	Std (σ)	Var (σ^2)	Sum
Cap rock	0.0001	24.2	24.2	2.2	4.5	20.5	25 372
Reservoir	10.2	440	429.7	168.3	107.1	11 471.7	1 986 070

Total number of cells defined in the entire property: 11800

Std – standard deviation

Var – variance

Delta=Max-Min

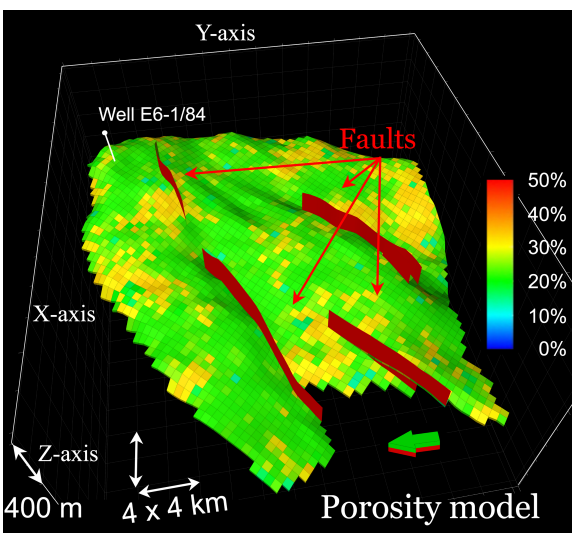
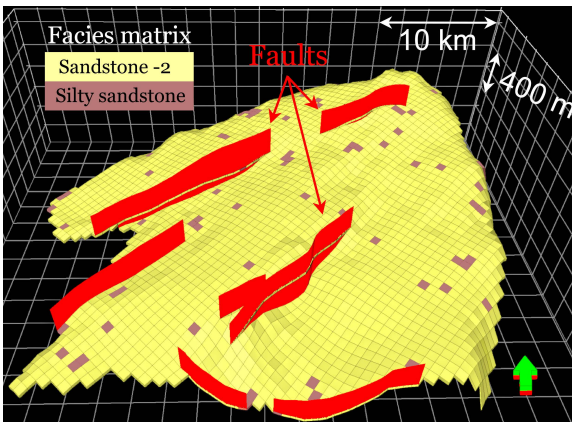


Figure 13. Top: 3D geological static facies model of the E6-A compartment of the E6 offshore structure, showing the lowermost layer 10 of the Cambrian Deimena sandstone-2 reservoir formation with rare clusters of silty sandstones and main faults. Bottom: 3D geological static porosity model of the E6-A compartment of the E6 offshore structure, with the lowermost layer 10 of the Deimena Formation and main faults.

3.5 Numerical seismic models of the E6 structure

3.5.1 Seismic properties of the reservoir formations

The bulk density ρ_{wet} decreased in the whole range of CO₂ saturation, accompanied by a drastic drop in V_{Pwet} and acoustic impedance, calculated for the reservoir rocks using the fluid substitution method (Table 3 in PAPER VI). Moreover, the mesoscopic attenuation showed a peak at about 5% CO₂ saturation in the reservoir rocks in all reservoir layers (Reservoir-1, Reservoir-2 and Reservoir-3) without and with a petrophysical alteration effect with minor differences. The decrease in P-wave velocity becomes insignificant in the range 10–50% CO₂ saturation. After 50% CO₂ saturation V_{Pwet} and V_{Swet} started to increase slightly due to decrease in bulk density. The velocity drop of the altered rocks (Scenario-2 and Scenario-4) is slightly higher than that of the non-altered rocks (Scenario-1 and Scenario-3; Tables 1–3 in PAPER VI). Figure 4 in PAPER VI shows the bulk density, velocities, acoustic impedance and attenuation of Reservoir-1 as a function of CO₂ saturation for the original (initial) and altered core samples.

3.5.2 Synthetic seismic sections

3.5.2.1 Plane-wave datasets

The baseline synthetic plane-wave seismic section of the E6 offshore structure before CO₂ injection (Fig. 14a) was produced and compared with six synthetic seismic sections, reproducing different CO₂ saturation levels (1, 5, 10, 15, 50 and 90%) of the Deimena Formation, considering homogeneous gas saturation (Scenario-1; Fig. 14-sc1-a). Repeated seismic simulations took the chemically induced petrophysical alteration effect of the reservoir rocks into account (Scenario-2; Fig. 14-sc2-a). Modelling provided seismic images of the CO₂ storage in the E6 offshore structure at different times over the same area. Plane-wave sections of the modelled CO₂ plume in the E6 structure without and with the petrophysical alteration effect were also computed (Scenario-3; Fig. 14-sc3-a and Scenario-4; Fig. 14-sc4-a, respectively).

The presence of CO₂ in the reservoir layers could be detected by direct comparison and interpretation of the baseline and repeated synthetic surveys with different CO₂ saturation levels in Scenario-1 (Fig. 14-sc1-a) and Scenario-2 (Fig. 14-sc2-a), already from 1% saturation. The seismic reflections corresponding to the top and bottom of three reservoirs became stronger with increasing CO₂ saturation showing the best contrast up to 5% CO₂ saturation. The evolution of the reflection strength in the considered sections after 5% CO₂ saturation was difficult to detect, as all synthetic plane-wave seismic sections in the range of 10–90% CO₂ saturation for a specific scenario were very similar. A slight variation in time shift or velocity push-down was also detectable on the plane-wave plots for the layers below the reservoir formation. The plane-wave sections of Scenario-3 (Fig. 14-sc3-a) and Scenario-4 (Fig. 14-sc4-a) clearly show the modelled CO₂ plume in the E6 storage site. Seismic reflections of the

reservoir rocks with a petrophysical alteration effect (Scenario-2 and Scenario-4) showed higher reflectivity in all cases compared to Scenario-1 and Scenario-3.

Using ‘Difference’ and NRMS metrics, CO₂ was clearly visible since low gas saturation (1%, Fig. 14). However, for saturation higher than 5% the amplitude of the signals delineating the reservoir and the interface below did not vary, similarly to the reflection amplitudes of the reservoirs in the synthetic plane-wave sections.

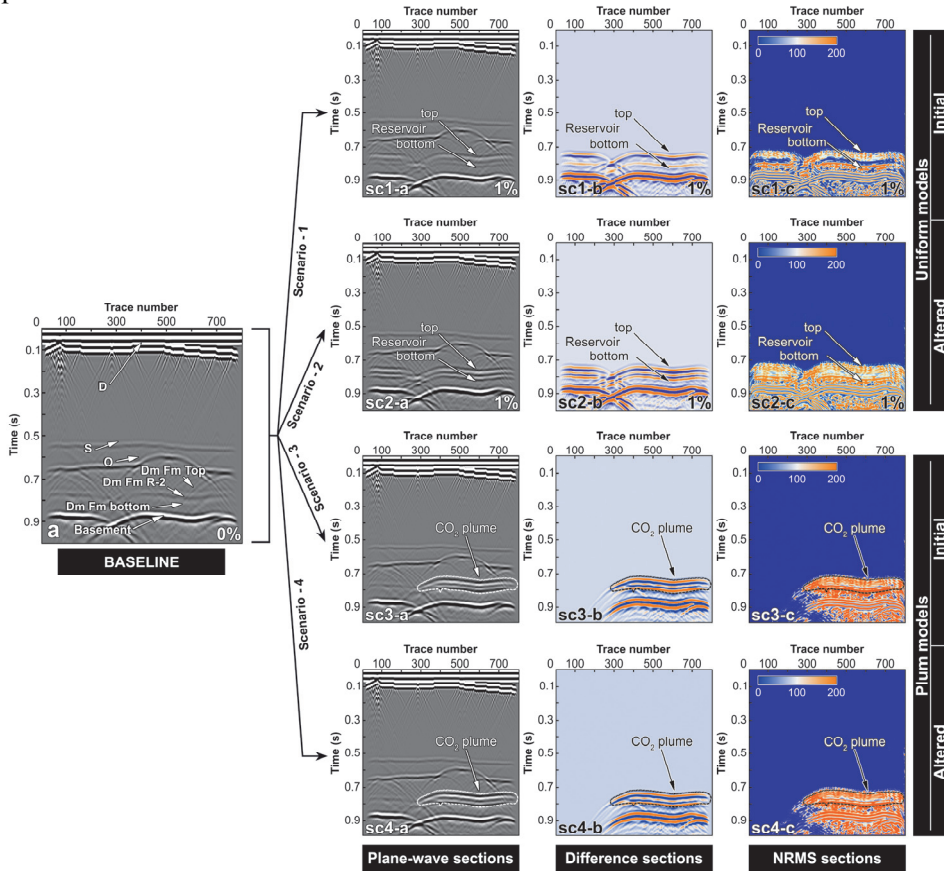


Figure 14. (a) Baseline synthetic plane-wave section of the E6 structure (before the injection of CO₂). Reflectors of the top of all geological formations (D–Devonian, S–Silurian, O–Ordovician), the top and bottom of the Deimena Formation reservoir (Dm Fm) and the middle part of the Deimena Formation Reservoir-2 (Dm Fm R-2) are indicated; (sc1-a) plane-wave section of Scenario-1 (uniform model without an alteration effect) with 1% CO₂ saturation; ‘Difference’ (sc1-b) and NRMS (sc1-c) sections of the synthetic baseline and the seismic section of Scenario-1 with 1% CO₂; (sc2-a–c) seismic sections of Scenario-2 (uniform model with an alteration effect) with 1% CO₂ saturation; arrows indicate the reservoir top and bottom; (sc3-a–c) seismic sections of Scenario-3 (plume model without an alteration effect); (sc4-a–c) seismic sections of Scenario-4 (plume model with an alteration effect); arrows indicate the CO₂ plume.

4. DISCUSSION

4.1 Storage site selection, characterization and risk assessment

Vintage hydrocarbon exploration reports were used in this study (Силантьев et al., 1970; Дмитриев et al., 1973; Бабуке et al., 1983; Андрющенко et al., 1985). The quality and amount of exploration data were different for various structures. The amount of rocks sampled for the experiments for this PhD research was lower than planned initially, due to the limited number of rocks permitted to sample. The reason was the limited number of drill cores stored in the LEGMC and their commercial approach in providing samples and data. Complete seismic data of these structures were not available. Shortage of exploration data and rock samples added uncertainties into the created 3D geological models and quality estimates of the storage reservoir.

The E6 structure that was selected for detailed modelling contains multiple faults. Uncertainties in the fault structure caused significant difficulties in the assessment of CO₂ storage risks and 3D geological modelling. Because of oil accumulation in the limestone of the Upper Ordovician Saldus Formation and oil impregnation of Cambrian Deimena and Devonian sandstones, the hypothesis of oil leakage from the E6 reservoir via faults could be assumed. There are two possible scenarios of the behaviour of the faults: (1) the faults still have open structure or (2) the faults were locked in the course of time by geological processes. The origin of faults and architecture of reservoirs need more detailed study, which would largely contribute to the estimation of the integrity of reservoirs.

These uncertainties can be clarified in two ways: (1) by conducting a modern geophysical exploration in the area of the studied structures or (2) by making pilot CO₂ injection into the structure and monitoring its behaviour. If the reservoirs are faulted and the faults have open structure, the CO₂ leakage could be determined using known monitoring methods. Seismic survey is the most effective method that has been implemented in the well-known world's largest CO₂ storage project in the Norwegian North Sea (Sleipner) for monitoring the injected CO₂ plume. During seismic survey the formation and migration of the injected CO₂ under impermeable layers can be observed from the surface (e.g. Chadwick et al., 2009; Hermanrud et al., 2009; Alnes et al., 2011).

The existing fault system in the E6 structure, interpreted by seismic data and oil impregnation of Cambrian sandstones revealed in drill core E6-1/84, would suggest two optional cases. The first case is a possible leakage of the geological trap. The opposite case is that the reservoir has good trapping mechanisms, but there is no trapped oil in the reservoir due to specific in situ conditions and geological history of the area. The first case was discussed by Chang et al. (2008). They developed a single-phase flow model to examine CO₂ migration along faults. The model simulated CO₂ migration from the fault into permeable

layers. Reaching these layers, CO₂ continued migration along the fault above them. The developed 1D model was compared with full-physics simulations in 2D. It was concluded that although more CO₂ escapes from a deeper storage formation through a fault, less CO₂ reaches the top of the fault. Thus, attenuation can reduce the risk associated with CO₂ reaching the top of the fault (Chang et al., 2008).

However, the presence of faults does not pose adverse impact on the security of storage. If the offset of a fault is less than the thickness of the cap rock, the likelihood of providing a migration pathway through the cap rock is lower (Bentham et al., 2013). The integrity of faults also plays a crucial role in reservoir security. According to studies carried out in the region, faults can propagate through all cap rocks (Ordovician and Silurian), reaching the Devonian sandstone layer. Thereby, faults were considered to be propagating through the cap rock in the 3D geological model of the E6 structure. No transmissivity values are available for the faults in the area. The vintage seismic reflection data were insufficient for a detailed geometrical characterization of faults. Nevertheless, the largest onshore Inčukalns structure, with a structural setting comparable to E6, has been successfully used for underground gas storage for many years, serving for gas supply to Latvia, Estonia and Lithuania. This fact indicates that faults in the region may have enclosed, impermeable structure (LEGMC, 2007) and as suggested in PAPER I, faults in the E6 structure can act as sealing surfaces.

The conditions of every reservoir for the geological storage of different gases are site-specific. For example, the properties of CO₂ and methane in deep in situ conditions can vary significantly. The migration of CO₂ via faults to depths shallower than 800 m is classified as a risk due to the properties of CO₂. In normal geothermal and pressure regimes CO₂ below 800 m is likely in its highly dense phase. Above this depth (depending on the exact pressure and temperature) the migrating CO₂ may undergo a phase change due to the decreasing pressure and temperature and become gaseous. Carbon dioxide would then expand and migrate faster, which may cause a more serious leakage of CO₂ depending on the surrounding geology (Bentham et al., 2013). Understanding faults integrity is a key for further studies that should clarify the storage potential and integrity risk of the studied structures. As mentioned above, the pilot injection of several thousands of CO₂ could clarify this uncertainty. Due to the splitting of the E6 structure by faults into two compartments E6-A and E6-B with areas of 553 and 47 km², respectively, we propose E6-A as the main CO₂ storage site within the structure and E6-B as an additional reserve structure. Using both substructures should be economical, considering the location of E6-A next to E6-B and the possibility of a common infrastructure. Thereby, E6-A, as the largest storage site in the region, is the main object in this study.

4.2 3D geological models

The reliability of geological static model depends on the amount of input data obtained during the exploration phases. Usually, modellers integrate large sets of various data into 3D numerical models: e.g. geological, structural, geophysical and borehole logging data and all measured parameters of rock samples, (e.g. Brun et al., 2001; Courrioux et al., 2001; Ledru, 2001; Zanchi et al., 2009; Salvi et al., 2010; Bigi et al., 2013). In our study we used a limited set of data from the vintage exploration survey (Андрющенко et al., 1985) and new laboratory measurements (PAPER I, PAPER II). Ideally, to provide a more realistic structural, geological, lithological and petrophysical representation of the E6 structure, additional exploration and new laboratory data are needed, including modern seismic surveys, borehole drilling, and laboratory studies of reservoir and cap rocks. Modern seismic exploration of the E6 structure was ordered in 2006 by the Danish oil company Odin Energi A/S, the owner of the license for oil exploitation in the structure, but the results are not available yet to the third parties. In many cases when the available data are scarce or irregular, an engineering software package such as Petrel can improve the quality of the geological models. The well-known mathematical algorithms of Geostatistical Software Library (Deutsch and Journel, 1998) implemented in Petrel provide a statistically justified image of the area.

4.3 CO₂ storage capacity

The difference between the maximum and average values of CO₂ storage capacity was higher in the E7 structure (48%) than in the E6 structure (37%), suggesting a lower homogeneity of sandstone porosity in the E7 reservoir. This difference was 27% in the Dobele and 22% in the South Kandava structure, whereas reservoir porosity was similar in the onshore structures but homogeneity was two times lower in the offshore structures (PAPER II).

The optimistic maximum and average storage potentials of the E6 structure (602 and 377 Mt) and its larger compartment E6-A (582 and 365 Mt) are higher and nearly the same as the previously reported total potential of all 16 onshore Latvian structures (400 Mt, Shogenova et al., 2009a). Even the average conservative capacities of E6 (152 Mt) and E6-A (146 Mt) are the largest among all Latvian onshore and offshore structures studied until now (PAPER II).

The average CO₂ storage capacity of the E7 structure, estimated both by the optimistic (34 Mt) and the conservative approach (7 Mt), was the lowest among the four studied structures and could be assessed as cautionary for the storage of large industrial emissions.

4.4 Assessment of reservoir quality

The permeability of the studied sandstones varies by six orders of magnitude and by four orders of magnitude at a single porosity. At the same time the porosity of these sandstones varies in the range 0.8–25.8% and can vary 2–2.5 times for a single permeability. Porosity and permeability are related to different properties of pore space geometry. This explains the correlation between porosity and permeability, but also the scattering of such correlations, indicating strong additional influences (Schön, 1996).

The wide range of porosity variation of the Cambrian sandstones in the Baltic Basin is explained by variation in composition, grain size and sorting, pore structure, cementation, diagenetic alteration, burial depth and compaction, tectonic and geothermal conditions, also by variation in onshore and offshore facies, especially in the northern and southern parts of the basin. As the sandstones of the Cambrian Deimena Formation are located in the central part of the Baltic Basin (700–1700 m depth) transitional from its northern shallow to the southern deep part, they can have properties of both shallow and deep parts of the basin. However, even the porosity and permeability of uncompacted Cambrian sandstones from the shallow part of the basin range from very low (1.5% and 0.001 mD, respectively), due to a high proportion of carbonate cement, to some 40% porosity and 1300 mD permeability in weakly cemented rocks (Shogenova et al., 2009a). The permeability and porosity of sandstones in the southwestern deep Lithuanian part of the basin (>1700 m) are distinguished mainly by a lower range of porosity 0.4–12.4%. This is explained by compaction and secondary quartz cementation in contrast to carbonate and clay cements prevailing in sandstones in the shallow and middle parts of the basin. The permeability of rocks in the southern part, however, varies in a rather wide range (0.003–960 mD) (Sliupa et al., 2001, 2008b; Čyžienė et al., 2006; Shogenova et al., 2009a). Considering these porosity and permeability ranges, the classification of the reservoir rocks for CO₂ storage (Table 4), proposed in this research for the middle Latvian–Lithuanian parts of the basin (700–1700 m depth), could be adopted to shallow and deep parts of the basin with some possible corrections of porosity ranges for the reservoir quality classes in the deep part.

The initial permeability and porosity of the sandstones studied in the experiment were mainly controlled by the amount and type of diagenetic cement. Sandstones of ‘very low’ reservoir quality class VIII with the highest content of carbonate and clay cement had the lowest permeability (0.001–0.7 mD). The porosity in carbonate-cemented sandstones for the given permeability was lower than in clay-cemented samples (Fig. 6a; Table 4; Table 3 in PAPER V). This corresponds to the results reported for the northern shallow part of the basin, where carbonate cementation has a higher influence on the porosity of Cambrian sandstones than clay cement, and grain size influences the porosity of these rocks to a lesser degree than cementation (Shogenova et al., 2001a).

Among sandstones from the offshore Lithuanian E7-1/82 and Latvian E6-1/84 boreholes, characterized by the same amount of cement, the more compacted sandstones from the deeper E7 structure (classes VII–VI) had lower permeability and porosity. Our study revealed a different rock microstructure of the sandstones of the Deimena Formation. For example, the sandstone from the E6 structure (E6-3, Fig. 8; PAPER V) was characterized in general by a fine grain size (0.25–0.125 mm, Krumbein phi scale; Krumbein, 1934), poor sorting of the material and the content of clay cement of 5%. The sandstone from the E7 structure (E7-3, Fig. 11; PAPER V) is medium- (0.5–0.25 mm) to fine-grained, well-sorted, with a high content of carbonate cement (about 50%). Sandstones from the South Kandava structure are medium- to very fine-grained (0.125–0.65 mm), poorly sorted to unsorted, with the presence of 50–100% carbonate in pore space and, in addition, several per cent clay cement. At the same time, due to heterogeneity, even in one geological structure (e.g. in E6) the rock properties could vary at different depths (PAPER II).

The main difference between previous classifications provided for hydrocarbon reservoirs, recommendations for reservoirs ‘appropriate’/‘not appropriate’ for CGS and the new classification proposed in this research for the sandstones of the Cambrian Deimena Formation is the overlapping porosity of rock groups divided by permeability (Table 4; PAPER V). For this reason every group is subdivided into classes distinguished by porosity. Therefore the petrophysical parameters depending on porosity, like bulk density and velocity can also overlap for some classes. However, every reservoir quality rock class is characterized by a unique set of the studied rock parameters, including petrophysical, chemical, mineralogical and microstructural features (Figs 7, 8, 11, 12; Table 2 in PAPER V).

4.5 Alteration experiment

The initial and altered effective porosity and permeability of the reservoir samples from the E6 structure were ranked as of ‘high-1’ and ‘good’ reservoir quality (classes I and III, respectively), or ‘very appropriate’ and ‘appropriate’ for CGS, respectively (groups 1 and 2, Table 4). The porosity and permeability of sandstones from the E7 structure were significantly lower (class VI) than in rocks from E6. The initial and altered permeability of the clay-cemented sandstones from the E7 structure (0.13–0.18 mD) and the initial permeability of the carbonate-cemented sandstones from South Kandava (0.001–0.28 mD) were in ‘very low’ reservoir quality class VIII. The reservoir quality of rocks decreases with increasing depth because of rock compaction, rising temperature, conformation of grains and increasing quartz cementation of sandstone with growing depth in the Baltic Basin (Sliupa et al., 2001; Shogenova et al., 2001a, 2001b, 2009a). Our study confirms these results. The shallowest offshore structure E6 has the best reservoir properties among the sandstones studied in this research.

The effective porosity did not change during treatment in most of the studied cases and was supported by stable (E7-1, E7-5) or little varying (E7-4, E7-6) permeability values (Table 6; PAPER V). Other samples showed some variations in effective porosity with stable permeability. At the same time, sample E7-3 was characterized by a slight decrease in effective porosity but a significant increase in permeability (up to 2 times after the alteration experiment). An increase in permeability, correlated with a decrease in grain density supported by unchanged initial porosity, could be explained by modifications of pore space geometry and grain shape changes that control capillary forces (Schön, 1996). A minor dissolution of sandstone cement, including dolomite and ankerite, was determined (Fig. 11; Table 3 in PAPER V), which was insignificant for effective porosity change but substantial for permeability increase. Mineral precipitation and/or cement dissolution, as well as relocation and displacement of clay cement, which blocks pores, took place in the samples characterized by decreased effective porosity. Thin section study showed that the clay fraction, represented by an insignificant amount of kaolinite and/or illite (about 5%) in porous media of the studied samples, was displaced from the pores after the alteration experiment (Figs 7, 8, 11; PAPER V). The type of the clay mineral present is important for the reservoir quality of sandstone. Different influence of kaolinite and illite on porosity and permeability change has been explained earlier. According to Tucker (2001), pore-filling kaolinite reduces the porosity of sandstone, but has little effect on permeability, whereas pore-lining illite reduces the permeability considerably by blocking pore throats, but has little effect on porosity. The present study does not focus on the clay fraction due to the minor presence of clay minerals in the studied samples and insignificant alteration of properties related to the clay cement displacement after the experiment.

Before the alteration experiment trans-res carbonate-cemented quartz sandstone samples Kn24-4 (ankerite-cemented) and Kn27-4 (calcite-cemented) were characterized by low and very low effective porosity and permeability (class VIII, Tables 4, 6; PAPER V). The dissolution of ankerite and calcite cements with minor displacement of clay cement, which blocks pores, was determined in both samples. However, the influence of both types of cement dissolution on the alteration of petrophysical properties was identified. A more significant increase in effective porosity and permeability was observed in calcite-cemented sandstone Kn27-4. The sample was relocated from the 'very low' reservoir quality class VIII rank, 'not appropriate' for CGS, to 'high-2' quality class II, 'very appropriate' for CGS due to final improvement of petrophysical properties (Tables 4, 6; PAPER V). These changes were supported by the dissolution of 3.5% CaO after the alteration experiment (Table 3 in PAPER V). Ankerite-cemented sandstone Kn24-4 showed dissolution of 1.7% CaO after the alteration experiment (Table 3 in PAPER V). The sample was relocated from 'very low' reservoir quality class VIII, 'not appropriate' for CGS, to 'moderate' quality class IV, 'appropriate' for CGS (Tables 4, 6;

PAPER V). Minor improvement of rock properties compared to calcite-cemented sandstone Kn27-4 was observed (Table 6; PAPER V).

Previously reported results of laboratory experiments, numerical modelling and field monitoring of CO₂-reservoir rock interactions (e.g. Czernichowski-Lauriol et al., 2006; Egermann et al., 2006; Izgec et al., 2008; Kaszuba & Janecky, 2009; Bemmer & Lombard, 2010; Bemmer et al., 2011; Nguyen et al., 2013) were confirmed in many cases by our laboratory experiments. Partial dissolution of carbonate cement (calcite, dolomite and ankerite) and other secondary minerals, associated with the increase, and in some places variation in porosity and permeability, was described for the reservoir rocks.

This section study allowed qualitative estimation of the mineral dissolution in carbonate cement. Although carbonate cement was expected to dissolve more intensely, it dissolved only on grains edges and partially inside the pore filling. This phenomenon could be explained by reduction in the acidity of brine and increase in pH equilibrium to the pre-experimental state during the alteration experiment, after the dissolution of a certain amount of carbonate cement material. This fact was confirmed by modelling provided by, e.g., Schumacher (2013), whose model represented the alkalinity and pH increase at all well locations at Sugar Creek, USA, for both the reservoir and seal rocks, directly after the CO₂ injection phase. The long-term modelling of the Sleipner storage site (Czernichowski-Lauriol et al., 2006) did not show possible leakage from the CO₂ storage reservoir through the cap rock. The batch- and reaction-diffusion simulations of the impact of CO₂ on the clayey cap rock at the North Sea Sleipner injection site performed by Gaus et al. (2005) showed that the effective diffusion coefficients are likely so low that the diffusion of CO₂ will only affect a few metres of the cap rock after thousands of years. Moreover, as CO₂ diffuses into the cap rock, silica, as well as other constituents, is released from the CO₂-cap rock interactions, leading to the precipitation of chalcedony, kaolinite and calcite, which may further reduce the diffusion into the cap rock. Bildstein et al. (2010) conducted a series of numerical simulations of cap rock responses to CO₂ injection using various reactive transport modelling codes. Both 1D and 2D single-phase flow scenarios in saturated porous media with or without fracture, and 1D multi-phase flow in unsaturated media without fracture, were modelled. Significant porosity changes were observed in the models for a period of 10 000 years, which were expected due to the high reactivity of the carbonate-rich cap rock with the acidic CO₂-rich fluid. However, the reactions were shown to be limited to the first decimetres to metres into the cap rock from the CO₂-cap rock interface in 10 000 years, and no leakage was reported. Their preliminary results on rock heterogeneity suggested, as indicated in experimental works (Angeli et al., 2009), that the reactivation of small cracks or fractures (especially those originally filled with calcite) could generate preferential pathways for CO₂ propagation in the cap rock.

It means that CGS in the areas with a high content of carbonate cementation of the reservoir rock will not cause a significant dissolution of cement in the

long term, which decreases the level of leakage risks. However, this statement is very site-specific and must be confirmed by fluid-flow modelling in every particular storage site.

The grain and bulk dry density and P-wave velocity measured in this research were mainly in the limits corresponding to the earlier reported data for the middle part of the Baltic Cambrian Basin, while the maximum values of P-wave velocity, measured before the experiment for carbonate-cemented sandstones from the South Kandava structure (5400–4556 m/s), were similar to those reported earlier for carbonate-cemented sandstones from the northern shallow part of the basin. A decrease in P-wave and S-wave velocity, measured in dry samples after the alteration experiment, was determined in most of the reservoir sandstones. This is explained by the increase in porosity and/or decrease in grain and bulk density (Fig. 10; PAPER V). The lowest acoustic velocity measured before alteration was in the range of the lowest values reported earlier (Shogenova et al., 2001a, 2001b), while after the experiment the P-wave velocity of sample E7-6 became the lowest among the earlier reported and recently measured velocities (Table 6). The grain density, measured before the alteration experiment for 12 sandstone samples, was in the limits of 2664–2746 kg/m³, decreasing after the experiment to 2635–2676 kg/m³ (Table 6; PAPER V).

The studied samples from the offshore reservoirs E6 and E7 are typical rocks of the Deimena Formation in the middle part of the Baltic Basin. Thereby, petrophysical alterations described in this study are an important piece of puzzle, when CGS will be modelled in the basin scale.

According to the measured and presented data (PAPER I, PAPER II) and the new presented classification (PAPER V), the Dobeles, South Kandava, E6 and E7 structures were re-estimated keeping in view the CGS in the Cambrian Deimena Formation in the Baltic Basin. The reservoir sandstones of the Deimena Formation in the Dobeles onshore structure were of ‘high-2’ average reservoir quality, assessed as ‘very appropriate’ for CGS (average porosity 19% and permeability 360 mD). The sandstones of the Deimena Formation in the South Kandava structure had an average porosity of 21%, identical to the porosity of rocks in the E6 structure, but two times higher average permeability, 300 mD (150 mD in E6). The estimated good reservoir quality of the sandstones in these structures was assessed as ‘appropriate’ for CGS. The reservoir quality of the sandstones of the E7 offshore structure estimated as ‘cautionary-2’ (average porosity 12% and permeability 40 mD), was the lowest in the studied structures and was assessed as ‘cautionary’ for CGS.

4.6 Numerical seismic models

Analysis of the changes in the seismic response of the reservoir structure with different CO₂ saturation levels clearly revealed small quantities of CO₂ within the host formation in the E6 structure in seismic models. This phenomenon is due to the change in seismic velocities, and consequently arrival

times, and reflection amplitudes with increasing CO₂ content already from 1% gas saturation. Therefore, the seismic monitoring of CO₂ injection within the considered E6 offshore structure is effective already from the very first steps of injection. Thus, the present research confirmed the results of previous studies, which suggest that accumulations of CO₂ as small as 500 tonnes may be detectable under favourable conditions (Chadwick et al., 2006). Pawar et al. (2006) presented results from the West Pearl Queen pilot CO₂ injection project in southeastern New Mexico, which suggest that surface 3D seismic can detect 2090 tonnes of CO₂ at a depth of 1372 m. But at the same time, the results showed that the response of the West Pearl Queen reservoir during the field experiment was significantly different from the predicted response based on the pre-injection data. According to Pawar et al. (2006) the latest numerical modelling algorithms do not capture the geochemical interactions, which are important elements in CGS modelling. In this PhD research for the first time the petrophysical alteration effect induced by CO₂ was incorporated into the numerical seismic modelling methodology (PAPER VI). Petrophysical properties of the host rocks measured before and after the alteration experiment were applied in modelling. This ‘alteration approach’ indicated the importance of implementing this effect in such a modelling routine for CGS monitoring and filled the gap in previous seismic models (Pawar et al., 2006).

Thus, in the last part of the thesis, the alteration of petrophysical properties of reservoir rocks from the E6 offshore structure, induced by CO₂–fluid–rock geochemical and mineralogical interactions during modelled CO₂ storage (PAPER IV; PAPER V), were considered (Scenario-2 and Scenario-4; Fig. 14). Nevertheless, for simplicity, the results of the laboratory alteration experiment were implemented equally for all CO₂ saturation seismic sections.

The interfaces defining the three units forming the reservoir in the Cambrian Deimena Formation and limestone oil reservoir in the Upper Ordovician Saldus Formation (Fig. 5a; PAPER VI) were impossible to distinguish on the baseline plane-wave seismic section due to relatively low frequency of the seismic source (35 Hz) considered, resulting in a single reflection.

The ‘Difference’ and NRMS sections of the layers overlying the reservoir rocks showed a zero amplitude for two-way travel times (TWT), which were lower than for the top of the reservoir reflection layer. In fact, the reflectors in this upper region of the seismogram were not influenced by the presence of CO₂, which changed the seismic characteristics of the lower reflectors, identifying the top of the reservoir and the reflectors below (longer TWT). This can be seen, e.g., in Figure 14-sc1-b and Figure 14-sc1-c (PAPER VI).

The decrease in P-wave velocity due to the injected CO₂ caused the velocity push-down recognizable in all the synthetic seismic sections for all provided scenarios below the reservoir. This phenomenon is well known and already documented in Arts et al. (2000), among others.

Previously published papers, based on theoretical (Domenico, 1977; Jain, 1987; Rossi et al., 2008; Picotti et al., 2012; Vera, 2012) and field experimental (Arts et al., 2003, 2004a, 2004b; Carcione et al., 2006; Chadwick et al., 2006)

studies, reported a significant drop in the P-wave velocity values of sandy reservoir rocks between 0 and 20% CO₂ saturation and a slow increase after 30% CO₂ saturation. Laboratory studies of unconsolidated sands by Domenico (1974, 1976) show that the presence of gas reduces V_{Pwet} by as much as 30%, while V_{Swet} has increased marginally (Jain, 1987). Vera (2012) reported only 7% as a maximum change in V_{Pwet} . In this part of the PhD study a 10–11% reduction in V_{Pwet} within 0–1% CO₂ saturation and a 20–22% decrease in V_{Pwet} after 5% CO₂ saturation were estimated (Tables 2, 3; Table 3 in PAPER VI). The V_{Swet} value did not increase significantly compared to V_{Pwet} (0.2–3%).

The trend of the acoustic impedance, i.e. the product of bulk density and P-wave velocity, was strongly dominated by velocity. It showed an elbow point approximately where V_{Pwet} stopped to decrease and a constant gentle decrease for increasing saturations (Fig. 4 in PAPER VI).

The reflectors, affected by the presence of CO₂, rapidly changed their characteristics (i.e. amplitude and frequency content) at the beginning of the injection phase, approximately up to 5% of gas saturation. For increasing CO₂ saturation the influence of gas on the reflected signals faded down. This phenomenon was explained by the relatively stable V_{Pwet} values in the reservoir rocks after fluid saturation of approximately 5% (Fig. 4; Table 3 in PAPER VI).

The time-lapse ‘Difference’ and NRMS section techniques supported the visualization of changes on the seismic datasets and allowed monitoring of possible CO₂ plume evolution within the studied storage site. The comparison of synthetic seismic sections of two corresponding scenarios (Scenario-1 and Scenario-2, and Scenario-3 and Scenario-4) clearly showed the expected difference in signals for all CO₂ saturation levels (Fig. 6a in PAPER VI), proving the effectiveness of the implementation of the petrophysical alteration effect. According to these results, the application of the presented methodology could be suggested to model the monitoring of CGS within the considered E6 structure or extrapolation to storage sites with similar stratigraphy, lithology, and geochemical and petrophysical properties of rocks in the Baltic sedimentary basin, as well as in other geological basins.

5. CONCLUSIONS

1. Four geological structures located onshore Latvia (South Kandava and Dobele) and in the Baltic Sea (E6 in Latvia and E7 in Lithuania), composed of the reservoir sandstones of the Cambrian Deimena Formation and overlain by an impermeable primary seal (Lower Ordovician Zebre Formation), were studied in detail using a multidisciplinary approach. The reservoir rocks are also covered by secondary cap rock represented by Ordovician and Silurian clayey carbonate sediments. The reservoir rocks in the studied structures were estimated as prospective for gas storage.
2. Based on the recently and earlier measured gas permeability and porosity, a classification of the reservoir quality for CO₂ geological storage was proposed for sandstones of the Deimena Formation of Cambrian Series 3 in the middle part of the Baltic Basin. According to their practical application to CGS, the rocks were divided into four groups by permeability (very appropriate, appropriate, cautionary and not appropriate) and eight reservoir quality classes were distinguished within the groups by porosity ('high-1' and 'high-2', 'good' and 'moderate', 'cautionary-1' and 'cautionary-2', 'low' and 'very low'). The proposed classification of the reservoir quality of sandstones helped to estimate the significance of their petrophysical changes caused by geochemical processes during the CO₂ injection-like alteration experiment.
3. The reservoir sandstones of the Deimena Formation in the Dobele onshore structure was characterized by 'high-2' estimated average reservoir quality, assessed as 'very appropriate' for CGS (average porosity 19% and permeability 360 mD). The reservoir sandstones in the South Kandava and E6 structures had an identical average porosity of 21%, but their average permeability differed twofold, being 300 and 150 mD, respectively. The good reservoir quality of sandstones in these structures was assessed as 'appropriate' for CGS. The reservoir quality of the sandstones of the E7 offshore structure, estimated as 'cautionary-2' (average porosity 12% and permeability 40 mD), was the lowest in the studied structures and was assessed as 'cautionary' for CGS.
4. The CO₂ storage capacities of the structures were estimated with different levels of reliability. The average capacities estimated by the optimistic approach in the onshore Dobele, South Kandava and offshore E6 and E7 structures were 106, 95, 377 and 34 Mt, respectively, by conservative approach 21, 25, 157 and 7 Mt, respectively.
5. Two compartments of the E6 structure split by faults were considered as separate substructures defined as E6-A and E6-B. Based on the optimistic approach, the CO₂ storage capacity of the E6-A part was 243–582 Mt (mean 365 Mt) and of the E6-B part 8–20 Mt (mean 12 Mt). The conservative capacity of E6-A was 97–233 Mt (mean 146 Mt) and of E6-B 4–10 Mt (mean 6 Mt).

6. The optimistic maximum and average storage potentials of the E6 structure (602 and 377 Mt) and its larger compartment E6-A (582 and 365 Mt) are higher and nearly the same as the previously reported total potential of all 16 onshore Latvian structures (400 Mt). Even the average conservative capacities of E6 (152 Mt) and E6-A (146 Mt) are the largest among all Latvian onshore and offshore structures studied until now.
7. The E6 structure offshore Latvia was estimated as the most prospective for CGS in the Baltic Cambrian Basin according to the reservoir thickness, area, quality and storage capacity. However, the risk of CO₂ leakage due to uncertainties of the fault system should be considered and further fault integrity risk assessment work is required.
8. The E7 offshore structure was estimated as ‘cautionary’ for CGS due to the relatively low average porosity and permeability of the reservoir sandstone, storage capacity and location at the Latvian–Lithuanian border. Storage in this structure could be considered as transboundary and will need regional agreements for CGS.
9. For the first time 4D time-lapse numerical seismic modelling based on rock physics studies was applied to monitor possible CO₂ storage in the largest geological structure E6 offshore Latvia in the Baltic Sea.
10. The novelty of the applied seismic numerical modelling approach was the coupling of the chemically induced petrophysical alteration effect of CO₂ hosting rocks measured in laboratory with time-lapse numerical seismic modelling.
11. Alteration of the petrophysical properties of the reservoir had a strong influence on the reflected signals in the seismic sections, showing the highest difference on seismic sections with 1% CO₂ saturation, increasing the detectability of the stored CO₂. The difference decreased with increase in CO₂ content. Up to 5% CO₂ saturation could be qualitatively estimated from the synthetic seismic data. For CO₂ saturation higher than 5% qualitative estimations of the saturation level are uncertain.
12. The obtained results of the alteration experiment indicate some possible physical processes that may occur during CGS in the studied onshore and offshore structures. These results, implemented in the seismic modelling in this research, and as the first of this type in the central part of the Baltic Basin, have also importance for the southern and western parts of the Baltic sedimentary basin, which have CO₂ storage capacity in the Cambrian aquifer (Lithuania, Sweden, Kaliningrad Region and offshore Poland). However, they should be supported by additional laboratory experiments and fluid-flow modelling of the CO₂ storage in the Cambrian sandstones both in structures and basin-scale for better assessment of the possible storage scenarios and their safety.

ACKNOWLEDGEMENTS

First of all, I would like to thank my mother and the main supervisor Dr Alla Shogenova, who was an initiator of this ambitious multidisciplinary project, for organizing different activities related to this study, for her support in all phases of the research, fast response in all cases, for review and input into the published articles as well as the present thesis.

I am indebted to my co-supervisor, the director of the petrophysical laboratory at IFP Energies nouvelles (IFPEN, French Petroleum Institute, Paris) Dr Olga Vizika-Kavvadias for all the arrangements at the experimental stage of the project. My sincere thanks are addressed to Jean Guelard (IFPEN) for permeability measurements and other guidance in petrophysical laboratory, Jean-François Nauroy (IFPEN) for acoustic velocity measurements and help with the preparation of PAPER IV and PAPER V, and the leaders of IFPEN for providing the experimental facilities, necessary for the study.

I appreciate the assistance of my colleagues Dr Olle Hints and Margus Voolma (IG TUT) with SEM adjustment and Dr Juri Ivask and Dr Anne-Liis Kleesment (IG TUT) for the help with English-Estonian translation.

This thesis would not have been completed without effective and rapid supervision of co-supervisor Davide Gei, senior researcher at National Institute of Oceanography and Experimental Geophysics (OGS, Trieste, Italy), in the last phase of study, related to seismic numerical modelling (PAPER III, PAPER VI). My special thanks go to Dr Geza Seriani for all arrangements during my stay at OGS that made the final step of my PhD research absolutely efficient. I am grateful to Edy Forlin (OGS) for his help and sharing with experience in 3D geological static modelling.

I am also grateful to the LEGMC for providing rock samples, exploration reports and structural maps, and to all the financial support sources without which this study would not have been possible: Estonian targeted funding programme (project SF0320080s07 and IUT19-22) of the Estonian Ministry of Education and Research, Archimedes Foundation programme DoRa, Estonian Doctoral School of Earth Sciences and Ecology, EU FP7 project CGS EUROPE, EU FP7 Programme, Marie Curie Research Training Network 'Quantitative Estimation of Earth's Seismic Sources and Structure' (QUEST), Contract No. 238007 and project 'ERMAS' of the Estonian national R&D Programme KESTA.

REFERENCES

- Alnes, H., Eiken, O., Nooner, S., Sasagawa, G., Stenvold, T. & Zumberge, M. 2011. Results from Sleipner gravity monitoring: Updated density and temperature distribution of the CO₂ plume. *Energy Procedia* 4, 5504–5511.
- API (American Petroleum Institute) 1998. Recommended practices for core analysis. Second Edition, Recommended Practice, 40, Exploration and Production Department.
- Angeli, M., Soldal, M., Skurtveit, E. & Aker, E. 2009. Experimental percolation of supercritical CO₂ through a caprock, *Energy Procedia*, 1, 3351–3358.
- Armitage, P. J., Faulkner, D. R., Worden, R. H., Aplin, A. C., Butcher, A. R. & Iliffe, J., 2011. Experimental measurement of, and controls on, permeability and permeability anisotropy of cap rocks from the CO₂ storage project at the Krechba Field, Algeria, *J. Geophys. Res.*, 116, B12208, doi:10.1029/2011JB008385.
- Arts, R., Eiken, O., Chadwick, R.A., Zweigel, P., van der Meer, L. & Zinszner, B. 2004a. Monitoring of CO₂ injected at Sleipner using time-lapse seismic data. *Energy*, Elsevier Science Ltd, Oxford, 29, 1383–1392.
- Arts, R., Eiken, O., Chadwick, R.A., Zweigel, P., Van der Meer, L. & Kirby, G.A. 2004b. Seismic monitoring at the Sleipner underground CO₂ storage site (North Sea). In: Baines, S. & Worden, R.J. (eds). *Geological Storage for CO₂ Emissions Reduction*. Geological Society, London, Special Publications, 233, 181–191.
- Arts, R., Eiken, O., Chadwick, R.A. Zweigel, P., Van der Meer, L. & Zinszner, B. 2003. Monitoring of CO₂ injected at Sleipner using time lapse seismic data. In: Gale, J. & Kaya, Y. (eds). *Greenhouse Gas Control Technologies*, Elsevier, Oxford, 347–352.
- Arts, R., Brevik, I., Eiken, O., Sollie, R., Causse, E. & van der Meer, B. 2000. Geophysical methods for monitoring marine aquifer CO₂ storage - Sleipner experiences. In: Williams, D., Durie, B., McMullan, P., Paulson, C., Smith, A. (eds.). *Proceeding of the 5th International Conference on Greenhouse Control Technologies*, Cairns, 366–371.
- Arts, R., Chadwick, A., Eiken, O., Thibeau, S. & Nooner, S. 2008. Ten years of experience of monitoring CO₂ injection in the Utsira Sand at Sleipner, offshore Norway. *First break*, 26, 65–72.
- Bachu, S. 2003. Screening and ranking sedimentary basins for sequestration of CO₂ in geological media in response to climate change. *Environmental Geology*, 44, 277–289.
- Bachu, S., Bonijoly, D., Bradshaw, J., Burruss, R., Holloway, S., Christensen, N.P. & Mathiassen, O.M. 2007. CO₂ storage capacity estimation: Methodology and gaps. *International Journal of Greenhouse Gas Control*, 1(4), 430–443.

- Bemer, E. & Lombard, J. M. 2010. From injectivity to integrity studies of CO₂ geological storage. *Oil & Gas Science and Technology - Rev. IFP*, 65(3), 445–459.
- Bemer, E., Nguyen, M. T. & Dormieux, L. 2011. Experimental poromechanics applied to CO₂ geological storage. *Proceedings of the Symposium on Mechanics and Physics of Porous Solids, Champs-sur-Marne, France, 18-20 April 2011*.
- Bentham, M. S., Green, A. & Grammer, D. 2013. The occurrence of faults in the Bunter Sandstone Formation of the UK sector of the Southern North Sea and the potential impact on storage capacity. *Energy Procedia*, 37, 5101–5109.
- Bertier, P., Swennen, R., Laenen, B., Lagrou, D. & Dreesen, R. 2006. Experimental identification of CO₂-water-rock interactions caused by sequestration of CO₂ in Westphalian and Buntsandstein sandstones of the Campine Basin (NE-Belgium). *Journal of geochemical exploration*, 89(1), 10–14.
- Bickle, M., Chadwick, A., Huppert, H.E., Hallworth, M. & Lyle, S. 2007. Modelling carbon dioxide accumulation at Sleipner: Implications for underground carbon storage. *Earth and Planetary Science Letters*, 255, 164–176.
- Bigi, S., Conti, A., Casero, P., Ruggiero, L., Recanati, R., Lipparini, L. 2013. Geological model of the central Periadriatic basin (Apennines, Italy). *Marine and Petroleum Geology*, 42, 107–121.
- Bildstein, O., Kervévan, C., Lagneau, V., Delaplace, P., Crédoz, A., Audigane, P., Per-fetti, E., Jacquemet, N. & Jullien, M. 2010. Integrative modeling of caprock integrity in the context of CO₂ storage: evolution of transport and geochemical properties and impact on performance and safety assessment. *Oil & Gas Science and Technology. – Rev. IFP*, 65, 485–502.
- Brun, J. P., Guennoc, P., Truffert, C. & Vairon, J. 2001. Cadomian tectonics in northern Brittany: a contribution of 3-D crustal-scale modelling. *Tectonophysics*, 331, 229–246.
- Carcione, J. M. 2007. Wave fields in real media: wave propagation in anisotropic, anelastic, porous and electromagnetic media. 2nd edition, revised and extended. *Handbook of Geophysical Exploration*, Elsevier, Amsterdam, 38.
- Carcione, J.M., Picotti, S., Gei, D. & Rossi, G. 2006. Physics and seismic modeling for monitoring CO₂ storage. *Pure and applied geophysics*, 163, 175–207.
- Carroll, S. A., McNab, W. W., Dai, Z. & Torres, S. C. 2013. Reactivity of Mt. Simon sandstone and the Eau Claire shale under CO₂ storage conditions. *Environmental Science and Technology*, 47(1), 252–261.
- Carroll, S. A., McNab, W. W. & Torres, S. C. 2011. Experimental study of cement – sandstone/shale – brine – CO₂ interactions. *Geochemical Transactions*, 12(9), doi:10.1186/1467-4866-12-9.

- Chadwick, A., Noy, D., Arts, R. J. & Eiken, O. 2009. Latest time-lapse seismic data from Sleipner yield new insights into CO₂ plume development. *Energy Procedia* 1, 2103–2110.
- Chadwick, A., Arts, R., Bernstone, C., May, F., Thibeau, S. & Zweigel, P. 2006. Best practice for the storage of CO₂ in saline aquifers. Keyworth, Nottingham, British Geological Survey Occasional Publication, 14, 277 pp.
- Chang, K. W., Minkoff, S. & Bryant, S. 2008. Modeling leakage through faults of CO₂ stored in an aquifer. SPE Annual Technical Conference and Exhibition, Denver, Colorado, USA.
- Courrioux, G., Nullans, S., Guillen, A. & Boissonnat, J. D. 2001. 3D volumetric modelling of Cadomian terranes (Northern Brittany, France): an automatic method using Voronoi diagrams. *Tectonophysics*, 331, 181–196.
- Czernichowski-Lauriol, I., Rochelle, C., Gaus, I., Azaroual, M., Pearce, J. & Durst, P. 2006. Geochemical interactions between CO₂, pore-waters and reservoir rocks: lessons learned from laboratory experiments, field studies and computer simulations. In: Lombardi, S., Altunina, S.E., Beaubien, S.E. (Eds.), *Advances in the geological storage of carbon dioxide: international approaches to reduce anthropogenic greenhouse gas emissions*. Springer, Dordrecht, Netherlands, 157–174.
- Čyžienė, J., Molenaar, N. & Šliaupa, S. 2006. Clay-induced pressure solution as a Si source for quartz cement in sandstones of the Cambrian Deimena Group. *Geologija*, 53, 8–21.
- Deutsch, C.V. & Journel, A.G. 1998. *GSLIB. Geostatistical Software Library and Users Guide*, 2nd. Oxford, New York: Oxford University Press.
- Domenico, S. N. 1977. Elastic properties of unconsolidated porous sand reservoirs. *Geophysics*, 42, 1339–1368.
- Domenico, S. N. 1976. Effect of brine-gas mixture on velocity in an unconsolidated sand reservoir. *Geophysics*, 41, 882–894.
- Domenico, S. N. 1974. Effect of water saturation on seismic reflectivity of sand reservoirs encased in shale. *Geophysics*, 39, 759–769.
- Egermann, P., Bemmer, E. & Zinszner, B. 2006. An experimental investigation of the rock properties evolution associated to different levels of CO₂ injection like alteration processes. In: *Proceedings of the International Symposium of the Society of Core Analysts*, paper SCA 2006-34, September 12-16, 2006, Trondheim, Norway.
- Fornel, A. & Estublier, A. 2013. To a dynamic update of the Sleipner CO₂ storage geological model using 4D seismic data. *Energy Procedia*, Elsevier, 37, 4902–4909, doi:10.1016/j.egypro.2013.06.401.
- Freimanis, A., Margulis, L.S., Brangulis, A., Kanev, S. & Pomerantseva, R. 1993. Geology and hydrocarbon prospects of Latvia. *OGJ*, 91(49), 71–74.
- Gaus, I., Azaroual, M. & Czernichowski-Lauriol, I. 2005. Reactive transport modeling of the impact of CO₂ injection on the clayey cap rock at Sleipner (North Sea), *Chemical Geology*, 217(3–4), 319–337.
- Gilfillan, S. M. V., Lollar, B. S., Holland, G., Blagburn, D., Stevens, S., Schoell, M., Cassidy, M., Ding, Z., Zhou, Z., Lacrampe-Couloume, G. &

- Ballentine, C. J. 2009. Solubility trapping in formation water as dominant CO₂ sink in natural gas fields. *Nature*, 458(7238), 614–618.
- Gorbatshev, R. & Bogdanova, S. 1993. Frontiers in the Baltic References Shield. *Precambrian Research*, 64, 3–21.
- Grigelis, A. 2011. Research of the bedrock geology of the Central Baltic Sea. *Baltica*, 24(1), 1–12.
- Grigg, R. B. & Svec, R. K. 2003. Co-injected CO₂-brine interactions with Indiana Limestone. In: Society of Core Analysts Symposium, paper SCA 2003-19, September 21-24, 2003, Pau, France.
- Halland, E. K., Johansen, W. T. & Riss, F., eds. 2013. CO₂ storage atlas, Norwegian Sea. The Norwegian Petroleum Directorate, 60 pp, <http://www.npd.no>.
- Halland, E. K., Johansen, W. T. & Riss, F., eds. 2011. CO₂ storage atlas, Norwegian North Sea. The Norwegian Petroleum Directorate, 72 pp, <http://www.npd.no>.
- Hermanrud, C., Andresen, T., Eiken, O., Hansen, H., Janbu, A., Lippard, J., Bolås, H.N. et al., 2009. Storage of CO₂ in saline aquifers – Lessons learned from 10 years of injection into the Utsira Formation in the Sleipner area. *Energy Procedia* 1, 1997–2004.
- Holloway, S. 2002. Underground sequestration of carbon dioxide - a viable greenhouse gas mitigation option. Proceedings of the 5th International Symposium on CO₂ Fixation and Efficient Utilization of Energy and the 4th International World Energy System Conference, Tokyo Institute of Technology, Tokyo, Japan, 4-6 March 2002, 373–380.
- Huppert, H. E. & Woods, A. W. 1995. Gravity flows in porous layers. *Journal of Fluid Mechanics*, 292, 55–69.
- IPCC (Intergovernmental Panel on Climate Change) 2005. IPCC Special Report on Carbon Dioxide Capture and Storage. Prepared by Working Group III of the Intergovernmental Panel on Climate Change [Metz, B., Davidson, O., de Coninck, H.C., Loos, M. & Meyer, L. A. (eds.)]. Cambridge University Press, Cambridge, United Kingdom and New York, NY, USA.
- IPCC 2014. IPCC Special Report. Climate change: Mitigation of climate change. Prepared by Working Group III Contribution of the Intergovernmental Panel on Climate Change to AR5.
- IEA (International Energy Agency) 2004. Prospects for CO₂ Capture and Storage. IEA/OECD, Paris, France.
- IEA (International Energy Agency) 2013. CO₂ Emissions from Fuel Combustion. Highlights. IEA/OECD, Paris, France.
- Izgec, O., Demiral, B., Bertin, H. & Akin, S. 2008. CO₂ injection into saline carbonate aquifer formations. Laboratory investigation. *Transport in Porous Media*, 72, 1–24.
- Jain, S. 1987. Amplitude-vs-offset analysis: a review with references to application in western Canada. *Canadian Society of Exploration Geophysicists Journal*, 23, 27–36.

- Kaszuba, J. P. & Janecky, D. R. 2009. Geochemical impacts of sequestering carbon dioxide in brine formations. In: Sundquist, E. & McPherson, B. Carbon Sequestration and its role in the global carbon cycle. Geophysical Monograph, 183(7).
- Kilda, L. & Friis, H. 2002. The key factors controlling reservoir quality of the Middle Cambrian Deimena Group sandstone in West Lithuania. Bulletin of the Geological Society of Denmark, 49(1), 25–39.
- Kleesment, A., Shogenova, A. 2005. Lithology and evolution of Devonian carbonate and carbonate-cemented rocks in Estonia. Proc. Estonian Acad. Sci. Geol., 54(3), 153–180.
- Krumbein, W. C. 1934. Size frequency distributions of sediments. Journal of Sedimentary Petrology, 4, 65–77.
- Ledru P. 2001. The Cadomian crust of Brittany (France): 3D imagery from multisource data (Géofrance 3D). Tectonophysics, 331, 300–320.
- LEGMC, 2007. Geological structures for the establishment of underground gas storages. Geological description for the information material ‘On the possibilities of use of the Latvian geological structures’. Riga, Latvia, 16 pp.
- Liu, F., Lu, P., Zhu, C. & Xiao, Y. 2011. Coupled reactive flow and transport modelling of CO₂ sequestration in the Mt. Simon sandstone formation. Midwest U.S.A. International Journal of Greenhouse Gas Control, 5(2), 294–307.
- Liu, F., Lu, P., Griffith, C., Hedges, S. W., Soong, Y., Hellevang, H. & Zhu, C. 2012. CO₂-brine-caprock interaction: Reactivity experiments on Eau Claire shale and a review of relevant literature. International Journal of Greenhouse Gas Control, 7, 153–167.
- Lyle, S., Huppert, H.E., Hallworth, M., Bickle, M. & Chadwick, A. 2005. Axisymmetric gravity currents in a porous medium. Journal of Fluid Mechanics, 543, 293–302.
- Metz, B., O. Davidson, H. C. de Coninck, M. Loos, and L. A. Meyer, (eds) 2005. IPCC Special Rep. Carbon Dioxide Capture and Storage. Prepared by Working Group III of the Intergovernmental Panel on Climate Change, Cambridge University Press, Cambridge, United Kingdom and New York, NY, USA.
- National Research Council 2010. Ocean Acidification: A National Strategy to Meet the Challenges of a Changing Ocean. Washington, DC. The National Academies Press.
- Nguyen, P., Fadaei, H. & Sinton, D. 2013. Microfluidics underground: A micro-core method for pore scale analysis of supercritical CO₂ reactive transport in saline aquifers. Journal of Fluids Engineering, 135(2), 1–7, doi:10.1115/1.4023644.
- Olivier, J.G.J., Janssens-Maenhout, G., Muntean, M. Peters, J.H.A.W. 2014. Trends in global CO₂ emissions - 2014 report, JRC report 93171 / PBL report 1490.

- Pawar, R. J., Warpinski, N. R., Lorenz, J. C., Benson, R. D., Grigg, R. B., Stubbs, B. A., Stauffer, P. H., Krumhansl, J. P. & Cooper, S. P. 2006. Overview of a CO₂ sequestration field test in the West Pearl Queen reservoir, New Mexico. The American Association of Petroleum Geologists/Division of Environmental Geosciences. *Environmental Geosciences*, 13(3), 163–180.
- Peng, S., Babcock, L. E. & Cooper, R. A. 2012. Chapter 19. The Cambrian Period. In: Gradstein, F., Ogg, J., Schmitz, M. & Ogg, G. (eds) *The Geologic Time Scale 2012*. Elsevier.
- Picotti, S., Carcione, J. M., Gei, D., Rossi, G. & Santos, J. E. 2012. Seismic modeling to monitor CO₂ geological storage: The Atzbach-Schwanenstadt gas field. *Journal of Geophysical Research*, B06103, 117(6), doi:10.1029/2011JB008540.
- Poprawa, P., Šliaupa, S., Stephenson, R., & Lazauskiene, J. 1999. Late Vendian-Early Palaeozoic tectonic evolution of the Baltic basin: regional tectonic implications from subsidence analysis. *Tectonophysics*, 314, 218–239.
- Rochelle, C. A., Czernichowski-Lauriol, I. & Milodowski, A. E. 2004. The impact of chemical reactions on CO₂ storage in geological formations: a brief review. *Geological Society, London, Special Publications*, 233, 87–106.
- Ross, G. D., Todd, A. C., Tweedie, J. A. & Will, A. G. 1982. The dissolution effects of CO₂-brine systems on the permeability of U.K. and North Sea calcareous sandstones. In: DOE Symposium on Enhanced Oil Recovery, paper SPE 10685, April 4-7, 1982, Society of Petroleum Engineers, Tulsa, OK, <http://dx.doi.org/10.2118/10685-MS>.
- Rossi, G., Gei, D., Picotti, S. & Carcione, J. M. 2008. CO₂ storage at the Atzbach-Schwanenstadt gas field: a seismic monitoring feasibility study. *First Break*, 26, 45–51.
- Salvi, F., Spalla, M. I., Zucali, M. & Gosso, G. 2010. Three-dimensional evaluation of fabric evolution and metamorphic reaction progress in polycyclic and polymetamorphic terrains: a case from the Central Italian Alps. *Geological Society Special Publication*, 332, 173–187.
- Schön, J. H. 1996. *Physical properties of rocks: fundamentals and principles of petrophysics*. Oxford, OX, UK: Pergamon.
- Schumacher, A. M. 2013. Modeling of CO₂-water-rock interactions in a Mississippian sandstone reservoir of Kentucky. Master theses and Dissertations-Earth and Environmental Sciences. Paper 11, http://uknowledge.uky.edu/ees_etds/1.
- Shogenova, A., Piessens, K., Holloway, S., Bentham, M., Martínez, R., Flornes, K.M., Poulsen, N.E., Wójcicki, A., Šliaupa, S., Kucharič, L., Dudu, A., Persoglia, S., Hladik, V., Saftic, B., Kvassnes, A., Shogenov, K., Ivask, J., Suárez, I., Sava, C., Sorin, A., Chikkatur, A. 2014. Implementation of the EU CCS Directive in Europe: results and development in 2013. *Energy Procedia*, 63, 6662–6670.

- Shogenova, A., Piessens, K., Ivask, J., Shogenov, K., Martínez, R., Suárez, I., Flornes, K. M., Poulsen, N. E., Wójcicki, A., Sliupa, S., Kucharic, L., Dudu, A., Persoglia, S., Holloway, S. & Saftic, B. 2013. CCS Directive transposition into national laws in Europe: progress and problems by the end of 2011, Elsevier. *Energy Procedia*, 37, 7723–7731.
- Shogenova, A., Shogenov, K., Vaher, R., Ivask, J., Sliupa, S., Vangkilde-Pedersen, T., Uibu, M. & Kuusik, R. 2011a. CO₂ geological storage capacity analysis in Estonia and neighboring regions. *Energy Procedia*, 4, 2785–2792.
- Shogenova, A., Shogenov, K., Pomeranceva, R., Nulle, I., Neele, F. & Hendriks, C. 2011b. Economic modelling of the capture–transport–sink scenario of industrial CO₂ emissions: the Estonian–Latvian cross-border case study. Elsevier, The Netherlands. *Energy Procedia*, 4, 2385–2392.
- Shogenova, A., Kleesment, A., Shogenov, K., Põldvere, A. & Jõelet, A. 2010. Composition and properties of Estonian Palaeozoic and Ediacaran sedimentary rocks. 72nd EAGE Conference & Exhibition incorporating SPE EUROPEC 2010, 14–17 June 2010, Barcelona. EAGE, The Netherlands, 1–5.
- Shogenova, A., Sliupa, S., Vaher, R., Shogenov, K. & Pomeranceva, R. 2009a. The Baltic Basin: structure, properties of reservoir rocks and capacity for geological storage of CO₂. *Estonian Journal of Earth Sciences*, 58(4), 259–267.
- Shogenova, A., Šliupa, S., Shogenov, K., Šliaupiene, R., Pomeranceva, R., Vaher, R., Uibu, M. & Kuusik, R. 2009b. Possibilities for geological storage and mineral trapping of industrial CO₂ emissions in the Baltic region. *Energy Procedia*, 1(1), 2753–2760.
- Shogenova, A., Kleesment, A. & Shogenov, K. 2005. Chemical composition and physical properties of the rock. In: Põldvere, A. (ed.). *Estonian Geological Sections. Bulletin 6. Mehikoorma (421) drill core*. Geological Survey of Estonia, Tallinn, 31–38.
- Shogenova, A., Kirsimäe, K., Bitjukova, L., Jõelet, A. & Mens, K. 2001a. Physical Properties and Composition of Cemented Siliciclastic Cambrian Rocks, Estonia. In: Fabricius, I.L. (ed.), *Research in Petroleum Technology*. Nordisk Energiforskning, Ås, Norway. 123–149.
- Shogenova, A., Šliupa, S., Rasteniene, V., Jõelet, A., Kirsimäe, K., Bitjukova, L., Lashkova, L., Zabele, A., Freimanis, Hoth, P. & Huenges, E. 2001b. Elastic properties of siliciclastic rocks from Baltic Cambrian basin. In: 63rd EAGE Conference and Technical Exhibition. Extended Abstracts, Volume 1, European Association of Geoscientists & Engineers, Amsterdam, The Netherlands. N-24, 1–4.
- Sikorska, M. & Paczesna, J. 1997. Quartz cementation in Cambrian sandstones and the background of their burial history of the East European Craton, *Geology Quarterly*, 41, 265–272.
- Sliupa, S., Rasteniene, V., Lashkova, L. & Shogenova, A. 2001. Factors controlling petrophysical properties of Cambrian siliciclastic deposits of

- central and western Lithuania. In: Fabricius, I.L. (Editor). *Nordic Petroleum Series: V. Research in Petroleum Technology*. Nordisk Energiforskning, Norway, 157–180.
- Sliaupa, S., Shogenova, A., Shogenov, K., Sliapiene, R., Zabele, A. & Vaher, R. 2008a. Industrial carbon dioxide emissions and potential geological sinks in the Baltic States. *Oil Shale*, 25(4), 465–484.
- Sliaupa, S., Cyziene, J., Molenaar, N. & Musteikyte, D. 2008b. Ferroan dolomite cement in Cambrian sandstones: burial history and hydrocarbon generation of the Baltic sedimentary basin, *Acta Geologica Polonica*, 58(1), 27–41.
- Sopher, D., Juhlin, C. & Erlström, M. 2014. A probabilistic assessment of the effective CO₂ storage capacity within a Swedish sector of the Baltic Basin. Elsevier. *International Journal of Greenhouse Gas Control*, 30, 148–170.
- Svec, R. K. & Grigg, R. B. 2001. Physical effects of WAG fluids on carbonate core plugs. In: *SPE Annual Technical Conference and Exhibition*, SPE 71496, New Orleans, LA.
- Sundberg, F. A., Zhao, Y. L., Yuan, J. L., Lin, J. P. 2011. Detailed trilobite biostratigraphy across the proposed GSSP for Stage 5 ('Middle Cambrian' boundary) at the Wuliu-Zengjiayan section, Guizhou, China. *Bulletin of Geosciences*, 423–464.
- Šliaupa, S., Lojka, R., Tasáryová, Z., Kolejka, V., Hladík, V., Kotulová, J., Kucharič, L., Fejdi, V., Wojcicki, A., Tarkowski, R., Uliasz-Misiak, B., Šliaupienė, R., Nulle, I., Pomeranceva, R., Ivanova, O., Shogenova, A. & Shogenov, K. 2013. CO₂ storage potential of sedimentary basins of Slovakia, The Czech Republic, Poland, and Baltic States. *Geological Quarterly*, 57(2), 219–232.
- Šteinerts, G. 2012. Maritime delimitation of Latvian waters, history and future prospects. *Journal of maritime transport and engineering*, 1(1), Latvian Maritime Academy, Latvia, Riga, 47–53.
- Tiab, D. & Donaldson, E. C. 2012. *Petrophysics. Theory and Practice of Measuring Reservoir Rock and Fluid Transport Properties* (3rd ed.). Oxford: Gulf Professional Pub..
- Tucker, M. E. 2001. *Sedimentary Petrology* (3rd ed.). Oxford: Blackwell Science.
- Van der Meer, L. G. H. 1993. The conditions limiting CO₂ storage in aquifers. *Energy Conversion and Management*, 34(9-11), 959–966.
- Van der Meer, B. & Egberts, P. 2008. A general method for calculating subsurface CO₂ storage capacity. *Offshore Technology Conference*, TA Utrecht, The Netherlands. OTC 19309, 1–9.
- Vangkilde-Pedersen, T. & Kirk, K. (eds). 2009. FP6 EU GeoCapacity Project, Assessing European Capacity for Geological Storage of Carbon Dioxide, Storage Capacity. D26, WP4 Report Capacity Standards and Site Selection Criteria. Geological Survey of Denmark and Greenland, 45 pp. .
- Vera, C. V. 2012. Seismic modelling of CO₂ in a sandstone aquifer. MSc Thesis, University of Calgary, <http://hdl.handle.net/1880/48934>.

- Vernon, R., O'Neil, N., Pasquali, R. & Nieminen, M. 2013. Screening of prospective sites for geological storage of CO₂ in the Southern Baltic Sea, VTT Technology 101, Espoo, Finland.
- US DOE (US Department of Energy) 2008. Methodology for development of geological storage estimates for carbon dioxide, 37 pp.
- USEPA (U.S. Environmental Protection Agency) 2013. Causes of climate change. Washington, D.C., U.S. Environmental Protection Agency Web site, accessed February 22, 2013, USGS CSRA Team (U.S. Geological Survey Geologic Carbon Dioxide Storage Resources Assessment Team) 2013.
- National assessment of geologic carbon dioxide storage resources. Results: U.S. Geological Survey Circular 1386, <http://pubs.usgs.gov/circ/1386/>.
- Zanchi, A., Francesca, S., Stefano, Z., Simone, S., Graziano, G. 2009. 3D reconstruction of complex geological bodies: examples from the Alps. *Computers and Geosciences*, 35 (1), 49–69.
- Zdanavičiute, O. & Sakalauskas, K. (eds). 2001. *Petroleum Geology of Lithuania and southeastern Baltic*. Vilnius, 204 pp.
- Zhang, Z. & Agarwal, R. 2014. Numerical simulation and optimization of Sleipner carbon sequestration project. *International Journal of Engineering & Technology*, 3(1), 1–13.
- Андрющенко, Ю., Вжосек, Р., Крочка, В., Хубльдигов, А. И., Лобанов, В., Новиков, Э. Л., Хафенштайн, К., Цимашевский, Л. и Лабусь, Р. 1985. Отчет о результатах бурения и геолого-геофизических исследований в поисковой скважине Е6-1/84. Неопубликованный отчет. Латвийский центр окружающей среды, геологии и метеорологии (LEGMC), Латвия, Рига.
- Бабуке, Б., Вжосек, Р., Найденов, В. Н., Крочка, В., Марков, П., Новиков, Э. Л., Цимашевский, Л. и Лабусь, Р. 1983. Геологическая отчетная документация скважины Е7-1/82. Неопубликованный отчет. Латвийский центр окружающей среды, геологии и метеорологии (LEGMC), Латвия, Рига.
- Дмитриев, Е. И., Фрейманис, А., Трацевский, Г. Д. и Павловский, А. А. 1973. Отчет о результатах бурения структурно-поисковых скважин 91 и 92 на Добельской структуре. Неопубликованный отчет. Латвийский центр окружающей среды, геологии и метеорологии (LEGMC), Латвия, Рига.
- Жданов, М. А. 1981. Основы промысловой геологии газа и нефти. 2-е изд., перераб. и доп., Москва: Недра, 453 с.
- Лашкова, Л. Н. 1979. Литология, фации и коллекторские свойства кембрийских отложений Южной Прибалтики. Москва: Недра, 102 с.
- Силантьев, В., Фрейманис, А., Михайловский, П., Павловский, А. и Карпитский, В. 1970. Геологическое строение и нефтеносность Южно-Кандавской структуры. Неопубликованный отчет. Латвийский центр окружающей среды, геологии и метеорологии (LEGMC), Латвия, Рига.

- Ханин, А. А. 1969. Породы-коллекторы нефти и газа и их изучение.
Москва: Недра, 368 с.
- Ханин, А. А. 1965. Основные учения о породах-коллекторах нефти и газа.
Москва: Недра, 362 с.

ABSTRACT

The aim of this PhD research was to compose petrophysical models of the CO₂ plume during possible CO₂ geological storage (CGS) in prospective deep subsurface structures in the Baltic sedimentary basin. The obtained results will support the implementation of CO₂ capture and geological storage (CCS) technology in the Baltic States as one of the effective measures to mitigate climate change.

The applied methodological approach for CGS modelling in the structure scale consisted of four stages: (1) storage site selection and data collection, (2) storage site characterization, (3) estimating the influence of CGS on rock properties, (4) numerical seismic modelling of CO₂ storage.

Four geological structures prospective for CGS in the Baltic Region, located onshore (South Kandava and Dobele) and offshore in Latvia (E6) and Lithuania (E7), were characterized using available data and new laboratory measurements of 24 samples of the reservoir and cap rocks from five boreholes. The reservoir sandstones of the Deimena Formation of the Cambrian Series 3 (earlier Middle Cambrian) are sealed in the studied structures by the Lower Ordovician clayey cap rocks of the Zebre Formation. Petrophysical properties, chemical and mineralogical composition and surface morphology of these rocks were interpreted together with the previously available data. Three-dimensional static models of the top of the reservoir sandstone of the Deimena Formation and cross sections of the reservoir and cap rocks for the four studied structures were constructed using geological, gamma-ray logging and laboratory data.

The CO₂ storage capacities of the four studied structures were estimated with different levels of reliability. The average capacities estimated by the optimistic approach in the onshore Dobele, South Kandava and offshore E6 and E7 structures were 106, 95, 377 and 34 Mt, respectively. The E6 structure was assessed as the most prospective for CGS in the Baltic Basin according to its reservoir quality, trap area and storage capacity. Its estimated optimistic CO₂ storage capacity was in the range 251–602 Mt (average 377 Mt) and was close to the earlier reported total potential of 16 onshore Latvian structures (400 Mt).

A new classification of the reservoir quality of rocks in terms of gas permeability and porosity was proposed for CGS in sandstones of the Deimena Formation based on data reported earlier and measured by the author. This classification was applied to estimate the quality of the reservoir rocks of the four studied structures. The quality of the reservoir sandstones ('high-2') was highest in the Dobele structure, and 'appropriate' for CGS in the South Kandava and E6 structures. The lowest quality, assessed as 'cautionary' for CGS, was recorded in the most compacted sandstones of the E7 structure.

Petrophysical, geochemical and mineralogical parameters of 12 sandstone samples from the South Kandava, E6 and E7 structures were measured and analysed before and after the CO₂ injection-like alteration experiment. The initial reservoir quality of the studied pure quartz sandstones from the offshore

structures was mainly preserved during the alteration experiment.

To analyse the feasibility of CO₂ storage monitoring in the largest E6 structure offshore Latvia, estimated as the most prospective for CGS, the 4D time-lapse numerical seismic modelling based on the rock physics studies was applied. Synthetic seismograms and seismic sections of the sandstone reservoir of the Deimena Formation homogeneously saturated with different concentrations of CO₂, computed for a CO₂ plume model, were compared with a baseline section within four scenarios (uniform and plume models without and with alteration effect) using 'Difference' and NRMS metrics. The novelty of the applied approach was the coupling of the chemically induced petrophysical alteration effect of CO₂ hosting rocks measured in the laboratory with time-lapse seismic numerical modelling. The alteration of the petrophysical properties of the reservoir had a strong influence on the reflected signals in the seismic sections. The highest difference was recorded in seismic sections with 1% CO₂ saturation, increasing the detectability of the stored CO₂. The difference decreased with increasing CO₂ content. Up to 5% CO₂ saturation could be qualitatively estimated from the synthetic seismic data. For CO₂ saturation higher than 5%, qualitative estimations of the saturation level are uncertain.

The obtained results and their novelty have a practical value for the demonstration of CGS and its monitoring in the Baltic Sea Region. The proposed methods were tested in the structure scale and the results of the CO₂ injection-like experiment could be applied to the basin-scale modelling of the CO₂ storage in the Baltic Cambrian Basin and in the other basins.

KOKKUVÕTE

PhD uuringu eesmärgiks oli koostada petrofüüsikalised mudelid Balti settebasseini perspektiivsetes sügavates pinnaalustes struktuurides võimaliku CO₂ geoloogilise ladustamise (CGS) käigus toimuva CO₂ voo kohta, et toetada CO₂ kinnipüüdmise ja ladustamise (CCS) tehnoloogia kui ühe efektiivsema kliimamuutust leevendava meetme kasutuselevõttu Balti riikides.

CGS-i struktuuriskaala modelleerimise metodoloogia koosnes neljast etapist: (1) ladustamiskoha valik ja andmete kogumine, (2) ladustamiskoha iseloomustamine, (3) CGS-i mõju kivimite omadustele, (4) CO₂ ladustamise numbriline seismiline modelleerimine.

Nelja geoloogilist struktuuri, mis on perspektiivsed CGS-i jaoks Balti regioonis (mandrilised Lõuna Kandava ja Dobeles struktuurid ning merelised struktuurid E6 Lätis ja E7 Leedus), iseloomustati, kasutades olemasolevaid ja uusi andmeid, mis saadi viiest puuraugust pärineva 24 reservuaariliivakivimi- ja katendikivimiproovi laboratoorsel analüüsimisel. Uuritud struktuuride Deimena ladestu Kambriumi seeria 3 (varem Kesk-Kambrium) reservuaarikivimid on kaetud Zebre ladestu Alam Ordoviitsiumi katendikivimitega. Kivimite petrofüüsikalisi omadusi, keemilist- ja mineraloogilist koostist ning pinnamorfoloogiat võrreldi varasema andmestikuga. Neljale uuritud struktuurile konstrueeriti geoloogiliste, gamma-karotaaži ja laboratoorsete andmete põhjal reservuaarisektsioonide ning katendikivimi läbilõigete ja Deimena ladestu ülaosa kolmemõõtmelised staatilised mudelid.

Struktuuride CO₂ ladustamise mahutavust hinnati erinevatel usaldusväärsuse tasemetel. Keskmise hinnanguline mahutavus, lähtudes optimistlikust tasemest, oli mandrilistel Dobeles ja Lõuna Kandava ning merelistel E6 ja E7 struktuuridel, vastavalt 106, 95, 377 ja 34 Mt. E6 struktuur hinnati Balti basseinis CGS-i jaoks kõige perspektiivsemaks, lähtudes selle reservuaarikvaliteedist, lukustuspindalast ja ladustamismahutavusest. Selle hinnanguline optimistlik CO₂ ladustamismahutavus oli 251–602 Mt (keskmise 377 Mt), mis on ligilähedane varem publitseeritud Läti 16 mandrilise struktuuri kogumahutavusele (400 Mt).

Gaasiläbilaskevõimele ja poorsusele tuginedes pakuti välja reservuaarikivimite CGS-i omaduste uus klassifikatsioon Balti settebasseini Deimena ladestu liivakivide jaoks, lähtudes varasematest ning autori poolt määratud parameetritest. Klassifikatsiooni rakendati seejärel nelja uuritud struktuuri reservuaarikivimite kvaliteedi hindamiseks. Reservuaari liivakivide kvaliteet oli kõrgeim ('kõrge-2') Dobeles struktuuris, samal ajal kui Lõuna Kandava ja E6 struktuuri kvaliteet oli 'sobiv' CGS-i jaoks. Madalaim kvaliteet, 'ettevaatust nõudev' CGS-i jaoks, oli kõige rohkem kokku surutud E7 struktuuri liivakividel.

Lõuna Kandava, E6 ja E7 struktuuridest pärit 12 liivakiviproovi petrofüüsikalisi, geokeemilisi ja mineraloogilisi parameetreid mõõdeti ning analüüsiti enne ja pärast CO₂ sisestamist imiteerivat mõjutuseksperimenti. Uuritud mereliste struktuuride peamiselt puhtast kvartsist liivakivireservuaaride

esialgne kvaliteet põhiliselt säilis mõjutuseksperimentide ajal.

Suurimas ja hinnanguliselt kõige perspektiivikamas Läti merelises struktuuris CO₂ ladustamise seire teostatavuse analüüsiks kasutati kivimite füüsikalistele uuringutele tuginevat 4D numbrilist seismilist modelleerimist. Erinevate CO₂ kontsentratsioonidega homogeenelt küllastatud ja arvutatud CO₂ voo mudeli alusel saadud Deimena ladestu liivakivireservuaari sünteetilisi seismogramme ja seismilisi sektsioone võrreldi nelja stsenaariumi raames (ühetaolised ja voomudelid ilma ja koos mõjutusefektiga) baastaseme sektsioonidega, kasutades diferents- ja normaliseeritud ruutkeskmise (NRMS) meetrikat. Kasutatud lähenemise uudsus seisnes laboratoorselt mõõdetud CO₂ siduvate kivimite keemiliselt indutseeritud petrofüüsikalise mõjutatuse ühendamises seismilise numbrilise modelleerimisega. Reservuaari petrofüüsikaliste omaduste mõjutamine avaldas tugevat mõju seismiliste sektsioonide peegeldunud signaalidele, kusjuures suurim erinevus esines 1% CO₂ küllastusega seismilistes sektsioonides, suurendades ladustatud CO₂ määratavust. Erinevus vähenes CO₂ sisalduse edasisel suurenemisel. CO₂ küllastatus kuni 5% on kvalitatiivselt hinnatav sünteetiliste seismiliste andmete põhjal. CO₂ küllastatuse puhul üle 5% pole küllastusastme kvalitatiivne hindamine praktiliselt enam võimalik.

Saadud tulemustel ja nende uudsusel on praktiline väärtus Balti mere regioonis CGS-i rakendatavuse demonstreerimisel. Struktuuriskaalas testitud pakutavaid meetodeid ning CO₂ sisestamist simuleeriva eksperimendi tulemusi saab rakendada Balti Kambriumi basseinis ja teistes basseinides CO₂ ladustamise basseiniskaalas modelleerimisel.

ELULOOKIRJELDUS

1. Isikuandmed

Ees- ja perekonnanimi: Kazbulat Šogenov

Sünniaeg ja -koht: 01.06.1982 Eesti

Kodakondsus: Eesti

E-posti aadress: kazbulat.shogenov@ttu.ee

2. Hariduskäik

Õppeasutus (nimetus lõpetamise ajal)	Lõpetamise aeg	Haridus (eriala/kraad)
Tallinna Tehnikaülikool (TTÜ)	2005	Geotehnoloogia/bakalaureuse- kraad
Tallinna Tehnikaülikool (TTÜ)	2008	Geotehnoloogia (Petrofüüsika)/magistrikraad

3. Keelteoskus (alg-, kesk- või kõrgtase)

Keel	Tase
Vene	emakeel
Inglise	kõrgtase
Eesti	kesktase
Araabia	algtase

4. Täiendusõpe

Õppimise aeg	Täiendusõppe korraldaja nimetus
2004	Geoloogilise kaardistamise treening. Välitööd korraldatud Taani Tehnikaülikooli poolt (Molinos, Hispaania)
2010	Marie Curie Research Training Networks (EU FP6) - GRASP (BRGM, Prantsusmaa, Orleans). Kursus: Pariisi basseini naftat sisaldavate reservuaaride liivakivide petrofüüsikalised ja mineraloogilised omadused: CO ₂ ladustamise ja nafta täiendava tootmise perspektiivid.
2010	Koolitus: Keemilise reaktsioonivõime modelleerimine CO ₂ geoloogilise ladustamise ajal (BRGM, Orleans)
2011	ARC-GIS modelleerimise ja kaardistamise kursused
2012–2013	Marie Curie Research Training Networks (EU FP7) - QUEST projekt (OGS, Itaalia, Trieste). Numbriline seisiline modelleerimine seiramaks CO ₂ ladustamist Läänemere struktuuris; 3D staatiline geoloogiline modelleerimine.

2013	Koolitusprogramm - Treener kui juht. Korraldatud Tallinna Ülikoolis
------	---

5. Teenistuskäik

Töötamise aeg	Tööandja nimetus	Ametikoht
2003–2005	TTÜ Geoloogia Instituut	Laborant
2005–2008	TTÜ Geoloogia Instituut	Insener
2008–2015	Tallinna Tehnikaülikooli Geoloogia Instituut	Erakorraline teadur
2010	BRGM (Prantsusmaa Geoloogiakeskus), Orleans	Erakorraline teadur
2012–2013	OGS (Riiklik Okeanograafia ja Eksperimentaalse Geofüüsika Instituut), Itaalia, Trieste	Erakorraline teadur

6. Teadustegevus, sh tunnustused ja juhendatud lõputööd

Auhinnad

2009: 1 preemia – Parim konkursitöö Eesti Geograafia Seltsi Noorteklubi tudengitööde konkursil 2009 teema: mäendus, geoloogia, geotehnika jt. maateadused

2007: Aasta geoloogia ja mäenduse tudengitööde konkurss - 3. koht (Lõuna-Eesti litoloogiline liigitamine gamma-karotaaži ja petrofüüsikaliste omaduste põhjal)

Teadusprojektid

2014–2018 Haridus- ja Teadusministeeriumi programm (projekt SF0320080s07, IUT19-22)

2010–2013 CGS EUROPE, (<http://www.cgseurope.net>), EC FP7

2006–2009 CO2NET EAST (<http://co2neteast.energnet.com>), EC FP6

2006–2008 EU GEOCAPACITY (<http://nts1.cgu.cz/geocapacity>), EC FP6

Muud tegevused

2010–2015 Kutsutud posterisessiooni kokkukutsuja ja teeside retsensent EAGE (European Association of Geoscientists and Engineers) konverentsil näitusel

2012–2013 - Magistrantide juhendamine (TTÜ: SEM- skaneeriv elektronmikroskoop, polarisatsioonmikroskoop, petrofüüsikalised laboratoorsed tööd)

- Uus CCS kursus TTÜ-s (praktilised tööd ja harjutused)

7. Publikatsioonid

Ajavahemikul 2003 - 2015 on avaldatud kokku 46 teadustööd esimese või kaasautorina. Üks esitatud artikkel (Paper VI) sisaldub ka käesolevas doktoritöös.

Eesti Teadusinfosüsteemi teadustegevuse tulemuste klassifikaator	Kirjeldus	Arv
1.1	Teadusartiklid, mis on kajastatud Thomson Reuters Web of Science andmebaasis (v.a. Thomson Reuters Conference Proceedings Citation Index poolt refereeritud kogumikud)	15
1.2	Teadusartiklid teistes rahvusvahelistes teadusajakirjades, millel on registreeritud kood, rahvusvaheline toimetus, rahvusvahelise kolleegiumiga eelretsenseerimine, rahvusvaheline levik ning kättesaadavus ja avatus kaastöödele	3
1.3	Eelretsenseeritud teadusartiklid Eesti ja teiste riikide eelretsenseeritavates teadusajakirjades, millel on kohalik toimetuskolleegium	2
3.1	Artiklid/peatükid lisas loetletud kirjastuste välja antud kogumikes (kaasa arvatud Thomson Reuters Book Citation Index, Thomson Reuters Conference Proceedings Citation Index, Scopus refereeritud kogumikud)	1
3.2	Artiklid/peatükid lisas mitte loetletud kirjastuste välja antud kogumikes	5
3.4	Artiklid/ettekanded, mis on avaldatud valdkonda 3.1. mittekuuluvates konverentsikogumikes	12
3.5	Artiklid/ettekanded, mis on avaldatud kohalikes konverentsikogumikes	2
5.1	Konverentsiteesid, mida kajastab Thomson Reuters Web of Science	1
5.2	Konverentsiteesid, mis ei kuulu valdkonda 5.1.	5

CURRICULUM VITAE

1. Personal data

Name: Kazbulat Shogenov

Date and place of birth: 01.06.1982 Estonia

E-mail: kazbulat.shogenov@ttu.ee

Nationality: Estonian

2. Education

Educational institution	Graduation year	Education (field of study/degree)
Tallinn University of Technology (TUT)	2005	Geo-technology/Bachelor
TUT	2008	Geo-technical Engineering (Petrophysics)/Master

3. Language competence/skills (fluent; average, basic skills)

Language	Level
Russian	Mother language
English	Fluent
Estonian	Average
Arabic	Basic skills

4. Special courses

Period	Educational or other organization
2004	Geological mapping course. Fieldwork organized by Danish Technical University (Molinos, Spain)
2010	Marie Curie Research Training Networks (EU FP6) - GRASP (BRGM, France, Orleans). Studied course – ‘Petrophysical and mineralogical properties of sandstones from the oil-bearing reservoirs in Paris Basin: prospects for CO ₂ storage and Enhanced Oil Recovery’
2010	Training course ‘Modelling chemical reactivity during CO ₂ geological storage’ (BRGM, Orleans)
2011	Courses for improving skill in ARC-GIS modelling and mapping
2012–2013	Marie Curie Research Training Networks (EU FP7) - QUEST project (OGS, Italy, Trieste). Studied course – ‘Seismic numerical modelling to monitor CO ₂ storage in the Baltic Sea offshore structure; 3D static geological modelling’.
2013	Training programme – Coach as a leader. Organized by Tallinn University.

5. Professional employment

Period	Organization	Position
2003– 2005	Institute of Geology at TUT	Technician
2005– 2008	Institute of Geology at TUT	Engineer
2008– 2015	Institute of Geology at TUT	Researcher
2010	BRGM (Geological Survey of France), Orleans, France	Researcher
2012– 2013	OGS (National Institute of Oceanography and Experimental Geophysics)	Researcher

6. Research activity, including honours and theses supervised

Awards

2009: 1st award – ‘The best M.Sc. student research work–2009’ by Estonian Geographical Society in the field of mining, geology and other earth sciences (‘Correlation of the Ordovician bedrock in the South Estonian boreholes by petrophysical and geochemical properties’)

2007: Student geology and mining award by the Department of Mining at Tallinn University of Technology – 3rd place (research work: ‘South Estonian lithological discrimination by gamma-ray logs and petrophysical data’)

Links to scientific projects

2014–2018 Estonian Ministry of Education and Research programme (projects SF0320080s07, IUT19-22)

2010–2013 CGS EUROPE, (<http://www.cgseurope.net>), EC FP7

2006–2009 CO2NET EAST (<http://co2neteast.energnat.com>), EC FP6

2006–2008 EU GEOCAPACITY (<http://nts1.cgu.cz/geocapacity>), EC FP6

Other activities

2010–2015 Invited poster session convener and abstracts reviewer for EAGE (European Association of Geoscientists and Engineers) Conference & Exhibition

2012–2013 Supervision of master students (TUT: SEM–Scanning electron microscope, polarizing microscope, petrophysical laboratory)
New CCS course (practical works and exercises) at TUT

7. Publications

A total of 46 scientific papers were published during 2003-2015 (as the first author or a co-author). Additionally PAPER VI submitted for publication is included in this thesis.

Classification of publications in Estonian Research Information System	Description	Number
1.1	Scholarly articles indexed by Thomson Reuters Web of Science (excluding articles indexed in Thomson Reuters Conference Proceedings Citation Index)	15
1.2	Peer-reviewed articles in other international research journals with an ISSN code and international editorial board, which are circulated internationally and open to international contributions	3
1.3	Scholarly articles in Estonian and other peer-reviewed research journals with a local editorial board	2
3.1	Articles/chapters in books published by the publishers listed in Annex (including collections indexed by the Thomson Reuters Book Citation Index, Thomson Reuters Conference Proceedings Citation Index, Scopus)	1
3.2	Articles/chapters in books published by the publishers not listed in Annex	5
3.4	Articles/presentations published in conference proceedings not listed in Section 3.1	12
3.5	Articles/presentations published in local conference proceedings	2
5.1	Conference abstracts indexed by Thomson Reuters Web of Science	1
5.2	Conference abstracts that do not belong to section 5.1.	5

ORIGINAL PUBLICATIONS

PAPER I. **SHOGENOV, K.**, SHOGENOVA, A. & VIZIKA-KAVVADIAS, O. 2013. Petrophysical properties and capacity of prospective structures for geological storage of CO₂ onshore and offshore Baltic. Elsevier, Energy Procedia, 37, 5036–5045.

GHGT-11

Petrophysical properties and capacity of prospective structures for geological storage of CO₂ onshore and offshore Baltic

*Kazbulat Shogenov^a, Alla Shogenova^a and Olga Vizika-Kavvadias^b

^aInstitute of Geology, Tallinn University of Technology, Ehitajate tee 5, Tallinn 19086, Estonia

^bIFP Energies nouvelles, Avenue de Bois-Préau 92852 Rueil-Malmaison Cedex, France

Abstract

This study is focused on the investigation of four prospective structures for geological storage of CO₂ in the Baltic region, specifically in the onshore structures South Kandava and Dobele, and offshore structures (E6 and E7) in Latvia. Using detailed petrophysical, mineralogical and geochemical analyses of the Middle Cambrian Deimena Formation sandstones in these structures, their CO₂ storage capacity was estimated with different levels of reliability. Different storage efficiency factors and porosities of the reservoir rocks were applied for optimistic and conservative estimates. Offshore structure E6 was estimated as the most prospective for CO₂ geological storage in the Baltic Region. Its optimistic CO₂ storage capacity was 264-631 Mt, and its average conservative capacity (158 Mt) is the largest among all the studied until now in Latvia onshore and offshore structures. Total capacity of four studied structures estimated using an optimistic approach was on average 630 Mt and using a conservative approach 210 Mt. Earlier capacity estimates made during the EU Geocapacity project of the Dobele and South Kandava onshore structures are in the range of our optimistic capacities.

© 2013 The Authors. Published by Elsevier Ltd.
Selection and/or peer-review under responsibility of GHGT

Keywords: CO₂ storage capacity; Baltic onshore and offshore structures; Cambrian sandstone; reservoir and cap rock properties; chemical and mineralogical composition

1. Introduction

Carbon capture and storage (CCS) and CO₂ geological storage (CGS) as a part of CCS technology are accepted by world scientific community as an effective measure to reduce the greenhouse gas effect and Earth's climate change. The International panel for climate change experts reported that we have to decrease CO₂ emissions by 50% before 2050 to stop drastic changes of the climate and stay below 2°C above pre-industrial average temperature [1]. CGS could account for about 19% of the necessary emission mitigation [2]. In 2007 Estonian power plants emitted 14.5 million tones (Mt) of CO₂ emissions, which is higher than all the other Baltic countries (Latvia and Lithuania) together. Estonian CO₂ emissions per capita are one of the highest in Europe (14.9 tonnes per capita in 2007) and in the world (15th place in 2007) due to the use of local oil shale for energy production. Geological conditions in

* Corresponding author. Tel.: +372-558-9001; fax: +372-620-3011
E-mail address: shogenov@gi.ee

Estonia are unsuitable for CGS because of the shallow sedimentary basin and potable water available in all known aquifers. The most suitable conditions for CGS in the Eastern Baltic region (Estonia, Latvia and Lithuania) are provided by 16 Cambrian onshore geological structures in Latvia [3, 4, 5]. There are also a number of prospective structures for CGS offshore Latvia, but their capacities haven't been estimated earlier. Two onshore geological structures (South-Kandava – Kn and Dobele - Db) and two offshore structures (E6 and E7) in Latvia prospective for CGS were estimated in detail in this research (Fig. 1). In 2008 Latvian oil-company was licensed for hydrocarbon exploration and production from the Upper Ordovician and Devonian oil-bearing reservoirs in the E6 structure. It gives opportunity for the future Enhanced Oil Recovery (EOR) project in the studied area. In the EU Geocapacity project CO₂ storage capacity of the Dobele structure was 56 Mt and South-Kandava 44 Mt respectively [5].

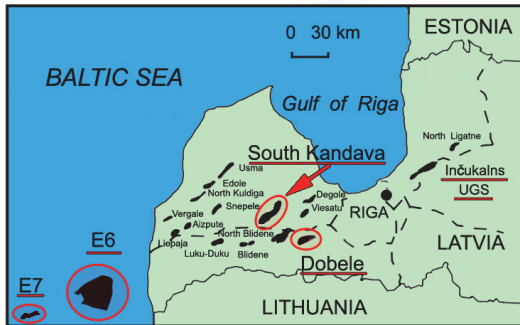


Fig. 1. Prospective structures in the Cambrian aquifer (CO₂ storage potential exceeding 2 Mt) and Inčukalns underground natural gas storage (UGS) in Latvia. The dashed line shows gas pipelines. Red circles shows locations of the studied offshore and onshore structures (modified after [5])

2. Data and Methods

Six onshore wells from the South Kandava and Dobele structures, as well as the E6-1/84 and E7-1/82 wells from offshore structures were selected for detailed study (Fig. 2). 24 samples of Middle Cambrian Deimena Formation (Dm) sandstone reservoir and Lower Ordovician (O₁) cap rock were taken from five drill cores stored in Latvian Environmental, Geological and Meteorological Center (LEGMC). 15 of these samples represent the reservoir across all four structures, while only nine samples from the onshore wells are taken from the caprock (Fig. 2). Three-dimensional (3-D) structural models were constructed in Golden Software Surfer 8 using structure maps of the top reservoir and wells cross sections. Four unpublished exploration reports (1970-1984, in Russian) stored in LEGMC were used. According to these reports open or effective porosity (W_{ef}) in the studied samples was estimated using the Preobrazhensky method (saturation of samples). Permeability (K_{gas}) has been determined whilst passing gas through the samples using the GK-5 apparatus. Only P-wave acoustic velocities of dry and wet rock samples were measured.

Within the present study petrophysical properties of new samples from these reservoirs were determined and compared to the old data. **Helium-density, helium-porosity, gas-permeability and acoustic wave velocities** were measured in the petrophysics laboratory of IFP Energies nouvelles (IFPEN) following the API recommendations [6]. Different properties were measured on 19 samples with 25 mm diameter and 11 to 27 mm height.

Permeability. The K_{gas} was measured using nitrogen injection. The sample is mounted in a Hassler cell under a confining pressure of 20 bars.

Acoustic wave velocity. Elastic properties of the rocks were measured only on dry samples. P-wave (P_w) and shear wave (S_w) velocities were measured using petro-acoustic equipment. This consisted of a pulser – Sofranel, Model 5072PR and two channel color digital phosphor oscilloscope – TDS 3032B (200MHz, 2,5 GS/s-DPO-Receiver, Tektronix). P_w was measured using 500 MHz wave transducers, while S_w was measured using 1 MHz wave transducers.

Measured and estimated porosity and gas permeability were used for CO₂ storage capacity estimates of the structures (Appendix A, A.1, A.3). Acoustic P_w and S_w velocities (Appendix A, A.1, A.2) were used for the interpretation of seismic data and further laboratory and numerical modelling of CO₂ plume behaviour underground.

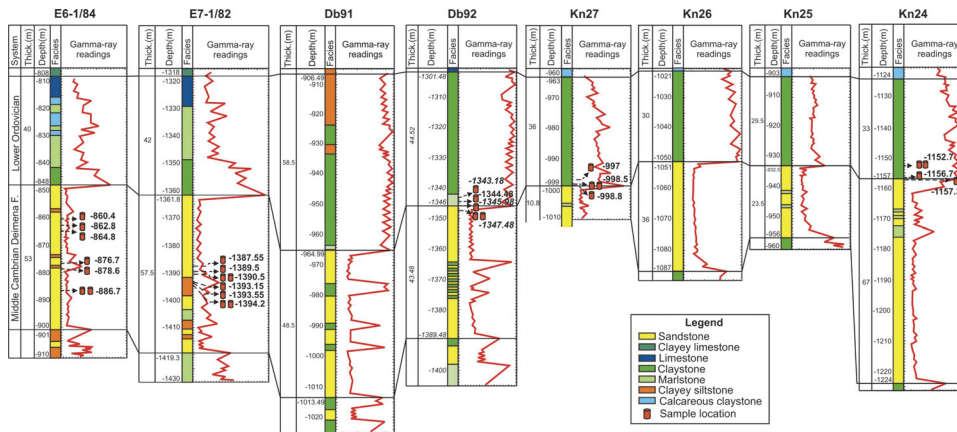


Fig. 2. Well correlation for the offshore (E6 and E7 structures) and onshore (Dobele and Kandava structures), focusing on the Middle Cambrian Deimena sandstone reservoir and Lower Ordovician cap rocks. Locations and depths of the studied samples are indicated by red cylinders

Chemical and mineralogical composition. Chemical, mineralogical composition and surface morphology of 24 rock samples were studied using X-Ray Fluorescence analyses (XRF), X-Ray Diffraction (XRD) and carbonate chemical analysis (CCA), Electron Microscope (EM) and Scanning Electron Microscope (SEM) studies. The XRF and XRD were measured in the ACME lab company (Canada), using the pressed pellet method for samples preparation. The CCA was done in the IGTUT [7]. The SEM and EM studies were conducted in the IGTUT with Zeiss EVO MA 15 Scanning Electron Microscope equipped with a Energy Dispersive Spectrometer (EDS) INCA x-act (Oxford Instruments Plc) and ZEISS Electron Microscope AxiosKop 40 respectively.

CO₂ Storage Capacity. Theoretical storage capacity in the studied structures was evaluated using a widely known formula for estimation of structural trap capacity [8]:

$$M_{CO_2t} = A \times h \times NG \times \varphi \times \rho_{CO_2r} \times S_{ef} \quad (1)$$

where M_{CO_2t} is storage capacity (kg), A is the area of an aquifer in the trap (m^2), h is the average thickness of the aquifer in the trap (m), NG is an average net to gross ratio of the aquifer in the trap (%), φ is the average porosity of the aquifer in the trap (%), ρ_{CO_2r} is the in situ CO₂ density at reservoir conditions, (kg/m^3), S_{ef} is the storage efficiency factor (for trap volume, %). We used different S_{ef} for each structure according to its reservoir properties and different methods to estimate these factors. According to [8] we estimated the efficiency factor as 10 and 20% in the E6 and E7 offshore structures respectively, and 20 and 15% in the Dobele and Kandava onshore structures respectively. We termed this approach “optimistic” due to the higher values of the factors in comparison with subsequent results obtained using other methods. With respect to the USA DOE report [9] we decided to decrease and to round the values of S_{ef} for the “conservative” estimation approach. The efficiency factor of 4% was selected for all the structures. In our simplified estimation model we did not consider pressure change and compressibility within the reservoir due to CO₂ injection [10]. We calculated optimistic and conservative M_{CO_2t} with minimum, maximum and average values (min-max/mean) of porosity determined by measured and reported data (Appendix A, A.1, A.3). We estimated the NG according to gamma-ray log readings (90% in E6, 80% in E7, 90% in Kandava, and 85% in Dobele) (Fig. 2).

The ρ_{CO_2r} depends on in situ reservoir pressure and temperature, which was estimated by the plot of supercritical state of CO₂ in situ conditions [11]. All measured laboratory data were compared with old exploration data for quality control (Fig. 3). According to reported and measured data we estimated minimum, maximum and average values of physical properties for each structure.

3. Results

3.1 E6 offshore structure

Geological background. The largest suitable trapping structure, offshore Latvia, is E6. The well E6-1/84 was drilled in 1984 in the central part of crest of the structure and crosses the anticline on the top of the Middle Cambrian Deimena Formation. The well is located 37 km from the Latvian coast and 47 km from the Liepaia harbor. The total depth of the well is 1068 m. The structure is an anticline fold bounded on three sides by faults (Fig. 4 a, b), which divide the main structure into two parts. According to seismic data faults are propagating only within the Cambrian and Ordovician horizons. The approximate area of the bigger part of the structure is 553 km², while the smaller part is 47 km². Total area of the structure is 600 km². The Deimena Formation (848-901 m depth) is represented by dark- and light-grey, fine-grained, loosely and medium cemented quartz sandstones. The reservoir interval contains thin layers of clayey

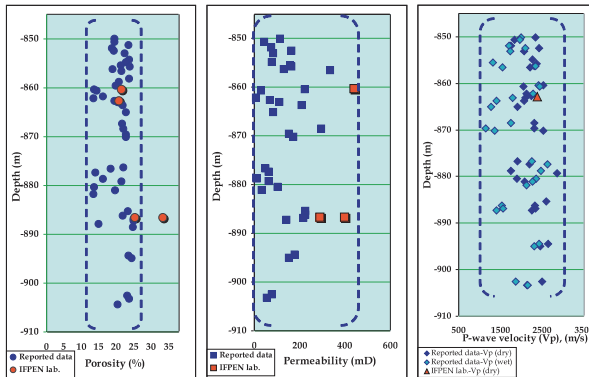


Fig. 3. Example of comparison plots (porosity, permeability and P-wave velocity (wet, dry) versus depth) of the measured samples with the old reported data (E6-1/84)

siltstones, clearly seen on gamma-ray logs. The reservoir rocks contain fractures (mostly open). The Deimena Formation unconformably overlain by impermeable Ordovician rocks, consisting mainly of claystones, carbonated clays (argillite), marlstones, limestones and clayey limestones. Thickness of the Deimena Formation in the well is 53 m and of Lower Ordovician cap rocks is 40 m. Total thickness of the Ordovician Formations is about 146 m. Approximately 120 m of non-porous Silurian mudstones overlie the Ordovician rocks, which play an additional role as a seal for Deimena structure.

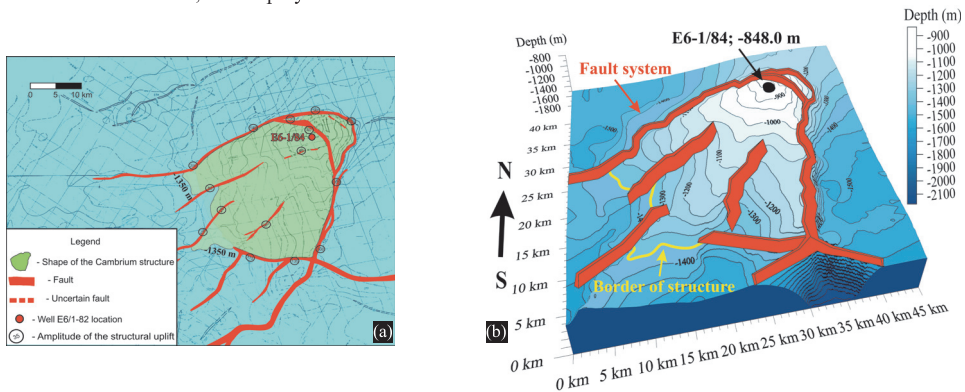


Fig. 4. (a) Local structure map of the offshore structure E6, drawn on the top of Deimena Formation and location of the well E6-1/84; (b) 3-D geological model of top of Deimena Formation in structure with estimated border of the structure (yellow isoline -1350 m). Faults bordered the structure are shown by red wall. Well location is shown by black circle with depth of top of Formation (-848 m)

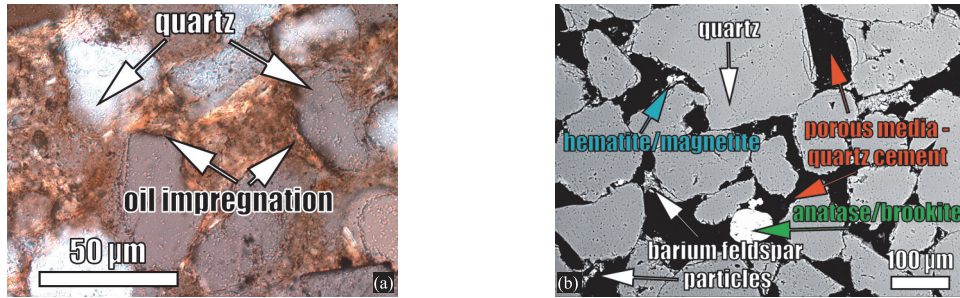


Fig. 5. Microphotograph of thin section in cross-polarized light (a) and SEM microphotograph (b) of the Deimena sandstones from the well E6-1/84 (a) Fine-grained quartz, carbonate and clayey cements presented in porous media were partially oil impregnated (876.7 m); (b) Minor amount of feldspar (sometimes barium feldspar) was found in all samples from the E6-1/84 borehole (886.7 m). Due to weak cementation this sample was broken into two parts, which had 26 and 33.5% of porosity, and 290 and 400 mD of permeability

Chemical and mineralogical composition. Pure sandstone samples studied from the E6 structure showed a good interparticulate and sometimes intraparticulate open porosity (Fig. 5 a, b). About 2% of chemical oxides (Al_2O_3 and TiO_2 used as indicators of clay content) in some loosely clay-cemented samples were determined. In general sandstone samples from the E6 structure can be considered to be “high quality” reservoir rocks.

CO₂ storage capacity in the E6 structure estimated using the optimistic approach was 264-631/396 Mt, and using the conservative approach was 106-252/158 Mt (Appendix A, A.3).

3.2 Offshore structure E7

Geological background. The structure E7 lies close to the E6 structure. The estimated approximate area of the E7 structure is 14 times less than E6 (43 km²). The E7-1/82 well was drilled in 1982. It was the first Baltic offshore deep well drilled in USSR. The total depth is 1650 m. The well is located in the Baltic Sea 85 km from the Latvian coast and 205 km from Gdansk harbor. The distance between the E6 and E7 boreholes is about 40 km. The E7 is an anticline fold within the Deimena Formation stretching from NE to SW and bounded at two sides faults (Fig.6 a, b). The well is located almost in the central part of the E7 on the crest and crosses the Deimena anticline on the top of the structure. The Deimena

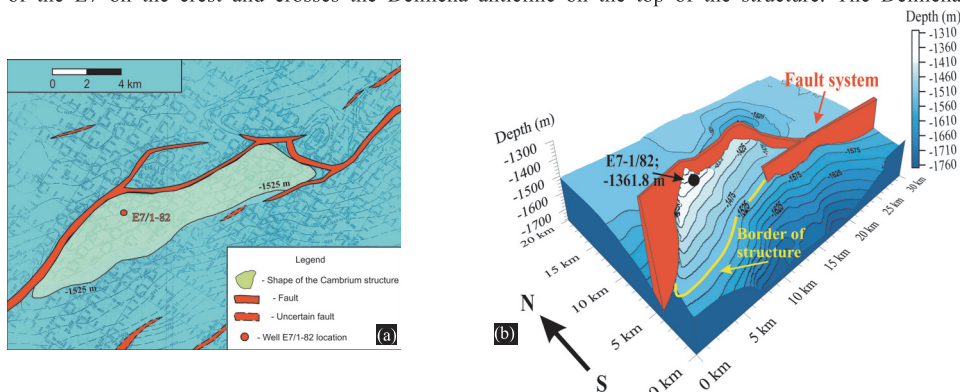


Fig. 6. (a) Local structure map of the E7 structure, drawn on the top of Deimena Formation, location of the well E7-1/82 is shown; (b) 3-D geological model of top of Deimena Formation in structure with estimated border of the structure (yellow isoline -1525 m). Faults bordered the structure are shown by red wall. Well location is shown by black circle with depth of top of Formation (-1361.8 m)

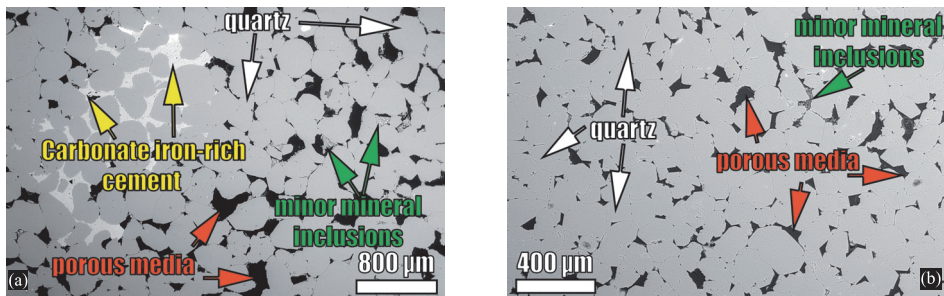


Fig. 7. SEM microphotograph of Deimena fine-grained quartz sandstones from the well E7-1/82. In all samples of E7 offshore structure the deterioration of reservoir properties was found compared to E6 structure. Samples contained about 2% of feldspar, some carbonates and mica. Heavy minerals such as zircon, tourmaline, pyrite are present. Clay fraction was presented by hydromica and kaolinite. (a) Medium to fine-grained quartz sandstone (1390.5 m) with spots of carbonate iron-rich cement, good porosity (14%) and low permeability (60 mD); (b) Very fine to fine-grained quartz sandstone (1389.5 m) with some inclusions of clayey fraction, 9% of porosity and 20 mD of permeability

sandstones are overlain by claystones, limestone, clayey limestone and marlstones of Ordovician Formation. Thickness of the Deimena Formation in the well is 58 m and depth 1362-1420 m and Lower Ordovician seal is 42 m thick. Total Ordovician Formation is 132 m thick. Thick non-porous Silurian mudstones (more than 190 m) overlie the Ordovician Formation. The Deimena Formation is represented by light grey and beige-grey fine-grained quartz sandstones interbedded by thin layers of sandy marlstones and clayey siltstones (4-5 cm), separated from pure sandstones by increased readings of the gamma-ray log. Sandstones are well sorted and sub-rounded, partly fractured. Essentially pure quartz sandstone samples from the E7 showed increase of clays and deterioration of free pore space compared with samples from the E6 (Fig. 7 a, b). Especially high clay cement content was observed in the samples from the clayey siltstone interbeds. Rocks of the upper part of the Deimena Formation are cemented mostly by quartz-regenerated cement. The lower part rocks are cemented by conformation of quartz grains due to dissolution under the pressure.

CO₂ storage capacity of the E7 structure was estimated using the optimistic approach 14-66/34 Mt, and the conservative estimate was 3-13/7 Mt (Appendix A, A.3).

3.3 South Kandava onshore structure

Geological background. The South Kandava structure was formed by uplift in the Pre-Devonian. The Brachy-anticlinal fold within the Deimena Formation with a flat NW flank and a steeper SE flank is prospective as a gas storage reservoir. The structure strikes from SW to NE. The structure is bounded by faults along two sides. The wells Kn25, Kn27 and Kn28 were drilled within the structure, while wells Kn24 and Kn26 are located outside the structure (Fig. 8 a). Estimated approximate area of the structure is 97 km². Thickness of the Deimena sandstones is 23-67 m, which are located at a depth of 933-1224 m. Quartz sandstones are white colored and contain small amounts of feldspar, biotite mica and muscovite. They are massive, fine-grained, well sorted, porous with good gas permeability and loosely cemented. Ordovician sediments overlie the Deimena sandstones with unconformity. The lower part of the cap rock consists of 5-10 cm of calcite cemented basal breccia consisting of marlstones. The Breccia is covered by 20-50 cm thick dark-green, glauconitic, weak cemented siltstones. Siltstones covered by dark-green, violet-brownish, strong, argillite carbonate clays with rare thin layers and lenses of limestone. The lower Ordovician cap rock is 30-36 m thick. The average thickness of Ordovician rocks in the structure is 224 m, while the Silurian Formation is 225 m.

Chemical and mineralogical composition. Both reservoir and cap rocks were studied in this structure. Reservoir quartz sandstone samples were cemented with calcite, as well as clayey material, regenerated quartz and siderite was found also in the studied reservoir samples (Fig. 8 b). Only few open pores were found in the calcium cement and between cement and grains. In general the main form of cementation within the South Kandava reservoir rocks consists of clayey cement. Regenerated borders

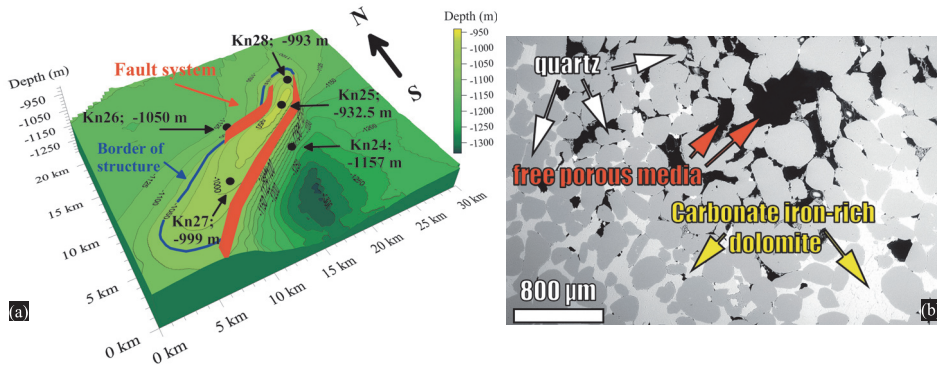


Fig. 8. (a) 3-D geological model of the South Kandava structure imposed on the top of Deimena Formation with estimated border of the structure (blue isoline -1050 m). Faults bordered the structure are shown by red wall. Wells locations with depths are shown by black circles; (b) SEM microphotograph of the Deimena quartz sandstone from the well Kn24 (1157.3 m). Quartz grains were almost completely cemented by carbonate iron-rich dolomite cement. It had low porosity (7%), close to 0 mD permeability and 81% of SiO_2 , 6% of CaO, 2% of MgO and 2% of Fe_2O_3 content. XRD analyzes showed ankerite as minor element in the sample

around the quartz grains partially form cement. The cap rock is represented by claystones, carbonate and clayey carbonate rocks. They are characterized by impermeable matrix composed of carbonate iron-rich dolomite and clayey material. The claystones have high clay content and minor dolomite and calcite content (Appendix A, A.2).

Estimated **CO₂ storage capacity** using the optimistic approach is 5-122/95 Mt, and using the conservative method 1-32/25 Mt. Estimated earlier within the EU Geocapacity project CO₂ storage capacity (44 Mt, [5]) is in the range with our optimistic capacities.

3.3 Dobeles onshore structure

Geological background. The studied wells Db91 and Db92 were drilled in 1971-1972 in the Dobeles structure, located in the limits of the East-Kurzema local high. Estimated area of the structure is 70 km², its surface altitude is 75-100 m. The structure is bounded only along one southern side by fault. The well Db91 is located almost on the crest of the structure close to the fault. The well Db92 was drilled near the fault, outside the uplift (Fig. 9 a). The core recovery of the Cambrian sandstones in these wells during

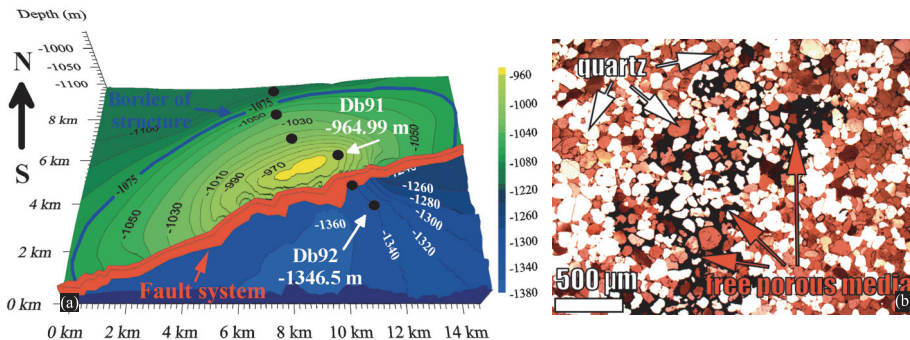


Fig. 9. (a) 3-D geological model of the Dobeles structure of the top of Deimena Formation. Wells location with index and depth is shown by white and indicated by black circles. Estimated border of the structure is shown by blue isoline (-1075 m). Fault bordered the structure is shown by red wall; (b) microphotograph in polarized light of the Deimena sandstone from the well Db92 (1347.5 m). The fine-grained sandstone had 91% of SiO_2 , 1,5% of CaO, 3% of Fe_2O_3 , 1% of Al_2O_3 content and had good intergranular 20% open porosity

exploration was only 20-30%. Cambrian reservoir is represented by white and light-grey fine- and very fine-grained quartz sandstones interbedded by thin layers of sandy siltstone and mudstones, reflected by higher gamma-ray readings. Deimena sandstones were found at the depth 965-1013 m in the Db91 well and 1346-1390 m in the Db92 well. Thickness of the sandstones is 44 m in the Db92 and 49 m in the Db91. Average thickness of reservoir sandstones in the structure is 52 m.

Chemical and mineralogical composition. Reservoir sandstones are mostly massive and loosely cemented with ore mineralization (halenite). The cement composition of sandstones and siltstones is clayey minerals (about 10%) and quartz regenerated cement.

The lower Ordovician Latorp Formation unconformably overlies the Deimena sandstones. These cap rocks are represented by claystones, marlstones, clayey siltstones and rare limestone interbeds. At the base of the formation a layer of greenish-grey glauconitic loosely cemented sandstones (0.5 m) was observed. The thickness of the Lower Ordovician cap rock is 59 m in the Db91 well and 45 m in the Db92 well. The average thickness of Ordovician Formation within the structure is 233 m. The Ordovician Formation is overlain by the Silurian Formation (> 100 m), which is represented by a thick succession of impermeable mudstones.

Measured porosity of reservoir sandstones was in the range of 17-20% (Appendix A, A.1). We determined a decrease in reservoir quality in the Dobe structure compared to offshore structures, as well as an increase of clay, calcite and dolomite cement. The reservoir rocks consist of 82%-100% quartz, about 9% feldspar and 6% mica (Fig. 9 b). Heavy minerals such as zircon, tourmaline, rutile and others are also observed accounting for 5% of the reservoir rock. The cap rocks are represented by clays with minor feldspar content and very low carbonate content. Due to weak cementation of samples it was possible to measure gas permeability only in one cap rock sample Db92-1344.48 (2 mD). This sample showed pretty high porosity for cap rock (15%) (Appendix A, A.2).

The estimated **CO₂ storage potential** in the Dobe structure using the optimistic approach is 56-145/106 Mt and using the conservative approach is 11-29/21 Mt (Appendix A, A.3). Estimated earlier within the EU Geocapacity project CO₂ storage capacity (56 Mt, [5]) corresponds to our minimum optimistic estimate.

4. Conclusions

- Geological structures in Latvia were estimated as prospective reservoirs for the gas storage. The structures lead to a structural high within the Cambrian saline aquifer and impermeable seal, which are suitable for both CO₂ and natural gas storage.
- The Cambrian Deimena Formation is clearly indicated by low natural radioactivity as observed on the gamma-ray log readings. Clayey interbeds and marlstone layers in the reservoir can easily be determined by increased gamma-ray readings. Cap rocks represented by clayey sediments of Ordovician and Silurian Formations are lead to the highest values on the gamma-ray logs.
- Good reservoir properties of the Cambrian sandstones were confirmed by new laboratory experiments in three studied boreholes (E6-1/84, E7-1/82 and Db92). Measured petrophysical properties confirm those reported in earlier data.
- The best reservoir properties (porosity and gas permeability) were found in sandstones from the Latvian E6 offshore structure. This structure was estimated as the most prospective for CGS in the Baltic Region. Its estimated optimistic CO₂ storage capacity was in the range of 264-631 Mt.
- Estimated optimistic CO₂ storage capacity was 14-66 Mt in the E7 offshore structure, 5-122 Mt in the South Kandava and 56-145 Mt in the Dobe onshore structures. The conservative CO₂ storage capacity was 105-252 Mt in the E6, 3-13 Mt in the E7 offshore and 1-32 Mt in the South Kandava and 11-29 Mt in the Dobe onshore structures. Total capacity of the four structures in the study estimated by optimistic approach was 340-965 Mt and average 630 Mt. Using the conservative approach it was 120-330 Mt and average 210 Mt.
- The difference between maximum and average values of CO₂ storage capacity was higher in the E7 structure (48%) than in the E6 structure (37%), suggesting a lower homogeneity of sandstone porosity in the E7 reservoir. This difference was 27% in the Dobe and 22% in the South Kandava structure, showing similar reservoir porosity in the onshore structures, but two times lower the homogeneity in the offshore structures.
- Optimistic maximum and average storage potential of the E6 structure (631 and 396 Mt) is higher and nearly the same as previously reported total potential of all 16 onshore Latvian structures (400

Mt). Even its average conservative capacity (158 Mt) is the largest among all the studied until now in Latvia onshore and offshore structures.

- The results obtained are giving new possibilities for economic and geochemical modeling of regional cross border CCS scenarios in the Baltic Sea Region and seismic modeling of the Baltic offshore reservoir structures. This study was continued with the determination of petrophysical properties of altered samples to investigate the impact of the CO₂ injection on the host reservoir. The alteration process called the “Homogeneous alteration method” is related to retarded acid treatment of the samples (IFPEN method simulating in situ conditions of CO₂-rich brine injection in an aquifer).

Acknowledgements

This research which is part of the PhD study was supported by the Estonian targeted funding program (project SF0320080s07) and partially funded by Archimedes Foundation program DoRa, Estonian Doctoral School of Earth Sciences and Ecology, EU FP7 project CGS EUROPE and Marie Curie Research Training Network "Quantitative Estimation of Earth's Seismic Sources and Structure" (QUEST), Contract No. 238007. We would like to thank Jean Guelard (IFPEN) for permeability measurements and other guidance in petrophysical laboratory, Jean-François Nauroy (IFPEN) for acoustic velocity measurements, Dan Bossie-Codreanu (IFPEN) for the fruitful discussion and helpful advices, and Daniel Sopher (Uppsala University) for grammar editing and essential comments. We are also very grateful to the LEGMC for providing samples and exploration reports for this study.

References

- [1] Solomon, S., Qin, D., Manning, M., Chen, Z., Marquis, M., Averyt, K.B., Tignor M., and Miller, H.L., (eds.). *Climate Change 2007: The Physical Science Basis*. IPCC Fourth Assessment Report (AR4). Contribution of Working Group I to the Fourth Assessment Report of the Intergovernmental Panel on Climate Change. Cambridge, United Kingdom and New York, NY, USA: Cambridge University Press; 2007, p. 1-996
- [2] Energy Technology Perspectives, Paris: OECD/IEA; 2010, p. 1-706
- [3] Sliapa, S., Shogenova, A., Shogenov, K., Sliapiene, R., Zabele, A., Vaher, R. *Industrial carbon dioxide emissions and potential geological sinks in the Baltic States*. Oil Shale, Vol. 25, No. 4; 2008, p. 465-484
- [4] Shogenova, A., Shogenov, K., Vaher R., Ivask J., Sliapa S., Vangkilde-Pedersen, T., Uibu, M., Kuusik, R. *CO₂ geological storage capacity analysis in Estonia and neighboring regions*, Energy Procedia, Volume 4; 2011, p. 2785-2792
- [5] Shogenova, A., Sliapa, S., Vaher, R., Shogenov, K., Pomeranceva, R. *The Baltic Basin: structure, properties of reservoir rocks and capacity for geological storage of CO₂*. Tallinn: Estonian Academy Publishers, Estonian Journal of Earth Sciences, 58(4); 2009, p. 259–267
- [6] American Petroleum Institute. *Recommended Practices for Core Analysis*. Second Edition, Recommended Practice 40, Exploration and Production Department; 1998, p.1-60
- [7] Shogenova, A., Kleesment, A., Hirt, A., Pirrus, E., Kallaste, T., Shogenov, K., Vaher, R. *Composition and properties of the iron hydroxides-cemented lenses in Estonian sandstone of Middle Devonian Age*. Stud. Geophys. Geod., 53(1); 2009, p. 111-131
- [8] Bachu, S., Bonijoly, D., Bradshaw, J., Burruss, R., Holloway, S., Christensen, N. P., Mathiassen, O. M. *International Journal of Greenhouse Gas Control*. 1; 2007, p. 430-443
- [9] US Department of Energy (DOE). *Methodology for development of geological storage estimates for carbon dioxide*. 2008, p. 1-37
- [10] van der Meer, B., and Egberts, P. *A general method for calculating subsurface CO₂ storage capacity*. Offshore Technology Conference, TA Utrecht, The Netherlands, OTC 19309; 2008, p. 1-9
- [11] Bachu, S. *Screening and ranking sedimentary basins for sequestration of CO₂ in geological media in response to climate change*. Environmental Geology, 44; 2003, p. 277–289

Appendix A

A.1. Studied parameters of the Middle Cambrian Deimena Formation sandstones

Structure	E6 offshore structure				E7 offshore structure				S. Kandava onshore structure				Dobele onshore structure			
	Min	Max	Mean	N	Min	Max	Mean	N	Min	Max	Mean	N	Min	Max	Mean	N
Wet density, kg/m^3	2704	2734	2720	4	2666	2746	2698	7	2664	2741	2702	2	2786	2877	2830	2
Porosity, % <i>estimated</i> *	13.5	33.5	21	50	5	23	12	56	1	27	21	-	10	26	19	7
Porosity, %	21	33.5	25	4	9.5	14	12	7	1	7	4	2	16.6	19.6	18	2
Permeability, mD <i>estimated</i> *	9	440	150	37	0.1	170	40	52	0.001	1250	300	-	0.1	670	360	5
Permeability, mD	290	440	380	3	0.1	70	20	7	0.001	0.3	0.1	2	-	-	-	-
P_w velocity, m/s	2383	2383	2383	1	2130	3583	2814	6	4556	5400	4978	2	-	-	-	-
S_w velocity, m/s	-	-	-	-	1725	2230	2050	3	3225	3600	3412	2	-	-	-	-
SiO ₂	95	98	97	6	87	99	95	6	70	81	76	2	91	91	91	1
Al ₂ O ₃	0.2	1.9	0.6	6	0.3	5.3	1.8	6	0.18	0.26	0.22	2	1.1	1.1	1.1	1
Fe ₂ O ₃	0.06	0.6	0.2	6	0.06	1.9	0.6	6	0.13	2.32	1.23	2	2.8	2.8	2.8	1
K ₂ O	0.07	0.3	0.14	6	0.03	0.9	0.3	6	<0.01	0.03	0.02	2	0.22	0.22	0.22	1
CaO	0.9	1.1	1.05	6	0.9	1.5	1.1	6	6.4	16.5	11.4	2	1.54	1.54	1.54	1
MgO	0.24	0.65	0.39	6	0.24	0.65	0.44	6	0.57	2.12	1.35	2	0.65	0.65	0.65	1

* (estimated porosity is averaged from measured and reported data)

A.2. Studied parameters of the Lower Ordovician cap rocks of the Dobele and South Kandava onshore structures

Structure	South Kandava				Dobele			
	Min	Max	Mean	N	Min	Max	Mean	N
Wet density, kg/m^3	2741	2753	2747	2	2.9	2.9	2.9	1
Porosity, %	4	5	4.4	2	14.9	14.9	14.9	1
Permeability, mD	0.004	0.004	0.004	2	2	2	2	1
P_w , m/s	4156	4630	4393	2	-	-	-	-
S_w , m/s	2493	2778	2636	2	-	-	-	-
SiO ₂	9.3	63	42	6	45	62	55	3
Al ₂ O ₃	2.6	15.6	10.7	6	4.5	16	12	3
Fe ₂ O ₃	0.8	4.4	3.1	6	4.6	10	6.5	3
K ₂ O	0.14	6.9	4.6	6	3.4	6.8	5.3	3
CaO	1.1	47.3	16.5	6	1.3	15.2	6	3
MgO	0.3	1.5	1	6	1.2	4.2	2.4	3

Chemical oxides measured in %: SiO₂, Al₂O₃, Fe₂O₃, K₂O by XRF, and CaO and MgO by CCA methods.
Min – minimum, max – maximum and mean – average values. N – number of samples

A.3. Physical parameters of the Latvian structural traps

Structure	Reservoir parameters							CO ₂ storage capacity, Mt						
	Depth of top, m	Thick-ness, m	Trap area, km^2	Sali-nity, g/l	Press-ure, mPa	T_r , °C	CO ₂ density, kg/m^3	S_{ef} Opt./Cons., %	Optimistic estimates			Conservative estimates		
									min	max	mean	min	max	mean
E6	848	53	600	99	9.3	36	658	10/4	264	631	396	106	252	158
E7	1362	58	43	125	14.7	46	727	20/4	14	66	34	3	13	7
S. Kandava	933	42	97	113	10.5	24.5	820	15/4	5	122	95	1	32	25
Dobele	950	52	70	114	13	18	900	20/4	56	145	106	11	29	21

The S_{ef} Opt./Cons. is a storage efficiency factors for the optimistic/conservative estimates. The NG in E6 was estimated by logging data as 90%, in E7 as 80%, S. Kandava as 90% and in Dobele as 85%. Estimated porosity (A.1) was used for capacity calculation

PAPER II. SHOGENOV, K., SHOGENOVA, A. & VIZIKAKAVVADIAS, O. 2013. Potential structures for CO₂ geological storage in the Baltic Sea: case study offshore Latvia. *Bulletin of the Geological Society of Finland*, 85(1), 65–81.

Potential structures for CO₂ geological storage in the Baltic Sea: case study offshore Latvia



KAZBULAT SHOGENOV¹⁾, ALLA SHOGENOVA¹⁾ AND
OLGA VIZIKA-KAVVADIAS²⁾

¹⁾ *Institute of Geology, Tallinn University of Technology, Ehitajate tee 5,
Tallinn 19086, Estonia*

²⁾ *IFP Energies nouvelles, Avenue de Bois-Préau 92852,
Rueil-Malmaison Cedex, France*

Abstract

This study is focused on two structures in the Baltic offshore region (E6 and E7 structures in Latvia) prospective for the geological storage of carbon dioxide (CO₂). Their CO₂ storage capacities were estimated recently with different levels of reliability. Petrophysical, geophysical, mineralogical and geochemical parameters of reservoir rocks represented by quartz sandstones of the Deimena Formation of Middle Cambrian in two wells and properties of Silurian and Ordovician cap rocks were additionally studied and interpreted in the present contribution. Extended methodology on rock measurements and estimation of conservative and optimistic storage capacity are presented. Uncertainties and risks of CO₂ storage in the offshore structure E6 estimated as the most prospective for CO₂ geological storage in the Baltic Region, and the largest among all onshore and offshore structures studied in Latvia, were discussed. We re-estimated the previous optimistic capacity of the E6 structure (265–630 Mt) to 251–602 Mt. Considering fault system within the E6 structure we estimated capacity of two compartments of the reservoir separately (E6-A and E6-B). Estimated by the optimistic approach CO₂ storage capacity of the E6-A part was 243–582 Mt (mean 365 Mt) and E6-B part 8–20 Mt (mean 12 Mt). Conservative capacity was 97–233 Mt (mean 146 Mt) in the E6-A, and 4–10 Mt (mean 6 Mt) in the E6-B. The conservative average capacity of the E6-B part was in the same range as this capacity in the E7 structure (6 and 7 Mt respectively). The total capacity of the two structures E6 and E7, estimated using the optimistic approach was on average 411 Mt, and using the conservative approach, 159 Mt.

Keywords: carbon dioxide, underground storage, offshore, reservoir rocks, sedimentary rocks, sandstone, physical properties, chemical composition, mineral composition, Latvia

Corresponding author email: shogenov@gi.ee

Editorial handling: Joonas Virtasalo

1. Introduction

Previous studies reported extremely high CO₂ emissions per capita in Estonia and need of carbon capture and storage technology (CCS) implementation to reduce the greenhouse gas effect and the Earth's climate change (Sliupa et al., 2008; Shogenova et al., 2009a, b, 2011a, b; Shogenov et al., 2013). According to these studies Estonia has unfavourable for CO₂ geological storage (CGS) conditions (shallow sedimentary basin and potable water available in all known aquifers) and storage capacity of Lithuanian geological structures was estimated as insufficient, due to small size of the structures (Fig. 1). The most suitable for CGS in the Eastern Baltic region (Estonia, Latvia and Lithuania) are 16 Cambrian onshore and 16 offshore deep anticline geological structures in Latvia. All the prospective Latvian structures are represented by uplifted Cambrian reservoir sandstones covered by Lower

Ordovician clayey carbonate rocks. In this study we focused on more detailed investigation of two offshore structures E6 and E7 (Fig. 2), which were briefly described in Shogenov et al., (2013). We expanded description of methods, measured petrophysical, geochemical and mineralogical properties of reservoir rocks, improved and clarified estimation of CO₂ storage capacity in the E6 structure.

2. Data and Methods

Two wells, E6-1/84 and E7-1/82, drilled in the Latvian offshore structures E6 and E7 respectively, were studied. Twelve samples from the Deimena Formation of Middle Cambrian sandstone reservoir were taken from two drill cores stored in the Latvian Environmental, Geological and Meteorological Centre (LEGMC) (Fig. 3). We interpreted an available seismic section of the E6 structure and,

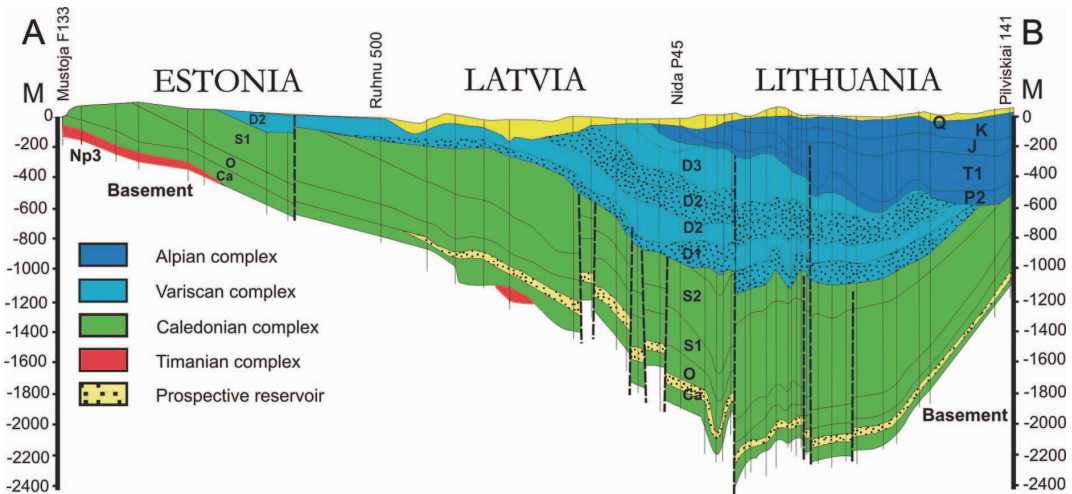


Fig. 1. Geological cross section across Estonia, Latvia and Lithuania. Cross section line A-B is shown on Fig. 2a. Major aquifers are indicated by dots. Dotted vertical lines show faults. The cross section clearly indicates that Estonia is out of the recommended depth frames for CGS (minimum recommended depth for CGS is 800 m). Devonian structures are unsuitable for CGS due to absence of impermeable cap rock formation that must overlay the reservoir. The size of Lithuanian Cambrian sandstone structures is too small for industrial scale. A number of structural uplifts in the Cambrian rocks bounded by faults are prospective reservoirs for CGS in Latvia. Np3 – Ediacaran (Vendian); Ca – Cambrian; O – Ordovician; S1 – Lower Silurian (Llandovery and Wenlock series); S2 – Upper Silurian (Ludlow and Pridoli series); D1, D2 and D3 – Lower, Middle and Upper Devonian, respectively; P2 – Middle Permian; T1 – Lower Triassic; J – Jurassic; K – Cretaceous; Q – Quaternary (modified from Shogenova et al., 2009a).

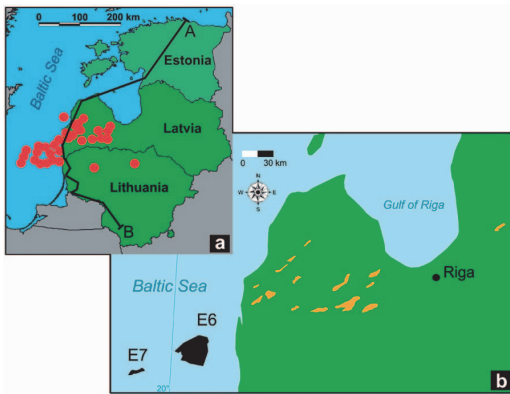


Fig. 2. (a) Approximate location of 16 onshore and 16 offshore Latvian structures in the Cambrian aquifer prospective for CGS (CO₂ storage potential exceeding 2 Mt), shown by red circles. Black line A-B represents geological cross section shown on Fig. 1. (b) 16 onshore (orange) and 2 studied offshore (E6 and E7) structures (black) in Latvia (maps built using ArcGis 9.2 software).

using structural maps of the E6 reservoir and cap rock top and cross section of the well E6-1/84, the geological cross section of the E6 structure was constructed (Fig. 4).

Two unpublished exploration reports (Babuke et al., 1983; Andrushenko et al., 1985), stored in the LEGMC, were used. According to these reports, open or effective porosity (W_{ef}) in the studied samples was estimated by saturation method (Zdanov, 1981). Permeability (K_{gas}) was determined when passing gas through the samples using the “GK-5” apparatus. More detailed description of K_{gas} measurements is given in Shogenova et al. (2009a). P-wave acoustic velocities of dry rock samples were measured with “DUK-20” equipment (100 KHz). Velocities were measured in two directions (X and Y) to consider anisotropy. Shogenov et al. (2013) reported petrophysical properties of new samples from reservoirs of the E6 and E7 structures, which were determined and compared to old data. More detailed description of petrophysical methods is presented here.

Helium density, helium porosity, gas permeability and acoustic wave velocities were measured in the petrophysical laboratory of IFP Energies nouvelles

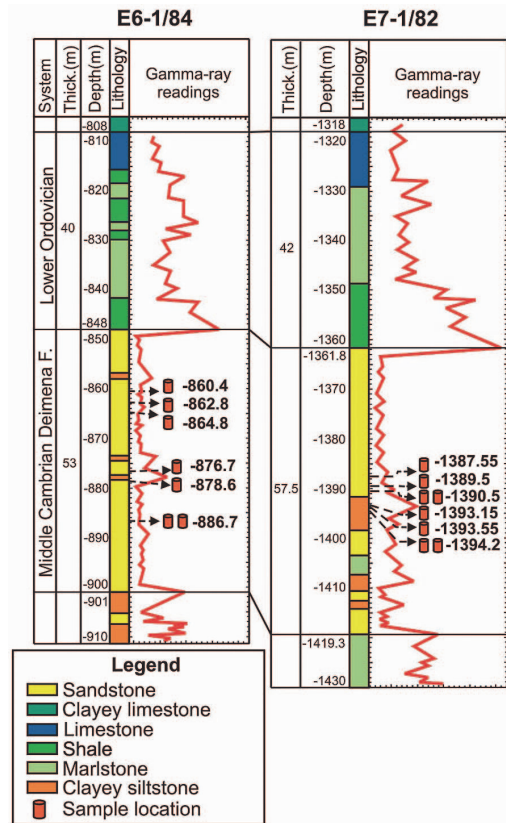


Fig. 3. Correlation of the E6 and E7 offshore structures based on drill core data (E6-1/84 and E7-1/82), focusing on the sandstone reservoir of the Deimena Formation of Middle Cambrian and Lower Ordovician cap rocks. Location and depth of the studied samples are indicated by red cylinders. Gamma-ray readings were digitized from analogue gamma-ray logging data.

(IFPEN) following the American Petroleum Institute recommendations (American Petroleum Institute, 1998). Various rock properties were determined on 11 samples with 25 mm diameter and 11–27 mm height. After drying of samples the solid volume (V_s) was calculated by gas displacement helium pycnometer AccuPyc 1330 (Micrometrics). Using sample weight (m), the grain or matrix density was calculated

$$\rho_g = \frac{m}{V_s}, \tag{1}$$

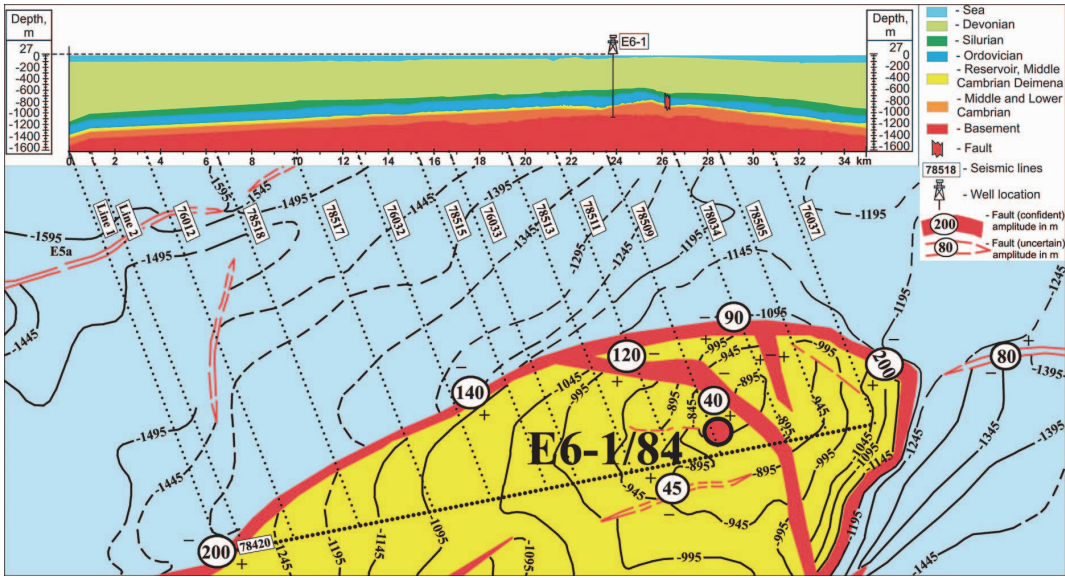


Fig. 4. Geological cross section corresponding to seismic line 78420, interpreted using reported seismic data, local structure map and lithological cross section in the well E6-1/84.

The total volume of sample (V_{total}) was measured on powder pycnometer GeoPyc 1360 (Micro-metrics). Applying V_{total} , the density of dry samples was calculated

$$\rho_{dry} = \frac{m}{V_{total}}, \quad (2)$$

Volume of pores V_{pore} was calculated using V_s and V_{total}

$$V_{pore} = V_{total} - V_s, \quad (3)$$

The effective porosity ϕ_{ef} (%) was calculated using the V_{pore} and V_{total}

$$\phi_{ef} = \frac{V_{pore}}{V_{total}} \times 100, \quad (4)$$

Permeability (K_{gas}) was measured using nitrogen injection. The sample is mounted in a Hassler cell under a confining pressure of 20 bars. Volume of the gas passed through the samples was measured

by gas meter. Flow rate Q (cm^3/s) was calculated by dividing the volume of the passed gas on time. Using the Q , length of samples (l , cm), area of sample (S , cm^2), viscosity of gas (μ_{gas} cP), atmospheric pressure (P_{atm} , bar), inlet and outlet pressures (P_1 , P_2 respectively, bar) and applying the Darcy law K_{gas} (mD) of the samples was calculated as

$$K_{gas} = Q \times \frac{1}{S} \times \mu_{gas} \times \frac{2 \times P_{atm}}{P_1^2 - P_2^2}, \quad (5)$$

Elastic properties of the rocks were determined only on dry samples. P-wave (P_w) and shear wave (S_w) velocities were measured with petro-acoustic equipment consisting of a pulser – Sofranel, Model 5072PR and a two-channel colour digital phosphor oscilloscope – TDS 3032B (200MHz, 2,5 GS/s-DPO-Receiver, Tektronix). P_w was measured with 500 MHz wave transducers, S_w with 1 MHz wave transducers.

On the basis of measured and estimated porosity and gas permeability, CO_2 storage capacity of the structures was estimated (Tables 1, 2).

The chemical and mineralogical composition and surface morphology of 12 rock samples were

Table 1. Studied parameters of the Middle Cambrian sandstones of the Deimena Formation.

Structure	E6 offshore structure				E7 offshore structure			
	Min	Max	Mean	N	Min	Max	Mean	N
Grain density, kg/m ³ estimated *	2630	2730	2690	12	2600	2930	2670	56
Grain density, kg/m ³ measured	2700	2730	2720	4	2670	2750	2700	7
Bulk density (dry), kg/m ³ estimated *	1810	2340	2090	45	2250	2940	2360	56
Bulk density (dry), kg/m ³ measured	1810	2170	2030	4	2310	2410	2370	7
Porosity, % estimated *	14	33,5	21	45	5	23	12	56
Porosity, % measured	21	33,5	25	4	9,5	14	12	7
Permeability, mD estimated *	10	440	160	34	0.13	170	40	52
Permeability, mD measured	290	440	380	3	0.13	70	20	7
P _w velocity (dry), m/s estimated *	1750	2850	2240	31	2130	3580	2920	15
P _w velocity (dry), m/s measured	2380	2380	2380	1	2130	3580	2815	6
S _w velocity, m/s measured	-	-	-	-	1725	2230	2050	3
XRF analysis, %								
SiO ₂	95	98	97	6	87	99	95	6
Al ₂ O ₃	0.2	1.9	0.6	6	0.3	5.3	1.8	6
Fe ₂ O ₃ total	0.06	0.6	0.2	6	0.06	1.9	0.6	6
K ₂ O	0.07	0.3	0.14	6	0.03	0.9	0.3	6
Na ₂ O	<0.01	0.04	0.03	6	<0.01	0.1	0.05	6
MnO	<0.01	<0.01	<0.01	6	<0.01	0.06	0.03	6
TiO ₂	0.09	0.18	0.13	6	0.06	0.5	0.23	6
P ₂ O ₅	<0.01	0.01	0.01	6	<0.01	0.04	0.02	6
Ba	0.07	0.28	0.16	6	<0.01	0.06	0.03	6
Titration method, %								
CaO	0.9	1.1	1.05	6	0.9	1.5	1.1	6
MgO	0,24	0.65	0.39	6	0,24	0.65	0,44	6
Gravimetric method, %								
Insoluble Residue	96.3	98.5	97.3	6	93.6	98.6	96.4	6

Chemical oxides measured in %: SiO₂, Al₂O₃, Fe₂O₃, K₂O, Na₂O, MnO, TiO₂, P₂O₅ and Ba by XRF, CaO and MgO by titration and insoluble residue by gravimetric methods. Min – minimum, max – maximum and mean – average values, N – number of samples.

* estimated rock properties were averaged from measured and reported data.

Table 2. Physical parameters of the Latvian offshore structural traps.

Structure	Reservoir parameters								CO ₂ storage capacity, Mt					
	Depth of top, m	Thickness, m	Trap area, km ²	Salinity, g/l	Pressure, mPa	T, °C	CO ₂ density, kg/m ³	S _{ef} Opt./Cons., %	Optimistic estimates			Conservative estimates		
									Min	Max	Mean	Min	Max	Mean
E6-A	848	53	553	99	9.3	36	658	10/4	243	582	365	97	233	146
E6-B	848	53	47	99	9.3	36	658	4/2	8	20	12	4	10	6
E6 total	848	53	600	99	9.3	36	658	10; 4/4; 2	251	602	377	101	243	152
E7	1362	58	43	125	14.7	46	727	20/4	14	66	34	3	13	7
<i>Total CO₂ storage capacity of E6 and E7, Mt</i>									265	668	411	104	256	159

The S_{ef} Opt./Cons. is a storage efficiency factor used for optimistic (Opt.) and conservative (Cons.) capacity calculation.

investigated using X-ray fluorescence analysis (XRF), X-ray diffraction (XRD), chemical analysis using gravimetric and titration methods, and transmission electron microscope (TEM) and scanning electron microscope (SEM) studies. The XRF and XRD analyses were performed in the Acme Analytical Laboratories Ltd. (Vancouver, <http://acmelab.com>), using the pressed pellet method for sample preparation. The SEM and TEM studies were conducted in the Institute of Geology at Tallinn University of Technology (IGTUT) with a Zeiss EVO MA 15 scanning electron microscope, equipped with an energy dispersive spectrometer (EDS) INCA x-act (Oxford Instruments Plc) and ZEISS light electron microscope AxiosKop 40, respectively (Shogenov et al., 2013), gravimetric and titration analyses were made in the IGTUT (Shogenova et al., 2009b).

The theoretical storage capacity of the structures was estimated using a well-known formula for estimation of the capacity of a structural trap (Bachu et al., 2007):

$$M_{\text{CO}_2t} = A \times h \times NG \times \varphi \times \rho_{\text{CO}_2r} \times S_{\text{ef}}, \quad (6)$$

where M_{CO_2t} is storage capacity (kg), A is the area of

an aquifer in the trap (m^2), h is the average thickness of the aquifer in the trap (m), NG is an average net to gross ratio of the aquifer in the trap (%), φ is the average porosity of the aquifer in the trap (%), ρ_{CO_2r} is the in situ CO_2 density in reservoir conditions (kg/m^3), S_{ef} is the storage efficiency factor (for the trap volume, %). CO_2 storage efficiency factor is the volume of CO_2 that could be stored in reservoir per unit volume of original fluids in place. In our previous study we used a different S_{ef} for each structure based on its reservoir properties and employed different methods to estimate these factors (Shogenov et al., 2013). Following Bachu et al., (2007), the efficiency factors 10 % and 20 % in the E6 and E7 offshore structures were estimated respectively. Bachu et al., (2007) proposed simplified model to estimate S_{ef} for open and semi-closed aquifers according the stratigraphic limitations in the connectivity between the trapped aquifer volume and the bulk aquifer volume and quality of reservoirs. Quality of reservoir depends on its petrophysical parameters (porosity and permeability). According to Bachu et al., (2007) and Vangkilde-Pedersen et al., (2009) S_{ef} of high quality reservoir limited by faults on two sides is 20 % and on three sides is 10 %. In Shogenov et al., (2013) we termed this

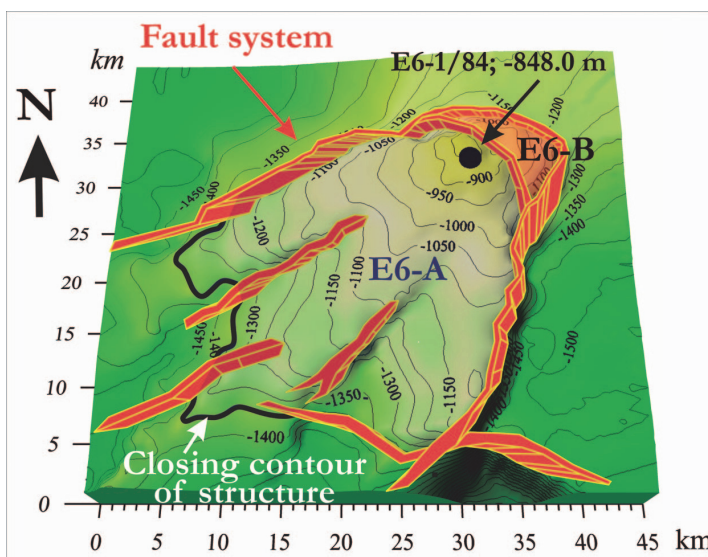


Fig. 5. 3D geological model of the top of the Deimena Formation in the E6 structure with the estimated closing contour of the structure (black contour is -1350 m). Faults bordering the structure are shown by a red wall. Location of the well is shown by a black circle with the depth of the top of the Deimena Formation (-848 m). Location of compartments E6-A and E6-B is indicated by red and green circle respectively (modified from Shogenov et al., 2013).

approach as “*optimistic*” due to the higher values of the factors in comparison with subsequent results obtained by other method. In this study we used the same optimistic S_{ef} for E7 structure (20 %), but we consider the E6 structure to be consisting of two different compartments divided by inner fault. We defined a bigger southern part as E6-A, and a smaller northern part as E6-B (Fig. 5). We determined the efficiency factors of 10 % and 4 % in the optimistic approach for the E6-A and E6-B respectively. The E6-A is limited by faults on three sides and the E6-B on four sides. High quality reservoirs bounded on all sides have S_{ef} 3-5 % (Vangkilde-Pedersen et al., 2009). Based on the US Department of Energy report (US DOE, 2008), we decided to lower and round the values of S_{ef} for the so-called “*conservative*” estimation approach (Shogenov et al., 2013). Obtained by US DOE, using Monte Carlo simulation, a range of S_{ef} values are between 1 % and 4 % for deep saline aquifers for a 15 to 85 % confidence range. The efficiency factor of 4 % was selected for the E6-A and E7 structures and 2 % for the E6-B in this simplified estimation model, which did not consider pressure change and compressibility within the reservoir due to CO₂ injection (van der Meer & Egberts, 2008). Optimistic and conservative M_{CO_2r} were calculated with minimum, maximum and average values (min-max/mean) of porosity determined using measured and reported data (Tables 1, 2). “Min-max/mean” approach was involved due to uncertainties related to lack of available experimental data (only one well within each structure). The average net to gross ratio was recorded from gamma-ray log readings (90 % in the E6, 80 % in the E7; Fig. 3).

The ρ_{CO_2r} value, which depends on in situ reservoir pressure and temperature, was estimated using a graph of the supercritical state of CO₂ under in situ conditions (Bachu, 2003). All measured laboratory data were compared with old exploration data for quality control (Figs. 6, 11). Using the reported and measured data, we estimated minimum, maximum and average values of physical properties for each structure (Shogenov et al., 2013).

All depths in our study are shown in meters below sea level.

3. Offshore structure E6

3.1 Geological background

The E6 offshore structure is already reported in our recent study as the largest suitable trapping structure offshore Latvia. It was explored in 1984 only by one well E6-1/84 (depth 1068 m), located 37 km from coast of Latvia (Shogenov et al., 2013). The structure is represented by uplifted Middle Cambrian 53 m thick reservoir rocks, covered by 40 m thick Lower Ordovician clayey cap rocks. The reservoir is overlain by Ordovician and Silurian (in total 266 m thick) clayey carbonate rocks and Devonian siliciclastic and carbonate rocks (Fig. 4). Reservoir quartz sandstones are fractured and all the E6 structure is bounded by faults on three sides. In addition the inner fault divided the E6 structure into two compartments, E6-A and E6-B (Fig. 5). We assumed that the E6-A and the E6-B are separated by the fault, which will prevent CO₂ move from one part to another during injection, and drilling of additional well in the part E6-B will be needed.

Upper part of the Ordovician succession is represented by 10.5 m thick oil-bearing limestone reservoir layer. Oil deposits are small and not significant for industrial use. The temperature within the reservoir is 36 °C, salinity of the Cambrian aquifer is 99 g/l (Table 2).

3.2 Petrophysical properties

The Deimena Formation of Middle Cambrian in the E6 structure could be subdivided into three depth intervals with slightly different petrophysical rock properties. Changes in reservoir properties are clearly reflected on the gamma-ray log and on porosity-permeability plots (Figs. 3, 6).

The uppermost interval (848–876 m) is characterized by very fine to medium-grained sandstones. Oil impregnation ranges from weak irregular to strong regular. The reservoir properties of sandstones of this interval were earlier reported as good: porosity 14–24 % (mean 21 %), permeability 10–300 mD (mean 140 mD), P_w of

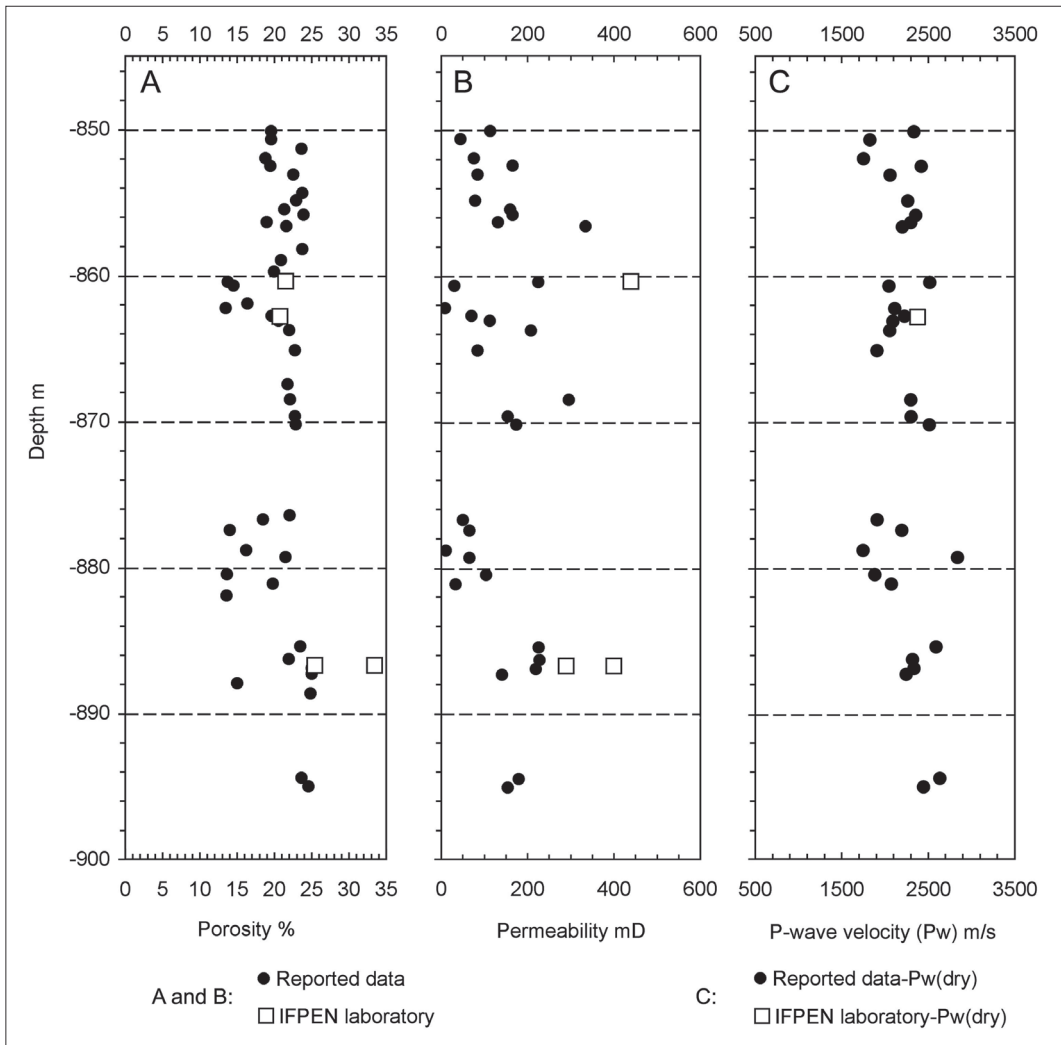


Fig. 6. Comparison plots of porosity, permeability and P-wave velocity versus depth of the measured samples (white squares) with the old reported data (black coloured figures) in the well E6-1/84 (modified from Shogenov et al., 2013).

dry samples 1750–2530 m/s (mean 2190 m/s), P_w of wet samples 1150–2440 m/s (mean 1800 m/s) (Andrushenko et al., 1985). Recently measured porosity (21–22 %) and P_w velocity of dry samples (2383 m/s) were in the range of the earlier data but new permeability was higher (440 mD) (Fig. 6, Shogenov et al., 2013).

The core interval 876–885 m is represented by very fine-grained silty sandstones interbedded by

silty clays. Oil impregnation is weak and irregular. Earlier the following characteristics have been reported: porosity 13–22 % (mean 17 %), permeability 10–100 mD (mean 55 mD), P_w of dry samples 1750–2850 m/s (mean 2110 m/s), P_w of wet samples 2120–2620 m/s (mean 2345 m/s). The reservoir properties of this interval are lower than in the upper level because of silty admixture in the rocks (about 30 % of reported samples), clayey

interlayers (no more than 5 cm) and poor sorting of the material.

The lower part of the formation (885–901 m) has regular but weak oil impregnation due to very well sorted sandstones and low clay content. The rocks are mostly massive, loosely cemented, strongly fractured and with very good reservoir properties: porosity 22–25 % (mean 24 %), permeability 140–230 mD (mean 190 mD), P_w of dry samples 2251–2643 m/s (mean 2435 m/s) (Andrushenko et al., 1985). New data on both porosity (25–33 %) and permeability (290–400 mD) were in the upper range of the old data or higher (Fig. 6, Shogenov et al., 2013).

Recently measured porosity of all samples from the well E6-1/84 was 21.5–33.5 % and gas permeability 290–440 mD. P_w of dry samples could be measured on only one sample, E6-862.8 m (2383 m/s). The properties of the E6 structure, estimated on the basis of reported and measured data, are as follows: total porosity 14–33.5 % (mean 21 %), permeability 10–440 mD (mean 180 mD), range of P_w velocity for dry samples 1750–2850 m/s (mean 2240 m/s) (Fig. 6, Table 1, Shogenov et al., 2013).

According to the classification of clastic oil and gas reservoirs by Hanin (1965), the reservoir rocks of the E6 structure are related to the 3rd and 4th classes of reservoir rocks (3rd class has permeability of 100–500 mD, 4th class permeability 10–100 mD). The residual water saturation of the 3rd class rocks is below 54.9 %, of the 4th class rocks more than 60 %.

Reported porosity and permeability of Upper Ordovician oil-bearing limestones are in the range of 10–23.5 % (mean 18 %) and 0.2–24 mD (mean 6 mD) respectively. Petrophysical measurements of other parts of Ordovician and Silurian cap rocks were not presented in the E6 exploration report. According to E7 report (Babuke et al., 1983) and reported measurements of more than 2000 samples from Baltic sedimentary basin (Shogenova et al., 2010) average porosity and permeability of Lower Ordovician (1) shales are 3 % and 0.001 mD respectively; (2) marlstones 3 % and 0.15 mD, respectively; (3) limestones 3 % and 6 mD respectively. Very few measurements of properties

of overlain Silurian rocks samples of the studied area are available in publications.

3.3 Chemical and mineralogical composition

Essentially pure sandstone samples (Table 1) studied from the E6 structure showed good interparticle and sometimes intraparticle open porosity (21–33.5 %). These sandstones include 95–98 % SiO₂ and 2–5 % other oxides, indicating clay (Al₂O₃ and TiO₂) and carbonate (CaO and MgO) cementation, and potassium feldspar admixture (K₂O) (Table 1, Fig. 7). Using SEM analyses accessory minerals were found in the cement matrix of the Deimena sandstone (iron sulphate, barite, anatase and brookite). However, cement content in the studied sample is insignificant (about 2–5 %). The results of XRD analyses supported the data obtained by XRF, chemical and SEM analyses. In general, sandstone samples from the E6 structure are considered as “high-quality” reservoir rocks (Shogenov et al., 2013).

3.4 CO₂ storage capacity

Shogenov et al. (2013) increased the closing contour of the E6 structure and determined it by the top depth contour of 1350 m (Fig. 5). The closing contour, reported by the LEGMC, was at 950 m (http://mapx.map.vgd.gov.lv/geo3/VGD_OIL_PAGE/). The line 76033 of the cross section, built on the basis of seismic data, crosses the Deimena Formation at a depth of 950 m. A propagation of a slope within the Deimena Formation could be clearly detected between the lines 76033 and Line1 (Fig. 4). We took into account depth range of the Deimena Formation and structural uplift within the E6 and fault system that separate the E6 structure from environing deposit surfaces. The total area of the structure is 600 km². With the 1350 m closure of the reservoir top, an approximate area of the larger part of the structure E6-A is 553 km², while the smaller part E6-B is 47 km². The thickness of the reservoir in the well is 53 m. The efficiency factor was taken to be 10 % (E6-A) and 4 % (E6-B) for

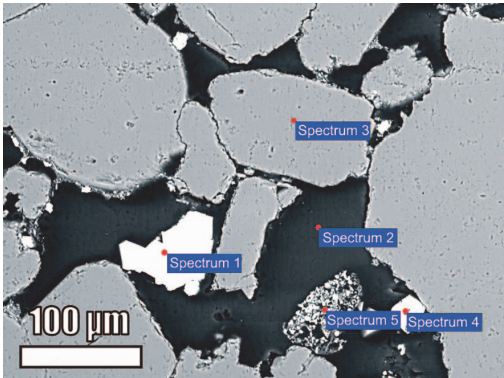


Fig. 7. SEM microphotograph of a thin section of the fine-grained porous (26–33 %) Deimena sandstone sample from the E6 structure, depth 886.7 m, and an example of SEM energy-dispersive x-ray spectroscopy (EDX) analyses (all results in weight %). The chemical composition of the sample is 97.4 % Si_2O , 0.3 % Al_2O_3 by XRF, and 1.1 % CaO and 0.25 % MgO by titration method. The white angular grain pointed by red called “Spectrum 1”, showing the content of Fe and S, is interpreted as iron sulphate. The black area (Spectrum 2) is porous space. Spectrum 3, located in grey subrounded to subangular grains (SiO_2), is quartz. The angular white grain analysed in point 4 with 33 % TiO_2 content (Spectrum 4) and the conglomeratic subrounded grain studied with 37 % TiO_2 in Spectrum 5 were interpreted as anatase and/or brookite accessory minerals.

Spectrum	C	Al	Si	P	S	Cl	Ca	Ti	Fe	Zr	O
Spectrum 1	8	-	2.6	-	18	-	-	-	15	0.94	56
Spectrum 2	25	-	4	-	0.08	0.07	-	0.09	0.07	-	71
Spectrum 3	10	-	29	-	-	-	-	-	-	-	60.6
Spectrum 4	8	0.6	6	-	-	-	-	33	0.18	-	51.7
Spectrum 5	-	3.4	11	2	0.5	-	0.5	37	0.6	-	44.5

the “optimistic” approach (Bachu et al., 2007) and 4 % (E6-A) and 2 % (E6-B) for the “conservative” approach (US DOE, 2008). In our previous study the optimistic CO_2 storage capacity of the E6 structure was estimated with efficiency factor 10 % (Shogenov et al., 2013). The NG was estimated as 90 % according to gamma-ray log data (Fig. 3). The value of ρ_{CO_2r} was 658 kg/m^3 , corresponding to a depth of 848 m and temperature 36 °C. The estimated minimum, maximum and average porosities of 14–33.5 % (mean 21 %) were used for calculation (Table 1). Estimated earlier theoretical CO_2 storage capacity of the E6 structure was 265–630 Mt (mean 395 Mt) based on the optimistic approach, and 105–250 Mt (mean 160 Mt) based on the conservative approach (Shogenov et al., 2013). In this study we reduced the optimistic storage capacity of the entire structure to 251–602 Mt (mean 377 Mt) (Table 2). We estimated the theoretical optimistic and conservative CO_2 storage capacity of two split parts of the reservoir separately. Based on the optimistic approach CO_2 storage capacity of the E6-A part was 243–582 Mt (mean

365 Mt) and E6-B part 8–20 Mt (mean 12 Mt). Conservative capacity of the E6-A was 97–233 Mt (mean 146 Mt) and capacity of the E6-B part was 4–10 Mt (mean 6 Mt).

4. Offshore structure E7

4.1 Geological background

The E7 structure is a brachyanticline fold within the Deimena Formation, stretching from NE to SW and bounded by faults at two sides (north and east) (Fig. 8). It was explored in 1982 only by one well E7-1/82 (depth 1623 m) located 85 km from the coast of Latvia (Shogenov et al., 2013). The structure is represented by uplifted Middle Cambrian 58 m thick reservoir rocks covered by 42 m thick Lower Ordovician clayey cap rocks (Fig. 3). The reservoir is overlain by Ordovician and Silurian (in total 322 m thick) clayey carbonate rocks and Devonian siliciclastic and carbonate rocks. The temperature within the reservoir is 46 °C, salinity of the Cambrian aquifer is 125 g/l (Table 2).

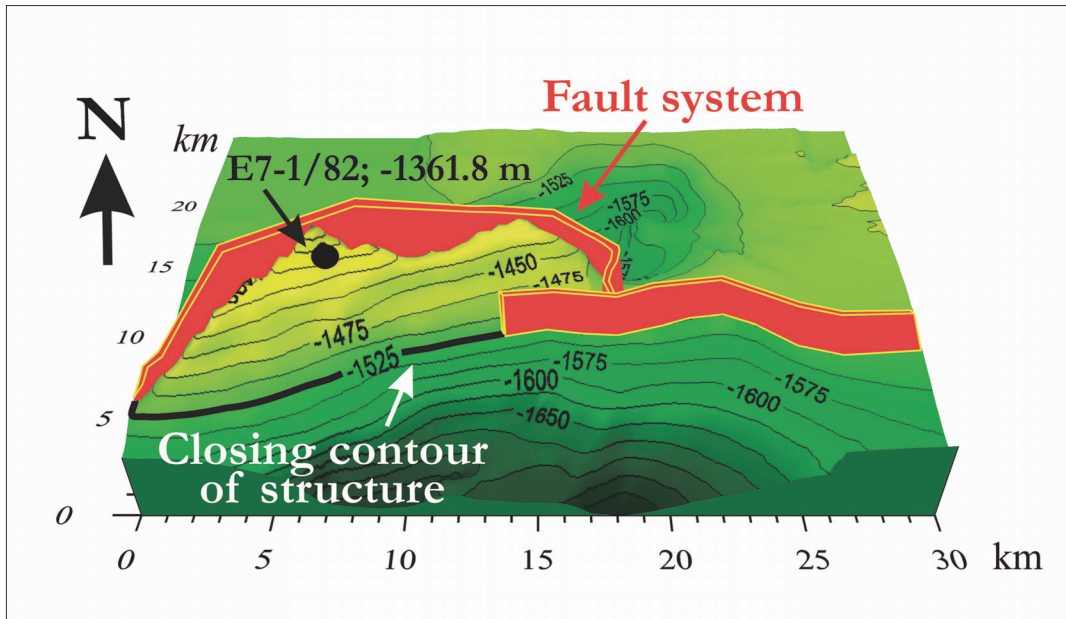


Fig. 8. 3D geological model of the top of the Deimena Formation in the E7 structure with the estimated closing contour of the structure (black contour -1525 m). Faults bordering the structure are shown by a red wall. Location of the well is shown by a black circle with the depth of the top of the formation (-1361.8 m) (modified from Shogenov et al., 2013).

4.2 Petrophysical properties

According to the reported in Babuke et al., (1983) data, sandstones from the E7 drill core have relatively good reservoir properties: porosity 5–23 % (mean 12 %), permeability 0.2–170 mD (mean 50 mD), P_w velocity in dry samples 2200–3515 m/s (mean 2990 m/s). The average porosity of siltstones presented in the reservoir is 12 % and permeability 20 mD (Fig. 9). Recently measured P_w velocity of dry samples was 2130–3580 m/s (mean 2814 m/s), S_w velocity of dry samples 1725–2230 m/s (mean 2050 m/s) (Shogenov et al., 2013). Considering both the reported and measured data, the range of porosity in the E7 structure is 5–23 % (mean 12%), gas permeability 0.1–170 mD (mean 40 mD), P_w velocity of dry samples 2130–3583 m/s (mean 2920 m/s), range of S_w velocity of dry samples 1725–2230 m/s (mean 2050 m/s) (Table 1, Fig. 9). Figure 9 clearly shows that measured values are totally in the range of reported data.

Oil impregnation within the E7 reservoir was

not observed. Reservoir properties of the E7 trapping rocks are significantly lower than in the E6 sandstones. According to the classification of clastic oil and gas reservoirs by Hanin (1965), the reservoir rocks of the E7 structure are related to the 3rd, 4th and 5th classes of reservoir rocks (5th class rocks have permeability of 1–10 mD).

Average porosity and permeability of Ordovician (1) shales are 3 % and 0.001 mD respectively; (2) marlstones 7 % and 0.29 mD, respectively; (3) limestones 3 % and 0.06 mD respectively. Very few measurements of Silurian shales properties are presented in the report (Babuke et al., 1983). Several measured marlstone samples showed good porosity (7–9 %) but very low permeability (0.001 mD).

4.3 Chemical and mineralogical composition

The Deimena Formation is represented by light-grey and beige-grey fine-grained quartz sandstones

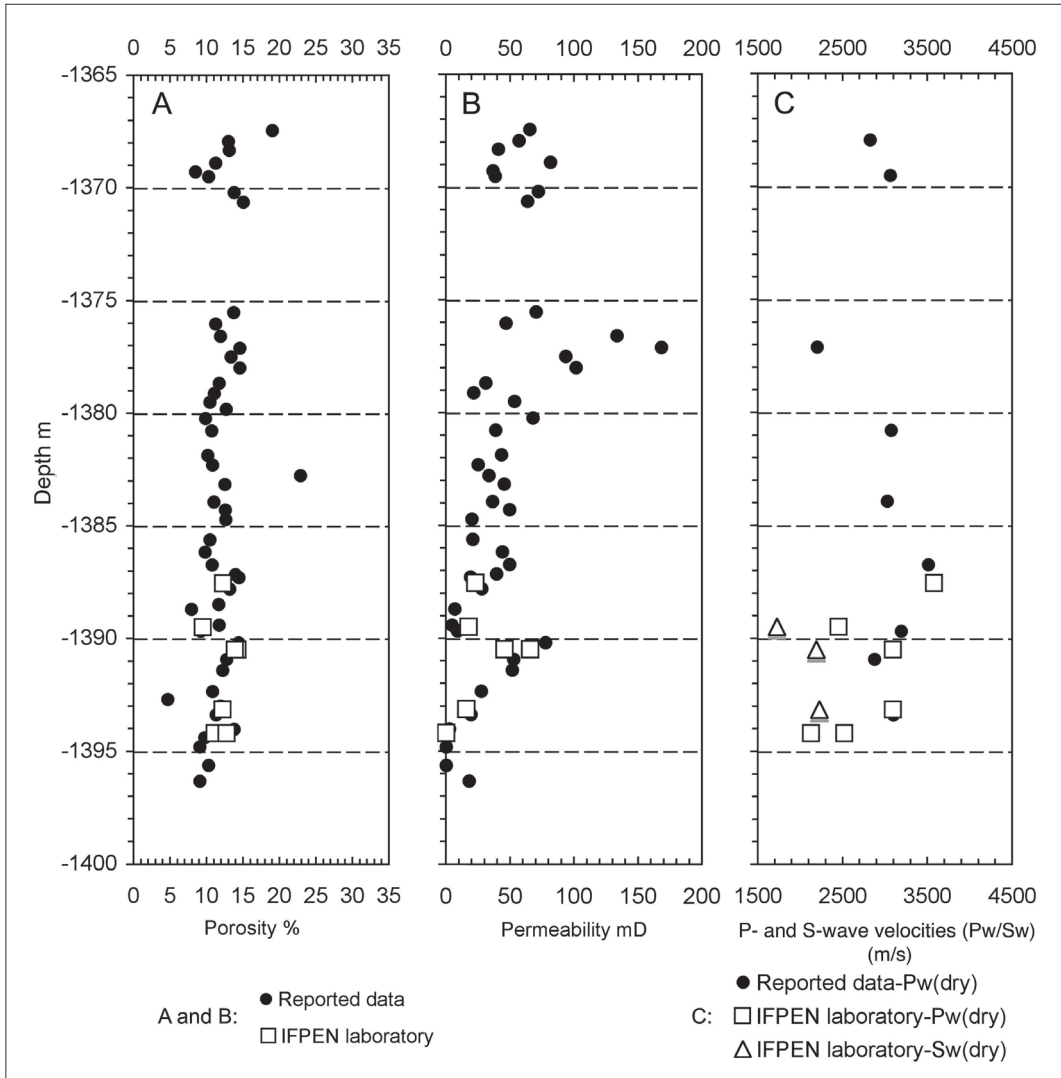


Fig. 9. Comparison plots of porosity, permeability and P-wave velocity of dry samples versus depth of the measured samples (white squares) with the old reported data (black circles) in well E7-1/82. S-wave velocity of the measured samples (white triangles) are shown on the velocity plot.

interbedded by thin layers of sandy marlstones and clayey siltstones (4–5 cm), reflected by increased readings of the gamma-ray log compared to pure sandstones (Fig. 3). Sandstones are well sorted and subrounded, partly fractured. Compared to the essentially pure quartz sandstone samples from the

E6-1/84 well, the samples from E7-1/82 showed an increase in clay content and a decrease in free pore space. Especially high clay cement content was observed in samples from the clayey siltstone interbeds. Rocks of the upper part of the Deimena Formation are mostly cemented by quartz-regenerated

cement, those of the lower part by conformation of quartz grains due to dissolution under the pressure (Shogenov et al., 2013).

Samples from the E7 structure contain on average 87–99 % SiO₂ and 1–13 % other oxides, indicating clay and carbonate cementation (Table 1). In two samples (1393.55 and 1394.2 m) the SiO₂ content was 90 and 87 %, Al₂O₃ content, indicating clay cement, 4 and 5 %, and Fe₂O₃ content 0.9 and 1.9 %, respectively. The content of carbonate minerals was lower (on average 1 % CaO and 0.4 % MgO). Samples also include admixture of feldspar and mica. Accessory minerals such as zircon, tourmaline and pyrite are present. Clay

fraction is represented by illite and kaolinite (Fig. 10).

Sandstones (depths 1389.5 and 1390.5 m), studied also by the SEM and XRD methods, showed lower porosity (14.3 and 9.5 % respectively) and higher cement content than the E6 sandstones (Fig. 10).

4.4 CO₂ storage capacity

The closing contour of the E7 reported by the LEGMC is 1450 m (http://mapx.map.vgd.gov.lv/geo3/VGD_OIL_PAGE/). According to depth range of the Deimena Formation and faults system

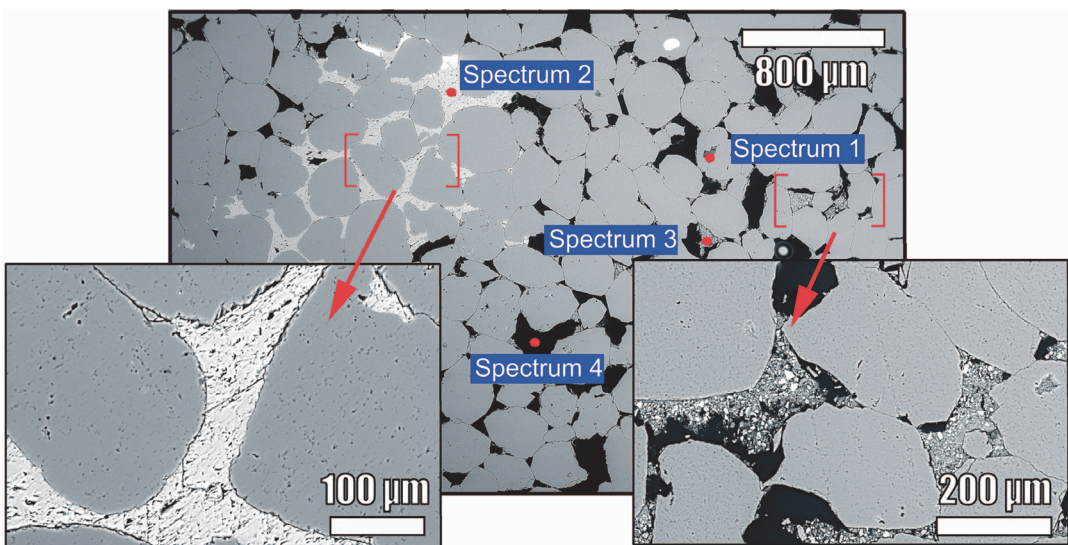


Fig. 10. SEM microphotographs of the thin section of the fine-grained porous Deimena sandstones sample in well E7/1-82 (1390.5 m) and an example of SEM energy-dispersive X-ray spectroscopy (EDX) analysis results (in weight %). Porous media studied by Spectrum 1 is partly filled by quartz cement (30 % SiO₂). White cement studied by Spectrum 2 is composed of iron-rich carbonate cementation including ankerite (15 % Ca, 5 % Mg and 8 % Fe). Some pores are filled by clay cement (4.5 % Al) and feldspar admixture (3 % K) (Spectrum 3). The black area studied by Spectrum 4 is porous media.

Spectrum	C	Mg	Al	Si	S	Cl	K	Ca	Mn	Fe	Ba	O
Spectrum 1	9.7	-	0.4	29.7	-	-	-	-	-	-	-	60
Spectrum 2	13.5	4.7	-	5	-	-	-	15	1	8	-	53
Spectrum 3	-	2	4.5	34	0.7	-	2.7	3.6	-	2.4	2.5	48
Spectrum 4	25.7	-	-	3	-	0.06	-	-	-	-	-	71.5

bounding the structure, and structural uplift within the E7 structure, we increased the boundaries of the structure and took the 1525 m depth as the closing contour of the reservoir top. In case of the 1525 m level, an approximate area of the E7 structure (43 km²) is 14 times less than that of the E6 (Shogenov et al., 2013).

The thickness of the reservoir in the well is 58 m. The efficiency factor of 20 % was taken for the “optimistic” approach (Bachu et al., 2007) and 4 % for the “conservative” approach (US DOE, 2008). The NG was found to be 80 % according to the gamma-ray log data (Fig. 3). The value of ρ_{CO_2} was taken 727 kg/m³, corresponding to a depth of 1362 m and temperature 46 °C. The estimated minimum, maximum and average porosities of 5–23 % (mean 12 %) were used for calculation (Table 1). The assessed CO₂ storage capacity of the E7 structure was 14–66 Mt (mean 34 Mt) by the optimistic approach and 3–13 Mt (mean 7 Mt) by the conservative approach (Table 2, Shogenov et al., 2013).

5. Discussion

In this study we used old exploration reports of years 1983–1985 (Babuke et al., 1983; Andrushenko et al., 1985). The quality of these reports is satisfactory, but characteristics of the E7 structure are worse than of E6. Earlier studies were made only in the frame of oil exploration. As the aims of the old and present studies are different, we lack necessary data and face uncertainties in existing information (only one well drilled in each structure, insufficient level of fault study, lack of necessary rock physical measurements, the reported values of the same parameters vary in different parts of the exploration reports, low quality of seismic map profiles). Complete seismic data on these structures were not available for this and previous (Shogenov et al., 2013) studies, which added uncertainties into the created 3D geological models and storage reservoirs quality estimates. The E6 structure contains multiple faults, and uncertainties in the fault structure could cause significant difficulties in the assessment and modelling of CO₂ storage risks. Due to fact of oil

accumulation in the Upper Ordovician limestone formation and Cambrian Deimena sandstones, and Devonian sandstones oil impregnation, the hypothesis of oil leakage from the E6 reservoir via faults could be assumed. There are two possible scenarios of the faults behaviour: (1) the faults still have open structure and (2) due to timing and geological processes the faults were locked. The origin of faults and reservoirs architecture need more detailed study, which would largely contribute to estimation of reservoirs integrity.

There are two ways to clarify these uncertainties: (1) to conduct a modern geophysical exploration in the studied structures area or (2) to make pilot CO₂ injection into the structure and monitor its behaviour. If the reservoirs are destructed and the faults have open structure, the CO₂ leakage could be determined using known monitoring methods. Seismic survey is the most effective method that has been implemented in the well-known world's largest CO₂ storage project in the Norwegian North Sea (Sleipner) for monitoring injected CO₂ plume. This method enables observation from the surface of the formation and migrating of CO₂, injected into the storage site, under impermeable layers (Chadwick et al., 2009; Hermanrud et al., 2009; Alnes et al., 2011).

Besides practical study, wide modelling possibilities are available in the field. In addition, a number of papers have been published during last years, including numerical modelling of CO₂ plume dissolution mechanisms in an aquifer (Audigane et al., 2011), CO₂ fluid flow studies and 2D/3D modelling, associated with the fault system in long and short terms (Audigane et al., 2007; Chang et al., 2008; Grimstad et al., 2009; Chadwick & Noy, 2010). The last seismic numerical modelling results represent performance of seismic techniques and methods in detection of presence, evolution, migration and leakage of CO₂ in the storage reservoir (Rossi et al., 2008; Picotti et al., 2012).

The existing fault system, interpreted by seismic data and oil impregnation of Cambrian sandstones revealed in drill core E6-1/84, would suggest two optional cases. The first case is possible leakage of the geological trap. The opposite one is that the

reservoir has good trapping mechanisms, but trapped oil in the reservoir could be lacking due to specific in situ conditions and geological history of the area. The first case is discussed by Chang et al., (2008). They developed a single-phase flow model to examine CO₂ migration along faults. The model simulated CO₂ migration from the fault into permeable layers. Reaching these layers, CO₂ continued migration along the fault above them. The developed 1D model was compared with full-physics simulations in 2D. It was concluded that although more CO₂ escapes from a deeper storage formation through a fault, less CO₂ reaches the top of the fault. Thus, attenuation can reduce the risk associated with CO₂ reaching the top of the fault (Chang et al., 2008).

However, the presence of faults does not mean that there would be an impact on security of storage. If the offset of a fault is less than the thickness of the cap rock the likelihood of providing a migration pathway through the cap rock is lower (Bentham et al., 2013). As well, faults integrity plays crucial role in reservoir security. According to available studies in the region, faults could propagate through the all cap rocks (Ordovician and Silurian) reaching Devonian sandstone layer. Nevertheless, the largest onshore Inčukalns structure with the relevant for the Baltic Basin fault offset has been successfully used for underground gas storage for many years and is applied for gas supply of Latvia, Estonia and Lithuania. This fact gives us opportunity to suggest that faults in the region could have enclosed, impermeable structure (LEGMC, 2007). The conditions of every reservoir for geological storage of different gases should be studied individually. For example properties of CO₂ and methane in deep in situ conditions could significantly vary. Migration of CO₂ via faults to depths shallower than 800 m is classified as a risk due to the properties of CO₂. In normal geothermal and pressure regimes CO₂ below 800 m is likely to be in its highly dense phase, above approximately this depth (depending on the exact pressure and temperature) the migrating CO₂ may undergo a phase change due to the decreasing pressure and temperature and become gaseous. The CO₂ would then expand and migrate faster. This

could cause a more serious leakage of CO₂ depending on the surrounding geology (Bentham et al., 2013).

Understanding of faults capacity is a key for further studies that should clarify the storage potential and integrity risk of the studied structures. As was mentioned above the pilot injection of several thousands of CO₂ could clarify this uncertainty.

Due to splitting of the E6 structure by faults into the two compartments the E6-A and the E6-B with area of 553 km² and 47 km² respectively, we propose the E6-A to be the main CO₂ storage site within the structure and the E6-B an additional reserve structure. Using the both substructures should be economic considering the location of the E6-A next to the E6-B and the common infrastructure to be used. Nevertheless, the E6-A, as a largest storage site in the region, will be an object of study in our next fluid flow and seismic numerical simulations.

6. Conclusions

Two offshore geological structures of Latvia E6 and E7 were estimated as prospective reservoirs for gas storage. These structures have structural closing contour within the Cambrian saline aquifer and are overlain by an impermeable seal. They are therefore suitable for CO₂ storage. Nevertheless, the lack of modern seismic data makes additional uncertainties of structural integrity. The Deimena Formation of Middle Cambrian is clearly indicated by low natural radioactivity on gamma-ray log readings. Clayey interbeds and siltstone layers in the reservoir can be easily determined (from 10 % to 20 % of reservoir rocks) by increased gamma-ray readings (Shogenov et al., 2013). The average net to gross ratio of the aquifer in the trap was defined by gamma-ray log readings (90 % in E6, 80 % in E7). Cap rock is represented by Ordovician and Silurian clayey carbonate sediments.

New estimated total optimistic CO₂ storage capacity in the most prospective for CGS in the Baltic Region offshore structure E6 was in the range of 251–602 Mt (average 377 Mt). However, the risk of CO₂ leakage due to uncertainties of fault system should be considered and further fault

integrity risk assessment work is required.

New re-estimated total capacity of two offshore structures E6 and E7 by the optimistic approach was 265–668 Mt (on average 411 Mt). The optimistic maximum (602 Mt) and average (377 Mt) storage potential of the E6 structure is higher and nearly the same respectively as previously reported total potential of all 16 onshore Latvian structures (400 Mt). Even its average conservative capacity (152 Mt) is the largest among all the onshore and offshore structures studied until now in Latvia.

Two split by faults compartments of the E6 structure were considered as separate substructures defined as E6-A and E6-B. Estimated theoretical CO₂ storage capacity of the E6-A was 243–582 Mt (mean 365 Mt) and E6-B part 8–20 Mt (mean 12 Mt) according to optimistic approach. Estimated conservative capacity of the E6-A was 97–233 Mt (mean 146 Mt) and of E6-B part 4–10 Mt (mean 6 Mt). Estimated area and conservative average capacity of E6-B part were in the same range as the area and conservative capacity of E7 structure (47 km² and 6 Mt in E6-B, respectively and 43 km² and 7 Mt in E-7, respectively).

This study is a basis for new 3D static geological, lithological and petrophysical numerical modelling of the E6-A substructure that will be applied in CO₂ storage fluid flow simulation. The last will be integrated into time-lapse (4D) rock physics and seismic numerical modeling.

Acknowledgements

This research, which is part of the first author's PhD study, was supported by the Estonian targeted funding programme (project SF0320080s07) and partially funded by the Archimedes Foundation programme DoRa, Estonian Doctoral School of Earth Sciences and Ecology, EU FP7 project CGS EUROPE, EU FP7 Programme, Marie Curie Research Training Network "Quantitative Estimation of Earth's Seismic Sources and Structure" (QUEST), Contract No. 238007 and project "ERMAS" of the Estonian national R&D Programme KES-TA. We would like to thank Jean Guelard (IFPEN) for permeability measurements and other guidance in petrophysical laboratory, Jean-François Nauroy (IFPEN) for acoustic velocity measurements, Dan Bossie-Codreanu (IFPEN) for the fruitful discussion and helpful advices, and Dr Nicolass Molenaar

(DTU) and Dr Joonas Virtasalo (GTK) for their useful recommendations made during revision of the article. We are also very grateful to the LEGMC for providing samples and exploration reports for this study.

References

- Alnes, H., Eiken, O., Nooner, S., Sasagawa, G., Stenvold, T. & Zumberge, M. 2011. Results from Sleipner gravity monitoring: Updated density and temperature distribution of the CO₂ plume. *Energy Procedia* 4, 5504–5511.
- American Petroleum Institute, 1998. Recommended Practices for Core Analysis. Second Edition, Recommended Practice 40, Exploration and Production Department. 60 p.
- Andrushenko, J., Vzosek, R., Krochka, V., Hubldikov, A., Lobanov, V., Novikov, E., Hafenshtain, K., Tsimashevski, K. & Labus, R., 1985. Report on the results of drilling and geological and geophysical studies in the exploration well E6-1/84. Unpublished exploration report of E6-1/84 offshore well. Latvian Environmental, Geology and Meteorology Centre (LEGMC), Latvia, Riga. (In Russian)
- Audigane, P., Gaus, I., Czernichowski-Lauriol, I., Pruess, K. & Xu, T. 2007. Two dimensional reactive transport modelling of CO₂ injection in a saline aquifer at the Sleipner site, North Sea. *American Journal of Science* 307, 974–1008.
- Audigane, P., Chiaberge, C., Mathurin, F., Lions, J. & Picot-Colbeaux, G. 2011. A workflow for handling heterogeneous 3D models with the TOUGH2 family of codes. Applications to numerical modeling of CO₂ geological storage. *Computers and Geosciences* 37, 610–620.
- Babuke, B., Vzosek, R., Grachev, A., Naidenov, V., Krochka, V., Markov, P., Novikov, E., Tsimashevski, L. & Labus, R., 1983. Geological report of the well E7-1/82. Unpublished exploration report of E7-1/82 offshore well. Latvian Environmental, Geology and Meteorology Centre (LEGMC), Latvia, Riga. (In Russian)
- Bachu, S. 2003. Screening and ranking sedimentary basins for sequestration of CO₂ in geological media in response to climate change. *Environmental Geology* 44, 277–289.
- Bachu, S., Bonijoly, D., Bradshaw, J., Burruss, R., Christensen, N.P., Holloway, S. & Mathiassen, O.M., 2007. Estimation of CO₂ storage capacity in geological media – phase 2. Work under the auspices of the Carbon Sequestration Leadership Forum (www.cslforum.org). Final report from the task force for review and identification of standards for CO₂ storage capacity estimation.
- Bentham, M.S., Green, A. & Grammer, D. 2013. The occurrence of faults in the Bunter Sandstone Formation of the UK sector of the Southern North Sea and the potential impact on storage capacity. *Energy Procedia*, 1–9 (in press).
- Chadwick, A., Noy, D., Arts, R.J. & Eiken, O. 2009. Latest time-lapse seismic data from Sleipner yield new insights

- into CO₂ plume development. *Energy Procedia* 1, 2103–2110.
- Chadwick, A. & Noy, D.J. 2010. History-matching flow simulations and time-lapse seismic data from the Sleipner CO₂ plume. Geological Society, London, Petroleum Geology Conference series 7, 1171–1182.
- Chang, K.W., Minkoff, S. & Bryant, S. 2008. Modeling leakage through faults of CO₂ stored in an aquifer. SPE Annual Technical Conference and Exhibition, Denver, Colorado, USA.
- Grimstad, A.A., Georgescu, S., Lindeberg, E. & Vuillaume, J.F. 2009. Modelling and simulation of mechanisms for leakage of CO₂ from geological storage. *Energy Procedia* 1, 2511–2518.
- Hanin, A.A. 1965. Oil and gas reservoir rocks. Moscow, Publishing House Nedra. 362 p. (In Russian)
- Hermanrud, C., Andresen, T., Eiken, O., Hansen, H., Janbu, A., Lippard, J., Bolås, H.N. et al., 2009. Storage of CO₂ in saline aquifers – Lessons learned from 10 years of injection into the Utsira Formation in the Sleipner area. *Energy Procedia* 1, 1997–2004.
- LEGMC, 2007. Geological structures for the establishment of underground gas storages. Geological description for the information material “On the possibilities of use of the Latvian geological structures”. Riga, Latvia. 16 p.
- Picotti, S., Carcione, J.M., Gei, D., Rossi, G. & Santos, J.E. 2012. Seismic modeling to monitor CO₂ geological storage: The Atzbach-Schwanenstadt gas field. *Journal of Geophysical Research* 117, B06103.
- Rossi, G., Gei, D., Picotti, S. & Carcione, J.M. 2008. CO₂ storage at the Atzbach-Schwanenstadt gas field: a seismic monitoring feasibility study. *First Break* 26, 45–51.
- Shogenov, K., Shogenova, A. & Vizika-Kavvadias, O. 2013. Petrophysical properties and capacity of prospective structures for geological storage of CO₂ onshore and offshore Baltic. *Energy Procedia*, in press, 1-8.
- Shogenova, A., Sliupa, S., Vaher, R., Shogenov, K. & Pomeranceva, R. 2009a. The Baltic Basin: structure, properties of reservoir rocks and capacity for geological storage of CO₂. *Estonian Journal of Earth Sciences* 58, 259–267.
- Shogenova, A., Šliaupa, S., Shogenov, K., Šliaupiene, R., Pomeranceva, R., Vaher, R., Uibu, M. & Kuusik, R. 2009b. Possibilities for geological storage and mineral trapping of industrial CO₂ emissions in the Baltic region. *Energy Procedia* 1, 2753–2760.
- Shogenova, A., Kleesment, A., Shogenov, K., Pöldvere, A. & Jõelet, A. 2010. Composition and properties of Estonian Palaeozoic and Ediacaran sedimentary rocks. 72nd EAGE Conference & Exhibition incorporating SPE EUROPEC 2010, 14-17 June 2010, Barcelona. EAGE, The Netherlands, p. 1-5.
- Shogenova, A., Shogenov, K., Vaher, R., Ivask, J., Sliupa, S., Vangkilde-Pedersen, T., Uibu, M. & Kuusik, R. 2011a. CO₂ geological storage capacity analysis in Estonia and neighboring regions. *Energy Procedia* 4, 2785–2792.
- Shogenova, A., Shogenov, K., Pomeranceva, R., Nulle, I., Neele, F. & Hendriks, C. 2011b. Economic modelling of the capture–transport–sink scenario of industrial CO₂ emissions: the Estonian–Latvian cross-border case study. Elsevier, The Netherlands. *Energy Procedia* 4, 2385–2392.
- Sliupa, S., Shogenova, A., Shogenov, K., Sliupiene, R., Zabele, A. & Vaher, R. 2008. Industrial carbon dioxide emissions and potential geological sinks in the Baltic States. *Oil Shale* 25, 465–484.
- US Department of Energy (US DOE), 2008. Methodology for development of geological storage estimates for carbon dioxide. 37 p.
- Van der Meer, B. & Egberts, P. 2008. A general method for calculating subsurface CO₂ storage capacity. Offshore Technology Conference, TA Utrecht, The Netherlands. OTC 19309, 1-9.
- Vangkilde-Pedersen, T. & Kirk, K. (eds.) 2009. FP6 EU GeoCapacity Project, Assessing European Capacity for Geological Storage of Carbon Dioxide, Storage Capacity. D26, WP4 report Capacity standards and site selection criteria, 45 pp., <http://www.geology.cz/geocapacity/publications>.
- Zdanov, M.A. 1981. Geology and evaluation of oil and gas. Second Edition, Publishing House “Nedra”, Moscow. 453 p. (In Russian)

PAPER III. SHOGENOV, K. & GEI, D. 2013. Seismic numerical modelling to monitor CO₂ storage in the Baltic Sea offshore structure. 10-13 June 2013, London, UK, Extended Abstract. EAGE, ID 16848, Tu-P08-13, 1–4.

Tu-P08-12

Seismic Numerical Modelling to Monitor CO₂ Storage in the Baltic Sea Offshore Structure

K. Shogenov* (OGS, Trieste) & D. Gei (OGS, Trieste)

SUMMARY

This study is a part of CO₂ geological storage research in the Baltic Region. Our research shows the effectiveness of seismic numerical modelling methodology, in particular, synthetic plane-wave and difference sections, to detect the presence of CO₂ in deep saline aquifer of Cambrian Deimena Sandstone Reservoir Formation in the E6 Baltic offshore structure for various saturation levels. Our results clearly show the applicability of seismic methods to monitor CO₂ plume within the studied Baltic Sea offshore storage site E6. This study plays a crucial role in developing an optimal seismic monitoring plan in the studied area.

Introduction

Our study is a part of CO₂ capture and geological storage (CCS/CGS) study in the Baltic Region. CCS plays an essential role in reducing the greenhouse gas effect and mitigating climate change on our planet. In this research we have applied time-lapse (4D) rock physics and seismic numerical modelling methodology, developed at the Istituto Nazionale di Oceanografia e di Geofisica Sperimentale (OGS), to compute synthetic seismograms and analyse seismic response while injecting CO₂ into a deep geological structure in the Baltic Sea Region and to design basis for further CGS monitoring plan in the region. This is an important technology to predict the seismic response to the presence of CO₂ in the storage site, to monitor CO₂ plume migration within the reservoir, estimate reservoir integrity and support possible leakage notification. This method allows to optimize the seismic surveys, which should be repeated over time to monitor the evolution of the injected CO₂ (Rossi et al., 2008; Picotti et al., 2012).

We selected the most prospective offshore oil-bearing geological structure E6 suitable for trapping of CO₂ in the Latvian offshore Baltic Sea Region. Middle Cambrian Deimena Sandstone Formation was estimated as a high quality reservoir for CGS in the E6 anticline structure prospective for CO₂ storage. The formation is 53 m thick saline aquifer with depth over 800 meters and salinity of 99000 ppm. The reservoir is unconformably overlain by 146 m thick impermeable Ordovician cap rock, consisting mainly of claystones, carbonated clays, marlstones and limestones (Shogenov et al., 2013). Input data play a critical role in sensitivity and quality of numerical modelling result. In this study a reliable description of CO₂ bearing reservoir rock properties is necessary. However, velocities from active seismic were not available. We have used rock physical properties of reservoir formation rocks measured in laboratory conditions. For layers above and below the storage formation we have considered laboratory measurements published in the exploration report of the E6 structure and in other studies of the Baltic Region (Shogenov et al., 2013, Shogenova et al. 2001), and values of rock properties estimated from empirical relations. We developed a geological model (Figure 1) defining the main formations, and populated it with petrophysical properties (temperature, pressure, solid rock composition, fluid saturation, porosity, density, acoustic wave velocities and quality factors). We have computed the seismic properties of the reservoir saturated with different saturation levels of CO₂, evaluated the seismic response and compared the results with initial conditions using difference sections and NRMS methodology.

Methodology

Using an available seismic section of the E6 offshore structure, interpreted in Shogenov et al. (2013), we set up a 2D model consisting of 10 main geological layers (Figure 1). We implemented vertical heterogeneity within the reservoir layer and split the Middle Cambrian Deimena Reservoir into three parts according their specific physical properties (Reservoir-1, -2 and -3 shown by yellow, pink and brown colours in the Figure 1, respectively). In the horizontal direction the reservoir was estimated to be homogeneous. Thin 10 meters black coloured layer between Ordovician and Silurian formations is Upper Ordovician oil reservoir. All the formations are characterized by specific constant rock properties (Table 1). Evaluated rock properties are strongly dependent on in situ conditions. We extrapolated temperature and pressure values for all layers of our model using measured data and gradients reported for the reservoir and cap rock layers.

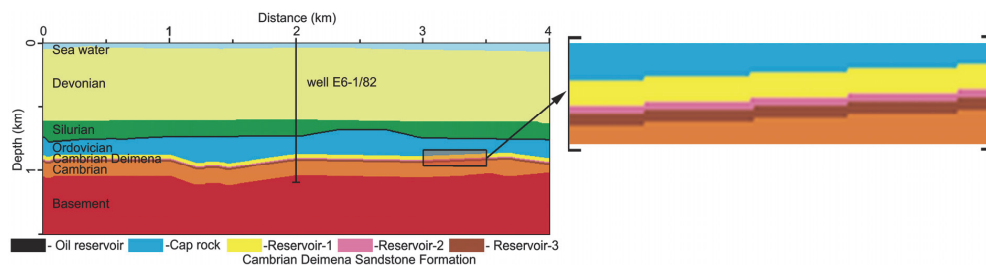


Figure 1 2D geological model extrapolated from E6 seismic section with well E6-1/82 in the centre.

Table 1 Seismic and physical properties of main rock formations shown in the model (Figure 1).

Formation	Lithology	T (°C)	P (MPa)	ρ_{wet} (kg/m ³)	Φ (%)	κ (mD)	V_P (m/s)	V_S (m/s)	Q_P	Q_S	μ (Gpa)	K (Gpa)
Sea water	-	10-7	0.1-0.8	1030	-	-	1480	0	-	-	-	-
Devonian	Sandstone	7-31	0.8-6.3	2226	15	2	2750	1355	81	26	4.1	-
Silurian	Claystone	31-35	6.3-8.4	2342	0	~ 0.01	3000	2369	97	81	13.1	-
Ordovician (Oil reservoir)	Limestone	35	8.4-8.6	2438	15	7	2970	1295	95	24	4.1	-
Ordovician (Cap rock)	Claystone-carbonated	35-37	8.6-9.3	2539	3	~ 0.001	4800	2220	248	71	12.5	-
Deimena (Reservoir-1)	Sandstone	37	9.3-9.7	2312	21	130	3271	1610	142	51	5.99	11.9
Deimena (Reservoir-2)	Sandstone	37	9.7-9.8	2375	17	80	3108	1435	147	48	4.89	9.72
Deimena (Reservoir-3)	Sandstone	37-38	9.8-10	2280	23	170	3233	1591	213	75	5.77	11.47
Cambrian	Siltstone	38-41	10-11.2	2324	0-19	0.2-23	3248	2141	114	66	10.7	-
Basement	Granite	41-...	11.2-...	2650	-	-	5800	3200	362	147	27.1	-

All formations except the Oil Reservoir are saturated with brine. Temperature (T) and pressure (P) of the formations top and bottom are shown. ρ_{wet} is the bulk density of brine saturated rock samples. Density of the brine at in situ conditions within the reservoir layers (1066.7 kg/m³) was computed using Batzle and Wang (1992) equations. Φ - average porosity; κ - average permeability; V_P and V_S - compressional (P) and shear (S) waves velocities, respectively; Q_P and Q_S - quality factors of P - and S -waves, respectively; μ and K - shear and bulk modules of dry rocks, respectively (K estimated for reservoir formations)

We applied the White's mesoscopic rock physics theory (White, 1975) to compute the P -wave velocity (V_P) and attenuation of a partially saturated medium. The S -wave (V_S) properties were computed as a function of shear modulus of dry rocks (μ) and bulk density of brine saturated rocks (ρ_{wet}). μ was estimated as function of V_S of dry rocks (V_{Sdry}) and density of dry rocks (ρ_{dry}). The V_{Sdry} was estimated as a function of V_P of dry samples (V_{Pdry}) and the ratio $V_{Pdry}/V_{Sdry}=1.41$, measured from the nearby offshore structure E7. The evaluated coefficient is in the range of common values for dry sandstone samples reported by Sudhir (1987). We estimated properties of reservoir rocks with different CO_2 saturations, specifically 5%, 10%, 15%, 50% and 90% (Table 2). White's theory provides realistic P -wave velocity and quality factors as a function of porosity, dry rock properties, gas saturation, fluid viscosity, permeability and dominant frequency of the seismic pulse. The saturation is assumed to be patchy, considering spherical gas pockets much larger than the solid grains of the sediment but much smaller than the wavelength. We computed plane-wave seismic sections (Figure 2 a, b) using time-domain equations for propagation in a heterogeneous viscoelastic medium (Carcione, 2007). The geological model (4 km in horizontal and 1.5 km in vertical directions, respectively) was discretized with a numerical mesh of 240000 (800 x 300) grid points and grid spacing of 5 m. In order to avoid wraparound effects in the modelling, absorbing strips of 40 grid-point lengths were implemented at the bottom and sides of the numerical mesh. A Ricker wavelet with a dominant frequency of 35 Hz was used as source time history. The differential equations were solved with a 4th-order Runge-Kutta time-stepping scheme and the staggered Fourier method for computing the spatial derivatives, which is noise-free in the dynamic range where regular grids generate artifacts that may have amplitudes similar to those of physical arrivals (Carcione, 2007). We performed plane-wave simulations that approximate non-migrated zero-offset sections by triggering simultaneously sources located in each grid point of the upper edge of the numerical mesh represented by the model. This procedure produces a plane wave propagating downward. Every time the plane-wave impinges upon the interface between two different formations, it is reflected back to upper edge of the geological model, coinciding with the sea surface, where seismic sensors record the seismic wave-field.

Difference and normalized root mean square (NRMS) sections of 4D seismic data are effective tools to indicate differences such as phase shifts of amplitude variations in time-lapse datasets (Picotti et al., 2012). We performed NRMS difference technique to compare seismic datasets before and after CO_2

injection simulating seismic acquisitions at different times over the same studied area (Kragh and Christie, 2002).

Table 2 Seismic properties of the Middle Cambrian Deimena Sandstone Formation partially saturated with CO₂.

Formation		Fluid saturation	ρ (kg/m ³)	V _P (m/s)	V _S (m/s)	Q _P	Q _S
Middle Cambrian Deimena Sandstone Formation	Reservoir-1	Brine (95%)+CO ₂ (5%)	2307	3012	1626	115	45
		Brine (90%)+CO ₂ (10%)	2302	2984	1623	169	67
		Brine (85%)+CO ₂ (15%)	2297	2973	1622	249	99
		Brine (50%)+CO ₂ (50%)	2262	2973	1628	2616	1046
		Brine (10%)+CO ₂ (90%)	2222	2996	1642	314957	126157
	Reservoir-2	Brine (95%)+CO ₂ (5%)	2371	2745	1454	89	34
		Brine (90%)+CO ₂ (10%)	2367	2697	1450	122	47
		Brine (85%)+CO ₂ (15%)	2363	2675	1447	175	68
		Brine (50%)+CO ₂ (50%)	2336	2652	1448	1723	685
		Brine (10%)+CO ₂ (90%)	2305	2662	1457	198576	79264
	Reservoir-3	Brine (95%)+CO ₂ (5%)	2275	2988	1605	140	54
		Brine (90%)+CO ₂ (10%)	2270	2957	1603	196	77
		Brine (85%)+CO ₂ (15%)	2265	2944	1602	283	112
		Brine (50%)+CO ₂ (50%)	2228	2942	1610	2877	1148
		Brine (10%)+CO ₂ (90%)	2187	2965	1624	338229	135321

Results

Figure 2 (a, b) shows an example of noise-free synthetic plane-wave sections computed with the pre-injection seismic properties (a) and with 5% of CO₂ saturation in the reservoir rocks (b). The Cambrian Deimena Reservoir is clearly detectable (Figure 2 a). After injection of 5% of CO₂ the plane-wave seismic section allows to distinguish the top and the bottom of the Reservoir (Figure 2 b). Figure 2 (c) shows the difference seismic section (difference between seismograms computed with different concentration of CO₂ in the fluid phase) for 0-5% CO₂ saturation. The Reservoir is clearly detectable, as well as the top of the Basement and some multiples below it.

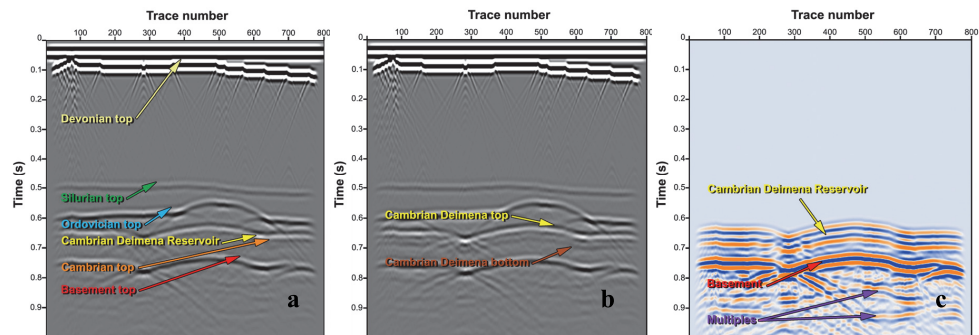


Figure 2 Examples of synthetic plane-wave (a and b) and difference sections (c). Plane-wave sections present 0% (a) and 5% (b) of CO₂ saturation. The seismograms are random noise-free. Approximate locations of the top of all geological formations (a) and the top and bottom of the Cambrian Deimena Sandstone Reservoir, saturated with CO₂ (b) are indicated. On the (c) introduced difference section of synthetic baseline (0% of CO₂) and the synthetic seismic line with 5% of CO₂ in the saturating fluid.

Discussion

We have explored behaviour of the seismic response using the plane-wave, difference and NRMS seismic sections in the modelled E6 structure reservoir and determined the ability to visualise a small quantities of injected CO₂. Arrival times and reflection strength from the reservoir and deeper formations varies with continuous changes of seismic properties due to the increasing CO₂ saturation.

This phenomenon is due to changing of magnitude of the reflection coefficient with increasing of CO₂ content, already with 5% of CO₂ saturation. Thin interbeds within the Reservoir (1, 2 and 3) implemented in the model and the Oil Reservoir (Figure 1) were impossible to define on the seismic sections due to the relatively low frequency of the seismic source (35 Hz), resulting in a single reflection. Reflectors on the difference section (Figure 2 c) characterized by two-way travel times lower than the reservoir are not influenced by the presence of CO₂ and give zero signal. The presence of CO₂ in the reservoir causes a decreasing of the P-wave velocity if compared with the brine saturated Deimena Sandstone and a variation of the quality factors (Table 2). These differences in the seismic properties determine a non-zero amplitude in the difference section for the reservoir and the reflectors located at higher depth. The lower part of the difference and NRMS sections was affected by multiple reflections.

Conclusions

The synthetic plane-wave and difference sections clearly indicate the presence of CO₂ in the Reservoir Formation in the E6 offshore structure for various saturation levels. Nevertheless, NRMS, which is one of the best methods suited for time-lapse seismic analysis, is affected by the presence of numerical noise and multiples. Our study shows effectiveness of seismic method to monitor the presence of CO₂ in the E6 Baltic Sea offshore structure already from the first stages of the injection. This study plays a crucial role in developing an optimal seismic monitoring plan in the studied area.

Acknowledgements

This study was funded by EU FP7 Marie Curie Research Training Network "Quantitative Estimation of Earth's Seismic Sources and Structure" (QUEST), Contract No. 238007 and is a part of K. Shogenov PhD research. We are grateful to Dr. Alla Shogenova from Tallinn University of Technology for her kind revision.

References

- Batzle, M. and Wang, Z. [1992] Seismic properties of pore fluids. *Geophysics*, **57**, 1396-1408.
- Carcione, J.M. [2007] Wave fields in real media: wave propagation in anisotropic, anelastic, porous and electromagnetic media. 2nd edition, revised and extended. *Handbook of Geophysical Exploration*, **38**, Elsevier, Amsterdam, 1-514.
- Kragh, E. and Christie, P. [2002] Seismic repeatability, normalized RMS and predictability. *The Leading Edge*, **21**, 642-647.
- Picotti, S., Carcione, J.M., Gei, D., Rossi, G. and Santos, J.E. [2012] Seismic modeling to monitor CO₂ geological storage: The Atzbach-Schwanenstadt gas field. *Journal of Geophysical Research*, **117**, B06103, doi:10.1029/2011JB008540.
- Rossi, G., Gei, D., Picotti, S. and Carcione, J.M. [2008] CO₂ storage at the Atzbach-Schwanenstadt gas field: a seismic monitoring feasibility study. *First Break*, **26**, 45-51.
- Shogenova, A., Šliaupa, S., Rasteniene, V., Jõelegt, A., Kirsimäe, K., Bitjukova, L., Lashkova, L., Zabele, A., Freimanis, Hoth, P., Huenges, E. [2001] Elastic properties of siliciclastic rocks from Baltic Cambrian basin. In: Extended Abstracts, Volume 1, *EAGE*, Amsterdam, The Netherlands, N-24, 1-4.
- Shogenov, K., Shogenova, A. and Vizika-Kavvadias, O. [2013] Petrophysical properties and capacity of prospective structures for geological storage of CO₂ onshore and offshore Baltic. *Elsevier, Energy Procedia*, in press, 1-8.
- Sudhir, J. [1987] Amplitude-%-offset analysis: a review with reference to application in Western Canada. *Journal of the Canadian Society of Exploration Geophysicists*, **23**, 27-36.
- White, J.E. [1975] Computed seismic speeds and attenuation in rocks with partial gas saturation. *Geophysics*, **40**, 224-232.

PAPER IV. SHOGENOV, K., SHOGENOVA, A., VIZIKA-KAVVADIAS, O. & NAUROY, J. F. 2015. Experimental modeling of CO₂-fluid-rock interaction: evolution of the composition and properties of host rocks in the Baltic Region. Earth and Space Science, AGU (accepted).

RESEARCH ARTICLE

Experimental modeling of CO₂–fluid–rock interaction: evolution of the composition and properties of host rocks in the Baltic Region

Key Points:

- Rocks from four onshore and offshore Baltic structures were studied
- The CO₂ injection-like experiment caused alterations in the rock composition and properties
- The dissolution of carbonate cement caused a high increase in porosity and permeability

Kazbulat Shogenov¹, Alla Shogenova¹, Olga Vizika-Kavvadias², and Jean-François Nauroy²

¹Institute of Geology, Tallinn University of Technology, Tallinn, Estonia, ²IFP Energies nouvelles, Rueil-Malmaison Cedex, France

Correspondence to:

K. Shogenov,
kazbulat.shogenov@ttu.ee

Abstract The objective of this study was to determine the influence of the possible CO₂ geological storage in the Baltic Region on the composition and properties of host rocks to support more reliable petrophysical and geophysical models of CO₂ plume. The geochemical, mineralogical and petrophysical evolution of Middle Cambrian reservoir sandstones and Lower Ordovician transitional clayey carbonate cap rocks from two offshore structures in Latvia and Lithuania and two onshore structures in Latvia, induced by laboratory-simulated CO₂ geological storage, was studied for the first time in the Baltic Region. The geochemical, mineralogical and petrophysical parameters were measured in 15 rock samples, before and after the alteration experiment. The diagenetic alteration of reservoir rocks was represented by carbonate cementation in the top of the onshore South Kandava structure, and quartz cementation and compaction, reducing the reservoir quality, in the deepest offshore E7 structure in Lithuania. The shallowest E6 structure offshore Latvia was least affected by diagenetic processes and had the best reservoir quality that was mainly preserved during the experiment.

Carbonate cement is represented by calcite and ankerite in the transitional reservoir sandstones of very low initial permeability in the upper part of the South Kandava structure. Its dissolution caused a significant increase in the effective porosity and

permeability of sandstones, a decrease in the weight of samples, bulk and matrix density, and P- and S- wave velocity, demonstrating short-term dissolution processes.

Only slight geochemical changes occurred during the experiment in offshore reservoir sandstones. Minor dissolution of carbonate and clay cements, feldspar and some accessory minerals and possible minor precipitation of pore-filling secondary minerals associated with slight variations in rock properties, demonstrating both short-term and long-term processes, were suggested.

As a novelty, this research shows the relationship between diagenetic alterations of Middle Cambrian reservoir sandstones and their changes caused by the CO₂ injection-like experiment.

1. Introduction

This research is related to one of the most promising technologies and fields of study, which is considered to be an effective measure for mitigating the climate change induced by greenhouse gases [IEA, 2004; Metz et al., 2005; Bachu et al., 2007; Arts et al., 2008; IPCC, 2014]. The scientific community agrees on the importance of reducing industrial carbon dioxide (CO₂) emissions in the atmosphere using CO₂ Capture and Geological Storage (CCS) in, for example, (1) deep saline aquifers, (2) depleted oil and gas fields, (3) un-mineable coal seams and (4) porous basalt formations. Worldwide, a number of known pilot storage and large-scale CCS demonstration projects are going on and/or monitored, the first of which (Sleipner, Norway) started in 1996. Nevertheless, there are gaps in the knowledge of short- and long-term (10–100 and 100–10,000 years, respectively) phenomena accompanying the process of the storage of CO₂ in deep geological formations, mostly related to site-specific reactions that have to be correctly evaluated and modeled.

Mineral trapping in saline aquifers may play a very insignificant role in terms of the storage volume. It may influence the injection rate by changing the porosity and permeability of the formation because of mineral dissolution or precipitation. In-depth analysis of the chemistry of rocks and their probable influence on sequestration can be conducted in a laboratory using available rock samples, with CO₂ injection in the reservoir conditions [Shafeen and Carter, 2010, pp. 235; Falk, 2014].

Our study is focused on CO₂ storage in deep saline aquifers overlain by the cap rock (seal). This is the most widespread worldwide option currently under consideration for CO₂ Geological Storage (CGS). The objective of the study was to determine the influence of possible CO₂ geological storage in the Baltic Region on the composition and properties of host rocks to support more

reliable petrophysical and geophysical models of CO₂ plume.

When injected into the aquifer or water-flooded oil reservoir, CO₂ has an impact on the pH level of in-situ brine, modifying it into a more acidic state. Isotope studies of natural analogues of CO₂ reservoirs suggest that the dissolution of CO₂ in formation brine is the main phenomenon in the long term, causing the acidification of native brine to a pH of approximately 3–5 [Gilfillan et al., 2009; Liu et al., 2011, 2012]. Chemically, this simple acid reaction is illustrated by equation (1), showing the formation and dissociation of carbonic acid (H₂CO₃⁰) from dissolved CO₂ in formation brine:



Acidic brine then reacts with the solid matrix of reservoir sediments (i.e. calcite, dolomite, anhydrite):



This exact phenomenon, induced by CO₂ injection into the aquifer, was applied as the main factor of the experiment and is a basis for further research.

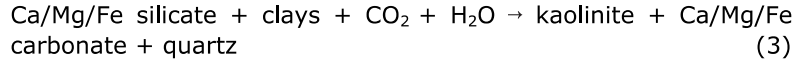
1.1 Reservoir rocks

A typical reservoir for CGS is a geological formation consisting of sandstone or carbonate characterized by good effective porosity and permeability. Effective (open) porosity is the porosity that is available for free fluids; it excludes all non-connected porosity, including the space occupied by the clay-bound water [Schön, 1996]. The ranges of “good” reservoir porosity and permeability are 15–20% and 50–250 millidarcy (mD), respectively [Tiab and Donaldson, 2012]. An ideal reservoir for CGS has permeability exceeding 200 mD to provide sufficient injectivity [Van Der Meer, 1993], however, the values greater than 300 mD are preferred. The porosities should be larger than 20%, while those below 10% should be treated with caution. The cumulative thickness of reservoirs should be greater than 50 m. The reservoirs less than 20 m thick are considered unsuitable for the storage of large amounts of CO₂.

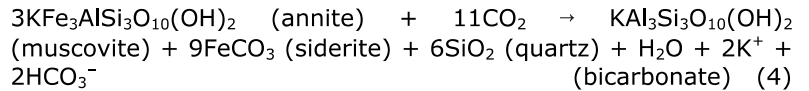
A number of recent papers have been dedicated to CO₂–brine–host reservoir rock interactions, both for sandstones and carbonate rocks [Ross et al., 1982; Svec and Grigg, 2001; Grigg and Svec, 2003; Rochelle et al., 2004; Bertier et al., 2006; Czernichowski-Lauriol et al., 2006; Egermann et al., 2006; Pawar et al., 2006; Izgec et al., 2008; Bemmer and Lombard, 2010; Bemmer et al., 2011; Carroll et al., 2011, 2013; Nguyen et al., 2013].

CGS-related laboratory experiments, numerical modeling and field monitoring of CO₂ storage sites have shown both partial

dissolution and precipitation of various minerals. A simplified equation for minor mineral dissolution/precipitation of host rock was given by Hitchon [1996]:

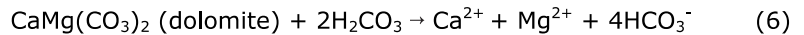
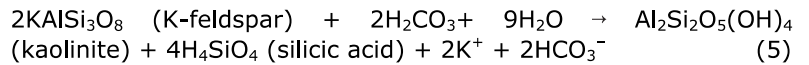


Computational and experimental simulations [Perkins and Gunter, 1995; Gunter et al., 1997; Gunter et al., 2000] of the siliciclastic glauconitic sandstone brine aquifer in the Alberta Basin suggest that CO₂ injection produces carbonate and quartz from aluminosilicate:



Ca- or Mg-bearing aluminosilicates would react in a similar fashion to consume CO₂ and precipitate calcite, dolomite or magnesium carbonate minerals, plus quartz [Gunter et al., 2000].

The reaction of carbonic acid with aluminosilicate or carbonate minerals produces significant alkalinity [Kaszuba and Janecky, 2009]:



Acid-dominated and related reactions will consume silicate minerals, produce secondary silicate assemblages and liberate silica. In addition to liberating silica, the acidity of these fluid-dominated systems accelerates fluid-silicate reaction rates, enhances silica solubility and inhibits quartz precipitation [Kaszuba and Janecky, 2009].

Gilfillan et al. [2008, 2009] studied stable carbon $\delta^{13}\text{C}$ (CO₂) isotope tracers from natural CO₂-bearing siliciclastic and carbonate gas reservoirs around the world. They explored CO₂ dissolution into formation brine at various pH values as the primary sink for CO₂ and precipitation of CO₂ as carbonate minerals. Nevertheless, this process is very site- and condition-dependent and, in several cases, no important rock-fluid interaction impact on the petrophysical properties of reservoir host rocks has been reported [Prieditis et al., 1991; Kamath et al., 1998].

1.2 Cap rocks

Cap rock is defined as a low-permeability (< 0.01 mD) rock (aquitard or aquiclude) that overlies a reservoir and retains hydrocarbons and/or other gases [Bachu et al., 2007]. However, its porosity can be relatively high, in the range of 15–30% [Armitage et al., 2011]. A cap rock less than 20 m thick is

cautionary, whereas thicknesses greater than 100 m are preferable [Chadwick et al., 2006].

The acidified brine may invade the pore space and trigger interactions with minerals. Due to their fast reaction kinetics, carbonate minerals may be affected by the most immediate attack. In the long run, acidified brine, even after carbonate buffering, may trigger reactions with the aluminosilicate minerals (feldspars and clays) present in the cap rock. Such reactions may occur on the order of tens, hundreds or thousands of years due to the slow rates of reactions with aluminosilicate minerals, but they may contribute significantly to the porosity/permeability alteration [Liu et al., 2012]. Numerical modeling of long timescale upward diffusion of dissolved CO₂ through the thick clay cap rock at the Sleipner storage site provided by Czernichowski-Lauriol et al. [2006] shows that only the bottom few meters of the cap rock adjacent to the reservoir is exposed to chemical reactions. Liu et al. [2012] reported new laboratory experiments on CO₂-brine-caprock interactions, indicating minor dissolution of K-feldspar (KAlSi₃O₈) and anhydrite (CaSO₄) and precipitation of pore-filling and pore-bridging illite ((K,H₃O)(Al,Mg,Fe)₂(Si,Al)₄O₁₀[(OH)₂, (H₂O)]) and/or smectite ((Na,Ca)_{0.33}(Al,Mg)₂(Si₄O₁₀)(OH)₂·nH₂O) and siderite (FeCO₃) in the vicinity of pyrite (FeS₂). A stable isotope study by Lu et al. [2009] has shown that CO₂ exists within the cap rock in both free and dissolved phases. As mentioned by Liu et al. [2012], previous experimental studies of CO₂-cap rock interaction have reported carbonate and feldspar mineral dissolution, along with secondary carbonate and clay mineral precipitation in the longer term [Kaszuba et al., 2005; Aplin et al., 2006; Busch et al., 2008; Soldal, 2008; Angeli et al., 2009; Credoz et al., 2009; Kohler et al., 2009; Wollenweber et al., 2010; Alemu et al., 2011; Berthe et al., 2011; Navarre-Sitchler et al., 2011].

1.3 Motivation of the study

Due to the use of local oil shale for energy production, Estonian CO₂ emissions per capita are among the highest in Europe and in the world [e.g. Shogenova et al., 2009a, 2009b, 2011a, 2011b]. The main target for the CGS study in the Baltic Region (Estonia, Latvia and Lithuania) is the Baltic sedimentary basin or Baltic Syncline, a 700 km x 500 km synclinal structure located in the western part of the East European Craton. The Middle Cambrian aquifer suits best for CO₂ storage in the Baltic Region. This aquifer includes potable water in the northern shallow part of the basin, mineral water (10 g/l) in southern Estonia and saline water (up to 120 g/l) in the central and southern parts of the basin at more than 800 m depths. The last mentioned geochemical and thermodynamic properties allow the use of the Middle Cambrian reservoir for CO₂ geological storage, whereas the geological conditions are most favorable in the uplifted structures in Latvia.

Prospective structures are located both on- and offshore the Baltic area [Grigelis 1991; Šliaupa et al., 2008a; Shogenova et al., 2009a; Šliaupa et al., 2013]. CO₂ geological storage has also prospects in Lithuanian and West Russian depleted oil fields and in the Swedish part of the Baltic Sea, in the Cambrian saline aquifer (Fallunden Member) covered by Ordovician Alum Shale Formation and Ordovician–Devonian rocks.

An EU CCS Directive was transposed into the Estonian laws by the end of 2011. While industrial-scale CO₂ storage is forbidden in the Estonian area, the regulations include a requirement for new large power plants to be “capture-ready”, with assessed possibilities for transboundary CO₂ transportation and storage [Shogenova et al., 2013]. In such a situation, the most probable scenarios for the storage of Estonian CO₂ emissions depend on regional decisions and cooperation with other Baltic Sea countries. Before implementation of the CO₂ storage technology in the Baltic Region, it is necessary to demonstrate its long-term safety for both humans and environment.

The Middle Cambrian stratigraphy is similar both on- and offshore Latvia [Grigelis, 1991]. The lithofacies implies the deepening of the sedimentation environment and maximum transgression at the beginning of the Middle Cambrian (Kybartai time). Rocks of the Middle Cambrian Deimena Formation deposited in a shallow regressing marine basin subjected to tides and storms and are dominated by quartz sandstones with subordinate claystone layers (mud shelf). The poorly sorted sandstones of various grain size, containing gravel fraction, were deposited at the end of Deimena time. The major Deimena reservoir, 50–70 m thick, lies regressively on the Kybartai Formation. The regression was associated with the more sandy composition of deposits. Three sedimentation cycles (Pajuris, Ablinga and Giruliai formations in Lithuania) resulted in the vertical lithological compartmentalization of the reservoir in the southern (Lithuanian) part of the basin. Each formation starts with a clayey base that grades into sandstones upward. Some tidal plain channels and sandy bars disrupt this regularity, providing pathways for vertical pore fluid migration. The subsidence rate drastically decreased in the Late Middle Cambrian, preceded by a break-off unconformity. The Middle–Upper Cambrian section, rarely exceeding 10 m in thickness, is represented by sandy sediments with clay layers dominating in the middle part. Numerous faults dissect the Cambrian reservoir body. They form important pathways for fluid migration, while high-amplitude faults provide a blockage for fluid migration in the uplifted structures. The Cambrian reservoir is sealed by Ordovician clay- and marlstones with low-porosity carbonates, except for the northern and southern extremes of the basin exposed to intense meteoric water infiltration [Paškevičius, 1997]. The Cambrian rocks were subjected to different diagenetic conditions across the

basin, with a wide spectrum of rock modification under shallow to deep burial conditions reflected in increasing clay mineral maturity with increasing depth, variations in the sandstone cement composition, with authigenic quartz prevailing in the deep part of the basin and carbonate cements prevailing in the basin periphery, changes in the porewater composition, grading from Ca-CO₃ type in the east to Na-Cl type in the west, etc. The carbonate cement of sandstones ranges in mineralogy from common ferroan dolomite and ankerite to less common calcite and siderite [Sliupa et al., 2008b]. In the Latvian part of the Baltic Syncline several structures have been singled out (Fig. 1).

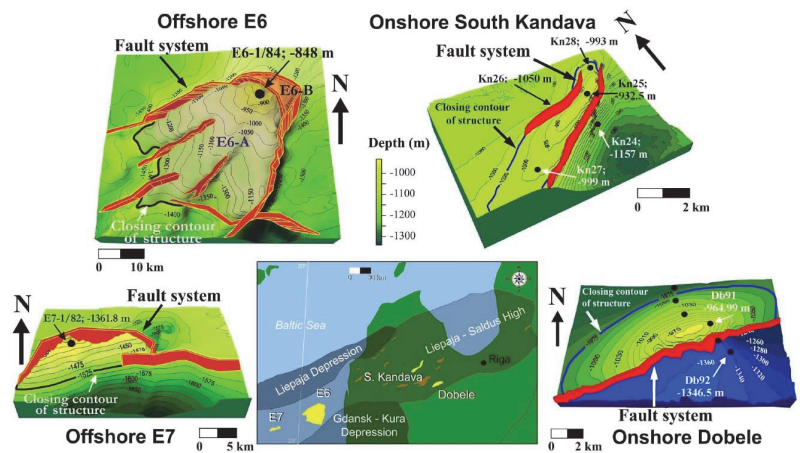


Fig. 1. Location of Latvian onshore structures prospective for CGS (CO₂ storage potential exceeding 2 Mt) in the Cambrian aquifer and the studied South Kandava and Dobele structures onshore Latvia, E6 structure offshore Latvia and E7 structure offshore Lithuania. Large regional structures complicating the Baltic Syncline in the study area are shown according to Freimanis [1993]. 3D geological models of the top of the Middle Cambrian Deimena Formation with location of the studied wells are shown [modified after Shogenov et al., 2013a, 2013b].

The Estonian-Latvian and Lithuanian monoclines are the marginal structures of the Baltic syncline. The Liepaja depression is a distinctly asymmetrical depression (length 200 km, width up to 70 km, trough amplitude 800 m) with a gentle northern and a steep near-fault southern edge. The Liepaja-Saldus zone of highs crosses the Baltic syncline, stretching from the Swedish offshore toward the northeast for about 400 km. The width of the zone is 25-80 km. From northeast to southwest, the basement submerges from 500 to 1,900 m. The Liepaja-Saldus zone is a complex system of disjunctive-plicative dislocations, the intensity of which exceeds that in other areas of the Baltic syncline. Fault amplitudes reach 600 m.

The Gdansk–Kura depression is only represented by its northern peripheral part. The South Latvian step, about 100 km long, is a sublatitudinal tectonic block in southern Latvia. The amplitudes of boundary faults reach 400–500 m [Freimanis et al., 1993].

Quartz cementation that formed during the late diagenetic stage [Lashkova, 1979; Sikorska and Paczesna, 1997] and increases with depth, is the main factor influencing the reservoir properties of rocks both in onshore and offshore structures. Another diagenetic process negatively influencing the reservoir properties is compaction. Pore reduction by mechanical compaction and quartz cement are the main controls of the petrophysical properties of Cambrian sandstones. The importance of mechanical compaction in reducing porosity and causing lithification is stressed by Čyžienė et al. [2006]. Compaction comprised the mechanical rearrangement of grains throughout the sandstones as well as the chemical compaction along shale–sandstone contacts and within shales. Grain breakage is rare, and no intergranular pressure solution in clay-free clean sandstones has been observed. In sandstones, detrital quartz grains mainly have point contacts. Differences in the degree of mechanical compaction are probably related to both maximum burial depth and variations in the depositional texture and susceptibility of sand to mechanical compaction. Quartz is the main cement mineral, occurring in the form of authigenic overgrowths on detrital quartz grains [Lashkova, 1979; Kilda and Friis, 2002]. According to Čyžienė et al. [2006], quartz cement is regionally widespread, but mainly confined to areas where present-day temperatures in the Cambrian are 50–90°C Sliupa et al. [2008b] stated that quartz cementation started at 1 km depth. The amount of quartz cement increases toward the deeper buried parts of the basin in West Lithuania, but is highly variable on a local scale and even within individual structures. Quartz cement contents show a negative correlation with porosity [Čyžienė et al., 2006] and with carbonate cement [Sliupa et al., 2008b].

The Deimena Formation is covered by up 46 m thick shales and clayey carbonate cap rocks of the Lower Ordovician Zebre Formation in the studied structures of Latvia. Shale rocks are dark, thin-layered (0.5–2 mm) and highly fissile. A layer of greenish-gray glauconite-bearing sandy marlstones (0.5 m) was observed at the base of onshore formations. The reservoir rocks are covered by 130–230 m thick Ordovician and 100–225 m thick Silurian impermeable clayey carbonate cap rocks. Clayey rocks could be easily determined by increased values of gamma-ray readings in all the studied wells, and they play an essential role as a seal for the studied structures (Fig. 2). The regional theoretical storage potential of the Cambrian sandstone saline aquifers below 900 m in the Baltic Sea region has been estimated as 16 Gt [Vernon et al., 2013]. For comparison, the total estimated storage capacity in the Jurassic sandstone formations

in the Norwegian Sea is 5.5 Gt [Halland et al., 2013]. The Utsira sandstone formation at the first in the world Sleipner storage site in the North Sea has a storage capacity of approximately 15 Gt [Halland et al., 2011]. More than 30 anticlinal deep geological structures on- and offshore Latvia and Lithuania, with different sizes and a storage capacity exceeding 2 Mt of CO₂, have been estimated as prospective for CGS [Šliaupa et al., 2008a; Shogenova et al., 2009a, 2009b, 2011a, 2011b; Šliaupa et al., 2013; Shogenov et al., 2013a, 2013b]. Four geological structures, located onshore (South Kandava and Dobele) and offshore Latvia (E6) and Lithuania (E7) and serving as prospective CGS sites in the Baltic Region (Fig. 1), were previously described in detail by Shogenov et al. [2013a, 2013b]. All the studied structures are situated within the tectonically dislocated Liepāja–Saldus zone of highs (Fig. 1). The deepest Deimena Formation rocks occur in the offshore E7 structure (Fig. 2). This structure is also characterized by the highest temperature of 46°C and water salinity of 125 g/l [Shogenov et al., 2013a, 2013b]. The shallowest offshore structure E6 shows a lower temperature (36°C) and the lowest salinity of Cambrian fluids (99 g/l). The studied onshore structures exhibit the average depth of the Deimena Formation (933–950 m) but a lower temperature than rocks in the offshore structures (18–24.5°C). The salinity of Cambrian fluids is also average, 113–114 g/l compared to the studied offshore structures. Sandstones at the top of the Deimena Formation in the South Kandava uplift and in its lowered wing have undergone diagenetic carbonate cementation represented by calcite, dolomite and ankerite [Shogenov et al., 2013a].

Geological and logging data were used for the construction of cross sections and 3D geological models (Figs 1, 2). The petrophysical properties, geochemical and mineralogical compositions of 24 samples of reservoir and cap rocks were studied, and structural theoretical CO₂ storage capacity was estimated with different levels of reliability. The selected structures have an average porosity of 12–21%, permeability of 40–360 mD and mean reservoir thickness of 42–58 m. The average CO₂ storage potentials (conservative-optimistic) of the Dobele, South Kandava, E7 and E6 structures were, respectively, 20–106, 25–95, 7–34 and 152–377 Mt. We estimated the E6 offshore structure as the largest suitable trapping structure prospective for CGS offshore Latvia with the highest CO₂ storage capacity [Shogenov et al., 2013a, 2013b]. Based on exploration report data [Babuke et al., 1983], we have treated E7 as a Latvian offshore structure in our earlier publications. However, according to the new Latvian–Lithuanian territorial agreement in the Baltic Sea, signed by Prime Ministers of Latvia and Lithuania in 1999, the E7 structure lies now offshore Lithuania [Šteinerts, 2012].

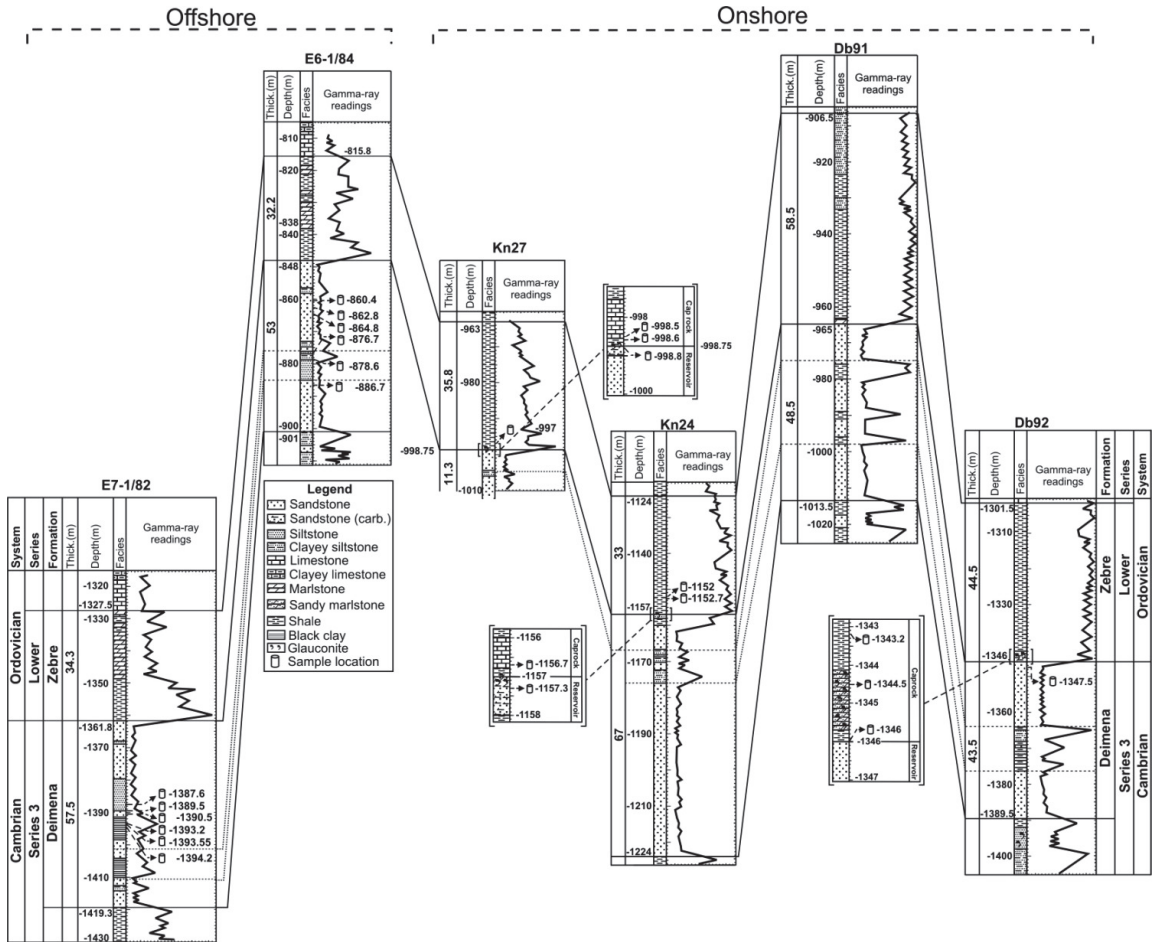


Fig. 2. Cross section of the studied wells showing correlation of the Deimena Formation by logging and drill core data [modified after Shogenov et al., 2013a]

The current study is focused on physical and geochemical alteration processes in the host reservoir rocks and cap rocks caused by acidic fluid, in association with CGS in the Cambrian saline aquifer in the Baltic Region. The results will be implemented in further studies of numerical dynamic fluid flow simulations and coupled time-lapse rock physics and numerical seismic modeling of CGS, supporting different scenarios of CO₂ plume evolution and monitoring.

Because chemical, mineralogical and petrophysical alterations are usually site-specific, this study has great importance for understanding the CO₂-fluid-host reservoir-cap rock interactions

for the prediction of CO₂ storage safety, integrity of the cap rock and possible risks.

A set of petrophysical, geochemical and mineralogical parameters, measured on reservoir and transitional cap rock samples from the Baltic sedimentary basin (Latvian offshore and onshore and Lithuanian offshore) before and after the CO₂ injection-like experiment, and the influence of CO₂-fluid-rock interactions on the properties and composition of rocks have been studied for the first time. The obtained results show some possible geochemical and physical processes that could occur during the CO₂ storage in the studied onshore and offshore structures in short and long terms. Being the first of this type in the Baltic Sea Region, these results are also significant for the southern parts of the region, which have CO₂ storage capacity in the Cambrian aquifer (Lithuania, Sweden, Kaliningrad Region and offshore Poland). However, the obtained data should be supported by additional laboratory experiments and fluid-flow modeling of the CO₂ storage in the Middle Cambrian sandstones in the Baltic Sea Region both in structures and basin-scale for better assessment of the possible storage scenarios and their safety.

2. Material and methods

Samples from the reservoir and cap rock were taken for this study from five drill cores stored in the Latvian Environmental, Geological and Meteorological Centre (LEGMC). Detailed descriptions of the methods applied to the study of 21 rock samples before the alteration experiment are available in our previous publications [Shogenov et al., 2013a, 2013b]. Fifteen of these samples were used in the alteration experiment. The total chemical composition of the samples was measured by X-ray fluorescence (XRF) analysis, and the total carbon (C) and total sulfur (S) contents were measured via the Leco method by Acme Analytical Laboratories Ltd. before and after the alteration experiment. CaO, MgO and insoluble residue (IR) were measured by the titration geochemical method only before the alteration experiment. Thin sections of the rock samples were studied in the Institute of Geology at Tallinn University of Technology using a Scanning Electron Microscope (SEM) equipped with an energy dispersive spectrometer (EDS). Only the chemical composition of the original shale cap rock samples (from the Dobele and South Kandava structures) was measured. Due to their weak consolidation these samples were not used for the petrophysical measurements or in the laboratory alteration experiment.

For this case, we simplified the CO₂ injection part in our alteration experiment by considering only the impact on the contact area between acidified fluid and the studied rocks. This simplification ensures a homogeneous dissolution of the brine on the core scale

and enables avoiding very local “worm-holing” effects on samples and erroneous physical measurements of rock [Egermann et al., 2006; Bemer and Lombard, 2010]. The homogeneous alteration method or retarded acid approach was conducted at the IFP Energies nouvelles (IFPEN, French Petroleum Institute, Paris). It constitutes in the placement of samples into the Hastelloy cell maintained under vacuum conditions and injection of an acid solution inside until 10 bar and the activation of the acid under the temperature of 60°C (for at least one day), simulating CO₂-rich brine in an aquifer characterized by lowered pH (approximately three units). This method has been developed and described in detail in Egermann et al. [2006], Bemer and Lombard [2010] and Bemer et al. [2011]. The day after, each sample was placed in a 25-mm-diameter cell and flooded by three pore volumes by 20 g/l NaCl brine at 20°C to stop the weathering. After this flooding, the samples were dried in an oven for three days. The procedure was repeated three times.

Siliciclastic rock samples with good reservoir properties are often weakly cemented; therefore, it could be problematic to keep their regular shape in experiments involving the flushing of samples with supercritical CO₂ and brine. The protocol of the implemented alteration method allows the use of samples with various sizes and shapes that simplify the investigation process.

In the present study, 15 rock samples from five wells (offshore E6-1/84 and E7-1/82 and onshore Dobele 92, South Kandava 24 and 27, Fig. 1) were treated with acid brine. Reservoir and cap rock samples were subdivided into lithological groups using the results of geochemical analyses. As a matrix for lithological determination of the rock samples, we used a geochemical model, developed and first published in Shogenova et al. [2003a, 2003b] and updated in Shogenova et al. [2005].

Bulk and matrix helium density, helium porosity, gas-permeability and acoustic wave velocities in dry samples, the chemical and mineralogical composition and surface morphology were studied both before and after the alteration experiment.

The XRF and SEM studies were conducted on 12 siliciclastic reservoir and three argillaceous carbonate rock samples (15 rock samples in total) after the experiment. Due to the partial destruction of several samples and the mostly complete destruction of the glauconite-bearing sandy marlstone Db92-2 (1344.5 m) from the Dobele structure after the alteration experiment, it was possible to measure porosity and permeability on only 14 rock samples, P-wave velocity on 10 samples and S-wave velocity on four samples (three sandstones and one argillaceous limestone).

The thin sections of samples were made after the alteration from the rock–fluid contact zone where the alteration was confirmed by

the high percentage of solubility of the studied samples. The change in the shape of the limestone sample Kn24-3 due to partial chemical weathering (dissolution of the rock material) during the alteration experiment is illustrated in Figure 3a, b. The experimental protocol did not support chemical measurements of the acid solution composition during the experiment. The alteration experiment involved all the 15 samples together in one solution under the same conditions. The changes in sample weights were caused by partial destruction of some samples.

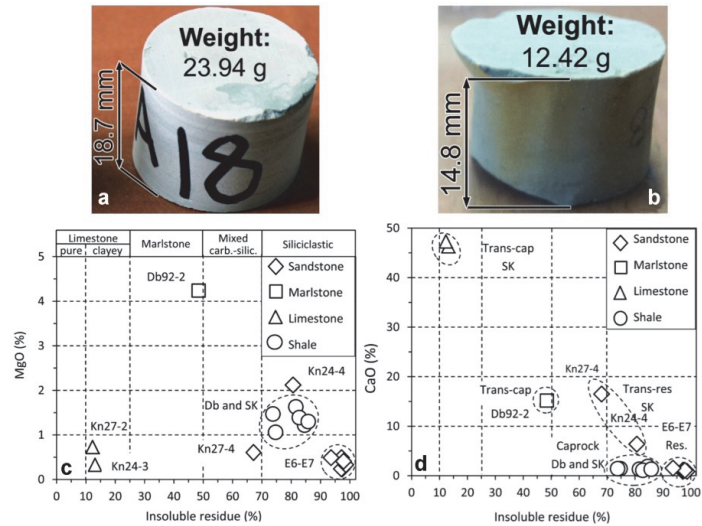


Fig. 3. Trans-cap limestone sample Kn24-3 before (a) and after (b) the alteration experiment. (c–d) Composition of the studied rock samples before the alteration experiment. (a) Initial MgO content versus insoluble residue content (IR). (b) Initial CaO content versus insoluble IR content. Trans-res sandstone samples (rhombs): Kn24-4 – characterized by a minor content of dolomite cement; Kn27-4 – mixed carbonate-siliciclastic calcite-cemented sandstone. The Dobele and South Kandava structures are indicated on the plot as Db and SK, respectively. Trans-cap glauconite-bearing sandy marlstone Db92-2 is located near the border between marlstones and mixed carbonate-siliciclastic rocks.

2.1 Experimental and interpretation uncertainties

Experimental uncertainties include the quality control of petrophysical measurements and uncertainties related to geochemical and mineralogical interactions. To distinguish between a real trend in a data set and variation due to the experimental uncertainty, the American Petroleum Institute [1998] has recommended reporting core analyses data together with a statement of the uncertainty with which these data were recorded.

Errors of the permeability and acoustic velocities measurements were quite high in the presented study due to sample sizes that differed from the standard ones at the IFPEN petrophysical and petro-acoustic laboratories. The standard samples were 40 mm in diameter and 80 mm in length, thus the length/diameter ratio should be higher or equal to two [Egermann et al., 2006]. The studied samples were 25 mm in diameter and 11–27 mm in length. Therefore, the experimentally established error (using replicate measurements of each sample) was 20% for permeability, and 10% for P- and S-wave velocity measurements for the used petro-acoustic installations.

The error of matrix density measurements was <0.7%. It consisted of an analytical balances (from Mettler Toledo) error of 0.2% (estimated experimentally) and a less than 0.5% pycnometer error for sample solid volume measurements (AccuPyc from Micromeritics) given as the default error. The error for the bulk density measurements due to the balances error (0.2%) and GeoPyc pycnometer (from Micromeritics) for total sample volume estimation with reported default error of 1.5% was 1.7%. The porosity measurements, supported by the high accuracy pycnometers from Micromeritics (GeoPyc and AccuPyc with 1.5% and 0.5% errors, respectively), provide a total of 2% accuracy.

Uncertainties and errors due to possible mistakes in the measurements of the altered petrophysical parameters were checked using well-known relationships: bulk density–porosity and acoustic velocity–porosity negative correlations; permeability–porosity–positive correlation in general and known possible scatter from this relationship in some cases; and acoustic velocity–matrix and bulk density positive correlations [Schön, 1996; Sliupa et al., 2001; Mavko et al., 2003; Shogenova et al., 2009a]. The correlated parameters were compared with each other after the alteration experiment.

Uncertainties in the interpretation of results are caused by the limited number of samples available for measurements, limitations of the laboratory experiment, the wide range of minerals that can be used to describe major element chemistry obtained by XRF analysis and semi-quantitative results provided by SEM-EDS.

3. Results

Based on the contents of IR, calcite (CaCO_3) and dolomite ($\text{CaMg}(\text{CO}_3)_2$), the studied rock samples were subdivided into the following groups (Table 1):

- 1) limestone [$\text{IR} < 25\%$, $\text{CaCO}_3 > \text{CaMg}(\text{CO}_3)_2$],
- 2) calcitic marlstone [$25\% < \text{IR} < 50\%$, $\text{CaCO}_3 > \text{CaMg}(\text{CO}_3)_2$],

- 3) mixed carbonate-siliciclastic rock ($50\% < IR < 70\%$),
- 4) siliciclastic rock ($IR > 70\%$).

Limestone samples could be classified as pure ($IR < 10\%$), slightly argillaceous ($10\% < IR < 15\%$) and strongly argillaceous rocks ($15\% < IR < 25\%$).

According to the lithological interpretation, petrophysical properties, XRD and XRF analyses, Leco and wet chemical analyses, the 21 studied samples were subdivided into seven groups [Shogenova et al., 2003a, 2003b, 2005, 2006; Shogenov, 2008]: (1) glauconite-bearing sandy marlstone, (2) pure "high-quality" quartz sandstone ($SiO_2 > 95\%$, porosity $> 20\%$, permeability > 250 Md), (3) pure quartz sandstone ($SiO_2 > 95\%$, porosity $< 20\%$, permeability < 250 Md), (4) quartz sandstone with clay cement ($85\% < SiO_2 < 95\%$, $Al_2O_3 > 5\%$), (5) sandstone with carbonate cement ($60\% < SiO_2 < 85\%$, $CaO > 5\%$), (6) limestone and (7) shale ($IR > 70\%$, $Al_2O_3 > 10\%$ and $K_2O > 5\%$), (Tables 1–4, Figs 3c, d, 4a, b). Only the chemical composition of the initial shale samples (before the alteration experiment) was measured (Figs 3c, d, 4a, Tables 1, 3). We subdivided all the samples into three clusters based on their location in the studied structures: (1) reservoir (10 samples), (2) trans-reservoir (two samples) and (3) trans-cap rock (three samples) samples. The trans-reservoir (trans-res) samples were taken from the uppermost 1 m of the reservoir rock, and trans-cap rock (trans-cap) samples were characterized by the lowermost 1 m of the cap rock (Table 1).

3.1 Reservoir rocks

The reservoir rock samples from the E6 structure were estimated as pure "high-quality" quartz sandstones (Tables 1, 4). According to our previous and present studies, these rocks are least of all changed by diagenetic processes and have the best reservoir properties. They are mainly composed of quartz, a minor amount of forming cement clay and carbonate minerals, admixture of feldspar (mainly potassium or barium feldspars) and accessory minerals represented by pyrite, barite, anatase and/or brookite and zircon [Shogenov et al., 2013a, 2013b].

The reservoir sandstones from the E7 offshore structure were estimated by XRD analysis as (1) pure quartz sandstones or (2) clay-cemented quartz sandstones (Table 1). These rocks were most of all subjected to diagenetic changes including mechanical compaction and authigenic quartz cementation, resulting in reduced reservoir properties. According to our studies, these rocks mainly consist of quartz and a higher amount of clay and carbonate minerals than in the E6 structure, including ankerite and dolomite, admixture of feldspar and accessory minerals represented by pyrite, barite, anatase and/or brookite, zircon and tourmaline. The clay fraction is represented by hydromica and kaolinite [Shogenov et al., 2013a, 2013b].

Table 1. List of studied rock samples*

Nº	Alteration experiment	Sample	Structure	Wells	Depth	Formation	Type	Lithology
Onshore								
1		Db92-1	Dobele	92	1343.2	O ₁ zb	Caprock	Shale
2	✓	Db92-2	Dobele	92	1344.5	O ₁ zb	Trans-cap	Sandy marlstone (glau.)
3		Db92-3	Dobele	92	1346.0	O ₁ zb	Caprock	Shale
4		Kn24-1	South Kandava	24	1152.0	O ₁ zb	Caprock	Shale
5		Kn24-2	South Kandava	24	1152.7	O ₁ zb	Caprock	Shale
6	✓	Kn24-3	South Kandava	24	1156.7	O ₁ zb	Trans-cap	Limestone
7	✓	Kn24-4	South Kandava	24	1157.3	E ₂ dm	Trans-res	Sandstone (carb.)
8		Kn27-1	South Kandava	27	997.0	O ₁ zb	Caprock	Shale
9	✓	Kn27-2	South Kandava	27	998.5	O ₁ zb	Trans-cap	Limestone
10		Kn27-3	South Kandava	27	998.6	O ₁ zb	Caprock	Shale
11	✓	Kn27-4	South Kandava	27	998.8	E ₂ dm	Trans-res	Sandstone (carb.)
Offshore								
12	✓	E6-1	E6	E6-1/84	860.4	E ₂ dm	Reservoir	Sandstone (HQ)
13	✓	E6-2	E6	E6-1/84	886.7	E ₂ dm	Reservoir	Sandstone (HQ)
14	✓	E6-3	E6	E6-1/84	886.7	E ₂ dm	Reservoir	Sandstone (HQ)
15	✓	E7-1	E7	E7-1/82	1387.6	E ₂ dm	Reservoir	Sandstone
16	✓	E7-2	E7	E7-1/82	1389.5	E ₂ dm	Reservoir	Sandstone
17	✓	E7-3	E7	E7-1/82	1390.5	E ₂ dm	Reservoir	Sandstone
18	✓	E7-4	E7	E7-1/82	1390.5	E ₂ dm	Reservoir	Sandstone
19	✓	E7-5	E7	E7-1/82	1393.2	E ₂ dm	Reservoir	Sandstone
20	✓	E7-6	E7	E7-1/82	1394.2	E ₂ dm	Reservoir	Sandstone (clay)
21	✓	E7-7	E7	E7-1/82	1394.2	E ₂ dm	Reservoir	Sandstone (clay)

*Localities in Latvia and Lithuania, geological age, formation, rock type and lithology; O₁zb, Zebre Formation of Lower Ordovician; E₂dm, Deimena Formation of Middle Cambrian; carb., carbonate-cemented; HQ, pure "high-quality" quartz sandstone; clay, clay-cemented; glauc., glauconite-bearing.

After the alteration experiment we determined changes in the chemical composition (Table 2) and petrophysical properties (Table 4) of the samples from the E6 and E7 structures. However, due to partial destruction of several rock samples, it was impossible to measure some petrophysical properties.

Thin section study of the altered sample from the E6 structure exhibited the dissolution of quartz and carbonate minerals in the cement matrix. At the same time, the determined dissolution of quartz was selective and often we did not find other signs of the dissolution of the quartz matrix around. Fractured remains of dissolved silica, carbonate and clay cement were detected in the middle part of the thin section (Fig. 5).

The study of thin sections of the E7 structure rocks after the alteration experiment revealed the dissolution of minor carbonate

Table 2. Chemical composition of rocks: (a) major oxides and insoluble residue^a

Nº	Sample	Type	Wet chemical analysis (%)		XRF analysis (%)												
			IR	CaO		MgO		SiO ₂		CaO		MgO		Al ₂ O ₃		Fe ₂ O ₃	
				before alteration	before	after	before	after	before	after	before	after	before	after	before	after	
1	Db92-2	Trans-cap	48.42	15.18	4.24	45.0	52.7	14.47	7.36	3.08	3.12	4.46	5.30	9.99	11.68		
2	Kn24-3	Trans-cap	13.12	46.31	0.33	10.8	7.40	46.27	49.29	0.73	0.61	2.98	2.06	0.96	0.67		
3	Kn24-4	Trans-res	80.64	6.38	2.12	81.1	85.4	5.61	3.95	1.98	1.40	0.26	0.43	2.32	1.74		
4	Kn27-2	Trans-cap	12.26	47.3	0.73	9.3	8.1	47.95	48.22	0.81	0.77	2.58	2.24	0.81	0.66		
5	Kn27-4	Trans-res	68.04	16.5	0.57	70.0	75.0	15.69	12.23	0.12	0.23	0.18	0.34	0.13	0.09		
6	E6-1	Reservoir	97.14	0.88	0.24	97.8	97.0	0.07	0.03	0.03	0.02	0.24	0.70	0.06	0.06		
7	E6-2	Reservoir	97.44	1.10	0.24	97.4	94.8	0.10	0.03	0.04	0.04	0.34	1.30	0.16	0.09		
8	E6-3	Reservoir	97.44	1.10	0.24	97.4	95.7	0.10	0.03	0.04	0.03	0.34	1.10	0.16	0.07		
9	E7-1	Reservoir	97.12	1.10	0.24	98.7	98.6	0.05	0.02	0.02	<0.01	0.27	0.72	0.08	0.02		
10	E7-2	Reservoir	98.64	0.88	0.33	98.3	98.7	0.04	0.02	0.01	<0.01	0.38	0.70	0.06	0.03		
11	E7-3	Reservoir	97.16	1.10	0.49	97.6	98.3	0.30	0.13	0.11	0.07	0.27	0.61	0.19	0.09		
12	E7-4	Reservoir	97.16	1.10	0.49	97.6	98.7	0.30	0.11	0.11	0.06	0.27	0.84	0.19	0.14		
13	E7-5	Reservoir	97.86	1.10	0.41	97.8	98.4	0.04	0.02	0.03	<0.01	0.59	0.72	0.31	0.06		
14	E7-6	Reservoir	93.60	1.54	0.49	87.2	90.2	0.16	0.05	0.34	0.20	5.26	4.96	1.85	1.10		
15	E7-7	Reservoir	93.60	1.54	0.49	87.2	86.4	0.16	0.07	0.34	0.33	5.26	6.63	1.85	1.54		

^aStudied rock samples are before and after alteration experiment; IR, Insoluble residue

cementation, occurring in spots on the grain edges and inside the pore fillings (Figs 6, 7), and the dissolution of quartz grains and second-phase quartz grain recrystallization (Fig. 8).

Sample Kn24-4 was estimated by XRD and XRF analyses as ankerite-cemented quartz sandstone (trans-res, 0.3 m below the cap rock formation, Fig. 9). The trans-res sample Kn27-4 (0.2 m below the cap rock formation) was estimated by XRD analysis as sandstone with abundant quartz and minor calcite (mixed carbonate-siliciclastic rock by geochemical interpretation). Changes in the chemical composition (Table 2) and drastic changes in petrophysical properties (Table 4) were determined after the alteration experiment in the trans-res samples from the uplifted South Kandava structure (Kn 27-4) and beyond the structure (Kn 24-4).

The thin section study of the South Kandava samples confirms the results of the petrophysical measurements of rock, showing the dissolution of carbonate cement after alteration (Fig. 9).

3.2 Trans-cap rocks

Argillaceous limestone and sandy marlstone samples, representing trans-cap rocks of the Dobele and South Kandava onshore structures, were studied (Tables 1–3).

Table 2. Chemical composition of rocks: (b) minor oxides, total carbon and total sulphur^a

N° Sample	Type	XRF analysis (%)														Leco method (%)					
		Na ₂ O		TiO ₂		K ₂ O		MnO		P ₂ O ₅		Ba		C		S					
		before	after	before	after	before	after	before	after	before	after	before	after	before	after	before	after				
1	Db92-2	Trans-cap	0.35	0.39	0.12	0.12	3.39	3.65	0.13	0.11	6.91	2.96	0.02	0.02	1.69	4.50	0.98	1.36			
2	Kn24-3	Trans-cap	0.11	0.10	0.16	0.09	0.32	0.30	0.23	0.28	0.04	0.03	0.01	<0.01	10.22	10.97	<0.02	<0.02			
3	Kn24-4	Trans-res	0.02	0.04	0.09	<0.01	0.03	0.03	0.21	0.15	0.06	0.07	<0.01	<0.01	2.07	2.14	0.19	0.10			
4	Kn27-2	Trans-cap	0.11	0.11	0.15	0.11	0.14	0.44	0.22	0.20	0.04	0.04	<0.01	<0.01	10.57	11.01	<0.02	<0.02			
5	Kn27-4	Trans-res	0.13	0.09	<0.01	0.01	0.06	<0.01	<0.01	0.13	0.07	0.07	0.43	0.35	3.38	3.48	0.03	0.04			
6	E6-1	Reservoir	0.03	0.06	0.13	0.06	0.10	0.04	<0.01	<0.01	0.01	0.01	0.28	0.22	0.19	1.19	0.05	0.06			
7	E6-2	Reservoir	0.03	0.14	0.17	0.09	0.14	0.09	<0.01	<0.01	0.01	0.01	0.24	0.18	2.04	2.04	0.10	0.10			
8	E6-3	Reservoir	0.03	0.06	0.17	0.17	0.14	0.05	<0.01	<0.01	0.01	0.01	0.24	0.16	0.24	1.62	0.10	0.08			
9	E7-1	Reservoir	0.02	0.03	0.10	0.11	0.04	0.04	<0.01	<0.01	<0.01	<0.01	0.06	0.01	0.03	0.10	0.03	<0.02			
10	E7-2	Reservoir	<0.01	0.01	0.13	0.11	0.03	0.02	0.01	<0.01	0.01	<0.01	<0.01	<0.01	0.03	0.05	<0.02	<0.02			
11	E7-3	Reservoir	0.03	0.05	0.06	0.03	0.07	0.05	0.01	<0.01	0.01	0.01	0.10	0.08	0.14	0.33	0.05	0.04			
12	E7-4	Reservoir	0.03	0.03	0.06	0.04	0.07	0.05	0.01	<0.01	0.01	<0.01	0.10	0.08	0.14	0.23	0.05	0.06			
13	E7-5	Reservoir	0.02	0.02	0.15	0.11	0.07	0.04	0.02	<0.01	0.01	0.01	<0.01	<0.01	0.07	0.05	0.04	<0.02			
14	E7-6	Reservoir	0.09	0.11	0.48	0.39	0.90	0.72	0.06	0.02	0.04	0.03	0.01	0.01	0.29	0.20	0.06	0.06			
15	E7-7	Reservoir	0.09	0.11	0.48	0.46	0.90	1.04	0.06	0.03	0.04	0.04	0.01	0.02	0.29	0.24	0.06	0.06			

^aStudied rock samples are before and after alteration experiment; IR, Insoluble residue

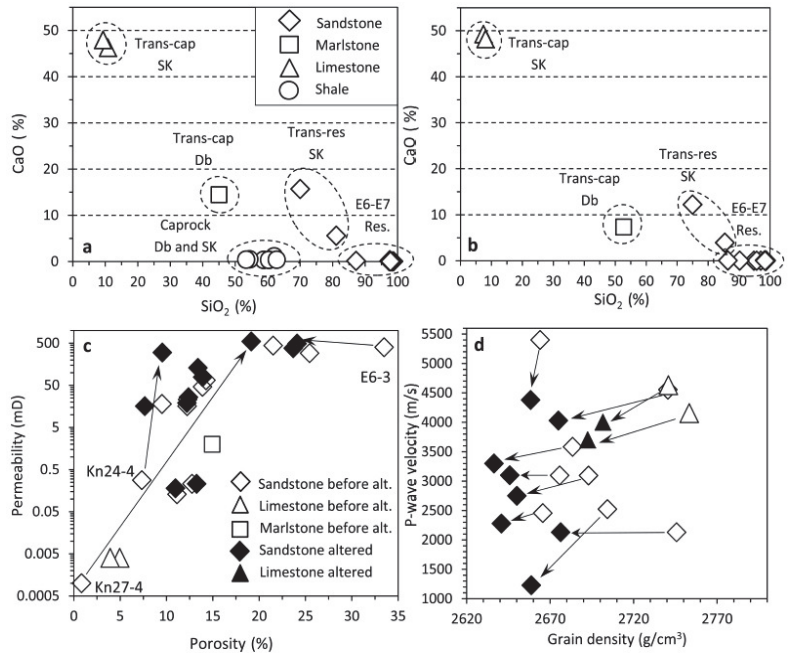


Fig. 4. Composition and properties of the studied rock samples from the Dobele (Db), South Kandava (SK), E6 and E7 structures before and after the alteration experiment. **(a–b)** CaO content versus SiO₂ content (XRF analysis, Tables 2, 3): (a) initial content before the alteration experiment; (b) final content after the alteration experiment. The CaO content decreased and SiO₂ increased in the trans-cap glauconite-bearing sandy marlstone Db92-2, and trans-res sandstones Kn24-4 and Kn27-4 compared to the initial content (Fig. 3c). The CaO content increased and SiO₂ content decreased in the trans-cap limestones Kn24-3 and Kn27-2 (South Kandava structure). Reservoir sandstones from the E6 and E7 structures underwent slight changes in SiO₂ and CaO contents. **(c–d)** Petrophysical parameters before and after the experiment (Table 4): (c) permeability versus porosity of the rocks before (white symbols) and after (black symbols) the experiment, showing a drastic increase in the permeability of trans-reservoir carbonate-cemented sandstones from the South Kandava structure; (d) P-wave velocity in dry samples versus matrix density, showing a decrease in the matrix density in all rocks and a decrease in velocity in most of the rocks after the experiment.

According to XRF analyses and thin section studies, the trans-cap rock Db92-2 of the Dobele structure, sampled at 1.5 m above the reservoir formation, is glauconite-bearing sandy marlstone (Fig. 10). Abundant glauconite grains with signs of diagenetic weathering and minor quartz grains cemented with carbonate and phosphate minerals (mainly calcite and apatite) were observed in the thin section before the alteration experiment. The admixture of pyrite could be interpreted in the original rock based on the

Table 3. Total chemical composition of shales^a

N° Sample	Type	Lithology	Wet chemical analysis (%)			XRF analysis (%)										Leco method (%)			
			IR	CaO	MgO	SiO ₂	CaO	MgO	Al ₂ O ₃	Fe ₂ O ₃	Na ₂ O	TiO ₂	K ₂ O	MnO	P ₂ O ₅	Ba	C	S	
1	Db92-1	Caprock	Shale	81.58	1.32	1.63	58.8	0.36	2.11	16.21	4.86	0.46	0.94	6.75	0.04	0.20	0.05	2.51	0.59
2	Db92-3	Caprock	Shale	84.58	1.87	1.22	62.0	1.11	1.82	15.04	4.57	0.26	0.68	5.87	0.05	0.09	0.03	1.22	1.09
3	Kn24-1	Caprock	Shale	74.68	1.43	1.06	54.4	0.47	1.63	13.38	3.98	0.65	0.75	6.79	0.03	0.24	0.04	8.26	0.85
4	Kn24-2	Caprock	Shale	82.78	1.10	1.39	60.4	0.36	1.99	14.97	4.36	0.78	0.84	6.88	0.03	0.18	0.05	2.51	0.52
5	Kn27-1	Caprock	Shale	85.82	1.32	1.30	62.8	0.40	2.20	15.57	4.31	0.86	0.86	6.86	0.03	0.18	0.05	0.54	0.10
6	Kn27-3	Caprock	Shale	73.78	1.43	1.47	53.4	0.41	1.69	14.76	4.27	0.72	0.81	6.35	0.03	0.10	0.04	7.36	1.01

^aRock samples are before alteration (in the initial state); IR, insoluble residue; C, total carbon content; S, total sulphur content.

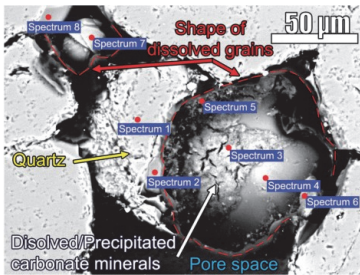
relatively high sulfur content and a high total iron content, although most of this iron is related to glauconite grains.

Samples Kn24-3 (Fig. 11) and Kn27-2 of the South Kandava structure, sampled 0.3 and 0.5 m above the reservoir formation from wells 24 and 27, respectively, were estimated by wet chemical and XRF analyses as slightly argillaceous trans-cap limestones (Tables 1, 2). After the alteration experiment we determined variations in the chemical composition and petrophysical properties in the trans-cap samples from the South Kandava structure (Tables 2, 4).

4. Discussion

In many cases our experiments confirmed previously reported results of laboratory experiments, numerical modeling and field monitoring of (1) CO₂-cap rock [e.g. Alemu et al., 2011; Berthe et al., 2011; Navarre-Sitchler et al., 2011; Liu et al., 2012] and (2) CO₂-reservoir rock interactions [e.g. Czernichowski-Lauriol et al., 2006; Egermann et al., 2006; Izgec et al., 2008; Kaszuba and Janecky, 2009; Bemmer and Lombard, 2010; Bemmer et al., 2011; Nguyen et al., 2013]. Carbonate and feldspar mineral dissolution along with secondary carbonate, clay (illite and smectite) and iron mineral (siderite and pyrite) precipitation in the longer term were recorded for cap rocks. Partial dissolution of carbonate cement (calcite, dolomite and ankerite) and other secondary minerals with an increase, in some places decrease, in porosity and permeability were described for the reservoir rocks.

This study provides a set of experimental data concerning the evolution of the geomechanical, petrophysical, geochemical and mineralogical properties of rocks under chemical alteration. The presented results do not yet allow the definition of constitutive laws taking the chemomechanical coupling into account.



Spectrum	C	Na	Mg	Al	Si	P	S	Cl	K	Ca	Fe	Br	O
Spectrum 1	10	-	-	-	29	-	-	-	-	-	-	-	61
Spectrum 2	13	-	-	-	25	-	-	-	0.1	-	-	-	62
Spectrum 3	-	2	0.6	1.3	28	0.8	1.4	0.9	0.9	18.5	0.8	-	45
Spectrum 4	-	3.9	1.3	0.5	39	-	0.4	-	0.7	5	-	-	50
Spectrum 5	20	0.2	-	-	12	-	0.1	-	-	0.5	0.4	0.4	67
Spectrum 6	19	0.4	-	-	5	-	0.1	-	-	13	-	-	62
Spectrum 7	13	-	-	-	25	-	-	-	-	-	-	-	62
Spectrum 8	15	-	-	-	22	-	-	-	-	-	-	-	64

Fig. 5. SEM microphotograph of the thin section of fine-grained porous Deimena reservoir sandstone sample E6-3 (Table 1) after alteration and SEM energy-dispersive X-ray spectroscopy (EDX) analyses (all results in weight %). EDX spots shown by circles are called "Spectrum". The black area is the pore space between white quartz grains. Dissolution of quartz is interpreted on spectrum sites 2, 7 and 8 and in other places on the edges of quartz grains. Dotted lines illustrate shapes of dissolved grains. Spectrum 3 is pointed at fractured remains of the dissolved illite-smectite, pyrite and carbonate remains of cement and precipitation of amorphous silica. Precipitation of silicate minerals (spectrum 4) and calcite (spectrum 6) is suggested.

4.1 Geochemical and mineralogical evolution

According to Carrol et al. [2011], provided a similar experimental approach is utilized, the addition of CO₂ lowers the pH and promotes silicate dissolution and amorphous silica, smectite and boehmite (γ-AlO(OH)) precipitation. The silica polymerization in mildly acidic to basic conditions begins with the condensation of monosilicic acid into cyclic oligomers, which grow to 3D polymer particles [Iler, 1979]. Gorrepati et al. [2010] reported silica particle formation and growth in low and negative pH solutions. These results were confirmed by XRF and SEM studies in our research.

We interpreted changes in the chemical composition of the reservoir sandstones from the E6 structure, caused by the alteration experiment (Fig. 5, Table 2), as the dissolution of minor and accessory minerals such as feldspar, dolomite, illite and barite, and assumed minor precipitation of amorphous silica, clay and carbonate minerals (according to XRF and SEM data). Such a phenomenon could be induced both by the alteration experiment performed in the laboratory and by natural diagenetic processes in the study area [Sliupa et al., 2008b]. However, the original rocks from the E6 structure were the least diagenetically altered and therefore we can suppose that minor precipitation of the mentioned minerals really happened during the performed CO₂-injection-like experiment.

The reservoir samples from the E7 structure showed slight diversity in the results of the geochemical/mineralogical alteration (Figs 6–8). Like in the samples from the E6 structure, we determined here minor dissolution of carbonate cement, clearly visible in Figs 6 and 7, dissolution of accessory minerals, such as barite, and precipitation of Fe-oxides/hydroxides, amorphous silica, dolomite, siderite, ilmenite, anatase, brookite and smectite (Table 2). The EDX study of thin sections revealed the second phase of the quartz mineral recrystallization phenomenon, confirming the precipitation of silica (Fig. 8). At the same time, the explored authigenic quartz mineralization could be subjected to different diagenetic conditions across the Baltic basin [Sliupa et al., 2008b]. Considering that the E7 structure is located in the conditions most favorable for such processes, including depth and increased temperature (46°C), we can suggest both diagenetic and experimental reasons for these alterations. The SEM study supports XRF analyses in terms of the presence of barium minerals in the form of barite due to the correlation of Ba with S (Fig. 6, Table 2). In marine sediments, Ba is associated with various particulate phases, including carbonates, organic matter, opal, ferromanganese oxyhydroxides, terrestrial and marine silicates, detrital material and barite [Gonnea and Paytan, 2006; Griffith and Paytan, 2012]. The major carrier of particulate Ba in

Table 4. Petrophysical parameters^a

№ Sample	Type	Weight, kg*10 ⁻³		Bulk density, kg/m ³		Matrix density, kg/m ³		Porosity, %		Permeability, mD		V _p , m/s		V _s , m/s	
		before	after	before	after	before	after	before	after	before	after	before	after	before	after
1	Db92-2 Trans-cap	15.2	-	2470	-	2900	-	14.9	-	2	-	-	-	-	-
2	Kn24-3 Trans-cap	23.9	12.4	2617	<i>2611</i>	2753	2693	4.95	3.0	0.004	-	4156	3700	2493	-
3	Kn24-4 Trans-res	35.3	31.6	2642	2148	2741	2675	7.3	9.6	0.28	300	4556	4030	3225	-
4	Kn27-2 Trans-cap	31.8	26.2	2633	2468	2741	2702	3.9	8.6	0.004	-	4630	4000	2778	<i>3034</i>
5	Kn27-4 Trans-res	35.0	27.1	2539	2419	2664	<i>2658</i>	0.8	19.1	0.001	550	5400	4380	3600	2540
6	E6-1 Reservoir	17.6	17.5	2123	2011	2705	2635	21.5	23.7	440	<i>380</i>	-	-	-	-
7	E6-2 Reservoir	12.0	<i>6.4*</i>	2031	1863	2725	2661	25.5	30.0	290	-	-	-	-	-
8	E6-3 Reservoir	10.2	10.0	1807	1999	2718	2633	33.5	24.1	400	490	-	-	-	-
9	E7-1 Reservoir	16.8	16.7	2354	2310	2683	2636	12.3	<i>12.4</i>	23	26	3583	<i>3300</i>	-	-
10	E7-2 Reservoir	26.5	<i>26.5</i>	2412	<i>2439</i>	2666	2641	9.5	7.7	18	16	2457	<i>2280</i>	1725	-
11	E7-3 Reservoir	24.8	24.6	2309	<i>2295</i>	2693	2650	14.3	13.4	66	130	3096	2750	2194	1850
12	E7-4 Reservoir	15.6	15.5	2339	2284	2716	2653	13.9	<i>13.9</i>	46	78	-	-	-	-
13	E7-5 Reservoir	24.9	<i>24.8</i>	2349	<i>2323</i>	2676	2646	12.2	<i>12.2</i>	16	19	3097	<i>3100</i>	2230	<i>2020</i>
14	E7-6 Reservoir	24.7	24.3	2403	<i>2367</i>	2704	2659	11.1	<i>11.0</i>	0.13	0.18	2524	1230	-	-
15	E7-7 Reservoir	24.8	<i>16.1*</i>	2395	2322	2746	2676	12.8	13.3	0.23	<i>0.23</i>	2130	<i>2130</i>	-	-

^aStudied rock samples are before and after the alteration experiment; V_p, P-wave velocity; V_s, S-wave velocity. **Bold** and *italic* numbers in the table correspond, respectively to "reliable" and "not reliable" changes of petrophysical parameters after the alteration experiment according to measurement errors. "Not reliable" values are also corresponding to the parameters not subjected to alteration.

*Change of the sample weight is due to destruction.

the water column is the mineral barite [Dymond et al., 1992]. Barite solubility (K_{BaSO₄}) grows with increasing pressure and temperature, up to 100°C, and then it progressively decreases with increasing temperature [Griffith and Paytan, 2012]. These conditions are close to those of our experiments, where XRF analysis showed a decrease in Ba content (Table 2). Most of Ba in the Earth's crust exists in association with K-bearing minerals, such as K-feldspars and K-micas, because its geochemistry is similar to the major rock-forming cation, K⁺. The XRF study confirmed a direct relationship between the decrease in Ba and K₂O contents after the alteration experiment in most of the studied samples (Table 2). Using XRF, we identified a slight increase in Ba in the clayey sandstone sample E7-7 after the experiment, assuming possible barite precipitation.

We assumed the dissolution of a significant amount of cement-forming carbonate minerals (ankerite in Kn24-4 and calcite in Kn27-4), induced by the chemical weathering and possible precipitation of silicate minerals in the trans-res samples from the South Kandava structure after the alteration (Table 2). Traces of

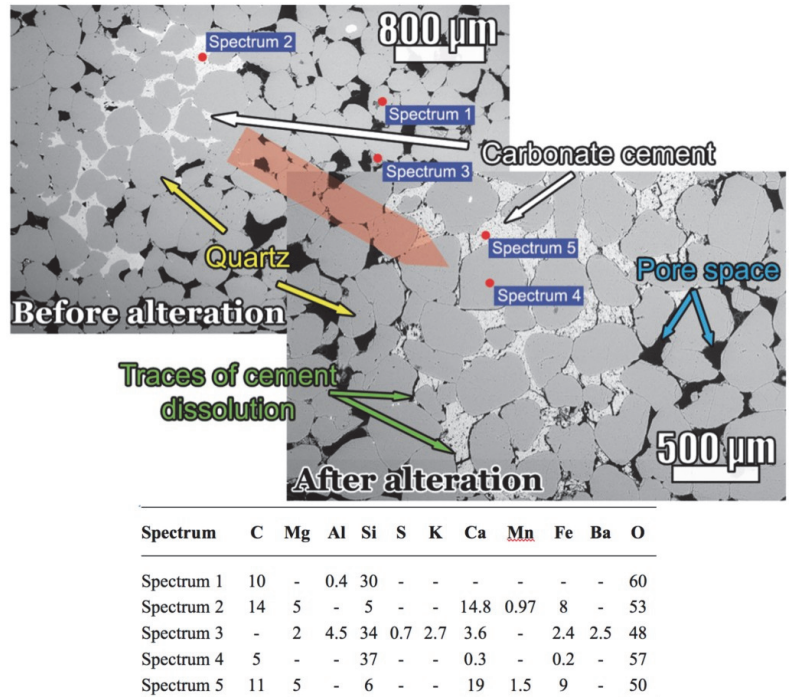
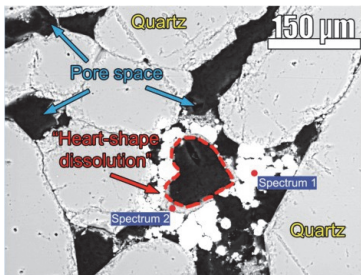


Fig. 6. SEM microphotographs of thin sections of fine-grained Deimena reservoir sandstone sample E7-3 (Table 1) before (left) and after (right) the alteration experiment and results of SEM energy-dispersive X-ray spectroscopy (EDX) analysis (in weight %). Large gray grains pointed by spectrum 4 are quartz grains. The black area is pore space. Spectra 2 and 5 are pointed at light gray-colored carbonate cement pore filling (calcite, ankerite and dolomite). Spectrum 3 is pointed at the clay and accessory minerals included in the cement pore filling (smectite, pyrite and barite). Traces of dissolved carbonate cement on the grain edges and inside the pore filling after alteration are indicated (right part).

carbonate cement dissolution could be clearly detected in thin sections of rock samples (Fig. 9). In addition, we found a minor increase in chemical oxides (Al_2O_3 , MgO and Na_2O) and decrease in MnO , Fe_2O_3 , TiO_2 and P_2O_5 . Carrol et al. [2011] discovered that Al/Fe silicate dissolution drives geochemical alterations within the reservoir and cap rock pore space. The dissolved Fe may be a source of long-term mineral trapping of CO_2 and the precipitation of secondary Fe-carbonates, clays and hydroxides could alter reservoir and seal permeability by clogging pores and fracture networks. The study of Liu et al. [2011] has shown that the acidic plume due to CO_2 dissolution into the brine could persist for thousands of years after the complete dissolution of CO_2 . Czernichowski-Lauriol et al. [2006] predicted that 50% of the CO_2



Spectrum	C	Al	Si	S	Cl	Ca	Ti	Fe	Zr	O
Spectrum 1	6	-	3	20	-	-	-	16	1.1	54
Spectrum 2	20	0.1	3.2	0.9	0.1	0.1	9	1.4	-	65

Fig. 7. SEM microphotograph of the thin section of reservoir sandstone sample E7-4 (Table 1) after the alteration experiment and results of SEM energy-dispersive X-ray spectroscopy (EDX) analysis (in weight %). Large dark-white grains are quartz grains. The black area is pore space. Spectrum 1 is pointed at white-colored inclusions of pyrite, siderite and minor content of zirconium silicate mineral (zircon). Spectrum 2 is pointed at secondary pore-filling minerals (aluminosilicates, anatase, pyrite and siderite). The heart-shaped dotted line shows freed space after dissolution.

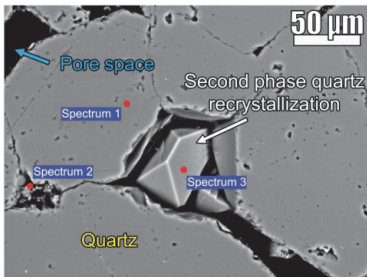
initially dissolved in the brine would be trapped in mineral phases (siderite, dawsonite) after 1,000 years. However, they mentioned that thermodynamic equilibrium is still not reached after 1,000 years. Proceeding from these conclusions, one could expect additional CO₂-fluid-rocks interactions in the long term and further research is needed in the field of geochemical-mineralogical evolution of the reservoir and cap rocks potentially used for the CGS.

The alteration of the glauconite-bearing sandy marlstone Db92-2, representing the trans-cap rock from the lowered wing of the Dobele structure, during modeling the CO₂ storage conditions in the aquifer, was in our study related to partial dissolution of carbonate and phosphate cement (calcite and apatite) and minor precipitation of pore-filling-bridging secondary clay minerals (illite and pyrite). It confirms that the implemented alteration experiment modeled the long-term conditions of CGS [Liu et al., 2012]. We assumed the dissolution of clay minerals and possible slight precipitation of calcite, supported by significant changes in the sample shape (Fig. 3a, b) and its weight decrease (up to 50%, Table 4), in the trans-cap limestone samples from the South Kandava structure (Kn24-3 and Kn27-2) (Fig. 11, Tables 2). The CO₂ mineral carbonation was proved by the increase in CaO and C contents after the laboratory alteration experiment. At the same time, we do not exclude that small changes in the chemical composition could also be connected with rock heterogeneity (considering the change in the sample size and weight during the alteration experiment) and with the accuracy of XRF measurements (different for every chemical element and depending depending on the element content).

4.2 Petrophysical evolution

Initial petrophysical properties of the studied reservoir rocks were controlled by primary sedimentation conditions, diagenetic processes including authigenic quartz cementation negatively correlated with carbonate cementation and porosity, clay maturity and mechanical compaction. These factors are controlled by paleoenvironmental conditions, present-day rock depth and fluid temperature, repeating tectonic movements and tectonic settings of the Baltic Syncline complicated by structures of the second order (Liepaja-Saldus high) and different fault settings in the studied structures of the third order.

The chemically induced petrophysical evolution of the reservoir rock samples from the two offshore structures (E6 and E7) was studied after modeling the CO₂ injection conditions in the storage sites. The initial and altered effective porosity and permeability of the reservoir samples from the E6 structure were ranked as "good" in terms of CGS. The porosity of the samples from the E7 structure before and after the experiment was estimated as "good" or "appropriate" for CGS but was significantly lower than



Spectrum	C	Al	Si	K	Ca	Fe	O
Spectrum 1	6	-	37	-	-	-	57
Spectrum 2	10	5	23	0.2	2.8	1	58
Spectrum 3	11	-	29	-	-	-	61

Fig. 8. SEM microphotograph of the thin section of reservoir sandstone sample E7-2 (Table 1) after the alteration experiment and results of SEM energy-dispersive X-ray spectroscopy (EDX) analysis (in weight %). Large gray grains are quartz. The black area is pore space. Spectrum 2 is pointed at secondary and clay minerals in the pore filling (illite/smectite). The gray crystal with white edges (indicated by spectrum 3) illustrates dissolution of quartz grains and the second phase of quartz grain recrystallization.

the properties of the E6 reservoir samples. The measured initial and altered permeability of the E7 samples was in the range of “low/impermeable–good/appropriate” in terms of CGS but significantly lower than in the E6 reservoir.

Similarly to the other studied rock samples, the reservoir sandstones from the E7 structure showed a slight reduction in the matrix density, correlated with a decrease in the bulk density and P-wave and S-wave velocity in some samples (Fig. 4c). The P-wave velocity of sample E7-6 decreased dramatically (more than 50%) after the alteration experiment. This was explained by a decrease in the sample weight caused by the dissolution of a significant amount of cement-forming ankerite and dolomite and minor feldspar and accessory minerals (e.g. pyrite and barite) (Table 2). Effective porosity was in most cases unchanged, supported by stable permeability (E7-1, E7-5) or some variation (E7-4, E7-6) in its value (Table 4, Fig. 4c). Other samples showed some variation in effective porosity with stable permeability. At the same time, sample E7-3 was characterized by a slight decrease in effective porosity but a significant increase in permeability (up to two times after the alteration experiment). A slight decrease in the matrix density in this sample correlated with a slight decrease in P-wave velocity (Table 4, Fig. 4c). An increase in permeability with a decrease in the matrix density, supporting unchanged native porosity, could be explained by pore space geometry modifications and grain shape changes that control capillary forces [Schön, 1996]. We determined a minor dissolution of cement in the samples, including dolomite and ankerite (Table 2, Fig. 6), which is insignificant for the effective porosity change but substantial for the permeability increase. The same interpretation could apply to the samples characterized by decreased effective porosity, where mineral precipitation and/or cement dissolution and relocation took place. In the case of the CO₂ storage in the E7 structure, there is some probability of a slight decrease in storage capacity and improvement of the CO₂ injection rate, but this conclusion should be supported by additional laboratory and modeling studies. A reliable decrease in the bulk density was determined in only two samples from that structure, E7-4 and E7-7. In E7-7, the bulk density decrease correlated with the effective porosity increase but in E7-4 the bulk density decrease correlated with the permeability increase.

All three reservoir rock samples from the E6 structure showed mechanical weakening due to decrease in the matrix density and sample weight after the experiment. However, the weight of sample E6-2 changed due to the destruction after the alteration. An increase in effective porosity, correlated with a decrease in the bulk density and unchanged permeability, was observed in sample E6-1. The same correlations (except permeability that was not measured after the experiment) were obtained in sample E6-2. A decrease in effective porosity correlated with an increase

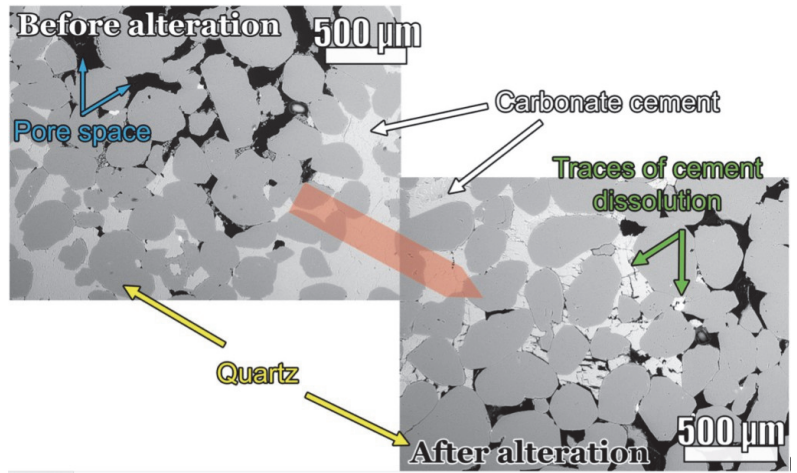


Fig. 9. SEM microphotographs of thin sections of trans-reservoir carbonate-cemented fine-grained Deimena sandstone sample Kn24-4 (Table 1) before (left) and after (right) the alteration experiment. XRD analyses revealed minor presence of ankerite ($\text{Ca}(\text{Fe,Mg,Mn})(\text{CO}_3)_2$) minerals. Large gray grains are quartz grains. The black area is pore space. The white area is ankerite cement pore filling. Traces of dissolved carbonate cement on grain edges and inside the pore filling after the alteration are indicated (right).

in the bulk density in sample E6-3, where also an increase in permeability was measured after the alteration (Table 4). These two rock samples have similar geochemical properties. Samples E6-1 and E6-3 were selected from two different depth intervals of the well E6-1/84 (Table 1), characterized by various lithological and petrophysical properties [Shogenov et al., 2013b]. Sample E6-2 (from the same depth as sample E6-3) showed an increase in effective porosity and, contrary to E6-3, petrophysical alterations after the experiment, thus proving the influence of rock heterogeneity on the obtained results.

The physical, geochemical and mineralogical studies of the trans-reservoir carbonate-cemented quartz sandstones Kn24-4 and Kn27-4 were carried out during this research. Before the alteration experiment, the samples had low effective porosity and permeability (Table 4). We determined a slight reduction in the weight, bulk and matrix density and P-wave velocity with an increase in effective porosity in Kn24-4 (Table 4). More significant changes were observed in sandstone Kn27-4 located in the uplift. Compared to Kn24-4 from the lowered wing of the structure, sample Kn27-4 showed a twofold decrease in weight and P-wave velocity and a significant increase in effective porosity (the final value of effective porosity increased from "very low" to almost "good"), as well as a significant decrease in S-wave velocity (Table 4). The matrix density did not change in sample Kn27-4,

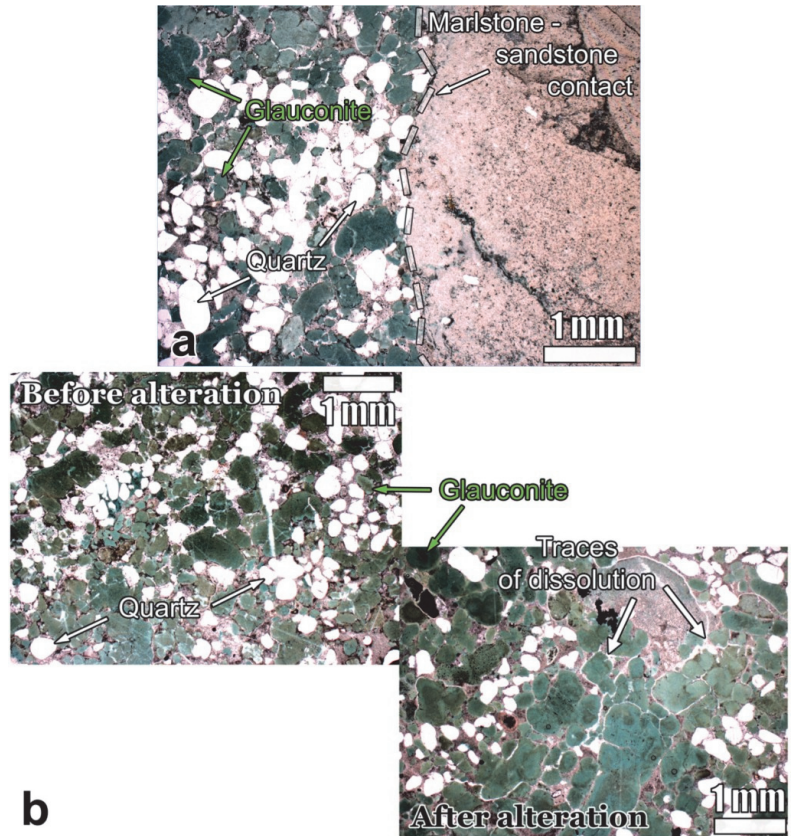
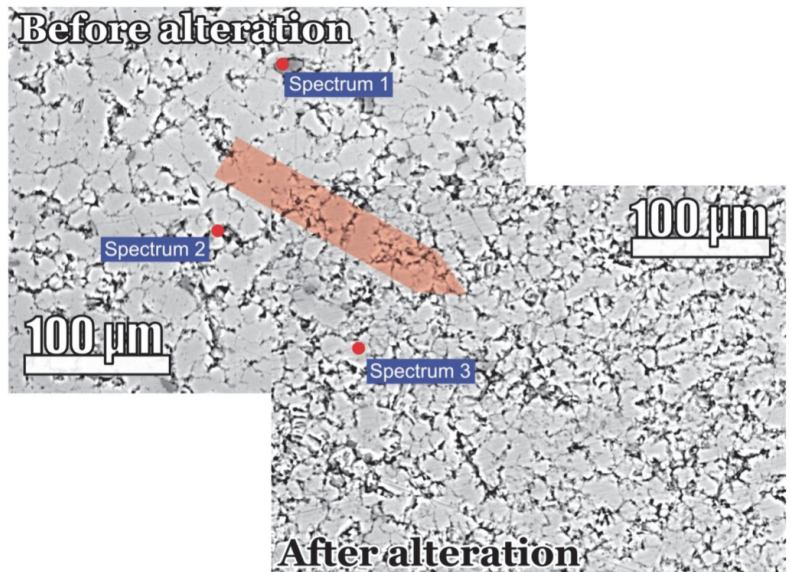


Fig. 10. (a) Microphotograph of the thin section in cross-polarized light of trans-cap glauconite-bearing sandy marlstone sample Db92-2 (Table 1) before the alteration experiment. The marlstone–sandstone contact shows sample heterogeneity and its transitional composition between carbonate and carbonate-siliciclastic rocks. (b) microphotographs of thin sections in cross-polarized light of sample Db92-2 before (left) and after (right) the alteration experiment. Natural diagenetic weathering of the original rock sample (left) was accelerated by acid-induced reactions during the alteration experiment (right). The original rock sample was partly destroyed and disaggregated due to the dissolution of calcite and apatite (Table 2) and it was not possible to measure its physical properties after the experiment.

and the bulk density decrease was four times lower than in sample Kn24-4. Both samples revealed a very similar drastic increase in permeability from a “low” rank to a “good” rank in terms of CGS (Table 4).

The effective porosity and permeability measurements of trans-cap limestone samples Kn24-3 and Kn27-2 before the alteration experiment showed low porosity (<10%) and low permeability



Spectrum	Mg	Al	Si	S	K	Ca	Ti	Mn	Fe	O
Spectrum 1	-	0.3	41.3	-	0.2	7.8	-	-	-	50.5
Spectrum 2	0.4	2.4	9.3	-	1.6	33.3	14.4	0.3	1.5	36.8
Spectrum 3	0.5	0.4	1.3	-	0.4	67.9	-	-	-	29.4

Fig. 11. SEM microphotographs of thin sections of trans-cap slightly argillaceous limestone sample Kn24-3 (Table 1) before (left) and after (right) the alteration experiment and results of SEM energy-dispersive X-ray spectroscopy (EDX) analysis (in weight %). Gray-white carbonate matrix is micritic calcite forming the limestone sample. The thin black net is porous space. The visually identified increase in porosity is supported by the measured decrease in P-wave velocity (Table 4) after the alteration (right).

(<0.01 mD, Table 4) appropriate for cap rock. Under chemical alteration, the matrix density and P-wave velocity decreased slightly in both samples (Table 4), while effective porosity decreased in sample Kn24-3 and increased in Kn27-2. Although changes in effective porosity had different trends (which could be explained by the heterogeneity of samples), they correspond to the requirements for good cap rocks, as the changed effective porosities after the experiment were still <10% in both samples (Table 4). The observed bulk density decrease in Kn27-2 was correlated with the effective porosity increase. We did not detect any reliable bulk density changes in sample Kn24-3. As due to a drastic change in the sizes of these samples it was impossible to measure their permeability after the experiment, we cannot assess how their sealing properties were changed in general. Still, considering the mechanical weakening of the sealing rocks reported earlier and confirmed by our CO₂-cap rock interaction

experiments, possible leakage from the CO₂ storage reservoir through the cap rock could be assumed. However, previous results of the long-term modeling of the Sleipner storage site [Czernichowski-Lauriol et al., 2006] permitted of another interpretation. The batch- and reaction-diffusion simulations of the impact of CO₂ on the clayey cap rock at the North Sea Sleipner injection site performed by Gaus et al. [2005] showed that the effective diffusion coefficients are likely so low that the diffusion of CO₂ will only affect a few meters of the cap rock after thousands of years. Moreover, as CO₂ diffuses into the cap rock, silica, as well as other constituents, is released from the CO₂-caprock interactions, leading to precipitation of chalcedony, kaolinite and calcite, which may further reduce the diffusion into the cap rock. Bildstein et al. [2010] conducted a series of numerical simulations of cap rock responses to CO₂ injection using various reactive transport modeling codes. Both 1D and 2D single-phase flow scenarios in saturated porous media with or without fracture, and 1D multi-phase flow in unsaturated media without fracture, were modeled. Significant porosity changes were observed in the models for a period of 10,000 years, which were expected due to the high reactivity of the carbonate-rich cap rock with the acidic CO₂-rich fluid. However, the reactions were shown to be limited to the first decimeters to meters into the cap rock from the CO₂-cap rock interface in 10,000 years, and no leakage was reported. Their preliminary results on rock heterogeneity suggested, as indicated in experimental works [Angeli et al., 2009], that the reactivation of small cracks or fractures (especially those originally filled with calcite) could generate preferential pathways for CO₂ propagation in the cap rock.

Although all the studied structures had a common stratigraphy of the Deimena Formation and were located within the Liepaja-Saldus high, they were characterized by different primary compositions of the Deimena rocks and their diagenetic changes, controlled by the present depth, temperature, which is higher offshore than onshore, and fluid salinity. We studied reservoir rock samples of different composition, cementation and compaction and some transitional clayey carbonate cap rocks from the onshore structures and their lowered wings. But, considering the limited number of the drill cores and samples used, it was not possible to make more general conclusions about paleoenvironmental conditions of sedimentation in the region. However, it was clearly shown that the interaction of rock with simulated CO₂-rich fluid was dependent on diagenetic changes, including authigenic quartz cementation, carbonate cementation, compaction and clay maturity. Additional studies, laboratory experiments and basin-scale modeling are needed to support more general conclusions about regional geology and interaction of rocks and fluids with CO₂ during its possible storage.

5. Conclusions

1. The 15 rock samples studied before and after the CO₂-injection-like experiment had undergone various diagenetic changes determining the alteration of rocks during the experiment and its degree.
2. Both short-term (mineral dissolution) and long-term processes (precipitation) were detected after the experiment.
3. Significant dissolution of the pore-filling carbonate cement (ankerite and calcite) in the trans-reservoir sandstones from the South Kandava onshore structure caused a high increase in effective porosity and permeability and a decrease in the weight of samples, bulk and matrix density, P- and S-wave velocity during the alteration experiment. In addition to the dissolution of accessory ankerite and calcite, we suggest possible minor precipitation of secondary silicate minerals.
4. Small changes in the "high-quality" reservoir sandstones from the E6 offshore structure during the alteration experiment were interpreted as minor dissolution of carbonate cement, feldspar and some accessory minerals (e.g. illite, barite, anatase/brookite), followed by some precipitation of amorphous silica, clay and carbonate minerals. Mineral dissolution caused slight mechanical weakening and a decrease in the weight of samples and matrix density, variations in the bulk density and an increase in effective porosity, and an increase in the permeability of the rock from the lowermost part of the E6 reservoir. Geochemical alterations induced a minor decrease in the bulk density and an increase in the effective porosity of the sandstone from the uppermost part of the E6 structure.
5. Only modest geochemical alteration of the reservoir sandstones from the E7 offshore structure caused minor dissolution of the cement-forming and accessory minerals (e.g. barite) and possible slight precipitation of Fe-oxides/hydroxides, amorphous silica, dolomite, siderite, ilmenite and smectite. These alterations caused some reduction in sample weight, bulk and matrix density, effective porosity, P- and S-wave velocities associated with a minor increase in permeability.
6. Initial reservoir properties of all the studied rocks did not decrease, but were significantly improved in the carbonate-cemented sandstones after the experiment.
7. The main effect of the CO₂ fluid on the trans-cap glauconite-bearing sandy marlstone from the Dobeles onshore structure was the dissolution of carbonate minerals (calcite and carbonate apatite) and minor precipitation of pore-filling-bridging secondary clay minerals (illite and pyrite).
8. The trans-cap limestones from the transitional zone between the reservoir and cap rock in the South Kandava onshore structure subjected to the alteration experiment showed slight dissolution of clay minerals and possible minor precipitation of

calcite. The chemical and mineralogical alteration was associated with a decrease in the weight of samples, bulk and matrix density and P-wave velocity.

Acknowledgements

This contribution is part of the PhD study by K. Shogenov. The research was partly supported by the institutional research funding programmes (projects SF0320080s07 and IUT19-22) of the Estonian Ministry of Education and Research) and the EU FP7 project CGS Europe project No. 256725. IFP Energies nouvelles (IFPEN) conducted the alteration experiment. All the data presented in the study are the property of the authors and available on request from the first author (kazbulat.shogenov@ttu.ee). We are grateful to the LEGMC for providing samples and to Jean Guelard (IFPEN) for help in permeability measurements and guidance in the petrophysical laboratory. We highly appreciate the fruitful discussions on thin sections of altered rock samples with Karl-Heinz Wolf from Delft University of Technology. The anonymous reviewers are thanked for their helpful comments improving the manuscript.

References

- Alemu, B. L., P. Aagaard, I. A. Munz, and E. Skurtveit (2011), Caprock interaction with CO₂: A laboratory study of reactivity of shale with supercritical CO₂ and brine, *Appl. Geoch.*, 26(12), 1975–1989, doi:10.1016/j.apgeochem.2011.06.028.
- American Petroleum Institute (1998), Recommended practices for core analysis, Second Edition, Recommended Practice, 40, Exploration and Production Department, <http://www.sprensky.com/bibliogs/tla.html>.
- Angeli, M., M. Soldal, E. Skurtveit, and E. Aker (2009), Experimental percolation of supercritical CO₂ through a caprock, *En. Proc.*, 1, 3351–3358, doi:10.1016/j.egypro.2009.02.123.
- Aplin, A. C., I. F. Matenaar, D. K. McCarty, and B. A. van der Pluijm (2006), Influence of mechanical compaction and clay mineral diagenesis on the microfabric and pore-scale properties of deep-water Gulf of Mexico mudstones, *Cl. Cl. Min.*, 54, 500–514.
- Armitage, P. J., D. R. Faulkner, R. H. Worden, A. C. Aplin, A. R. Butcher, and J. Iliffe (2011), Experimental measurement of, and controls on, permeability and permeability anisotropy of caprocks from the CO₂ storage project at the Krechba Field, Algeria, *J. Geophys. Res.*, 116, B12208, doi:10.1029/2011JB008385.
- Arts, R., A. Chadwick, O. Eiken, S. Thibeau, and S. Nooner (2008), Ten years of experience of monitoring CO₂ injection in the Utsira Sand at Sleipner, offshore Norway, *First break*, 26(1), 65–72.
- Babuke, B., R. Vzosek, A. Grachev, V. Naidenov, V. Krochka, P. Markov, E. Novikov, L. Tsimashevski, and R. Labus (unpublished data, 1983), Geological Rep. of the well E7-1/82, available from Latvian Environmental, Geology and Meteorology Centre (LEGMC), Latvia, Riga, (in Russian).
- Bachu, S., D. Bonijoly, J. Bradshaw, R. Burruss, S. Holloway, N. P. Christensen, and O. M. Mathiassen (2007), CO₂ storage capacity estimation: Methodology and gaps, *Int. J. Greenh. Gas Con.*, 1(4), 430–443, doi:10.1016/S1750-5836(07)00086-2.
- Bemer, E. and J. M. Lombard (2010), From injectivity to integrity studies of CO₂ geological storage, *Oil & Gas Sci. Tech. - Rev. IFP*, 65(3), 445–459, doi:10.2516/ogst/2009028.
- Bemer, E., M. T. Nguyen, and L. Dormieux (2011), Experimental poromechanics applied to CO₂ geological storage, paper presented at Symposium on Mechanics and Physics of Porous Solids, Champs-sur-Marne, France.
- Berthe, G., S. Savoye, C. Wittebroodt, and J. L. Michelot (2011), Effect of CO₂-enriched fluid on three argillite type caprocks, paper presented at Goldschmidt Conference, Prague, Czech Republic, *Mineral. Mag.*, pp.523, <http://goldschmidt.info/2011/abstracts/finalPDFs/523.pdf>.
- Bertier, P., R. Swennen, B. Laenen, D. Lagrou, and R. Dreesen (2006), Experimental identification of CO₂-water-rock interactions caused by sequestration of CO₂ in Westphalian and Buntsandstein sandstones of the Campine Basin (NE-Belgium). *J. Geochem. Explor.*, 89(1), 10–14, doi:10.1016/j.gexplo.2005.11.005.
- Bildstein, O., C. Kervévan, V. Lagneau, P. Delaplace, A. Crédoz, P. Audigane, E. Per-fetti, N. Jacquemet, and M. Jullien (2010), Integrative modeling of caprock integrity in the context of CO₂ storage: evolution of transport and geochemical properties and impact on performance and safety assessment. *Oil & Gas Sci. Tech. - Rev. IFP*, 65, 485–502, dx.doi.org/10.2516/ogst/2010006.
- Busch, A., S. Alles, Y. Gensterblum, D. Prinz, D. N. Dewhurst, M. D. Raven, H. Stanjek, and B. M. Krooss (2008), Carbon dioxide storage potential of shales, *Int. J. Greenh. Gas Con.*, 2(3), 297–308, doi:10.1016/j.ijggc.2008.03.003.

- Carroll, S. A., W. W. McNab, and S. C. Torres (2011), Experimental study of cement –sandstone/shale-brine-CO₂ interactions, *Geochem. Trans.*, 12(9), doi:10.1186/1467-4866-12-9.
- Carroll, S. A., W. W. McNab, Z. Dai, and S. C. Torres (2013), Reactivity of Mt. Simon sandstone and the Eau Claire shale under CO₂ storage conditions, *Environ. Sci. Technol.*, 47(1), 252-261, doi:10.1021/es301269k.
- Chadwick, A., R. Arts, C. Bernstone, F. May, S. Thibeau, and P. Zweigel (2006), Best practice for the storage of CO₂ in saline aquifers, Keyworth, Nottingham, British Geological Survey Occasional Publication, 14, ISBN: 978-0-85272-610-5.
- Creodoz, A., O. Bildstein, M. Jullien, J. Raynal, J. C. Pétronin, M. Lillo, C. Pozo, and G. Geniaut (2009), Experimental and modeling study of geochemical reactivity between clayey caprocks and CO₂ in geological storage conditions, *En. Proc.*, 1(1), 3445–3452, doi:10.1016/j.egypro.2009.02.135.
- Čyžienė, J., N. Molenaar, S. Šliaupa (2006), Clay-induced pressure solution as a Si source for quartz cement in sandstones of the Cambrian Deimena Group, *Geol.*, 53, 8–21, ISSN 1392-110X.
- Czernichowski-Lauriol, I., C. Rochelle, I. Gaus, M. Azaroual, J. Pearce, and P. Durst (2006). Geochemical interactions between CO₂, pore-waters and reservoir rocks: lessons learned from laboratory experiments, field studies and computer simulations, In: Lombardi, S., Altunina, S.E., Beaubien, S.E. (Eds.), *Advances in the geological storage of carbon dioxide: international approaches to reduce anthropogenic greenhouse gas emissions*. Springer, Dordrecht, Netherlands, 157–174, ISBN: 9781402044700.
- Dymond, J., E. Suess, and M. Lyle (1992), Barium in deep-sea sediment: a geochemical proxy for paleoproductivity, *Paleoceanogr.*, 7(2), 163–181, doi:10.1029/92PA00181.
- Egermann, P., E. Bemer, and B. Zinszner (2006), An experimental investigation of the rock properties evolution associated to different levels of CO₂ injection like alteration processes, paper presented at International Symposium of the Society of Core Analysts, paper SCA 2006-34, Trondheim, Norway.
- Falk, E. S. (2014), Carbonation of peridotite in the Oman Ophiolite, Ph.D. thesis, Columbia Univ., Columbia, USA.
- Freimanis, A., L.S. Margulis, A. Brangulis, S. Kanev, and R. Pomerantseva (1993), Geology and hydrocarbon prospects of Latvia. *OGJ*, 91(49), 71-74.
- Gaus, I., M. Azaroual, and I. Czernichowski-Lauriol (2005), Reactive transport modeling of the impact of CO₂ injection on the clayey cap rock at Sleipner (North Sea), *Chem. Geol.*, 217(3-4), 319–337, doi:10.1016/j.chemgeo.2004.12.016.
- GCCI (Global CCS Institute) (2013), *The Global Status of CCS: 2013*, Melbourne, Australia (<http://www.globalccsinstitute.com/publications/global-status-ccs-2013>).
- Gilfillan, S. M. V., C. J. Ballentine, G. Holland, D. Blagburn, B. S. Lollar, S. Stevens, M. Schoell, and M. Cassidy (2008), The noble gas geochemistry of natural CO₂ gas reservoirs from the Colorado Plateau and Rocky Mountain provinces, USA, *Geochimica et Cosmochimica Acta*, 72, 1174–1198, doi:10.1016/j.gca.2007.10.009.
- Gilfillan, S. M. V., B. S. Lollar, G. Holland, D. Blagburn, S. Stevens, M. Schoell, M. Cassidy, Z. Ding, Z. Zhou, G. Lacrampe-Couloume, and C. J. Ballentine (2009), Solubility trapping in formation water as dominant CO₂ sink in natural gas fields, *Nat.*, 458(7238), 614–618, doi:10.1038/nature07852.
- Gonneea, M. E. and A. Paytan (2006), Phase associations of barium in marine sediments, *Mar. Chem.*, 100, 124–135, doi:10.1016/j.marchem.2005.12.003.
- Gorrepati, E. A., P. Wongthahan, S. Raha, and H. S. Fogler (2010), Silica precipitation in acidic solutions: mechanism, pH effect, and salt effect, *Langmuir*, 26(13), 10467–10474, doi: 10.1021/la904685x.
- Griffith, E. M. and A. Paytan (2012), Barite in the ocean – occurrence, geochemistry, and paleoceanographic applications, *Sediment.*, 59(6), 1817-1835, doi:10.1111/j.1365-3091.2012.01327.x.
- Grigelis, A. A. (1991), editor. *Geology and geomorphology of the Baltic Sea. Explanatory note of the geological maps, scale 1:500 000*, Leningrad, Nedra, (in Russian).

- Grigg, R. B. and R. K. Svec (2003), Co-injected CO₂-brine interactions with Indiana Limestone, paper presented at Society of Core Analysts Symposium, paper SCA 2003-19, Pau, France.
- Gunter, W. D., B. Wiwchar, and E. H. Perkins (1997), Aquifer disposal of CO₂-rich greenhouse gases: extension of the time scale of experiment for CO₂-sequestering reactions by geochemical modeling, *Miner. Pet.*, 59(1-2), 121-140.
- Gunter, W. D., E. H. Perkins, and I. Hutcheon (2000), Aquifer disposal of acid gases: modeling of water-rock reactions for trapping of acid wastes, *Appl. Geochem.*, 15(8), 1085-1095, doi:10.1016/S0883-2927(99).00111-0.
- Halland, E. K., W. T. Johansen, and F. Riss (2011), CO₂ storage atlas - Norwegian North Sea. The Norwegian Petroleum Directorate, <http://www.npd.no/Global/Norsk/3-Publikasjoner/Rapporter/PDF/CO2-ATLAS-lav.pdf>.
- Halland, E. K., W. T. Johansen, and F. Riss (2013), CO₂ storage atlas - Norwegian Sea. The Norwegian Petroleum Directorate, <http://www.npd.no/Global/Norsk/3-Publikasjoner/Rapporter/CO2-ATLAS-Norwegian-sea-2012.pdf>.
- Hitchon, B., ed. (1996), *Aquifer Disposal of Carbon Dioxide*, Sherwood Park, Alberta, Canada: Geoscience Publishing Ltd.
- IEA-International Energy Agency (2004), *Prospects for CO₂ Capture and Storage*, paper presented at IEA/OECD, Paris, France.
- Iler, R. K. (1979), *The chemistry of silica: solubility, polymerization, colloid and surface properties, and biochemistry*, John Wiley & Sons, New York, ISBN:978-0-471-02404-0.
- IPCC (2014), *IPCC Special Rep. Climate change: Mitigation of climate change*. Prepared by Working Group III Contribution of the Intergovernmental Panel on Climate Change to AR5.
- Izgec, O., B., Demiral, H. Bertin, and S. Akin (2008), CO₂ injection into saline carbonate aquifer formations. Laboratory investigation, *Transp. Porous Med.*, 72, 1–24, doi:10.1007/s11242-007-9132-5.
- Kamath, J., F. M. Nakagawa, R. E. Boyer, and K. A. Edwards (1998), Laboratory investigation of injectivity losses during WAG in West Texas Dolomites, paper presented at Permian Basin Oil and Gas Conference, paper SPE 39791, Midland, TX, <http://dx.doi.org/10.2118/39791-MS>.
- Kaszuba, J. P., D. R. Janecky, and M. G. Snow (2005), Experimental evaluation of mixed fluid reactions between supercritical carbon dioxide and NaCl brine: relevance to the integrity of a geologic carbon repository, *Chem. Geol.*, 217, 277–293, doi:10.1016/j.chemgeo.2004.12.014.
- Kaszuba, J. P. and D. R. Janecky (2009), *Geochemical impacts of sequestering carbon dioxide in brine formations*, American Geophysical Union, Washington D.C., *Geoph. Monogr.*, 183(7), doi:10.1029/2006GM000353.
- Kilda, L., and H. Friis (2002), The key factors controlling reservoir quality of the Middle Cambrian Deimena Group sandstone in West Lithuania, *Bulletin of the Geological Society of Denmark*, 49(1), 25–39.
- Kohler, E., T. Parra, and O. Vidal (2009), Clayey cap-rock behavior in H₂O–CO₂ media at low pressure and temperature conditions: an experimental approach, *Cl. Cl. Min.*, 57(5), 616–637, doi:10.1346/CCMN.2009.0570509.
- Lashkova L. N. 1979. *Lithology, facies and reservoir properties of Cambrian deposits of South Baltic region*. Moscow: Nedra, pp. 102 (in Russian).
- Liu, F., P. Lu, C. Zhu, and Y. Xiao (2011), Coupled reactive flow and transport modeling of CO₂ sequestration in the Mt. Simon sandstone formation, Midwest U.S.A, *Int. J. Greenh. Gas Con.*, 5(2), 294–307, doi:10.1016/j.ijggc.2010.08.008.
- Liu, F., P. Lu, C. Griffith, S. W. Hedges, Y. Soong, H. Hellevang, and C. Zhu (2012), CO₂-brine-caprock interaction: Reactivity experiments on Eau Claire shale and a review of relevant literature, *Int. J. Greenh. Gas Con.*, 7, 153-167, doi:10.1016/j.ijggc.2012.01.012.
- Lu, J., M. Wilkinson, R. S. Haszeldine, and A. E. Fallick (2009), Long-term performance of a mudrock seal in natural CO₂ storage, *Geol.*, 37(1), 35–38, <http://dx.doi.org/10.1130/G25412A.1>.

- Mavko, G., T. Mukerji, and J. Dvorkin (2003), *Rock physics handbook - Tools for seismic analysis in porous media*, Cambridge University Press.
- Metz, B., O. Davidson, H. C. de Coninck, M. Loos, and L. A. Meyer, (eds) (2005), *IPCC Special Rep. Carbon Dioxide Capture and Storage*. Prepared by Working Group III of the Intergovernmental Panel on Climate Change, Cambridge University Press, Cambridge, United Kingdom and New York, NY, USA.
- Navarre-Sitchler, A., K. Muouzakis, J. Heath, T. Dewers, G. Rother, X. Wang, J. Kaszuba, and J. McCray (2011), Changes to porosity and pore structure of mud-stones resulting from reaction with CO₂ and brine, paper presented at Goldschmidt Conference, Prague, Czech Republic, *Mineral. Mag.*, pp. 1527, <http://goldschmidtabstracts.info/2011/1527.pdf>.
- Nguyen, P., H. Fadaei, and D. Sinton (2013), Microfluidics underground: A micro-core method for pore scale analysis of supercritical CO₂ reactive transport in saline aquifers, *J. Flu. Eng.*, 135(2), 1-7, doi:10.1115/1.4023644.
- Paškevičius J. 1997. *The Geology of the Baltic Republics*. Vilnius. 387 p
- Pawar, R. J., N. R. Warpinski, J. C. Lorenz, R. D. Benson, R. B. Grigg, B. A. Stubbs, P. H. Stauffer, J. P. Krumhansl, and S. P. Cooper (2006), Overview of a CO₂ sequestration field test in the West Pearl Queen reservoir, New Mexico, *The American Association of Petroleum Geologists/Division of Environmental Geosciences, Env. Geosci.*, 13(3), 163-180, doi:10.1306/eg.10290505013.
- Perkins, E. H. and W. D. Gunter (1995), Aquifer disposal of CO₂-rich greenhouse gasses: modeling of water-rock reaction paths in a siliciclastic aquifer, paper presented at 8th International Symposium on water-rock Interaction, edited by Y. K. Kharaka and O. V. Chudaev, A.A. Balkema, Vladivostok, Russia, 895-898.
- Prieditis, J., C. R. Wolle, and P. K. Notz (1991), A laboratory and field injectivity study: CO₂ WAG in the San Andres formation of West Texas, paper presented at Annual Technical Conference and Exhibition, paper SPE 22653, October 6-9, 1991, Dallas, TX, doi:10.2118/22653-MS.
- Rochelle, C. A., I. Czernichowski-Lauriol, and A. E. Milodowski (2004), The impact of chemical reactions on CO₂ storage in geological formations: a brief review, *Geological Society, London, Special Publications*, 233, 87-106, doi:10.1144/GSL.SP.2004.233.01.07.
- Ross, G. D., A. C. Todd, J. A. Tweedie, and A. G. Will (1982), The dissolution effects of CO₂-brine systems on the permeability of U.K. and North Sea calcareous sandstones, paper presented at DOE Symposium on Enhanced Oil Recovery, paper SPE 10685, Society of Petroleum Engineers, Tulsa, OK, <http://dx.doi.org/10.2118/10685-MS>.
- Schön, J. H. (1996), *Physical properties of rocks: fundamentals and principles of petrophysics*, Oxford, OX, UK: Pergamon.
- Shafeen, A. and T. Carter (2010), Geological Sequestration of Greenhouse Gases, in *Environmentally Conscious Fossil Energy Production*, edited by M. Kutz and A. Elkamel, John Wiley & Sons. Canada, Inc., Hoboken, NJ, USA. doi:10.1002/9780470432747.ch6.
- Shogenov, K. (2008), Correlation of the Ordovician bedrock in the South Estonian boreholes by petrophysical and geochemical properties, M.S. thesis, AKG34LT, Department of Mining, Tallinn Univ. of Techn., Tallinn, Estonia, (in Estonian).
- Shogenov, K., A. Shogenova, and O. Vizika-Kavvadias (2013a), Petrophysical properties and capacity of prospective structures for geological storage of CO₂ onshore and offshore Baltic, *Elsevier, En. Proc.*, 37, 5036-5045, doi:10.1016/j.egypro.2013.06.417.
- Shogenov, K., A. Shogenova, and O. Vizika-Kavvadias (2013b), Potential structures for CO₂ geological storage in the Baltic Sea: case study offshore Latvia, *Bulletin of the Geological Society of Finland*, 85(1), 65-81, ISSN:0367-5211, http://www.geologinenseura.fi/bulletin/Volume85/Bulletin_vol85_1_2013_Shogenov_ea.pdf.
- Shogenova, A., A. Jõelet, R. Einasto, A. Kleesment, K. Mens, and R. Vaher (2003a), Petrophysical model of sedimentary rocks from Ruhnu borehole,

- Estonia, paper presented at International Geophysical Conference and Exhibition, Russia, Moscow, Sovincenter, Extended Abstract Volume, 1-4.
- Shogenova, A., A. Jõelet, R. Einasto, A. Kleesment, K. Mens, and R. Vaher (2003b), Chemical composition and physical properties of rocks, In: Põldvere, A. (ed.). Estonian Geological Sections. Bulletin 5. Ruhnu 500 drill core, Geological Survey of Estonia, Tallinn, 34–39.
- Shogenova, A., A. Kleesment, and K. Shogenov (2005), Chemical composition and physical properties of the rock. In: Põldvere, A. (ed.). Estonian Geological Sections. Bulletin 6. Mehikoorma (421) drill core. Geological Survey of Estonia, Tallinn, 31-38.
- Shogenova, A., A. Kleesment, and K. Shogenov (2006), Lithologic determination of Devonian dolomitic carbonate-siliciclastic rocks from Estonia by physical parameters, paper presented at 68th EAGE Conference & Exhibition, Extended Abstracts & Exhibitors` Catalogue, P207, European Association of Geoscientists & Engineers, Vienna 2006, Houten, The Netherlands, 1-5.
- Shogenova, A., S. Šliaupa, R. Vaher, K. Shogenov, and R. Pomeranceva (2009a), The Baltic Basin: structure, properties of reservoir rocks and capacity for geological storage of CO₂, In: Estonian Academy Publishers, Est. J. Earth Sci., 58(4), 259-267, doi:10.3176/earth.2009.4.04.
- Shogenova, A., S. Šliaupa, K. Shogenov, R. Šliaupiene, R. Pomeranceva, R. Vaher, M. Uibu, and R. Kuusik (2009b), Possibilities for geological storage and mineral trapping of industrial CO₂ emissions in the Baltic region, En. Proc., 1(1), 2753-2760, doi:10.1016/j.egypro.2009.02.046.
- Shogenova, A., K. Shogenov, R. Vaher, J. Ivask, S. Šliaupa, T. Vangkilde-Pedersen, M. Uibu, and R. Kuusik (2011a), CO₂ geological storage capacity analysis in Estonia and neighboring regions, En. Proc., 4, 2785-2792, doi:10.1016/j.egypro.2011.02.182.
- Shogenova, A., K. Shogenov, R. Pomeranceva, I. Nulle, F. Neele, and C. Hendriks (2011b), Economic modeling of the capture–transport–sink scenario of industrial CO₂ emissions: the Estonian–Latvian cross-border case study, Elsevier, The Netherlands, En. Proc., 4, 2385-2392, doi:10.1016/j.egypro.2011.02.131.
- Shogenova, A., K. Piessens, J. Ivask, K. Shogenov, R. Martínez, I. Suárez, K. M. Flornes, N. E. Poulsen, A. Wójcicki, S. Šliaupa, L. Kucharic, A. Dudu, S. Persoglia, S. Holloway, and B. Saftic (2013), CCS Directive transposition into national laws in Europe: progress and problems by the end of 2011, Elsevier. En. Proc., 37, 7723-7731, doi:10.1016/j.egypro.2013.06.718.
- Sikorska, M. and J. Paczesna (1997), Quartz cementation in Cambrian sandstones and the background of their burial history of the East European Craton, Geol. Quart., 41, 265-272.
- Šliaupa, S., V. Rasteniene, L. Lashkova, and A. Shogenova (2001), Factors controlling petrophysical properties of Cambrian siliciclastic deposits of central and western Lithuania, paper presented at Nordic Petroleum Series: V. Research in Petroleum Technology, Nordisk Energiforskning, 5, Fabricius, I.L. (Editor), Norway, 157–180.
- Šliaupa, S., A. Shogenova, K. Shogenov, R. Šliaupiene, A. Zabele, and R. Vaher (2008a), Industrial carbon dioxide emissions and potential geological sinks in the Baltic States, Oil Shale, 25(4), 465-484, doi:10.3176/oil.2008.4.06.
- Šliaupa, S., J. Cyziene, N. Molenaar, and D. Musteikyte (2008b), Ferroan dolomite cement in Cambrian sandstones: burial history and hydrocarbon generation of the Baltic sedimentary basin, Acta Geol. Polonica, 58(1), 27-41, <http://yadda.icm.edu.pl/baztech/element/bwmeta1.element.baztech-article-BGPK-2015-7504>.
- Soldal, M. (2008), Caprock interaction with CO₂, M.S. thesis, Fac. of Math. and Natur. Sci., Univ. of Oslo, Oslo, Sweden.
- Svec, R. K. and R. B. Grigg (2001), Physical effects of WAG fluids on carbonate core plugs, paper presented at SPE Annual Technical Conference and Exhibition, SPE 71496, New Orleans, LA.
- Šliaupa, S., R. Lojka, Z. Tasáryová, V. Kolejka, V. Hladík, J. Kotulová, L. Kucharic, V. Fejdi, A. Wojcicki, R. Tarkowski, B. Uliasz-Misiak, R. Šliaupienė, I. Nulle, R. Pomeranceva, O. Ivanova, A. Shogenova, and K. Shogenov (2013),

- CO₂ storage potential of sedimentary basins of Slovakia, The Czech Republic, Poland, and Baltic States, *Geol. Quart.*, 57(2), 219-232, doi:10.7306/gq.1088.
- Šteinerts, G. (2012), Maritime delimitation of Latvian waters, history and future prospects, *J. Marit. Trans. Eng.*, 1(1), Latvian Maritime Academy, Latvia, Riga, 47-53, ISSN:2255-758X.
- Tiab, D. and E. C. Donaldson (2012), *Petrophysics, Theory and Practice of Measuring Reservoir Rock and Fluid Transport Properties* (3rd ed.), Oxford: Gulf Professional Pub., ISBN:978-0-12-383848-3.
- Van der Meer, L. G. H. (1993), The conditions limiting CO₂ storage in aquifers, *En. Conv. Manag.*, 34(9-11), 959 – 966, doi:10.1016/0196-8904(93)90042-9.
- Vernon, R., N. O'Neil, R. Pasquali, and M. Nieminen (2013), Screening of prospective sites for geological storage of CO₂ in the Southern Baltic Sea, *VTT Technology 101*, Espoo, Finland, ISSN:2242-122X, <http://www.vtt.fi/inf/pdf/technology/2013/T101.pdf>.
- Wollenweber, J., S. A. Alles, A. Busch, B. M. Krooss, H. Stanjek, and R. Littke (2010), Experimental investigation of the CO₂ sealing efficiency of caprocks, *Int. J. Greenh. Gas Con.*, 4(2), 231–241, doi:10.1016/j.ijggc.2010.01.003.

PAPER V. **SHOGENOV, K.**, SHOGENOVA, A., VIZIKA-KAVVADIAS, O. & NAUROY, J. F. 2015. Reservoir quality and petrophysical properties of Cambrian sandstones and their changes during the experimental modelling of CO₂ storage in the Baltic Basin. *Estonian Journal of Earth Science*, 64(3), (accepted).

Reservoir quality and petrophysical properties of Cambrian sandstones and their changes during the experimental modelling of CO₂ storage in the Baltic Basin

Kazbulat Shogenov^a, Alla Shogenova^a, Olga Vizika-Kavvadias^b and Jean-François Nauroy^b

^a Institute of Geology at Tallinn University of Technology, Ehitajate tee 5, 19086 Tallinn, Estonia; kazbulat.shogenov@ttu.ee

^b IFP Energies nouvelles, 1 & 4 avenue de Bois-Préau 92852ueil-Malmaison Cedex, France

Received 5 January 2015, accepted 20 April 2015

Abstract. The objectives of this study were (1) to review current recommendations on storage reservoirs and classify their quality using experimental data of sandstones of the Deimena Formation of Cambrian Series 3, (2) to determine how the possible CO₂ geological storage (CGS) in the Deimena Formation sandstones affects their properties and reservoir quality and (3) to apply the proposed classification to the storage reservoirs and their changes during CGS in the Baltic Basin.

The new classification of the reservoir quality of rocks for CGS in terms of gas permeability and porosity was proposed for the sandstones of the Deimena Formation covered by Lower Ordovician clayey and carbonate cap rocks in the Baltic sedimentary basin. Based on permeability the sandstones were divided into four groups showing their practical usability for CGS ('very appropriate', 'appropriate', 'cautionary' and 'not appropriate'). According to porosity, eight reservoir quality classes were distinguished within these groups.

The petrophysical, geochemical and mineralogical parameters of the sandstones from the onshore South Kandava and offshore E6 structures in Latvia and the E7 structure in Lithuania were studied before and after the CO₂ injection-like alteration experiment. The greatest changes in the composition and properties were determined in the carbonate-cemented sandstones from the uppermost part of the South Kandava onshore structure. Partial dissolution of pore-filling carbonate cement (ankerite and calcite) and displacement of clay cement blocking pores caused significant increase in the effective porosity of the samples, drastic increase in their permeability and decrease in grain and bulk density, P- and S-wave velocity, and weight of the dry samples. As a result of these alterations, carbonate-cemented sandstones of initially 'very low' reservoir quality (class VIII), 'not appropriate' for CGS, acquired an 'appropriate' for CGS 'moderate' quality (class IV) or 'very appropriate' 'high-2' reservoir quality (class II). The permeability of the clay-cemented sandstones of 'very low' reservoir quality class VIII from the lower part of the E7 reservoir was not improved. Only minor changes during the alteration experiment in the offshore pure quartz sandstones from the E6 and E7 structures caused slight variations in their properties. The initial reservoir quality of these sandstones ('high-1' and 'good', classes I and III, respectively, in the E6 structure, and 'cautionary-2', class VI in the E7 structure) was mainly preserved.

The reservoir sandstones of the Deimena Formation in the South Kandava structure had an average porosity of 21%, identical to the porosity of rocks in the E6 structure, but twice higher average permeability, 300 and 150 mD, respectively. The estimated good reservoir quality of these sandstones was assessed as 'appropriate' for CGS. The reservoir quality of the sandstones from the E7 offshore structure, estimated as 'cautionary-2' (average porosity 12% and permeability 40 mD), was lowest among the studied structures and was assessed as 'cautionary' for CGS.

Petrophysical alteration of sandstones induced by laboratory-simulated CGS was studied for the first time in the Baltic Basin. The obtained results are important for understanding the physical processes that may occur during CO₂ storage in the Baltic onshore and offshore structures.

Key words: CO₂ geological storage, Deimena Formation, porosity, permeability, reservoir quality, rock properties, Baltic Basin, offshore structure.

INTRODUCTION

The reduction of the greenhouse effect of the Earth's atmosphere is a major concern for researchers and everyone who cares about the future of our planet. This research is related to one of the most promising technologies and fields of study, which is considered to be an effective measure for mitigating the climate

change induced by greenhouse gases (Metz et al. 2005; Bachu et al. 2007; Arts et al. 2008; IPCC 2014). The scientific community agrees on the importance of reducing industrial carbon dioxide (CO₂) emissions in the atmosphere using CO₂ Capture and Geological Storage (CCS) in, for example, (1) deep saline aquifers, (2) depleted oil and gas fields, (3) unmineable coal seams and (4) porous basalt formations. The global economic

potential of CCS would amount to 220–2200 Gt of CO₂ cumulatively, which would mean that CCS contributes 15–55% of the total mitigation effort worldwide until 2100, averaged over a range of baseline scenarios (Metz et al. 2005). Worldwide, a number of known pilot storage and large-scale CCS demonstration projects are ongoing and/or monitored, the first of which, Sleipner (Norway), started in 1996. Nevertheless, there are gaps in the knowledge of short- and long-term (10–100 and 100–10 000 years, respectively) phenomena accompanying the process of the storage of CO₂ in deep geological formations.

Our study concentrates on CO₂ storage in deep saline aquifers (>800 m depth, >35 g L⁻¹ salinity), composed of reservoir rocks overlain by the cap rock (seal). This is the most widespread worldwide option currently under consideration for CO₂ Geological Storage (CGS). The sandstones of the Deimena Formation of Cambrian Series 3 (earlier Middle Cambrian; Sundberg et al. 2011; Peng et al. 2012) in the Baltic Basin are characterized by highly variable porosity and permeability, which are not considered in the available classifications of reservoir rocks and recommendations on CO₂ storage reservoirs.

The current research aims at the assessment of the quality of reservoir rocks for CGS based on the properties of reservoir quartz sandstones and their changes caused by acidic fluid during experimentally modelled CGS. Because mineralogical and petrophysical alterations are usually site-specific, this study is important for gaining parameters for the petrophysical modelling of the CO₂ plume to predict the CO₂ fate in short and long term, and to demonstrate the effectiveness of the geophysical monitoring of the storage site before, during and after the CO₂ injection in the Baltic sedimentary basin.

The objectives of this study were (1) to review the available recommendations on storage reservoirs and offer a classification of their quality using experimental data of the Deimena Formation sandstones of Cambrian Series 3, (2) to determine the influence of possible CGS in the sandstones of the Deimena Formation on their properties and reservoir quality and (3) to apply the proposed classification to the storage reservoirs and their evolution during CGS in the Baltic Basin.

The obtained data will be used in 4D time-lapse numerical seismic modelling to support more reliable petrophysical and geophysical models of the CO₂ plume.

GEOLOGICAL BACKGROUND

The main target for the CGS study in Estonia, Latvia and Lithuania is the Baltic Basin (700 km × 500 km synclinal structure), a Late Ediacaran–Phanerozoic poly-

genetic sedimentary basin that developed in a pericratonic setting in the western part of the East European Platform. It overlies the Palaeoproterozoic crystalline basement of the East European Craton, specifically the West Lithuanian Granulite Domain, flanked by terranes of the Svecofennian Orogen southeast of the Baltic Sea (Gorbatshev & Bogdanova 1993). Basin fill consists of Ediacaran–Lower Palaeozoic, Devonian–Carboniferous and Permian–Mesozoic successions, coinciding with what are referred to as the Caledonian, Variscan and Alpine stages of the tectonic development of the basin, respectively. These are separated by regional unconformities and overlain by a thin cover of Cenozoic deposits (Poprawa et al. 1999). The Cambrian Series 3 saline aquifer (depth 650–1700 m), located in the central-western part of the Baltic Basin, suits best for the CO₂ storage in the Baltic Region. It is composed of 25–80 m thick Deimena Formation sandstone, covered by up to 46 m thick shales and clayey carbonate primary cap rocks of the Lower Ordovician Zebre Formation. Shale rocks are dark, thin-layered (0.5–2 mm) and highly fissile. A 0.5 m layer of greenish-grey glauconite-bearing sandy marlstones with minor limestone lenses is observed at the base of the onshore Zebre Formation. The reservoir rocks are also covered by 130–230 m thick Ordovician and 100–225 m thick Silurian impermeable clayey carbonate secondary cap rocks. Clayey rocks can be easily determined by increased values of gamma-ray readings in all the studied wells, and they play an essential role as a seal for the studied structures (Fig. 1).

The regional theoretical storage potential of Cambrian sandstone saline aquifers below 800 m in the Baltic Sea Region has been estimated as 16 Gt (Vernon et al. 2013). The average storage capacity of the Cambrian reservoir is 145 Mt in the western part of the Baltic Basin in the S41/Dalders structure of the Swedish offshore sector, while the average capacity of the regional Cambrian Faludden trap is 5.58 Gt (Sopher et al. 2014). For comparison, the total estimated storage capacity in the Jurassic sandstone formations in the Norwegian Sea is 5.5 Gt (Halland et al. 2013). The Utsira sandstone formation at the first storage site in the world, Sleipner in the North Sea, has a storage capacity of approximately 15 Gt (Halland et al. 2011).

The Cambrian aquifer includes potable water in the northern shallow part of the Baltic Basin, mineral water (salinity 10 g L⁻¹) in southern Estonia and saline water in the Deimena Formation at more than 800 m depths, with salinity up to 120 g L⁻¹ in the central and 150–180 g L⁻¹ in the southern and western parts of the basin, where fluid temperature reaches 88 °C (Zdanavičiute & Sakalauskas 2001). The last mentioned geochemical and pressure–temperature conditions of formation fluids allow the use of the Deimena Formation reservoir for

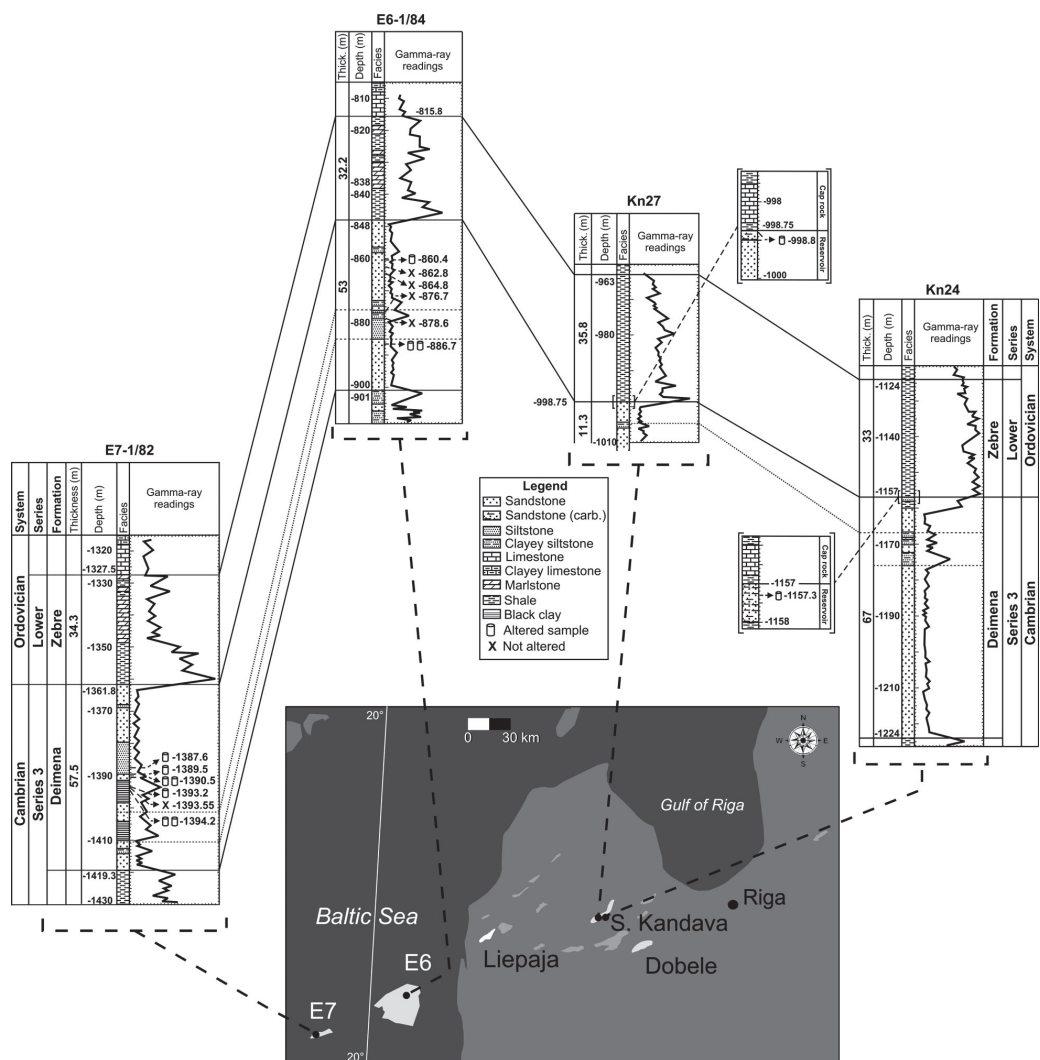


Fig. 1. Correlation of boreholes from the studied offshore E6 and E7 structures (E6-1/84 and E7-1/82) and onshore South Kandava (S. Kandava, Kn24, Kn27) focusing on the sandstone reservoir of the Deimena Formation of Cambrian Series 3. Cap rocks are represented by the Lower Ordovician Zebre Formation (primary cap rock) and part of the secondary cap rock (Middle Ordovician Kriukai Formation). Gamma-ray readings were digitized from analogous gamma-ray logging data. Approximate locations of the studied structures (white) and boreholes (black points) are indicated on the map. Other onshore Latvian structures prospective for CGS (CO₂ storage potential exceeding 2 Mt) are shown in light grey.

CGS at depths of 800–2500 m, where CO₂ can be stored in a supercritical state (>31 °C and >73 atm). The geological conditions are most favourable in the uplifted structures in Latvia, where more than 30 anticlinal deep geological structures onshore and offshore Latvia, with

different sizes and a storage capacity exceeding 2 Mt of CO₂, have been estimated as prospective for CGS (Šliaupa et al. 2008a; Shogenova et al. 2009a, 2009b, 2011a, 2011b; Shogenov et al. 2013a, 2013b; Šliaupa et al. 2013). Four geological structures, located onshore

(South Kandava and Dobele) and offshore Latvia (E6) and Lithuania (E7) and serving as prospective CGS sites in the Baltic Sea Region (Fig. 1), were previously described in detail by Shogenov et al. (2013a, 2013b).

The petrophysical properties and geochemical and mineralogical composition of 24 samples of the Deimena Formation reservoir and Zebre Formation cap rocks from four Baltic onshore and offshore structures were studied and analysed together with previously reported data. The properties of reservoir rocks, cross sections and 3D geological models, constructed using geophysical and geological data, were used for the estimation of the theoretical CO₂ storage capacity of these structures in our earlier studies. The selected structures have an average porosity of 12–21%, permeability of 40–360 mD and mean reservoir thickness of 42–58 m. The average CO₂ storage potentials ('conservative'–'optimistic') of the Dobele, South Kandava, E7 and E6 structures were, respectively, 20–106, 25–95, 7–34 and 152–377 Mt. We estimated the E6 offshore structure as the largest trapping structure prospective for CGS offshore Latvia with the highest CO₂ storage capacity (Shogenov et al. 2013a, 2013b). Based on exploration report data (Babuke et al. 1983), we have treated E7 as a Latvian offshore structure in our earlier publications (Shogenov et al. 2013a, 2013b). However, according to the new Latvian–Lithuanian territorial agreement in the Baltic Sea, signed by Prime Ministers of Latvia and Lithuania in 1999, the E7 structure belongs now to Lithuania (Steinerts 2012).

DIAGENETIC MODIFICATION OF RESERVOIR PROPERTIES

The studied Cambrian rocks were subjected to different diagenetic conditions across the basin, with a wide spectrum of rock modification under shallow to deep burial conditions, reflected in growing clay mineral maturity with increasing depth, variations in the composition of sandstone cement, with authigenic quartz prevailing in the deep part of the basin and carbonate cements prevailing in the basin periphery, etc. The carbonate cement of sandstones is varying in mineralogy from common ferroan dolomite and ankerite to less common calcite and siderite (Sliupa et al. 2008b). Quartz cementation that formed during the late diagenetic stage (Lashkova 1979; Sikorska & Paczesna 1997) and increases with depth is the main factor influencing the reservoir properties of rocks both in onshore and offshore structures.

Quartz is the main cement mineral, occurring in the form of authigenic overgrowths on detrital quartz grains (Lashkova 1979; Kilda & Friis 2002). According to

Čyžienė et al. (2006), quartz cement is regionally widespread, but mainly confined to areas where present-day temperatures in the Cambrian are 50–90 °C. Sliupa et al. (2008b) stated that quartz cementation started at 1 km depth. The amount of quartz cement increases towards the deeper buried parts of the basin in West Lithuania, but is highly variable on a local scale and even within individual structures. Quartz cement contents show a negative correlation with porosity (Čyžienė et al. 2006) and with carbonate cement (Sliupa et al. 2008b).

Another diagenetic process negatively influencing the reservoir properties is compaction. Pore reduction by mechanical compaction is one of the main controls of the petrophysical properties of Cambrian sandstones. The importance of mechanical compaction in reducing porosity and causing lithification is stressed by Čyžienė et al. (2006). Compaction comprised the mechanical rearrangement of grains throughout the sandstones as well as the chemical compaction along shale–sandstone contacts and within shales. Grain breakage is rare and no intergranular pressure solution in clay-free clean sandstones has been observed. In sandstones detrital quartz grains mainly have point contacts. Differences in the degree of mechanical compaction are probably related to both maximum burial depth and variations in the depositional texture and susceptibility of sand to mechanical compaction.

REQUIREMENTS FOR RESERVOIR ROCKS

A typical reservoir for CGS is a geological formation consisting of sandstone or carbonate rock characterized by 'good' effective porosity and permeability. Effective (open) porosity is the porosity that is available for free fluids; it excludes all non-connected porosity, including the space occupied by clay-bound water (Schön 1996). The ranges of 'good' reservoir porosity and permeability for oil and gas reservoirs are 15–20% and 50–250 millidarcy (mD), respectively (Tiab & Donaldson 2012).

Until now there is no unified classification specifying requirements for 'high-', 'good-' or 'low-quality' reservoirs for CO₂ storage. As a general rule the formation permeability must exceed 200 mD for a specific reservoir to provide sufficient injectivity (Van der Meer 1993). However, the values greater than 300 mD are preferred and considered as positive indicators to start the screening process of the possible storage site (Chadwick et al. 2006; Vangkilde-Pedersen & Kirk 2009). The porosities should be larger than 20%, while those below 10% and permeability below 200 mD are considered 'cautionary' by these authors (Table 1). The cumulative thickness of reservoirs should be greater than 50 m. The reservoirs less than 20 m thick are

Table 1. Classification of the reservoir rocks according to permeability and porosity

Hydrocarbon reservoirs (Khanin 1965, 1969)				CO ₂ storage standards*				Classification of the studied rocks for CO ₂ storage**							
Group	Class	Reservoir quality	K (mD)	φ (%)	Group	Class	Reservoir quality	K (mD)	φ (%)	Group	Application for CGS	Class	Reservoir quality	K (mD)	φ (%)
1	I	Very high	≥1000	≥20	1	I	High	>500	>25	1	Very appropriate	I	High-1	>300	≥20
			500–1000	18–20			Preferred	>300	>20				High-2	9–20	
	II	High	100–500	14–18	III	III	Good	50–250	15–20	2	Appropriate	III	Good	100–300	>18
			Average	8–14			Moderate	50–250	10–15				Moderate	9–18	
2	IV	Reduced	10–100	8–14	2	IV	Cautious	<200	<10	3	Cautious	V	Cautious-1	10–100	18–23
			1–10	2–8			Low	<10	<15				4	Not appropriate	VII
	V	Low	<1	<2	VI	VI	Very low	<50	<5	4	Not appropriate	VIII	Very low	<1	<18
			Very low	<1			<2	<5	<5				<1	<18	

* CO₂ storage standards modified after Van der Meer (1993), Chadwick et al. (2006), Vangkilde-Pedersen & Kirk (2009), Tiab & Donaldson (2012), Halland et al. (2013): group 1, acceptable for CGS; group 2, cautious.

** New classification based on the studied data (reported and measured in laboratory before the alteration experiment), proposed by the authors for the studied region and geological structures. K, gas permeability; φ, porosity.

considered unsuitable for the storage of large amounts of CO₂. According to Halland et al. (2013), a homogeneous 50 m thick reservoir with a permeability >500 mD and porosity >25% is estimated as a ‘high-quality’ reservoir, while heterogeneous 15 m thick reservoir with a permeability <10 mD and porosity <15% is considered as a ‘low-quality’ reservoir for CGS.

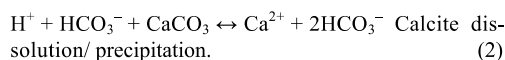
The classification of hydrocarbon reservoirs proposed by Khanin (1965, 1969) was used during exploration for hydrocarbon deposits on the territory of the Baltic States and later for the characterization of petroleum geology in the region (Zdanavičiute & Sakalauskas 2001). Based on porosity and permeability, Khanin divided hydrocarbon reservoirs into six classes without any overlapping of these parameters in reservoir quality classes (Table 1). In his classification the hydrocarbon reservoirs of ‘high’ and ‘very high’ quality have a permeability more than 500 and 1000 mD, respectively, while requirements for porosity (18–20 and >20%) are close to the positive indicators for CO₂ storage reservoirs (>20%) given by Chadwick et al. (2006) and Vangkilde-Pedersen & Kirk (2009).

CO₂–RESERVOIR ROCK INTERACTION

When injected into the aquifer or water-flooded oil reservoir, CO₂ has an impact on the pH level of in situ brine, modifying it into a more acidic state. Isotope studies of natural analogues of CO₂ reservoirs suggest that the dissolution of CO₂ in formation brine is the main phenomenon in the long term, causing the acidification of native brine to a pH of approximately 3–5 (Gilfillan et al. 2009; Liu et al. 2011, 2012). Chemically, this simple acid reaction is illustrated by equation (1), showing the formation and dissociation of carbonic acid (H₂CO₃⁰) from dissolved CO₂ in formation brine:



Acidic brine then reacts with the solid matrix of reservoir sediments (i.e. calcite, dolomite and anhydrite):

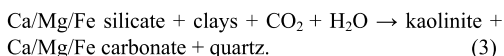


This exact phenomenon, induced by CO₂ injection into the aquifer, was applied as the main factor of the experiment and is a basis for further research.

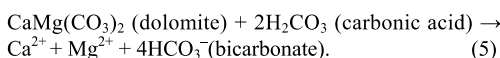
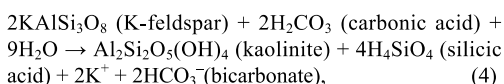
A number of recent papers have been dedicated to CO₂–brine–host reservoir rock interactions, both for sandstones and carbonate rocks (Ross et al. 1982; Svec & Grigg 2001; Grigg & Svec 2003; Rochelle et al. 2004; Bertier et al. 2006; Czernichowski-Lauriol et al. 2006;

Egermann et al. 2006; Pawar et al. 2006; Izgec et al. 2008; Bemer & Lombard 2010; Carroll et al. 2011, 2013; Nguyen et al. 2013).

The CGS-related laboratory experiments, numerical modelling and field monitoring of CO₂ storage sites have shown both partial dissolution and precipitation of various minerals. A simplified equation for minor mineral dissolution/precipitation of host rock was given by Hitchon (1996):



The reaction of carbonic acid with aluminosilicate or carbonate minerals produces significant alkalinity (Kaszuba & Janecky 2009):



The alkalinity of in situ brine cannot overcome the acidity within the repository that was produced by the dissolution of supercritical CO₂ fluid. However, due to the separation of brine from supercritical CO₂ and the prevailing chemical potential of carbonic acid, alkalinity in brine can neutralize the acidity, yielding near-neutral pH (Kaszuba & Janecky 2009).

Gilfillan et al. (2008, 2009) studied stable carbon $\delta^{13}\text{C}$ (CO₂) isotope tracers from natural CO₂-bearing siliciclastic and carbonate gas reservoirs around the world. They explored CO₂ dissolution into formation brine at various pH values as the primary sink for CO₂ and precipitation of CO₂ as carbonate minerals. Nevertheless, this process is very site- and condition-dependent and, in several cases, no important rock–fluid interaction impact on the petrophysical properties of the reservoir host rocks has been reported (Prieditis et al. 1991; Kamath et al. 1998).

MATERIAL AND METHODS

The porosity (Φ) and gas permeability (K) data of 115 samples, including those from six drill cores (E6-1/84, E7-1/82, South Kandava 24 and 27, Dobele 91 and 92) described in old exploration reports (Silant'ev et al. 1970; Dmitriev et al. 1973; Babuke et al. 1983; Andrushenko et al. 1985), from the Liepaja-San borehole (GEOBALTICA project, Shogenova et al. 2009a) and the ones recently measured in IFP Energies nouvelles (IFPEN, French

Petroleum Institute, Paris) (Shogenov et al. 2013a, 2013b), were used for the classification of the reservoir quality of sandstones. Gas permeability was calculated as an average value of reported permeability measured in horizontal and vertical directions. A more detailed description of permeability measurements from the Liepaja structure (Liepaja-San borehole) is given in Shogenova et al. (2009a). The physical properties of 139 samples from seven boreholes (offshore E6-1/84 and E7-1/82, onshore South Kandava 24 and 27, Dobele 91 and 92, Liepaja-San), measured recently or reported earlier, were used in this study. The K values of 127 samples and Φ values of 128 samples, grain density of 102 samples, bulk density of 129 dry samples, P-wave velocity (V_P) in 60 dry samples and S-wave velocity (V_S) in 10 dry samples comprised the recent and earlier data (Shogenova et al. 2001b; Shogenov et al. 2013a, 2013b).

Twelve rock samples of the reservoir sandstones of the Deimena Formation from four boreholes drilled onshore in the South Kandava structure and offshore in the E6 and E7 structures (Fig. 1, Table 1) and stored in the Latvian Environmental, Geological and Meteorological Centre were used for the CO₂ injection-like alteration experiment conducted at the IFPEN. Detailed descriptions of the methods applied are available in Shogenov et al. (2013a, 2013b). Bulk and grain helium density, helium porosity, gas permeability and acoustic wave velocities in dry samples, the chemical and mineralogical composition and surface morphology were studied in the 12 selected rocks both before and after the experiment. Due to partial destruction of several samples during the experiment, it was possible to measure K values in 11, V_P in nine and V_S in three samples. The total chemical composition of the samples was measured by X-ray fluorescence (XRF) analysis by Acme Analytical Laboratories Ltd. before and after the alteration experiment. CaO, MgO and insoluble residue (IR) were measured by the titration geochemical method only before the experiment. Thin sections of the samples were studied in the Institute of Geology at Tallinn University of Technology (IG TUT) using a Scanning Electron Microscope (SEM) equipped with an energy dispersive spectrometer (EDS). The thin sections were made after the experiment from the rock–fluid contact zone where alteration was confirmed by the high solubility of the samples. Due to partial destruction of some rocks, the weight of the samples was measured both before and after the experiment.

The CO₂ injection part in our experiment was simplified to consider only the impact on the contact area between acidified fluid and the studied rocks. This simplification ensures a homogeneous distribution of brine on the core scale and allows us to avoid very local ‘worm-holing’ effects on samples and erroneous physical

measurements (Egermann et al. 2006; Bemer & Lombard 2010). The homogeneous alteration method, or retarded acid approach, was conducted at IFPEN. It constitutes in the placement of samples into the Hastelloy cell maintained under vacuum conditions and injection of an acid solution. Acid treatment was performed at 10 bar pressure and temperature of 60°C (for at least one day), simulating CO₂-rich brine in an aquifer characterized by lowered pH (approximately three units). This method has been developed and described in detail in Egermann et al. (2006) and Bemer & Lombard (2010). The day after, each sample was placed in a 25-mm-diameter cell and flooded by three pore volumes of 20 g L⁻¹ NaCl brine at 20°C to stop the weathering. After this flooding the samples were dried in an oven for three days. The procedure was repeated three times.

Siliciclastic rock samples with good reservoir properties are often weakly cemented. In order to keep their regular shape in the experiments involving the flushing of samples with supercritical CO₂ and brine, the use of samples of various sizes and shapes was allowed by the implemented alteration method.

EXPERIMENTAL AND INTERPRETATION UNCERTAINTIES

Experimental uncertainties include the quality control of petrophysical measurements. To distinguish between a real trend in a data set and variation due to the experimental uncertainty, the American Petroleum Institute (API 1998) has recommended reporting core analyses data together with a statement of the uncertainty with which these data were recorded.

Variations in the permeability and acoustic velocity measurements were quite high in the presented study due to the sample sizes that differed from the standard ones at the IFPEN petrophysical and petroacoustic laboratories. The standard samples were 40 mm in diameter and 80 mm in length, thus the length/diameter ratio should be higher or equal to two (Egermann et al. 2006). The studied samples were 25 mm in diameter and 11–27 mm long. Therefore, the experimentally established accuracy (using replicate measurements of each sample) was 20% for the *K* values, and 10% for P- and S-wave velocity measurements for the used petroacoustic installations.

The accuracy of grain density measurements was <0.7%. It consisted of an analytical balances (from Mettler Toledo) accuracy of 0.2% (estimated experimentally) and less than 0.5% pycnometer accuracy for sample solid volume measurements (AccuPyc from Micromeritics), given as the default error. The accuracy of bulk density measurements due to the balances accuracy

(0.2%) and GeoPyc pycnometer (from Micromeritics) for the estimation of the total sample volume with reported default accuracy of 1.5% was 1.7%. The porosity measurements, supported by the high accuracy pycnometers from Micromeritics (GeoPyc and AccuPyc with 1.5% and 0.5% accuracy, respectively), provided a total of 2% accuracy.

The uncertainties and variations due to the accuracy of the measurements of altered petrophysical parameters and possible mistakes caused by changes in the sizes and shapes of rock samples were checked using well-known relationships: bulk density–porosity and acoustic velocity–porosity negative correlations; permeability–porosity positive correlation in general and available scatter from this relationship for the sandstones of the Deimena Formation in the studied region; and acoustic velocity–matrix and bulk density positive correlations (Schön 1996; Sliupa et al. 2001; Mavko et al. 2003; Shogenova et al. 2009a).

RESULTS

Assessment of the quality of the reservoir rocks

Considering the permeability and porosity requirements for CO₂ geological storage (Van der Meer 1993; Chadwick et al. 2006; Vangkilde-Pedersen & Kirk 2009; Tiab & Donaldson 2012; Halland et al. 2013), hydrocarbon reservoir classification by these parameters proposed by Khanin (1965, 1969) and earlier and recent data of 115 sandstone samples (Shogenova et al. 2009a; Shogenov et al. 2013a, 2013b), we subdivided the reservoir sandstones of the Deimena Formation into four groups and eight classes based on reservoir quality (Tables 1, 2, Fig. 2). The groups were distinguished using the permeability limits of 300, 100, 10 and 1 mD. Each group was subdivided into two classes of various porosity. The reservoir rocks of the first group that are ‘very appropriate’ for CGS, having the highest permeability and high porosity, were subdivided into ‘high-1’ (porosity ≥20%) and ‘high-2’ (porosity 9–20%) quality classes I and II, respectively. The second group, ‘appropriate’ for CGS, composed of rocks with a permeability of 100–300 mD, was subdivided into ‘good’ and ‘moderate’ quality classes III and IV (porosity >18% and 9–18%, respectively). The third group, ‘cautionary’ for CGS, contains rocks with a permeability of 10–100 mD and was subdivided into ‘cautionary-1’ and ‘cautionary-2’ classes V and VI (porosity 18–23% and 7–18%, respectively). The last group, ‘not appropriate’ for CGS, comprises rocks with a permeability <10 mD. It was subdivided into ‘low’ and ‘very low’ quality classes VII and VIII. Class VII comprises rocks with a permeability of 1–10 mD and porosity 7–18%, and class VIII contains rocks with a permeability <1 mD and porosity <18%.

Table 2. Average properties of the sandstones of the Deimena Formation before the alteration experiment

Group	Class	Reservoir quality	K (mD)		Φ (%)		Grain density (kg m^{-3})		Bulk density dry (kg m^{-3})	
			min–max/mean(N)	min–max/mean(N)	min–max/mean(N)	min–max/mean(N)				
1	I	High-1	334–763/525(11)	20.1–25.8/22.3(10)	2670–2718/2694(10)	1807–2150/2034(11)				
	II	High-2	347–600/440(9)	12.5–19.2/17.2(10)	2680–2730/2707(10)	2110–2260/2167(10)				
2	III	Good	113–295.5/183(17)	19–25.5/22.5(17)	2680–2725/2700(2)	1980–2130/2050(17)				
	IV	Moderate	102–261/186(8)	12–17.8/14.8(8)	2640–2750/2693(6)	2200–2330/2274(8)				
3	V	Cautionary-1	33–84/62(12)	18.5–22.9/20.8(12)	2630–2720/2677(6)	2020–2310/2133(12)				
	VI	Cautionary-2	16–94/45(41)	8.5–16.2/12.1(41)	2600–2820/2661(39)	2250–2430/2334(41)				
4	VII	Low	1.5–10/6.2(8)	7.95–17.5/13.1(8)	2660–2730/2683(7)	2210–2450/2315(8)				
	VIII	Very low	0.001–0.7/0.2(10)	0.8–16.3/8.9(10)	2664–2840/2712(10)	2200–2780/2452(10)				

K , gas permeability; Φ , porosity; min, minimum; max, maximum; mean, average; N , number of studied samples (measured and reported).

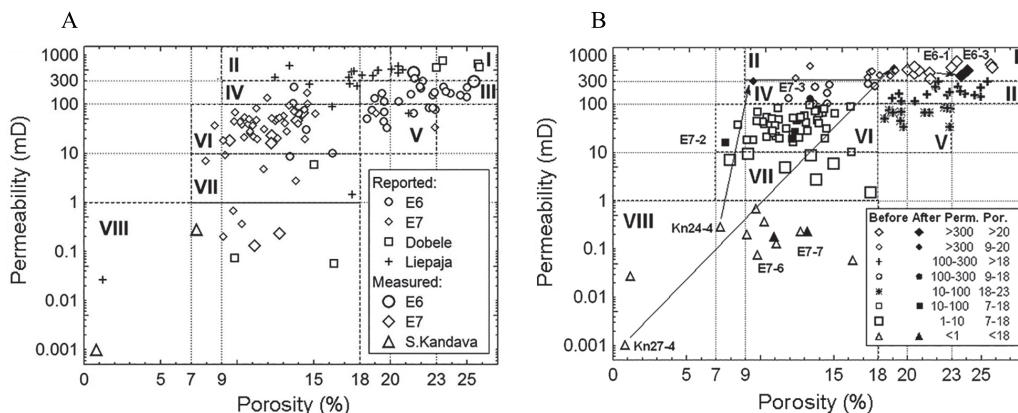


Fig. 2. Gas permeability versus porosity of the reported and measured sandstones of the Deimena Formation from two offshore and three onshore structures in eight reservoir quality classes I–VIII (Tables 1, 2) based on: (A) 115 samples reported and measured before the alteration experiment in terms of five structures; (B) 115 samples reported and measured before the alteration experiment (empty symbols) and 12 samples measured after alteration (black symbols) in terms of eight reservoir quality classes. Perm., gas permeability; Por., porosity.

Every reservoir quality class is characterized by a unique set of petrophysical parameters. However, rocks in groups one and two, ‘very appropriate’ and ‘appropriate’ for CGS, respectively, differ mainly in permeability, but have a common range of porosities, determining their similarities in other physical properties (Tables 1, 2).

The first group, ‘very appropriate’ for CGS (classes I and II), includes samples from the offshore E6, onshore Dobele-92 and Liepaja-San boreholes.

The second group, ‘appropriate’ for CGS, class III, is composed of rocks from the E6-1/84 borehole, while class IV also includes rocks from the E7-1/82 and Liepaja-San boreholes.

The third group, ‘cautionary’ for CGS, ‘cautionary-1’ class V, includes samples mainly from the E6-1/84 borehole, while ‘cautionary-2’ class VI contains mostly rocks from the E7-1/82 borehole.

The last, ‘very low’ reservoir quality class VIII from the fourth group, ‘not appropriate’ for CGS, includes clay-cemented samples from the E7 structure and carbonate-cemented samples from the South Kandava structure, supplemented by three samples from the Dobele and Liepaja structures (Fig. 2A). Class VII includes the samples (E6, E7, Liepaja and Dobele structures) which had higher permeability and porosity, lower grain and bulk density and P-wave velocity than the rocks of class VIII.

Assessment of the reservoir quality of sandstones before and after alteration

According to the chemical and lithological classification proposed by Shogenova et al. (2005, 2006), sample Kn27-4 is a mixed carbonate-siliciclastic sandstone ($50 < IR < 70\%$), while the other studied samples (E6-1–E6-3, E7-1–E7-7 and Kn24-4) are siliciclastic sandstones ($IR > 70\%$) of different quality, clay and carbonate cement content (Table 3).

According to our classification based on permeability and porosity (Table 1), offshore sandstones from the E6 structure are mainly of ‘good’ and ‘high-1’ reservoir quality (classes III and I, respectively), with a small number of samples of ‘cautionary-1’ class V and rare samples of classes IV, VI and VII. Offshore sandstones from the E7 structure are mainly of ‘cautionary-2’ reservoir quality class VI, while rest of the samples belong to classes IV–VII. Clay-cemented samples from the downward part of the E7 reservoir ($70 < SiO_2 < 90\%$ and $Al_2O_3 > 5\%$, Table 3) and carbonate-cemented samples ($65 < SiO_2 < 85\%$ and $CaO > 5\%$, Table 3) from the upward part of the onshore South Kandava structure are in ‘very low’ quality class VIII.

The ‘high-1’ and ‘good’ reservoir quality (classes I and III, respectively) quartz sandstones from the E6 structure are mainly composed of quartz, with minor amounts of clay (illite and/or kaolinite) and carbonate cement forming minerals, admixture of feldspar and accessory minerals represented by pyrite, barite, anatase and/or brookite and zircon (Shogenov et al. 2013a, 2013b). Increase in effective porosity, supported by decrease in bulk and grain density, and slight decrease in sample weight, due to the dissolution of minor carbonate cement, displacement of clay cement after the experiment and minor increase in microfractures in grains, were determined after the alteration experiment in the samples from this structure (Tables 3, 4, Figs 3, 4). However, the changes in permeability and porosity did not cause a significant change in their reservoir quality and samples from the E6 structure remained in the same ‘high-1’ and ‘good’ reservoir quality classes after the experiment (Table 4, Fig. 2).

The sandstones from the E7 offshore structure are also mainly composed of quartz. Compared to sandstones present in the E6 structure, sandstones in the E7 structure in some parts of the Deimena Formation contain more clay and carbonate minerals, including ankerite, dolomite, admixture of feldspar and clay fraction represented by kaolinite and illite. Sandstones in the upper part of the Deimena Formation are mostly cemented by quartz-generated cement. Rocks in the lower part of the formation are characterized by conformation of quartz grains due to dissolution under pressure (Shogenov

Table 3. Chemical composition of the sandstones of the Deimena Formation before and after the alteration experiment (major oxides and insoluble residue)

Sample	Depth (m)	Wet chemical analysis (%)			XRF analysis (%)									
		IR	Before alteration		SiO ₂	CaO		MgO		Al ₂ O ₃		Fe ₂ O ₃		
			CaO	MgO		Before	After	Before	After	Before	After	Before	After	
E6-1	860.4	97.14	0.88	0.24	97.8	97.0	0.07	0.03	0.03	0.02	0.24	0.70	0.06	0.06
E6-2	886.7	97.44	1.10	0.24	97.4	94.8	0.10	0.03	0.04	0.04	0.34	1.30	0.16	0.09
E6-3	886.7	97.44	1.10	0.24	97.4	95.7	0.10	0.03	0.04	0.03	0.34	1.10	0.16	0.07
E7-1	1387.6	97.12	1.10	0.24	98.7	98.6	0.05	0.02	0.02	<0.01	0.27	0.72	0.08	0.02
E7-2	1389.5	98.64	0.88	0.33	98.3	98.7	0.04	0.02	0.01	<0.01	0.38	0.70	0.06	0.03
E7-3	1390.5	97.16	1.10	0.49	97.6	98.3	0.30	0.13	0.11	0.07	0.27	0.61	0.19	0.09
E7-4	1390.5	97.16	1.10	0.49	97.6	98.7	0.30	0.11	0.11	0.06	0.27	0.84	0.19	0.14
E7-5	1393.2	97.86	1.10	0.41	97.8	98.4	0.04	0.02	0.03	<0.01	0.59	0.72	0.31	0.06
E7-6*	1394.2	93.60	1.54	0.49	87.2	90.2	0.16	0.05	0.34	0.20	5.26	4.96	1.85	1.10
E7-7*	1394.2	93.60	1.54	0.49	87.2	86.4	0.16	0.07	0.34	0.34	5.26	6.63	1.85	1.54
Kn24-4**	1157.3	80.64	6.38	2.12	81.1	85.4	5.61	3.95	1.98	1.40	0.26	0.43	2.32	1.74
Kn27-4**	998.8	68.04	16.5	0.57	70.0	75.0	15.69	12.23	0.12	0.23	0.18	0.34	0.13	0.09

Before, samples measured before the alteration experiment; after, samples measured after the alteration experiment; * clay-cemented; ** carbonate-cemented sandstones from the South Kandava structure; IR, insoluble residue.

Table 4. Reservoir quality classes and petrophysical properties of the Deimena Formation studied in the alteration experiment

Sample	Depth (m)	Reservoir quality class		Weight (kg 10 ⁻³)		Bulk density (kg m ⁻³)		Grain density (kg m ⁻³)		Porosity (%)		Permeability (mD)		V _p (m s ⁻¹)		V _s (m s ⁻¹)	
		Before	After	Before	After	Before	After	Before	After	Before	After	Before	After	Before	After	Before	After
E6-1	860.4	I	I	17.6	17.5	2123	2011	2705	2635	21.5	23.7	440.0	380.0	—	2310	—	—
E6-2	886.7	III	III	12.0	6.4*	2031	1863	2725	2661	25.5	30.0	290.0	—	—	—	—	—
E6-3	886.7	I	I	10.2	10.0	1999	2633	2718	2633	—	24.1	400.0	490.0	—	—	—	—
E7-1	1387.6	VI	VI	16.8	16.7	2354	2310	2683	2636	12.3	12.4	23.0	26.0	3583	3300	—	—
E7-2	1389.5	VI	VI	26.5	26.5	2412	2439	2666	2641	9.5	7.7	18.0	16.0	2457	2280	1725	—
E7-3	1390.5	VI	IV	24.8	24.6	2309	2295	2693	2650	14.3	13.4	66.0	130.0	3096	2750	2194	1950
E7-4	1390.5	VI	VI	15.6	15.5	2339	2284	2716	2653	13.9	13.9	46.0	78.0	—	—	—	—
E7-5	1393.2	VI	VI	24.9	24.8	2349	2323	2676	2646	12.2	12.2	16.0	19.0	3097	3100	2230	2020
E7-6*	1394.2	VIII	VIII	24.7	24.3	2403	2367	2704	2659	11.1	11.0	0.13	0.18	2524	1230	—	—
E7-7*	1394.2	VIII	VIII	24.8	16.1*	2395	2322	2746	2676	12.8	13.3	0.23	0.23	2130	2130	—	—
Kn24-4**	1157.3	VIII	IV	35.3	31.6	2642	2148	2741	2675	7.3	9.6	0.28	300.0	4556	4030	3225	—
Kn27-4**	998.8	VIII	II	35.0	27.1	2539	2419	2664	2658	0.8	19.1	0.001	550.0	5400	4380	3600	2540

Before, samples measured before the alteration experiment; after, samples measured after the alteration experiment; V_p, P-wave velocity; V_s, S-wave velocity; * clay-cemented; ** carbonate-cemented sandstones from the South Kandava structure.

Bold and *italic* numbers in the table correspond, respectively, to 'reliable' and 'not reliable' changes in petrophysical parameters after the alteration experiment according to measurement errors. 'Not reliable' values also correspond to the parameters not subjected to alteration.

et al. 2013a, 2013b). Reliable changes in the physical properties of rock were detected in the nearly pure (estimated by XRD) quartz sandstones E7-2–E7-5, sampled from the depth interval 1389.5–1393.2 m (Table 4; Figs 2, 5). The grain density in these samples and the effective porosity in samples E7-2 and E7-3 were found to decrease. A reliable decrease in weight and a significant increase in permeability were detected in sample E7-3 (Fig. 6). Additionally, a reliable decrease in P- and S-wave velocity was determined in sample E7-3. A reliable decrease in bulk density was recorded only in sample E7-4 (Table 4). However, the only sample E7-3 from class VI ('cautionary-2') improved its reservoir quality up to class IV ('moderate') owing to its permeability increase, while the quality of the other samples was not improved after the experiment.

Only slight decrease in sample weight and grain density, and a significant reduction in P-wave velocity, supported by some insignificant variations in permeability and porosity, were determined in clay-cemented sandstones E7-6 and E7-7 of initially 'very low' quality class VIII. After the alteration both samples remained in the same reservoir quality class (Table 4, Fig. 2).

The transitional reservoir (trans-res) sandstones from the South Kandava onshore structure (located 0.2–0.3 m below the Lower Ordovician cap rock formation) are characterized by a higher carbonate cement content than the other studied pure reservoir sandstones. Trans-res sandstone Kn24-4 (0.3 m below the cap rock formation, Figs 1, 7) was estimated by XRD and XRF analyses as ankerite-cemented almost pure quartz sandstone of 'very low' reservoir quality (class VIII). Sample weight decreased after the alteration experiment due to the dissolution of cement (expressed by a decrease in CaO content from 5.61% before to 3.95% after alteration, Table 3). Also bulk and grain density and P-wave velocity decreased, associated with a significant rise in effective porosity and drastically increased permeability (Table 4, Figs 2B, 3B, 5). Thin section study confirmed the results of the physical measurements of rock, showing the dissolution and microfracturing of carbonate cement and the displacement of clay cement, which previously blocked pores, after alteration (Fig. 7). Owing to drastic changes in porosity and permeability, the reservoir quality of this rock sample was improved up to 'moderate' reservoir quality class IV 'appropriate' for CGS (group 2, Table 4).

Trans-res rock sample Kn27-4 (0.2 m below the cap rock formation, Figs 1, 8) was estimated by XRD analysis as sandstone with abundant quartz and minor calcite (mixed carbonate-siliciclastic rock by geochemical interpretation) and was assigned to 'low' reservoir quality (class VII). Sample weight decreased after the experiment

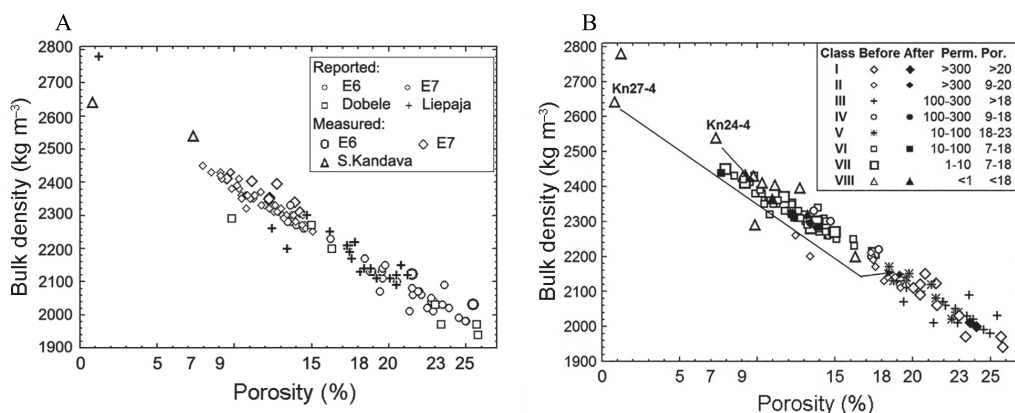


Fig. 3. Bulk density measured on dry samples versus porosity of the sandstones of the Deimena Formation from two offshore and three onshore structures: (A) for 115 samples reported and measured from seven boreholes before alteration; (B) for 115 samples reported and measured before alteration (empty symbols) and 12 samples measured after alteration (black symbols) in terms of reservoir quality classes I–VIII (Tables 1, 2). Perm., gas permeability; Por., porosity.

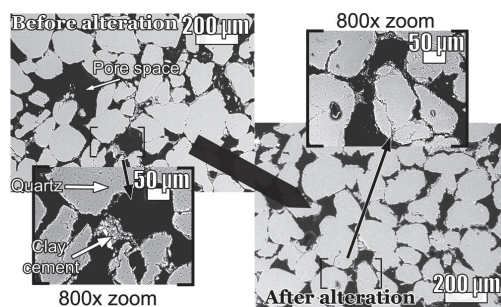


Fig. 4. SEM microphotographs of thin sections of reservoir fine-grained poorly sorted Deimena Formation sandstone sample E6-3 (Table 3) before (left) and after (right) the alteration experiment. The composition is oligomictic, characterized by predominantly subrounded to subangular quartz grains. Clay cement indicated on zoomed photos locally blocks porous media and accounts for about 5%. Open porosity is mostly interparticle, locally also intraparticle. The measured porosity of E6-3 after the alteration experiment (24.1%) was confirmed by visual analysis of thin sections (20–30% by Shvetsov 1948, Table 4). Slightly increased permeability (Table 4) could be explained by the dissolution of minor carbonate cement (Table 3), displacement of clay cement after the experiment and minor increase in microfractures in grains (right part). Sample E6-3 is of ‘high-1’ (class I) reservoir quality sandstone, very appropriate for CGS with no changes in the reservoir quality after the experiment.

due to partial dissolution of carbonate cement (expressed by a decrease in CaO content from 15.69% before to 12.23% after alteration, Table 3). It was accompanied

by reduction in P- and S-wave velocity and bulk density, associated with dramatically increased effective porosity and permeability induced by chemical alteration (Table 4, Figs 2B, 3B, 5, 8). This caused an improvement of the reservoir quality of this sample up to ‘high-2’ reservoir quality class II, ‘very appropriate’ for CGS (group 1).

DISCUSSION

This study provides a set of experimental data concerning the change in the petrophysical properties of rocks under chemical alteration. The presented results do not allow yet the definition of constitutive laws taking the chemomechanical coupling into account.

The permeability of the studied sandstones varies by six orders of magnitude and by four orders of magnitude at a single porosity. At the same time the porosity of these sandstones varies in the range of 0.8–25.8% and can vary 2–2.5 times for a single permeability. Porosity and permeability are related to different properties of pore space geometry. This explains the correlation between porosity and permeability, but also the scattering of such correlations indicating strong additional influences (Schön 1996).

Great variability of the porosity of Cambrian sandstones in the Baltic Basin is explained by variation in their composition, grain size and sorting, pore structure, cementation, diagenetic alteration, burial depth and compaction, tectonic and geothermal conditions, and variation in onshore and offshore facies, especially in the northern and southern parts of the basin. As the

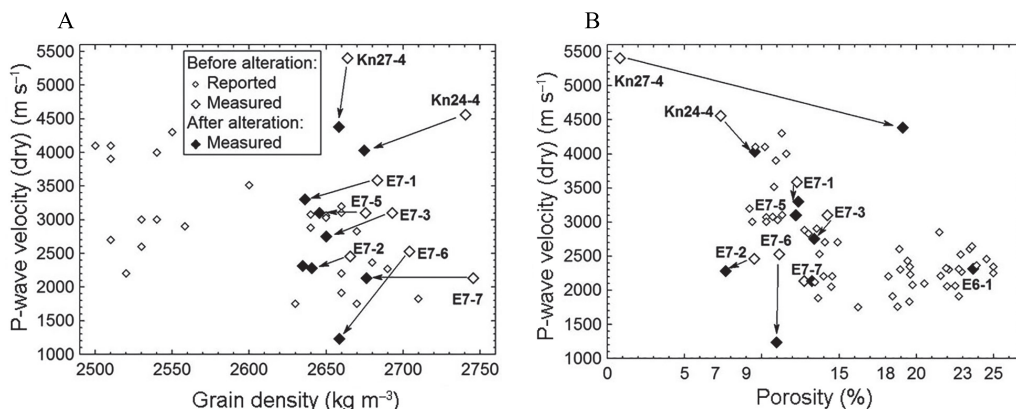


Fig. 5. (A) P-wave velocity versus grain density in dry sandstones of the Deimena Formation, reported (27 samples), and measured before (8 samples) and after (9 samples) the alteration experiment; (B) P-wave velocity versus porosity in dry sandstones, reported (52 samples), and measured before (8 samples) and after (9 samples) the alteration experiment (for legend see Fig. 5A). A decrease in the grain density in all samples and a decrease in the velocity in most of the samples were determined after the experiment.

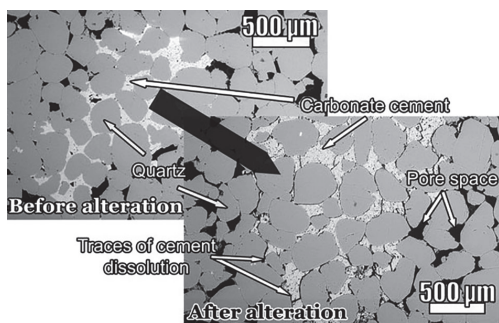


Fig. 6. SEM microphotographs of thin sections of reservoir carbonate-cemented medium- to fine-grained well-sorted Deimena Formation sandstone sample E7-3 (Table 3) before (left) and after (right) the alteration experiment. The sandstone composition is oligomictic, characterized by predominantly subrounded quartz grains. The sample is characterized by tight compaction of grains. Interparticle porosity is connected by very thin intermediate channels responsible for low permeability before alteration (Table 5). Visual analysis of thin sections (left and right) confirmed the measured results (10–15% by Shvetsov 1948, Table 5). The light-coloured area is carbonate cement (calcite, ankerite and dolomite), locally making more than 50% of the rock pore volume. Traces of the dissolution and microfracturing of carbonate cement on the edges of grains and inside the pore filling and the displacement of clay cement blocking pores were determined after the experiment (right). Increase in microporosity is responsible for increase in permeability measured after alteration (Table 5). Sample E7-3 is of ‘cautionary-2’ reservoir quality (class VI) with improved quality up to ‘moderate’ (class IV) after alteration.

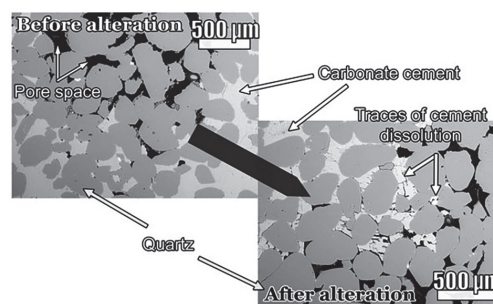


Fig. 7. SEM microphotographs of thin sections of trans-reservoir carbonate-cemented medium-grained poorly sorted Deimena sandstone sample Kn24-4 (Table 4) before (left) and after (right) the alteration experiment. The composition is oligomictic, predominantly characterized by subrounded quartz grains. XRD analyses revealed very minor presence of ankerite ($\text{Ca}(\text{Fe,Mg,Mn})(\text{CO}_3)_2$) minerals. The light-coloured area is pore filling ankerite cement, occupying more than 50% of pores in the thin section. The presence of about 5% clay-supported matrix was determined before the alteration experiment. Clay-supported matrix is locally blocking interparticle porous media (left). The porosity has very thin intermediate channels responsible for very low permeability before alteration. Visual analysis of thin sections confirmed the measured porosity (5–10% by Shvetsov 1948, Table 4). Traces of the dissolution and microfracturing of carbonate cement on the edges of grains and inside the pore filling and displacement of the clay-supported matrix blocking pores after the experiment were determined (right). This phenomenon explains drastically increased permeability measured after alteration (Table 4). Sample Kn24-4 was of ‘very low’ reservoir quality before the alteration experiment and became of ‘moderate’ reservoir quality (class IV) after the experiment.

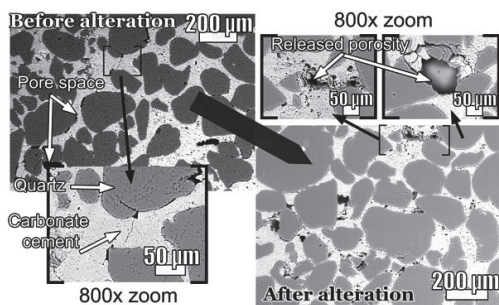


Fig. 8. SEM microphotographs of thin sections of trans-reservoir carbonate-cemented sample Kn27-4 from medium- to very fine-grained (fine-grained in general) unsorted Deimena sandstone (Table 3) before (left) and after (right) the alteration experiment. The composition is oligomictic, characterized by predominantly subrounded–subangular quartz grains. XRD analyses revealed minor calcite. The white-coloured area is pore filling calcite cement (carbonate), occupying almost 100% of pore space in the thin section. The appearance of new pores, which take up 1–5% of intragrain volume, was determined before the alteration experiment (left). Visual analysis confirms laboratory measurement data (Table 5). The zoomed image (lower left) of the thin section before alteration shows very thin interconnections between pores within carbonate cement, which makes the propagation of gases and liquids almost impossible (permeability = 0.001, Table 5). Spotted dissolution of cement with the destruction of cement matrix and locally quartz grains was observed after alteration (right). This phenomenon is responsible for drastically increased porosity and permeability after alteration (Table 5). Sample Kn27-4 was of ‘very low’ reservoir quality sandstone. During the alteration experiment its reservoir quality improved up to ‘high-2’ (class II), ‘very appropriate’ for CGS (Table 1).

studied sandstones of the Deimena Formation are located in the central middle part of the Baltic Cambrian Basin (700–1700 m depth), transitional from its northern shallow to southern deep part, they could have properties of both parts of the basin. However, even the porosity and permeability of uncompacted Cambrian sandstones from the shallow part of the basin range from very low values (1.5% and 0.001 mD, respectively), due to a high share of carbonate cement, to some 40% and 1300 mD in weakly cemented rocks (Shogenova et al. 2009a). The porosity of sandstones in the southwestern deep Lithuanian part of the basin (>1700 m) is mostly lower than that in carbonate- and clay-cemented sandstones in the shallow and middle parts of the basin, ranging within 0.4–12.4%. This is explained by compaction and secondary quartz cementation. However, the permeability of rocks in the southern part is varying in a rather wide range (0.003–960 mD) (Sliupa et al. 2001, 2008b; Čyžienė et al. 2006; Shogenova et al. 2009a). Considering these porosity and permeability ranges, the classifi-

cation of the reservoir rocks for CO₂ storage (Table 1), proposed in this research for the middle Latvian–Lithuanian parts of the basin (700–1700 m depth), could be adopted to shallow and deep parts of the basin with some possible corrections of porosity ranges for the reservoir quality classes in the deep part.

The initial permeability and porosity of the sandstones studied in the experiment were mainly controlled by the amount and type of diagenetic cement. Sandstones of ‘very low’ reservoir quality class VIII with the highest content of carbonate and clay cement had the lowest permeability (0.001–0.7 mD). The porosity of carbonate-cemented sandstones with the given permeability was lower than in clay-cemented samples (Tables 1, 3, Fig. 2). This corresponds to the results reported for the northern shallow part of the basin, where carbonate cementation has higher influence on the reduction of the porosity of Cambrian sandstones than clay cement, and grain-size influences the porosity of these rocks to a lesser degree than cementation (Shogenova et al. 2001a).

In sandstones from the offshore Lithuanian E7-1/82 and Latvian E6-1/84 boreholes, characterized by the same amount of clay and carbonate cement, lower permeability and porosity values were detected in the more compacted sandstones from the deeper E7 structure (class VI). Our study revealed different rock microstructure of sandstones of the Deimena Formation. For example, sandstone from the E6 structure (E6-3, Fig. 4) was characterized in general by fine grain size (0.25–0.125 mm, Krumbein phi scale, Krumbein 1934), poor sorting of the material and clay cement content of 5%. Sandstone from the E7 structure (E7-3, Fig. 6) is medium- (0.5–0.25 mm) to fine-grained, well-sorted with a high content of carbonate cement (about 50%). Sandstones from the South Kandava structure are medium- to very fine-grained (0.125–0.63 mm), poorly sorted to unsorted, with 50–100% carbonate in pore space and, in addition, several per cent of clay cement. At the same time, due to heterogeneity, the rock properties could vary at different depths even in one geological structure (e.g. in E6) (Shogenov et al. 2013b).

The main difference between previous classifications, given for hydrocarbon reservoirs, recommendations for reservoirs ‘appropriate’/‘not appropriate’ for CGS and the new classification proposed in this research for the sandstones of the Deimena Formation is the overlapping porosity of rock groups divided by permeability (Table 1). For this reason every group is subdivided into classes distinguished by porosity. Still, the petrophysical parameters depending on porosity, like bulk density and velocity, can also overlap for some classes. However, every reservoir quality rock class is characterized by a unique set of petrophysical, chemical, mineralogical and microstructural parameters (Table 2, Figs 4, 6–8).

The initial and altered effective porosity and permeability of the reservoir samples from the E6 structure were ranked as of 'high-1' and 'good' reservoir quality (classes I and III, respectively), or 'very appropriate' and 'appropriate' for CGS, respectively (groups 1 and 2, Table 1). The porosity and permeability of sandstones from the E7 structure were significantly lower (class VI) than in rocks from E6. The initial and altered permeability of the clay-cemented sandstones from the E7 structure (0.13–0.18 mD) and the initial permeability of the carbonate-cemented sandstones from the South Kandava structure (0.001–0.28 mD) were in 'very low' reservoir quality class VIII. The reservoir quality of rocks decreases with increasing depth because of rock compaction, rising temperature, conformation of grains and increasing quartz cementation of sandstone with growing depth in the Baltic Basin (Shogenova et al. 2001a, 2001b, 2009a; Sliupa et al. 2001). Our study confirms these results – the shallowest offshore structure E6 has the best reservoir properties of sandstones.

The effective porosity of most samples did not change during treatment and was supported by stable (E7-1, E7-5) or little varying (E7-4, E7-6) permeability values (Table 4, Fig. 2). Other samples showed some variation in effective porosity with stable permeability. At the same time, sample E7-3 revealed a slight decrease in effective porosity but a significant increase in permeability (up to 2 times after the alteration experiment). An increase in permeability, correlated with a decrease in grain density and supported by unchanged initial porosity, could be explained by modifications of pore space geometry and grain shape changes that control capillary forces (Schön 1996). We determined a minor dissolution of sandstone cement, including dolomite and ankerite (Table 3, Fig. 6), which was insignificant for effective porosity change but substantial for permeability increase. Mineral precipitation and/or cement dissolution, as well as relocation and displacement of clay cement, which blocks pores, took place in the samples characterized by decreased effective porosity. Thin section study showed that the clay fraction, represented by an insignificant amount (about 5%) of kaolinite and/or illite in porous media of the studied samples, was displaced from the pores after the alteration experiment (Figs 4, 6, 7). The type of clay mineral present is important for the reservoir quality of sandstone. Different influence of kaolinite and illite on porosity and permeability change has been explained earlier. According to Tucker (2001), pore-filling kaolinite reduces the porosity of sandstone, but has little effect on permeability, while pore-lining illite reduces permeability considerably by blocking pore throats but has little effect on porosity. We are not focusing on the clay fraction due to the minor presence of clay minerals in

the studied samples and insignificant alteration of properties related to the clay cement displacement after the experiment.

Before the alteration experiment trans-res carbonate-cemented quartz sandstone samples Kn24-4 (ankerite-cemented) and Kn27-4 (calcite-cemented) had low and very low effective porosity and permeability (class VIII, Tables 1, 4). In both samples we determined the dissolution of ankerite and calcite cements with minor displacement of clay cement blocking pores. However, both types of cement dissolution affected the alteration of petrophysical properties. We observed a more significant increase in effective porosity and permeability in calcite-cemented sandstone Kn27-4. The sample was relocated from the 'very low' reservoir quality class VIII rank ('not appropriate' for CGS) to 'high-2' quality class II ('very appropriate' for CGS) due to final improvement in petrophysical properties (Tables 1, 4). These changes were supported by the dissolution of the carbonate mineral phase, expressed in the decrease in CaO values (3.5%) measured by XRF analysis after the alteration experiment (Table 3). The dissolution of the carbonate mineral phase in ankerite-cemented sandstone Kn24-4 is also expressed by the decrease in CaO (1.7%) measured by XRF analysis after the alteration experiment (Table 3). This sample was relocated from 'very low' reservoir quality class VIII ('not appropriate' for CGS) to 'moderate' quality class IV ('appropriate' for CGS) (Tables 1, 4). Minor improvement of the rock properties compared to calcite-cemented sandstone Kn27-4 was observed (Table 4).

Previously reported results of laboratory experiments, numerical modelling and field monitoring of CO₂-reservoir rock interactions (e.g. Czernichowski-Lauriol et al. 2006; Egermann et al. 2006; Izgec et al. 2008; Kaszuba & Janecky 2009; Bemer & Lombard 2010; Nguyen et al. 2013) concur with our data. Partial dissolution of carbonate cement (calcite, dolomite and ankerite) and other secondary minerals associated with significant increase, and in some places slight variation in porosity and permeability were determined in the reservoir rocks.

Thin section study allowed qualitative estimation of the mineral dissolution in carbonate cement. Although we expected carbonate cement to dissolve more intensely, it dissolved only on the edges of grains and partially inside the pore filling. This phenomenon could be explained by the reduction in the acidity of brine and increase in pH to the pre-experimental level during the experiment due to the dissolution of a certain amount of carbonate cement material. This means that CGS in the areas with substantial carbonate cementation of reservoir rock will not cause a significant dissolution of cement in the long term, which lowers the level of leakage risks.

However, this statement is very site-specific and must be approved by fluid-flow modelling in every certain storage site.

The grain and bulk dry density and P-wave velocity measured in this research were mainly within the limits corresponding to the data earlier reported for the middle part of the Baltic Cambrian Basin. Maximum values of P-wave velocity measured before the experiment for carbonate-cemented sandstones from the South Kandava structure (5400–4556 m s⁻¹) were similar to the data measured earlier for carbonate-cemented sandstones of the northern shallow part of the basin. The decrease in P-wave and S-wave velocity in the dry samples after the alteration experiment, determined in most of the reservoir sandstones, is explained by the increase in porosity and/or decrease in grain and bulk density (Fig. 5). The lowest acoustic velocity before the alteration was in the range of the lowest previously obtained values (Shogenova et al. 2001a, 2001b), while after the experiment the P-wave velocity of sample E7-6 became the lowest among earlier and recently measured velocities (Table 4). The grain density, measured before the alteration experiment for 12 sandstone samples, was in the limits of 2664–2746 kg m⁻³, decreasing after the experiment to 2635–2676 kg m⁻³ (Table 4).

The studied samples from the offshore reservoirs (E6 and E7) are typical rocks of the Deimena Formation of Cambrian Series 3 in the Baltic Basin. Thereby, petrophysical alterations described in this study are an important piece of the puzzle when CGS will be modelled in the basin scale.

According to the data in Shogenov et al. (2013a, 2013b) and the classification presented herein, the South Kandava, E6 and E7 structures were re-estimated for CGS in the Cambrian Deimena Formation in the Baltic Basin. The reservoir sandstones of the Deimena Formation in the South Kandava and E6 structures had an identical average porosity of 21%, while their average permeability differed twofold, being 300 and 150 mD, respectively. The estimated good reservoir quality of sandstones in these structures was assessed as ‘appropriate’ for CGS. The reservoir quality of the sandstones of the E7 offshore structure, estimated as ‘cautionary-2’ (average porosity 12% and permeability 40 mD), was the lowest in the studied structures and was assessed as ‘cautionary’ for CGS.

CONCLUSIONS

1. Based on the recently and earlier measured gas permeability and porosity, a classification of the reservoir quality for CO₂ geological storage was proposed for sandstones of the Deimena Formation of Cambrian Series 3 in the middle part of the Baltic Basin. According to their practical application to CGS, the rocks were divided into four groups by permeability (very appropriate, appropriate, cautionary and not appropriate) and eight reservoir quality classes were distinguished within the groups by porosity (high-1 and high-2, good and moderate, cautionary-1 and cautionary-2, low and very low). The proposed classification of the reservoir quality of sandstones helped to estimate the significance of their petrophysical changes caused by geochemical processes during the CO₂ injection-like alteration experiment.
2. The rocks of the initially four reservoir quality classes were studied both before and after the CO₂ injection-like alteration experiment. The greatest changes in the composition and properties of the rocks, caused by geochemical alteration during the experiment, were determined in two carbonate-cemented transitional reservoir sandstones from the uppermost part of the South Kandava onshore reservoir (0.2–0.3 m below cap rock). Partial dissolution of pore filling carbonate cement (ankerite and calcite) and displacement of clay cement, which blocks pores, caused a significant increase in effective porosity, drastic increase in permeability and a decrease in samples’ weight, bulk and grain density and P- and S-wave velocity. As a result of these alterations carbonate-cemented sandstones of initially ‘very low’ reservoir quality (class VIII), ‘not appropriate’ for CGS, acquired an ‘appropriate’ for CGS ‘moderate’ (class IV) or ‘very appropriate’ for CGS ‘high-2’ reservoir quality (class II).
3. Significant increase in effective porosity and permeability after the alteration experiment was detected in calcite-cemented sandstone Kn27-4 compared to ankerite-cemented sandstone Kn24-4. Only partial carbonate cement dissolution occurred on the edges of grains and inside the pore filling in the samples with carbonate cement (e.g. E7-3, Kn24-4 and Kn24-7), which is explained by reduction in the acidity of brine and increase in pH equilibrium during the experiment compared to the pre-experimental state.
4. The composition and properties of clay-cemented sandstone with initially ‘very low’ reservoir quality (class VIII), ‘not appropriate’ for CGS, from the lower part of the offshore E7 structure changed slightly. Its permeability (0.18–0.23 mD) was not improved during the experiment and these rocks remained in the ‘very low’ reservoir quality class.
5. Variation in the properties of sandstones from the middle and upper parts of the E7 structure of initially ‘cautionary-2’ reservoir quality (class VI) did not cause significant changes in their reservoir quality, except for one sample with notably increased perme-

ability, rising its reservoir quality into ‘moderate’ (class IV), ‘appropriate’ for CGS.

6. Slight variations in the composition and properties of the ‘high-1’ reservoir quality sandstones from the E6 offshore structure did not cause significant changes in reservoir quality and they remained in their initial quality classes (‘high-1’ and ‘good’ quality classes I and III). These changes were interpreted as insignificant mineral dissolution and some displacement of clay cement from the pore space, which caused slight mechanical weakening and a decrease in the weight, grain and bulk density, possible slight increase in the effective porosity in all the structure, as well as probable increase in the permeability of the rocks from the lowermost part of the E6 reservoir.
7. The reservoir sandstones of the Deimena Formation in the South Kandava and E6 structures had an identical average porosity of 21%, but their average permeability differed twofold, being 300 and 150 mD, respectively. The good reservoir quality of sandstones in these structures was assessed as ‘appropriate’ for CGS. The reservoir quality of the sandstones of the E7 offshore structure, estimated as ‘cautionary-2’ (average porosity 12% and permeability 40 mD), was the lowest in the studied structures and was assessed as ‘cautionary’ for CGS.
8. The obtained results indicate some possible physical processes that could occur during CGS in the studied onshore and offshore structures. These results, being the first of this type in the central part of the Baltic Basin, are also important for the southern and western parts of the Baltic sedimentary basin, which have CO₂ storage capacity in the Cambrian aquifer (Lithuania, Sweden, Kaliningrad Region and offshore Poland). However, they should be supported by additional laboratory experiments and fluid-flow modelling of the CO₂ storage in the Cambrian sandstones both in the structures and basin scale for better assessment of the possible storage scenarios and their safety.

Acknowledgements. This contribution is a part of K. Shogenov’s PhD study and is partly supported by the institutional research funding programmes (projects SF0320080s07 and IUT19-22) of the Estonian Ministry of Education and Research and the EU FP7 ‘CGS Europe’ project No. 256725. IFP Energies nouvelles (IFPEN) performed the alteration experiment. All the data presented in the study are the property of the authors and available on request from the first author (kazbulat.shogenov@ttu.ee). We are grateful to the Latvian Environmental, Geological and Meteorological Centre for providing samples, to Jean Guelard (IFPEN) for help in permeability measurements and guidance in the petrophysical laboratory, our colleagues Olle Hints and Maarjuss Voolma

from the IG TUT for their kind assistance with SEM adjustment and Jüri Ivask (IG TUT) for help during article preparation. We highly appreciate the fruitful discussions on thin sections of altered rock samples with Karl-Heinz Wolf from Delft University of Technology. We are also grateful to reviewers Ģirts Stinkulis from Latvia and Argo Jõelett from Estonia for their great contribution improving the manuscript.

REFERENCES

- Andrushenko, J., Vzosek, R., Krochka, V., Hubldikov, A., Lobanov, V., Novikov, E., Hafenshtain, K., Tsimashevskij, K. & Labus, R. 1985. *Geological Report of the Well E6-1/84*. Unpublished exploration report, Latvian Environmental, Geology and Meteorology Centre (LEGMC), Latvia, Riga [in Russian].
- [API] American Petroleum Institute. 1998. *Recommended Practices for Core Analysis*. Second Edition, Recommended Practice, 40, Exploration and Production Department, 236 pp.
- Arts, R., Chadwick, A., Eiken, O., Thibeau, S. & Nooner, S. 2008. Ten years of experience of monitoring CO₂ injection in the Utsira Sand at Sleipner, offshore Norway. *First break*, **26**, 65–72.
- Babuke, B., Vzosek, R., Grachev, A., Naidenov, V., Krochka, V., Markov, P., Novikov, E., Tsimashevskij, L. & Labus, R. 1983. *Geological Report of the Well E7-1/82*. Unpublished exploration report, Latvian Environmental, Geology and Meteorology Centre (LEGMC), Latvia, Riga [in Russian].
- Bachu, S., Bonijoly, D., Bradshaw, J., Burruss, R., Holloway, S., Christensen, N. P. & Mathiassen, O. M. 2007. CO₂ storage capacity estimation: methodology and gaps. *International Journal of Greenhouse Gas Control*, **1**, 430–443.
- Bemer, E. & Lombard, J. M. 2010. From injectivity to integrity studies of CO₂ geological storage. *Oil & Gas Science and Technology – Rev. IFP*, **65**, 445–459.
- Bertier, P., Swennen, R., Laenen, B., Lagrou, D. & Dreesen, R. 2006. Experimental identification of CO₂–water–rock interactions caused by sequestration of CO₂ in Westphalian and Buntsandstein sandstones of the Campine Basin (NE-Belgium). *Journal of Geochemical Exploration*, **89**, 10–14.
- Carroll, S. A., McNab, W. W. & Torres, S. C. 2011. Experimental study of cement–sandstone/shale–brine–CO₂ interactions. *Geochemical Transactions*, **12**:9.
- Carroll, S. A., McNab, W. W., Dai, Z. & Torres, S. C. 2013. Reactivity of Mt. Simon sandstone and the Eau Claire shale under CO₂ storage conditions. *Environmental Science and Technology*, **47**, 252–261.
- Chadwick, A., Arts, R., Bernstone, C., May, F., Thibeau, S. & Zweigel, P. 2006. Best practice for the storage of CO₂ in saline aquifers. Keyworth, Nottingham. *British Geological Survey Occasional Publication*, **14**, 1–277.
- Čyžienė, J., Molenaar, N. & Šliaupa, S. 2006. Clay-induced pressure solution as a Si source for quartz cement in sandstones of the Cambrian Deimena Group. *Geologija (Vilnius)*, **53**, 8–21.
- Czernichowski-Lauriol, I., Rochelle, C., Gaus, I., Azaroual, M., Pearce, J. & Durst, P. 2006. Geochemical interactions

- between CO₂, pore-waters and reservoir rocks: lessons learned from laboratory experiments, field studies and computer simulations. In *Advances in the Geological Storage of Carbon Dioxide: International Approaches to Reduce Anthropogenic Greenhouse Gas Emissions* (Lombardi, S., Altunina, S. E. & Beaubien, S. E., eds), pp. 157–174. Springer, Dordrecht, Netherlands.
- Dmitriev, E., Freimanis, A., Tratsevski, G. & Pavlovski, A. 1973. *Geological Report of Wells 91 and 92 on the Dobele Structure*. Unpublished exploration report, Latvian Environmental, Geology and Meteorology Centre (LEGMC), Latvia, Riga [in Russian].
- Egermann, P., Bemer, E. & Zinszner, B. 2006. An experimental investigation of the rock properties evolution associated to different levels of CO₂ injection like alteration processes. In *Proceedings of the International Symposium of the Society of Core Analysts, September 12–16, 2006, Trondheim, Norway*, paper SCA 2006-34.
- Gilfillan, S. M. V., Ballentine, C. J., Holland, G., Blagburn, D., Lollar, B. S., Stevens, S., Schoell, M. & Cassidy, M. 2008. The noble gas geochemistry of natural CO₂ gas reservoirs from the Colorado Plateau and Rocky Mountain provinces, USA. *Geochimica et Cosmochimica Acta*, **72**, 1174–1198.
- Gilfillan, S. M. V., Lollar, B. S., Holland, G., Blagburn, D., Stevens, S., Schoell, M., Cassidy, M., Ding, Z., Zhou, Z., Lacrampe-Couloume, G. & Ballentine, C. J. 2009. Solubility trapping in formation water as dominant CO₂ sink in natural gas fields. *Nature*, **458**, 614–618.
- Gorbatshev, R. & Bogdanova, S. 1993. Frontiers in the Baltic References Shield. *Precambrian Research*, **64**, 3–21.
- Grigg, R. B. & Svec, R. K. 2003. Co-injected CO₂-brine interactions with Indiana Limestone. In *Society of Core Analysts Symposium, September 21–24, 2003, Pau, France*, paper SCA 2003-19.
- Halland, E. K., Johansen, W. T. & Riss, F. 2011. *CO₂ Storage Atlas – Norwegian North Sea*. The Norwegian Petroleum Directorate, <http://www.npd.no/Global/Norsk/3-Publikasjoner/Rapporter/PDF/CO2-ATLAS-lav.pdf> [accessed 20 April 2015].
- Halland, E. K., Johansen, W. T. & Riss, F. 2013. *CO₂ Storage Atlas – Norwegian Sea*. The Norwegian Petroleum Directorate, <http://www.npd.no/Global/Norsk/3-Publikasjoner/Rapporter/CO2-ATLAS-Norwegian-sea-2012.pdf> [accessed 20 April 2015].
- Hitchon, B. (ed.). 1996. *Aquifer Disposal of Carbon Dioxide*. Geoscience Publishing Ltd., Sherwood Park, Alberta, Canada, 165 pp.
- IPCC. 2014. *IPCC Special Report. Climate Change: Mitigation of Climate Change*. Prepared by Working Group III Contribution of the Intergovernmental Panel on Climate Change to AR5, 1435 pp.
- Izgec, O., Demiral, B., Bertin, H. & Akin, S. 2008. CO₂ injection into saline carbonate aquifer formations. Laboratory investigation. *Transport in Porous Media*, **72**, 1–24.
- Kamath, J., Nakagawa, F. M., Boyer, R. E. & Edwards, K. A. 1998. Laboratory investigation of injectivity losses during WAG in West Texas Dolomites. In *Permian Basin Oil and Gas Conference, March 23–26, 1998, Midland, TX*, paper SPE 39791.
- Kaszuba, J. P. & Janecy, D. R. 2009. Geochemical impacts of sequestering carbon dioxide in brine formations. In *Carbon Sequestration and Its Role in the Global Carbon Cycle* (Sundquist, E. & McPherson, B., eds), *Geophysical Monograph*, **183**, 239–248.
- Khanin, A. A. 1965. *Osnovnye ucheniya o porodakh-kollektorakh nefi i gaza [Main Studies of Oil and Gas Reservoir Rocks]*. Publishing House Nedra, Moscow, 362 pp. [in Russian].
- Khanin, A. A. 1969. *Porody-kollektory nefi i gaza i ikh izuchenie [Oil and Gas Reservoir Rocks and Their Study]*. Publishing House Nedra, Moscow, 368 pp. [in Russian].
- Kilda, L. & Friis, H. 2002. The key factors controlling reservoir quality of the Middle Cambrian Deimena Group sandstone in West Lithuania. *Bulletin of the Geological Society of Denmark*, **49**, 25–39.
- Krumbein, W. C. 1934. Size frequency distributions of sediments. *Journal of Sedimentary Petrology*, **4**, 65–77.
- Lashkova, L. N. 1979. *Litologiya, fatsii, i kollektorskie svoystva kembrijskikh otlozhenij Yuzhnoj Pribaltiki [Lithology, Facies and Reservoir Properties of Cambrian Deposits of the South Baltic Region]*. Publishing House Nedra, Moscow, 102 pp. [in Russian].
- Liu, F., Lu, P., Zhu, C. & Xiao, Y. 2011. Coupled reactive flow and transport modelling of CO₂ sequestration in the Mt. Simon sandstone formation. Midwest U.S.A. *International Journal of Greenhouse Gas Control*, **5**, 294–307.
- Liu, F., Lu, P., Griffith, C., Hedges, S. W., Soong, Y., Hellevang, H. & Zhu, C. 2012. CO₂-brine-caprock interaction: reactivity experiments on Eau Claire shale and a review of relevant literature. *International Journal of Greenhouse Gas Control*, **7**, 153–167.
- Mavko, G., Mukerji, T. & Dvorkin, J. 2003. *Rock Physics Handbook – Tools for Seismic Analysis in Porous Media*. Cambridge University Press, 329 pp.
- Metz, B., Davidson, O., de Coninck, H. C., Loos, M. & Meyer, L. A. (eds). 2005. *IPCC Special Report. Carbon Dioxide Capture and Storage*. Prepared by Working Group III of the Intergovernmental Panel on Climate Change. Cambridge University Press, Cambridge, United Kingdom and New York, NY, USA, 431 pp.
- Nguyen, P., Fadaei, H. & Sinton, D. 2013. Microfluidics underground: a micro-core method for pore scale analysis of supercritical CO₂ reactive transport in saline aquifers. *Journal of Fluids Engineering*, **135**(2), 7 pp.
- Pawar, R. J., Warpinski, N. R., Lorenz, J. C., Benson, R. D., Grigg, R. B., Stubbs, B. A., Stauffer, P. H., Krumhansl, J. P. & Cooper, S. P. 2006. Overview of a CO₂ sequestration field test in the West Pearl Queen reservoir, New Mexico. *The American Association of Petroleum Geologists/Division of Environmental Geosciences, Environmental Geosciences*, **13**, 163–180.
- Peng, S., Babcock, L. E. & Cooper, R. A. 2012. Chapter 19. The Cambrian Period. In *The Geologic Time Scale 2012* (Gradstein, F., Ogg, J., Schmitz, M. & Ogg, G., eds), pp. 437–488. Elsevier.
- Poprawa, P., Šliaupa, S., Stephenson, R. & Lazauskiene, J. 1999. Late Vendian–Early Palaeozoic tectonic evolution of the Baltic basin: regional tectonic implications from subsidence analysis. *Tectonophysics*, **314**, 218–239.

- Prieditis, J., Wolle, C. R. & Notz, P. K. 1991. A laboratory and field injectivity study: CO₂ WAG in the San Andres formation of West Texas. In *Annual Technical Conference and Exhibition, October 6–9, 1991, Dallas, TX*, paper SPE 22653.
- Rochelle, C. A., Czermichowski-Lauriol, I. & Milodowski, A. E. 2004. The impact of chemical reactions on CO₂ storage in geological formations: a brief review. *Geological Society, London, Special Publications*, **233**, 87–106.
- Ross, G. D., Todd, A. C., Tweedie, J. A. & Will, A. G. 1982. The dissolution effects of CO₂–brine systems on the permeability of U.K. and North Sea calcareous sandstones. In *DOE Symposium on Enhanced Oil Recovery, April 4–7, 1982, Society of Petroleum Engineers, Tulsa, OK*, paper SPE 10685.
- Schön, J. H. 1996. *Physical Properties of Rocks: Fundamentals and Principles of Petrophysics*. Pergamon, Oxford, UK, 583 pp.
- Shogenov, K., Shogenova, A. & Vizika-Kavvadias, O. 2013a. Petrophysical properties and capacity of prospective structures for geological storage of CO₂ onshore and offshore Baltic. *Energy Procedia*, **37**, 5036–5045.
- Shogenov, K., Shogenova, A. & Vizika-Kavvadias, O. 2013b. Potential structures for CO₂ geological storage in the Baltic Sea: case study offshore Latvia. *Bulletin of the Geological Society of Finland*, **85**, 65–81.
- Shogenova, A., Kirsimäe, K., Bitjukova, L., Jõelet, A. & Mens, K. 2001a. Physical properties and composition of cemented siliciclastic Cambrian rocks, Estonia. In *Research in Petroleum Technology* (Fabricius, I. L., ed.), pp. 123–149. Nordisk Energiforskning, Ås, Norway.
- Shogenova, A., Šliaupa, S., Rasteniene, V., Jõelet, A., Kirsimäe, K., Bitjukova, L., Lashkova, L., Zabele, A., Freimanis, A., Hoth, P. & Huenges, E. 2001b. Elastic properties of siliciclastic rocks from Baltic Cambrian basin. In *63rd EAGE Conference and Technical Exhibition. Extended Abstracts, Volume 1*, pp. 1–4. European Association of Geoscientists & Engineers, Amsterdam, The Netherlands. N-24.
- Shogenova, A., Kleesment, A. & Shogenov, K. 2005. Chemical composition and physical properties of the rock. In *Mehikoorma (421) Drill Core* (Pöldvere, A., ed.), *Estonian Geological Sections*, **6**, 31–38.
- Shogenova, A., Kleesment, A. & Shogenov, K. 2006. Lithologic determination of Devonian dolomitic carbonate-siliciclastic rocks from Estonia by physical parameters. In *68th EAGE Conference & Exhibition, Extended Abstracts & Exhibitors' Catalogue, P207*, pp. 1–5. European Association of Geoscientists & Engineers, Vienna 2006, Houten, The Netherlands.
- Shogenova, A., Šliaupa, S., Vaher, R., Shogenov, K. & Pomeranceva, R. 2009a. The Baltic Basin: structure, properties of reservoir rocks and capacity for geological storage of CO₂. *Estonian Journal of Earth Sciences*, **58**, 259–267.
- Shogenova, A., Šliaupa, S., Shogenov, K., Šliaupiene, R., Pomeranceva, R., Vaher, R., Uibu, M. & Kuusik, R. 2009b. Possibilities for geological storage and mineral trapping of industrial CO₂ emissions in the Baltic region. *Energy Procedia*, **1**, 2753–2760.
- Shogenova, A., Shogenov, K., Vaher, R., Ivask, J., Šliaupa, S., Vangkilde-Pedersen, T., Uibu, M. & Kuusik, R. 2011a. CO₂ geological storage capacity analysis in Estonia and neighboring regions. *Energy Procedia*, **4**, 2785–2792.
- Shogenova, A., Shogenov, K., Pomeranceva, R., Nulle, I., Neele, F. & Hendriks, C. 2011b. Economic modelling of the capture–transport–sink scenario of industrial CO₂ emissions: the Estonian–Latvian cross-border case study. *Energy Procedia*, **4**, 2385–2392.
- Shvetsov, M. S. 1948. *Petrografiya osadochnykh porod* [*Petrography of Sedimentary Rocks*], GosGeolTehlzdat, 385 pp. [in Russian].
- Sikorska, M. & Paczesna, J. 1997. Quartz cementation in Cambrian sandstones and the background of their burial history of the East European Craton. *Geological Quarterly*, **41**, 265–272.
- Silant'ev, V., Freimanis, A., Mikhailovskij, P., Pavlovskij, A. & Karpitskij, V. 1970. *Geology and Oil Potential of South Kandava Structure*. Unpublished exploration report, Latvian Environmental, Geology and Meteorology Centre (LEGMC), Latvia, Riga [in Russian].
- Šliaupa, S., Rasteniene, V., Lashkova, L. & Shogenova, A. 2001. Factors controlling petrophysical properties of Cambrian siliciclastic deposits of central and western Lithuania. In *Research in Petroleum Technology* (Fabricius, I. L., ed.), pp. 157–180. Nordic Petroleum Series, V, Nordisk Energiforskning, Norway.
- Šliaupa, S., Shogenova, A., Shogenov, K., Šliaupiene, R., Zabele, A. & Vaher, R. 2008a. Industrial carbon dioxide emissions and potential geological sinks in the Baltic States. *Oil Shale*, **25**, 465–484.
- Šliaupa, S., Cyziene, J., Molenaar, N. & Musteikyte, D. 2008b. Ferroan dolomite cement in Cambrian sandstones: burial history and hydrocarbon generation of the Baltic sedimentary basin. *Acta Geologica Polonica*, **58**, 27–41.
- Šliaupa, S., Lojka, R., Tasáryová, Z., Kolejka, V., Hladík, V., Kotulová, J., Kucharič, L., Fejdi, V., Wojcicki, A., Tarkowski, R., Uliasz-Misiak, B., Šliaupienė, R., Nulle, I., Pomeranceva, R., Ivanova, O., Shogenova, A. & Shogenov, K. 2013. CO₂ storage potential of sedimentary basins of Slovakia, The Czech Republic, Poland, and Baltic States. *Geological Quarterly*, **57**, 219–232.
- Sopher, D., Juhlin, C. & Erlström, M. 2014. A probabilistic assessment of the effective CO₂ storage capacity within a Swedish sector of the Baltic Basin. *International Journal of Greenhouse Gas Control*, **30**, 148–170.
- Šteinerts, G. 2012. Maritime delimitation of Latvian waters, history and future prospects. *Journal of Maritime Transport and Engineering*, **1**, 47–53.
- Sundberg, F. A., Zhao, Y. L., Yuan, J. L. & Lin, J. P. 2011. Detailed trilobite biostratigraphy across the proposed GSSP for Stage 5 (“Middle Cambrian” boundary) at the Wuliu-Zengjiayan section, Guizhou, China. *Bulletin of Geosciences*, **86**, 423–464.
- Svec, R. K. & Grigg, R. B. 2001. Physical effects of WAG fluids on carbonate core plugs. In *SPE Annual Technical Conference and Exhibition, SPE 71496, New Orleans, LA*, 10 pages.
- Tiab, D. & Donaldson, E. C. 2012. *Petrophysics. Theory and Practice of Measuring Reservoir Rock and Fluid Transport Properties*, 3rd ed. Gulf Professional Publishing, Oxford, 950 pp.

- Tucker, M. E. 2001. *Sedimentary Petrology*, 3rd ed. Blackwell Science, Oxford, 272 pp.
- Van der Meer, L. G. H. 1993. The conditions limiting CO₂ storage in aquifers. *Energy Conversion and Management*, **34**, 959–966.
- Vangkilde-Pedersen, T. & Kirk, K. (eds). 2009. *FP6 EU GeoCapacity Project, Assessing European Capacity for Geological Storage of Carbon Dioxide, Storage Capacity. D26, WP4 Report Capacity Standards and Site Selection Criteria*. Geological Survey of Denmark and Greenland, 45 pp., <http://www.geology.cz/geocapacity/publications> [accessed 20 April 2015].
- Vernon, R., O'Neil, N., Pasquali, R. & Nieminen, M. 2013. *Screening of Prospective Sites for Geological Storage of CO₂ in the Southern Baltic Sea*. VTT Technology 101, Espoo, Finland, 70 pp.
- Zdanavičiute, O. & Sakalauskas, K. (eds). 2001. *Petroleum Geology of Lithuania and Southeastern Baltic*. Institute of Geology, Vilnius, 204 pp.

Kambriumi liivakivide reservuaarikvaliteet ja petrofüüsikalised omadused ning nende evolutsioon Balti basseinis CO₂ geoloogilise ladustamise eksperimentaalse modelleerimise vältel

Kazbulat Shogenov, Alla Shogenova, Olga Vizika-Kavvadias ja Jean-François Nauroy

Käesoleva uurimistöö eesmärkideks olid: 1) anda ülevaade kehtivatest soovutest ladustamisreservuaaridele ja välja pakkuda nende kvaliteediklassifikatsioon, kasutades Kambriumi Seeria 3 Deimena ladestu katseandmeid; 2) kindlaks teha võimaliku CO₂ geoloogilise ladustamise (CGS) mõju Deimena ladestu liivakivide omadustele ja reservuaarikvaliteedile; 3) rakendada ettepanud klassifikatsiooni ladustamisreservuaaridele ja nende evolutsioonile CGS-i kestel Balti basseinis.

Baseerudes gaasiläbilaskevõimele ja poorsusele, pakuti välja reservuaarikivimite CGS-i kvaliteedi uus klassifikatsioon Balti settebasseini Deimena ladestu liivakividele, mis on kaetud Alam-Ordoviitsiumi savi- ning karbonaatsete kattekihivitega. Liivakivid jagati läbilaskevõime alusel nelja gruppi vastavalt nende CGS-i praktilisele kasutatavusele ('väga sobivad', 'sobivad', 'ettevaatust nõudvad' ja 'ebasobivad') ning täiendavalt jagati grupid poorsuse alusel kaheksaks reservuaarikvaliteediklassiks.

Mandrilise Lõuna-Kandava ja mereliste E6 struktuuri (Lätis) ning E7 struktuuri (Leedus) petrofüüsikalised, geo-keemilised ja mineraloogilised parameetrid määrati enne ning pärast CO₂ sisestamist imiteerivat muutmiskspereinti. Kõige märkimisväärsed muutused uuritud kivimite koostises ja omadustes leiti Lõuna-Kandava mandrilise struktuuri ülemiste kihtide karbonaatse tsemendiga liivakivides. Uuritud proovide poore täitva karbonaatse tsemendi (ankeriit ja kaltsiit) osaline lahustumine ning poore blokeeriva savitsemendi eemaletõrjumine põhjustasid nende efektiivse poorsuse märkimisväärse suurenemise, läbilaskevõime drastilise suurenemise ja tera- ning massitiheduse, P- ja S-laine kiiruse ning kuivproovide massi vähenemise. Nende muutuste tulemusel omandasid karbonaatse tsemendiga liivakivid, mis olid algselt 'väga madala' reservuaarikvaliteediga (klass VIII) ja CGS-iks 'ebasobivad', nüüd CGS-iks 'sobiva' 'keskpärase' kvaliteediklassi (klass IV) või CGS-iks 'väga sobiva' 'kõrge-2' kvaliteediklassi (klass II). 'Väga madala' (klass VIII) kvaliteediklassiga reservuaari savitsemendiga liivakivide läbilaskevõime ei paranenud. Muutmiskatsed, mis tehti uuritud mereliste puhaste kvartslivakividega E6 ja E7 struktuuridest, põhjustasid nende kivimite omadustes vaid tähtsusetuid muutusi. Nende liivakivide algsed reservuaarikvaliteedi näitajad ('kõrge-1' ja 'hea' ning klassid I ja III E6-s ning 'ettevaatust nõudvad-2' ja klass VI E7-s) peamiselt säilisid.

Lõuna-Kandava Deimena ladestu struktuuri reservuaari liivakivid keskmise poorsusega 21% on poorsuse poolest identsed kivimitega E6 struktuurist, kuid neil on kaks korda suurem läbilaskevõime: vastavalt 300 ja 150 mD. Hinnanguline hea liivakivide reservuaarikvaliteet nendes struktuurides hinnati CGS-iks 'sobivaks'. E7 merelise struktuuri liivakivide reservuaarikvaliteet, mis oli hinnanguliselt 'ettevaatust nõudev-2' (keskmine poorsus 12% ja läbilaskevõime 40 mD), oli uuritud struktuuridest madalaim ning hinnati kui CGS-iks 'ettevaatust nõudev'.

Esmakordselt uuriti laboratoorselt simuleeritud CGS-ile allutatud liivakivide petrofüüsikalist evolutsiooni. Saadud tulemused on olulised, mõistmaks füüsikalisi protsesse, mis võivad toimuda CO₂ ladustamisel Baltikumi mandrilistes ja merelistes struktuurides.

PAPER VI. SHOGENOV, K., GEI, D., FORLIN, E. & SHOGENOVA, A.
Petrophysical and numerical seismic modelling of CO₂ geological storage in the E6 structure, Baltic Sea, Offshore Latvia. Petroleum Geoscience (submitted).

Petrophysical and Numerical Seismic Modelling of CO₂ Geological Storage in the E6 structure, Baltic Sea, Offshore Latvia

Shogenov Kazbulat^{1,*}, Davide Gei², Edy Forlin² & Alla Shogenova¹

¹*Institute of Geology, Tallinn University of Technology, Ehitajate tee 5, Tallinn 19086, Estonia*

²*Istituto Nazionale di Oceanografia e di Geofisica Sperimentale (OGS)*

Borgo Grotta Gigante, 42/c, 34010 Sgonico Trieste, Italy

**Corresponding author (e-mail: kazbulat.shogenov@ttu.ee)*

ABSTRACT: For the first time 4D time-lapse numerical seismic modelling based on rock physics studies was applied to analyse feasibility of CO₂ storage monitoring in the largest offshore Latvia geological structure E6 in the Baltic Sea. The novelty of the applied approach was the coupling of the chemically induced petrophysical alteration effect of CO₂ hosting rocks measured in laboratory with time-lapse numerical seismic modelling. Synthetic seismograms were generated for the E6 structure, where the sandstone reservoir of the Deimena Formation of the Cambrian Series 3 (earlier Middle Cambrian), was homogeneously saturated with different concentrations of CO₂. The synthetic seismograms obtained after CO₂ injection, were compared with a baseline. The following four scenarios were considered: (1) uniform model without alteration effect, (2) uniform model with alteration effect, (3) plume model without alteration effect and (4) plume model with alteration effect.

The presence of CO₂ could be clearly indicated by direct interpretation of the plane-wave synthetic seismic sections, and is clearly observed when one displays the difference between the baseline and post CO₂ injection synthetics. The normalized root mean square (NRMS) imaging techniques also clearly highlights the time-lapse differences between the baseline and CO₂ plume models.

Application of measured in laboratory alteration of the petrophysical properties of the reservoir had a strong influence on the reflected signals in the seismic sections, showing the highest difference on seismic sections with 1% of CO₂ saturation, increasing the detectability of the stored CO₂. The difference decreased with increasing CO₂ content.

Up to 5% CO₂ saturation could be qualitatively estimated from the synthetic seismic data. CO₂ saturation higher than 5% produced a strong signal in the repeatability matrix, but P-wave velocity varied so slightly, that qualitative estimations challenging. A time shift or push-down effect of the reflectors below CO₂ storage area was observed.

Seismic models could detect CO₂ injected into the deep aquifer formations even with low CO₂ saturation values according to changes in amplitude and two-way travel times in the presence of CO₂.

Our results showed effectiveness of the implemented time-lapse rock physics and seismic methods to plan monitoring of the CO₂ plume evolution and migration in the E6 offshore oil-bearing structure, which could be applied for other prospective structures in the Baltic Region.

KEY WORDS: *CO₂ geological storage, numerical seismic modelling, NRMS, petrophysical alteration, seismic monitoring, CO₂ plume, offshore Latvia, Baltic Sea*

INTRODUCTION

Carbon Dioxide (CO₂) is an important greenhouse gas responsible for recent global climate change. It is capable of absorbing the heat radiation from the Earth's surface and contributes to the increase of the atmosphere's temperature. Nevertheless, if the level of CO₂ in the atmosphere drastically changes, the greenhouse effect could alter the conditions on the planet (National Research Council 2010). The Intergovernmental Panel on Climate Change (IPCC 2005), U.S. Environmental Protection Agency (USEPA 2013), etc. stated that fossil fuel combustion is a major source of CO₂ emissions to

the atmosphere (USGS CSRA Team 2013). Our previous studies show that the Estonian power plants emit more CO₂, than the energy sector of all other Baltic countries (Latvia and Lithuania) together. Estonian CO₂ emissions per capita are one of the highest in Europe and in the world due to the use of local oil shale for energy production (e.g. Shogenova *et al.* 2009a, b, 2011a, b).

Carbon Capture and Storage (CCS) is one of the most effective measures and plays an essential role in reducing the greenhouse effect and mitigating climate change on our planet (Holloway 2002; IEA 2004; IPCC 2005; Bachu *et al.* 2007;

Arts *et al.* 2008; IEA 2013; IPCC 2013). The overall reduction of CO₂ emissions will likely involve some combination of technologies, but for the immediate future, industrial CO₂ storage in geologic reservoirs (CGS) is an available technology because existing knowledge derived from the oil and gas production industries has helped to solve some of the major engineering challenges. A detailed estimate of the national geologic CO₂ storage resources is required to make informed decisions about the implementation of CGS in the study area (USGS CSRA Team 2013).

The Estonian territory is unsuitable for CGS because of its geological setting, i.e., shallow sedimentary basin and potable water available in all known aquifers. The most prospective structures for CGS in the East Baltic region (Estonia, Latvia and Lithuania) are located in Latvia and consist in a number of onshore and offshore anticlines (Sliampa *et al.* 2008; Shogenova *et al.* 2009a, b, 2011a, b; Shogenov *et al.* 2013a, b; Šliampa *et al.* 2013).

In this study we focus on a coupled petrophysical and numerical seismic modelling methodology to study the feasibility of monitoring CGS in a Latvian offshore deep geological structure E6 oil-bearing in the Saldus Formation of the Upper Ordovician secondary cap rock. This structure was selected as one of the most prospective in the Latvian area of the Baltic Region in our earlier published studies (Fig. 1, Shogenov *et al.* 2013a, b).

The E6 structure is located in the Baltic Sea, 37 km from the coast of Latvia. Estimated conservative and optimistic CO₂ storage capacity (160-400 Mt respectively) makes it the largest among all the studied onshore and offshore structures in the Baltic Region (Shogenov *et al.* 2013a, b). The prospective reservoir for CGS is represented by the Deimena Formation of the Cambrian Series 3 (earlier Middle Cambrian) (848–901 m depth in the well E6-1/84) composed by dark- and light-grey, fine-grained, loosely and medium-cemented, oil-impregnated sandstones. The oil impregnation ranges from weak irregular to strong regular (Shogenov *et al.* 2013b). According to a new classification of reservoir rock quality for CO₂ storage by permeability and porosity proposed in our previous study (Shogenov *et al.* 2015, accepted), the reservoir rocks from the E6 structure are presented mostly by sandstones of a 'good' reservoir quality of class III 'appropriate' (second group) for CGS (permeability 100-300 mD and porosity >18%) interbedded by sandstones of 'cautionary-2' reservoir quality class VI related to 'cautionary' for CGS group three (permeability 10-

100 mD and porosity 7-18%). In this study we did not consider oil impregnation of the reservoir rocks due to its very low saturation. The structure is an anticline fold bounded on three sides by faults. The total area of the structure is 600 km² with the closing contour line (or spill point) of the reservoir located at a depth of 1350 m below sea level (bsl) interpreted by Shogenov *et al.* (2013b), using structural maps of the study area and an available seismic profile. The closing contour line reported by the Latvian Environmental, Geology and Meteorology Centre (LEGMC) was at 950 m bsl (http://mapx.map.vgd.gov.lv/geo3/VGD_OIL_PAGE/).

The E6 is consisting of two different compartments (E6-A and E6-B) divided by an inner fault (Fig. 1). Shogenov *et al.* (2013b) assumed that the fault separated these compartments, preventing CO₂ movement from one part to another during injection, and drilling of additional well in the part E6-B will be needed.

An approximate area of the larger part (E6-A) of the structure is 553 km², while the smaller part (E6-B) is 47 km². The Deimena reservoir formation in the well E6-1/84 is a 53 m thick

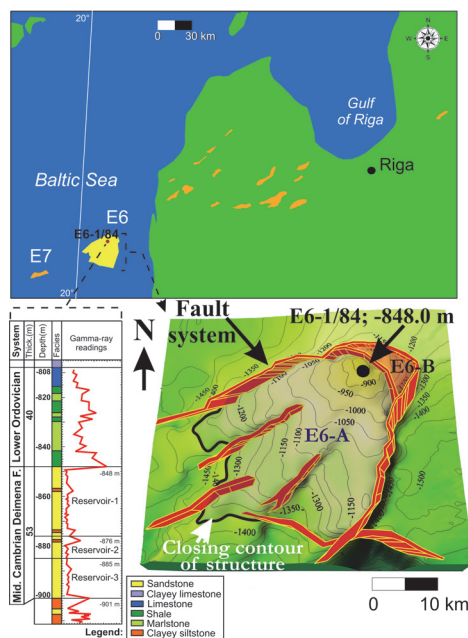


Fig. 1. Location map of Latvian onshore and Lithuanian offshore E7 structure (orange) prospective for CGS (CO₂ storage potential exceeding 2 Mt) in the Cambrian aquifer and studied structure E6 offshore Latvia (yellow) with location of well, lithological cross section and gamma-ray logging data and 3D geological model of the top of the Cambrian Deimena Formation of the E6 structure (modified after Shogenov *et al.* 2013b).

aquifer at 848 meters depth bsl (the top of the Deimena Formation), with salinity of 99000 ppm (98.89 g/l). The bigger part E6-A (553 km²) was considered for the modelling. The Deimena Sandstone Formation is unconformably covered by 40 m thick Lower Ordovician clayey primary cap rock. The reservoir located at the depth exceeding 850 m bsl is overlain by the Ordovician and Silurian (in total 266 m thick) clayey carbonate rocks and Devonian siliciclastic and carbonate rocks (Table 1). Upper part of the Upper Ordovician represents a small oil deposit in the Saldus Formation limestones (10.5 m; Shogenov *et al.* 2013a, b). The Cambrian Deimena Formation overlain by 117 m thick argillaceous siltstones, sandstones and claystones of the Cambrian Formations (Kybartai, Rausve, Vergale and Talsi). The basement is represented in the structure by Precambrian Neoproterozoic Ediacaran tuffaceous sediments and Paleoproterozoic gneissose granites at the depth 1018 m in the well E6-1/84 (Grigelis 2011; Shogenov *et al.* 2013a, b).

Time-lapse seismic method

Time-lapse seismic method is known as a highly suitable geophysical technique for monitoring CO₂ injection into a saline aquifer. The effects of the CO₂ on the seismic data are large both in terms of seismic amplitudes and in observed velocity push-down (Arts *et al.* 2000). In this research we have applied a 4D time-lapse rock physics and numerical seismic modelling method (Carcione 2007) to compute synthetic seismograms before and after CO₂ injection into the E6 structure and to provide the basis for further CGS monitoring plan in the study area. This is an important technology to predict the seismic response of CO₂ in the storage site, to plan the monitoring of the plume migration, to estimate reservoir integrity and support possible leakage notification. This method allows us to optimise the seismic surveys, which should be repeated over time to monitor the evolution of injected CO₂ (Rossi *et al.* 2008; Picotti *et al.* 2012).

A relevant number of cognate studies were made during last several years in operating CO₂ storage sites, e.g. the Sleipner in Norway (Arts *et al.* 2003, 2004a, b; Carcione *et al.* 2006; Chadwick *et al.* 2006) and prospective for CGS sites, such as Atzbach-Schwandenstadt in Austria (Rossi *et al.* 2008; Picotti *et al.* 2012) and Calgary in Canada (Vera 2012) showing similar results: (1) CO₂ injected into the geological storage site can be detected using time-lapse seismic surveys even with low CO₂ saturation values; (2) P-wave

velocity drops quickly from 0 to 20% CO₂ saturation in the reservoir, with slight decrease of velocities at higher saturations; (3) The magnitude of S-wave velocity change is very small in comparison with P-wave velocity variations; (4) The presence of the CO₂ plume could be detected by direct interpretation of seismic sections in the injection zone, but more effectively by performing the difference between the baseline and repeated surveys or considering more sophisticated repeatability metrics such as NMRS. These difference techniques are extremely sensitive for imaging the smallest changes between seismic baseline and repeated seismic sections data and were used to compare seismic datasets before and after CO₂ injection, simulating seismic acquisitions at different times over the same study area (Kragh & Christie 2002).

Shogenov *et al.* (2015, submitted-accepted; 2015, accepted) performed a CO₂ injection-like storage experiment simulated in the laboratory and studied petrophysical alterations in the reservoir rocks caused by geochemical and mineralogical CO₂-fluid-rock interactions. In the present study, for the first time according to our knowledge, the petrophysical alteration effect induced by the CO₂ was incorporated into the numerical seismic modelling methodology. Petrophysical properties of the host rocks before and after the alteration experiment were applied in the modelling. This alteration approach should indicate the importance of implementing this effect in such modelling routine for CGS monitoring and fill the gap in the previous seismic models (Pawar *et al.* 2006).

The uniform model without alteration effect of the offshore oil-bearing structure E6 from the Baltic Sea was presented in Shogenov & Gei (2013). In this paper we updated some properties implemented in the previous study with data from the petrophysical alteration analysis.

DATA AND METHODS

Two different approaches of CO₂ distribution in the hosting rock were applied for the numerical seismic modelling: (i) CO₂ homogeneous saturation of reservoir (uniform model) and (ii) CO₂ plume accumulation (plume model). Therefore, we produced synthetic datasets for four scenarios: (1) uniform model without alteration effect, (2) uniform model with alteration effect, (3) plume model without alteration effect and (4) plume model with alteration effect. Synthetic seismic sections were produced, analysed and compared with the baseline dataset (before injection of CO₂). We considered the first two

scenarios to explore the effectiveness of the seismic technique for CGS monitoring in the long term, when CO₂ has homogeneously spread within the storage reservoir. The third and fourth scenarios present more realistic approaches in short term and involve more complex study (plume shape and inhomogeneous CO₂ saturation).

2D uniform modelling

Figure 2 shows the 2D geological model implemented for the numerical seismic modelling simulations and extrapolated for the interpretation of the E6 seismic section. The well E6-1/84 is located approximately in the middle of the model. The Deimena Reservoir was split, according their specific rock physics properties, into three parts: Reservoir-1, Reservoir-2 and Reservoir-3. Due to shortage of experimental data (only one well drilled in the structure), the three sub-reservoirs were approximated to be homogeneous without vertical or lateral heterogeneity. The Saldus Formation of the Upper Ordovician oil reservoir is shown by 10 meters-thick black coloured layer between the Ordovician and Silurian formations (Fig. 2).

All the layers in the geological model were characterized and populated with specific lithology and measured or computed petrophysical properties recalculated at in-situ conditions (Table 1).

CO₂ plume modelling

A simplified CO₂ plume accumulation model was based on studies of gravity flows within a permeable medium for an axisymmetric geometry (Huppert & Woods 1995; Lyle *et al.* 2005; Bickle *et al.* 2007) and considered field monitoring and

numerical modelling studies of existing offshore storage site (Sleipner, North Sea, e.g. Fornel & Estublier 2013; Zhang & Agarwal 2014). The possible evolution and migration of the CO₂ plume within the reservoir layers in the E6 potential storage site was described at a specific time and with a given amount of injected CO₂. The fluid saturation has been assumed according to the structural, stratigraphic, lithological and petrophysical properties of different reservoir layers (Scenario-3 and Scenario-4; Fig. 3).

Seismic and poro-viscoelastic properties

The seismic parameters of the reservoir layers were computed using properties of the rocks (grain and dry-rock density, ρ_{solid} and ρ_{dry} , respectively, effective porosity and permeability, ϕ and κ , respectively, and P-wave velocity, $V_{P,dry}$) measured on dry-rock samples before and after alteration experiments at the IFP Energies nouvelles (IFPEN) rock physics laboratories (Shogenov *et al.* 2013a, b; Shogenov & Gei 2013; Shogenov *et al.* 2015, submitted-accepted; Shogenov *et al.* 2015, accepted). The measured parameters were coupled with data available in the exploration report for the E6 structure (Andrushenko *et al.* 1985). The measured, reported or estimated data (average from measured and reported for different parts of the reservoir layer) were applied. Estimated ρ_{solid} was used for the Reservoir-1, reported for the Reservoir-2 and measured for the Reservoir-3. Estimated ρ_{dry} , ϕ and κ were applied for the Reservoir-1 and Reservoir-3, and reported for the Reservoir-2. Estimated $V_{P,dry}$ was used for the Reservoir-1 and reported for the Reservoir-2 and Reservoir-3 (Table 1).

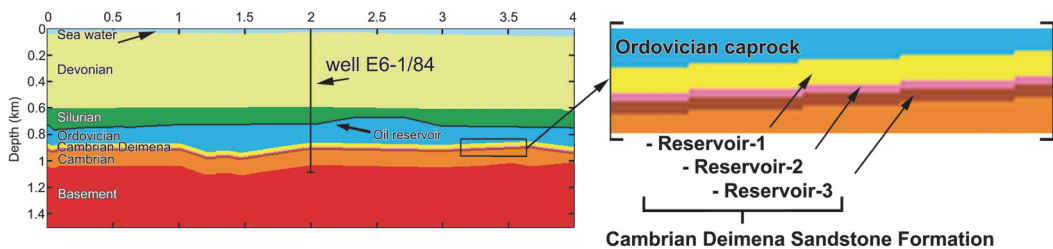


Fig. 2. 2D geological model of the E6 offshore structure implemented for seismic modelling and a magnification of the three reservoirs (modified after Shogenov & Gei 2013).

Table 1. Characteristics and physical properties of the main rock formations shown in the model (Figure 2)

Formation	Lithology	Depth (m)	T (°C)	P (MPa)	ρ_{wet} (kg/m ³)	ϕ_{ef} (%)	κ (mD)	V_P (m/s)	V_S (m/s)	Q_P	Q_S	μ (Gpa)	K_{dry} (Gpa)
Sea water	-	0	10	0.1	1030	-	-	1480	-	-	-	-	-
Devonian	Sandstone	36.5	7	0.8	2226	15	2	2474	1133	66	18	2.86	-
Silurian	Carbonate shales	580	31	6.3	2244	6-16	<0.1	2570	1043	71	16	2.44	-
Ordovician Saldus Fm. (Oil reservoir)	Limestone	702	35	8.4	2342	18	6	2970	1395	95	28	4.56	-
Ordovician (Cap rock)	Carbonate shales	712.5	35	8.6	2540	3	<0.01	2628	1093	74	17	3.04	-
Deimena (Reservoir-1)	Sandstone	848	37	9.3	2341	21	160	2836	1400	250	94	4.59	4.21
Deimena (Reservoir-2)	Sandstone	876	37	9.7	2400	17	60	2873	1349	761	255	4.37	4.00
Deimena (Reservoir-3)	Sandstone	885	37	9.8	2306	25	230	2872	1510	211	87	5.26	4.82
Cambrian	Siltstone	901	38	10	2324	3-18	0.2-23	2746	1675	81	40	6.52	-
Basement	Granite	1018	41	11.2	2675	-	-	5800	3454	362	171	31.9	-

* Depth of the top of the formation in well E6-1/84

All formations except for the Oil reservoir are saturated with brine. Temperature (T) and pressure (P) of the formations top; ρ_{wet} – the bulk density of brine-saturated rock samples; ϕ_{ef} – effective porosity; κ – permeability; V_P and V_S – compressional (P) and shear (S) waves velocities, respectively; Q_P and Q_S – quality factors of P- and S-waves, respectively; μ and K_{dry} – shear and bulk modules of dry rocks, respectively (K_{dry} estimated only for reservoir formations).

For the reservoir rock properties after the alteration experiment we applied results of the petrophysical alteration of the E6 structure for the Reservoir-1 and Reservoir-3 (Shogenov *et al.* 2015, submitted-accepted; Shogenov *et al.* 2015, accepted). Due to lack of samples characterising rock properties change in the Reservoir-2 and the V_{Pdry} change in the Reservoir-1 and Reservoir-3, we have applied alteration results of the identical reservoir samples (with similar properties before the alteration) from the Lithuanian offshore structure E7 located in about 40 km S–W from the E6 structure in the Baltic Sea (Fig. 1, Shogenov *et al.* 2013b; Shogenov *et al.* 2015, submitted-accepted; Shogenov *et al.* 2015, accepted).

For the layers above and below the storage formation we considered experimental P-wave velocities (V_{Pwet}) obtained from published results of active seismic surveys, laboratory measurements of dry and wet samples of the Saldus Formation of the Upper Ordovician oil reservoir from the well E6-1/84 (Andrushenko *et al.* 1985) and reported measurements of more than 2000 rock samples of the northern part of the Baltic sedimentary basin

(Shogenova *et al.* 2010).

Seismic properties of the different formations (Tables 1 & 2; Shogenov & Gei 2013) were computed considering rock physics theories described in the following sections.

Reservoir formation

The velocity and attenuation of compressional seismic waves for the reservoir rocks partially saturated with carbon dioxide were computed with the White's mesoscopic rock physics theory (White 1975). A detailed review of White's theory can be found in Carcione *et al.* (2006) or Picotti *et al.* (2012). This model of attenuation gives realistic seismic properties (P-wave velocity and quality factor) when dry rock moduli, porosity, bulk density, permeability, fluid saturation and the dominant frequency of the seismic signal are provided. The saturation is assumed to be patchy, considering that spherical gas pockets are much larger than solid grains of the sediment but much smaller than the wavelength (White 1975; Carcione *et al.* 2003, 2006; Carcione 2007; Carcione *et al.* 2012).

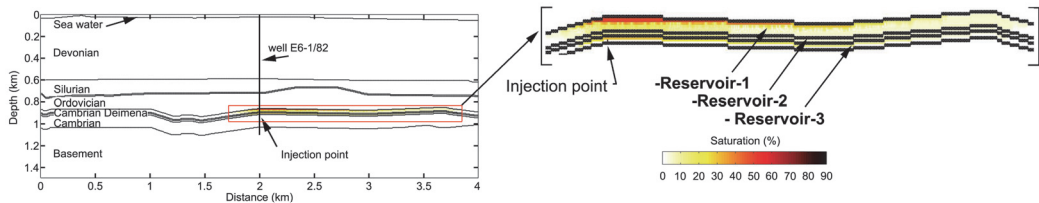


Fig. 3. Plume saturation model of CO₂ injected into the reservoir formation in the E6 structure. Different CO₂ saturation of reservoir formation fluids is indicated. Black lines within the structure are formations borders.

Table 2. Estimated seismic (poro-viscoelastic) properties of the reservoir rock formations after the alteration experiment shown in the seismic model (Figure 2)

Formation	Lithology	ρ_{wet} (kg/m ³)	φ_{ef} (%)	κ (mD)	V_P (m/s)	V_S (m/s)	Q_P	Q_S	μ (Gpa)	K_{dry} (Gpa)
Reservoir-1	Sandstone	2270	23	140	2743	1319	189	68	3.95	3.62
Reservoir-2	Sandstone	2388	16	90	2856	1283	1163	360	3.93	3.61
Reservoir-3	Sandstone	2188	30	280	2735	1415	202	81	4.38	4.01

All reservoir formations are saturated with brine

We applied a fluid substitution procedure to compute the seismic properties of brine-saturated rocks and the same rocks partially saturated with CO₂. Physical properties of the saturating fluids are needed for the modelling. Seismic velocity and density of brine were computed at in situ conditions using Batzle & Wang (1992) empirical relationships. The compressibility and density of CO₂ at in situ pressure and temperature are computed with the Peng-Robinson equation of state (Peng & Robinson 1976; Picotti *et al.* 2012).

Assuming a Poisson's ratio (ν) for unconsolidated sands equal to 0.1 (Gregory 1977), the S-wave velocity of the dry rocks (V_{Sdry}) can be computed using relation provided by White (1965) and Castagna *et al.* (1985):

$$V_{Sdry} = \frac{V_{Pdry}}{1.5} \quad (1)$$

The bulk modulus of the dry rock K_{dry} and the shear modulus μ are computed from:

$$K_{dry} = V_{Pdry}^2 \rho_{dry} - \frac{4}{3} \mu \quad (2)$$

and

$$\mu = V_{Sdry}^2 \rho_{dry} \quad (3)$$

The shear and bulk modulus assume positive values, based on thermodynamic restrictions (Gercek 2007). The Poisson's ratio ν varies between 0 and 0.5 and a value of 0.25 is often assumed (De Waals 1986). The Poisson's ratio of the E6 wet sandstones, ν_{wet} , (Reservoir-1, Reservoir-2 and Reservoir-3) before and after alteration is between 0.31–0.37, within the range of values reported by Gercek (2007) (from 0.4 for unconsolidated sands to values well below 0.05 for tight rocks). The ν could be estimated with equation (e.g. Bacon *et al.* 2003):

$$\nu = 0.5 \frac{3K - 2\mu}{2\mu + 6K} \quad (4)$$

The density of the partially saturated rock is given by:

$$\rho_{wet} = \rho_{solid}(1 - \Phi) + \rho_{fluid} \Phi \quad (5)$$

where ρ_{fluid} is the density of the gas–brine mixture:

$$\rho_{fluid} = \rho_{brine} s_{brine} + \rho_{gas} s_{gas} \quad (6)$$

where s_{brine} and s_{gas} are relative saturations such that $s_{brine} + s_{gas} = 1$.

The S-wave velocities of the partially saturated reservoir rocks are computed with:

$$V_{Swet} = \sqrt{\mu / \rho_{wet}} \quad (7)$$

Since White's theory does not predict any shear dissipation, we describe attenuation with a Zener element according to the theory described in Carcione *et al.* (2012).

Other formations

As mentioned above, properties of the cap rock and underlying layers (Table 1) were obtained from the E6 structure exploration report (Andrushenko *et al.* 1985), when available. The missing parameters were estimated with empirical relations offered by Ludwig *et al.* (1970), Castagna *et al.* (1985, 1993), Saxena (2004) and Brocher (2005) for different rock types as described below.

Average V_{Swet} for the Devonian Sandstone Formation was estimated using reported V_{Pwet} (Andrushenko *et al.* 1985) and empirical equation, derived from laboratory V_P – V_S data for water-saturated sandstones (Castagna *et al.* 1993):

$$V_{Swet} = (0.804 \times V_{Pwet} - 0.856) \cdot 10^3 \text{ (m/s)} \quad (8)$$

The ρ_{wet} of the Devonian sandstones was estimated using Eq. (5), the reported average ρ_{solid} (Shogenova *et al.* 2010) and φ_{ef} (Andrushenko *et al.* 1985) and ρ_{brine} computed at in situ conditions using Batzle & Wang (1992) empirical relationships.

Average V_{Swet} of the Silurian and Ordovician cap rocks (claystones and shales) were estimated using reported V_{Pwet} (Andrushenko *et al.* 1985) and famous in situ 'mudrock line', obtained from relations for shales by Castagna *et al.* (1985):

$$V_{Swet} = (0.862 \times V_{Pwet} - 1.172) \cdot 10^3 \text{ (m/s)} \quad (9)$$

The ρ_{wet} of the Silurian cap rock layer was estimated using polynomial and power-law forms of Gardner *et al.* (1974) velocity–density relationship, presented in Castagna *et al.* (1993):

$$\rho_{wet(shales)} = -0.0261 \times V_{Pwet}^2 + 0.373 \times V_{Pwet} + 1.458 \quad (10)$$

The ρ_{wet} of the Ordovician cap rock layer was estimated using Eq. (5). Rock physical properties (ρ_{solid} and φ) were derived from the reported laboratory data (Andrushenko *et al.* 1985).

The V_{Swet} of the limestone oil reservoir of the Ordovician Formation was estimated with Eq. (7), using μ obtained with Eq. (3) and ρ_{wet} with Eq. (5). The V_{Pdry} , V_{Pwet} , ρ_{dry} , ρ_{solids} , ρ_{fluid} (oil) and ϕ were derived from the reported laboratory data (Andrushenko *et al.* 1985). The V_{Sdry} , necessary for the calculation of μ , was derived using $V_{Pdry}-V_{Sdry}$ theoretical relationship for dry limestones (Saxena 2004):

$$V_{Sdry} = \frac{V_{Pdry}}{1.8} \quad (11)$$

Average V_{Sdry} , μ and V_{Swet} of the Cambrian siltstone layer, underlying the reservoir, were estimated using Eq. (1), (3) and (7), respectively, and the ρ_{wet} , ρ_{dry} , V_{Pdry} were derived from the laboratory measurement data reported in Shogenova *et al.* (2010). The V_{Pwet} was derived from the well E6-1/84 report (Andrushenko *et al.* 1985).

The V_{Pwet} for the basement layer was derived from an average reported laboratory data of measured more than 4000 water-saturated basement samples from the drill cores of Kola Peninsula (Baltic Shield), Ukraine, Caucasus, Urals, Kazakhstan, Transbaikal and Primorsky Krai (Dortman 1992). Average V_{Swet} for the basement was estimated from the V_{Pwet} using a ‘Brocher’s regression fit’ (Brocher 2005):

$$V_{Swet} = 0.7858 - 1.2344 \times V_{Pwet} + 0.7949 \times V_{Pwet}^2 - 0.1238 \times V_{Pwet}^3 + 0.0064 \times V_{Pwet}^4 \quad (\text{km/s}) \quad (12)$$

The ρ_{wet} of the basement layer was derived using a Nafe-Drake relation ‘Nafe-Drake curve’, published by Ludwig *et al.* (1970) for a wide variety of sedimentary and crystalline rock types (for compressional wave velocities between 1.5 and 6.1 km/s):

$$\rho_{wet} = 1.6612 \times V_{Pwet} - 0.4721 \times V_{Pwet}^2 + 0.0671 \times V_{Pwet}^3 - 0.0043 \times V_{Pwet}^4 + 0.000106 \times V_{Pwet}^5 \quad (13)$$

The quality factors (Q) of all the formations except the reservoir were computed from the V_{Pwet} and V_{Swet} by empirical relationships proposed by Waters (1978) and Udias (1999), and given also in Haase & Stewart 2004:

$$Q_s = Q_p \frac{4}{3} \left(\frac{V_s}{V_p} \right)^2 \quad (14)$$

where Q_p is a the P-wave and Q_s is a S-wave quality factors.

Numerical seismic modelling

For the numerical seismic modelling we considered the 2D viscoelastic wave equation,

which was solved with a 4-th order Runge-Kutta time-stepping scheme and the staggered Fourier method to compute the spatial derivatives. This method is noise-free in the dynamic range where regular grids generate artifacts that may have amplitudes similar to those of physical arrivals (Carcione 2007; Picotti *et al.* 2012).

The seismic simulation is performed over a numerical mesh obtained by discretizing the geological model given in Figure 2. A mesh of 240 000 (800 x 300) points with a grid point spacing of 5 m was built. We considered plane-wave simulations, approximating non-migrated zero offset sections, by triggering simultaneously sources, located in each grid point of the upper edge of the numerical mesh. This procedure produces a plane-wave propagating downward. Every time the plane-wave impinges upon the interface between two different formations, it is reflected back to the upper edge of the geological model, coinciding with the sea surface, where the seismic wave-field is recorded at each gridpoint. We computed synthetic seismograms of the baseline and after CO₂ injection considering the homogeneous and plume gas distribution into the reservoir. Specific repeatability metrics – ‘Difference’ and normalized root mean square (NRMS) sections of 4D seismic data were used to qualitatively estimate changes in seismic reflection and to indicate differences, such as phase shifts and amplitude variations in time-lapse datasets (Kragh & Christie 2002; MacBeth *et al.* 2006; Vedanti *et al.* 2009; Lacombe *et al.* 2011; Picotti *et al.* 2012). The source time history is a Ricker wavelet with a dominant frequency of 35 Hz. Absorbing boundary conditions are implemented in absorbing strips of 40 grid-point lengths, located at the bottom and sides of the numerical mesh to damp the wraparound phases.

RESULTS

Seismic properties of the reservoir formations

The bulk density ρ_{wet} decreased in all the range of CO₂ saturation, accompanied with a drastic drop of the V_{Pwet} and acoustic impedance, calculated for the reservoir rocks using the fluid substitution method (Table 3). Moreover, the mesoscopic attenuation showed a peak at about 5% of CO₂ saturation in the reservoir rocks in all reservoir layers (Reservoir-1, Reservoir-2 and Reservoir-3) without and with petrophysical alteration effect with minor differences. The decrease of the P-wave velocity becomes insignificant in the range of 10-50% of CO₂ saturation. After 50% of CO₂ saturation the

V_{Pwet} and V_{Swet} started to increase slightly due to decrease in the bulk density. The velocity drop of the altered rocks (Scenario-2 and Scenario-4; Tables 1–3) is slightly higher if compared with non-altered rocks (Scenario-1 and Scenario-3; Tables 1–3). Figure 4 shows the bulk density, velocities, acoustic impedance and attenuation of Reservoir-1 as a function of CO₂ saturation for the original (initial) and altered core samples.

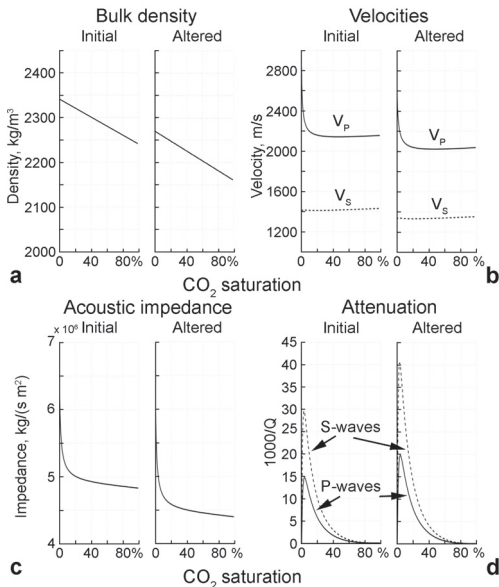


Fig. 4. a) Bulk density, b) P- and S-wave velocities (V_P and V_S respectively), c) acoustic impedance and d) P- and S-wave attenuation ($1000/Q$) in the uppermost layer of reservoir formation (Reservoir-1) of the Cambrian Deimana Formation sandstones versus CO₂ saturation at initial state before injection of CO₂ (without alteration effect) and at altered conditions.

Synthetic seismic sections

Plane-wave datasets

Firstly, we produced synthetic plane-wave seismic section of the E6 offshore structure before CO₂ injection (Fig. 5a; baseline). Then, six seismic sections, reproducing different CO₂ saturation levels (1, 5, 10, 15, 50 and 90%) of the Deimana Formation were computed, considering homogeneous gas saturation (Scenario-1; Fig. 5-sc1-a). We repeated the seismic simulations, taking into account the chemically induced petrophysical alteration effect of the reservoir rocks (Scenario-2; Fig. 5-sc2-a). The modelling provided seismic images of CO₂ storage in the E6 offshore structure at different times over the same area. Plane-wave sections computed considering the modelled CO₂

plume in the E6 structure without and with the petrophysical alteration effect were further produced (Scenario-3; Fig. 5-sc3-a & Scenario-4; Fig. 5-sc4-a, respectively).

The presence of CO₂ in the reservoir layers could be detected by a direct comparison and interpretation of the baseline and repeated synthetic surveys with different CO₂ saturation levels in the Scenario-1 (Fig. 5-sc1-a) and Scenario-2 (Fig. 5-sc2-a), already from 1% saturation. The seismic reflections corresponding to the top and bottom of three reservoirs became stronger with increasing CO₂ saturation showing the best contrast up to 5% of CO₂ saturation. The evolution of the reflection strength increase in the considered sections after 5% of CO₂ saturation became difficult, as all synthetic plane-wave seismic sections in the range of 10–90% of CO₂ saturation for specific scenario look like very similar. A slight variation of time shift or velocity push-down is also detectable on the plane-wave plots for the layers below the reservoir formation. The plane-wave sections of the Scenario-3 (Fig. 5-sc3-a) and 4 (Fig. 5-sc4-a) clearly show the modelled CO₂ plume in the E6 storage site. Seismic reflections of the reservoir rocks with petrophysical alteration effect (Scenario-2 and Scenario-4) showed higher reflectivity in all the cases compared to the Scenario-1 and Scenario-3.

'Difference' and NRMS sections

To monitor the presence of CO₂ within the storage site in more details, the modelled numerical seismic baseline section of the E6 structure was compared with repeated synthetic sections at different CO₂ saturations. 'Difference' and NRMS techniques were applied for each scenario (Fig. 5). In addition, in order to understand the effect of the alteration on the reflectivity of the reservoir, we compared each seismic line without and with petrophysical alteration (Fig. 6). Using 'Difference' and NRMS metrics CO₂ is highly visible since low gas saturation (1%, Fig. 5). However, for saturation higher than 5% the amplitude of the signals delineating the reservoir and the interface below does not vary, similarly to the reflection amplitudes of the reservoirs in the synthetic plane-wave sections.

DISCUSSION

By analysing the changes of the seismic response of the reservoir structure with different CO₂ saturation levels, we clearly monitored the presence of small quantities of CO₂ within the host formation.

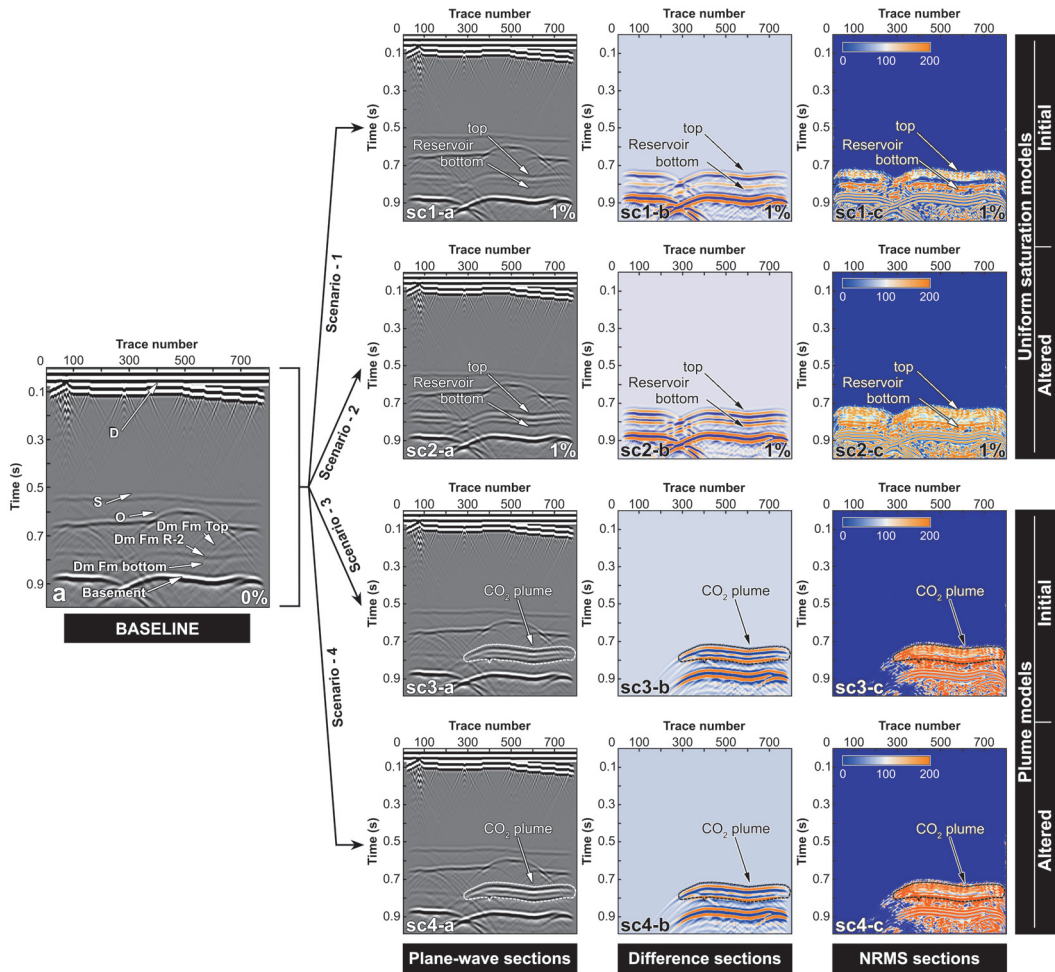


Fig. 5. (a) Baseline synthetic plane-wave section of the E6 structure (before the injection of CO₂). Reflectors of the top of all geological formations (D–Devonian, S–Silurian, O–Ordovician), the top and bottom of the Cambrian Deimena Sandstone Reservoir (Dm Fm) and middle part of the reservoir formation Reservoir-2 (Dm Fm R-2) are indicated; (sc1-a) plane-wave section of Scenario-1 (uniform model without an alteration effect) with 1% CO₂ saturation; ‘Difference’ (sc1-b) and NRMS (sc1-c) sections of the synthetic baseline and the seismic section of Scenario-1 with 1% CO₂; (sc2-a-c) seismic sections of Scenario-2 (uniform model with an alteration effect) with 1% CO₂ saturation; arrows indicate the reservoir top and bottom; (sc3-a-c) seismic sections of Scenario-3 (plume model without an alteration effect); (sc4-a-c) seismic sections of Scenario-4 (plume model with an alteration effect); arrows indicate the CO₂ plume.

This phenomenon is due to changing of seismic velocities, and consequently arrival times, and reflection amplitudes with increasing CO₂ content already from 1% of gas saturation. Therefore, the seismic monitoring of CO₂ injection within the considered E6 offshore structure is effective already from the very first steps of injection. Thus, we confirmed results of previous studies which suggest that accumulations of CO₂ as small as 500 tonnes may be detectable under favourable conditions (Chadwick *et al.* 2006). Pawar *et al.* (2006) presented results from the West

Pearl Queen pilot CO₂ injection project in South Eastern New Mexico, which suggests that surface 3D seismic can detect 2090 tonnes of CO₂ at a depth of 1372 m. But at the same time, results showed that the response of the West Pearl Queen reservoir during the field experiment was significantly different than predicted response based on the pre-injection characterization data. Pawar *et al.* (2006) reported that latest numerical modelling algorithms are not capturing the geochemical interactions, which are important elements in a CGS modelling. In previous studies,

Table 3. Seismic properties of the Deimena Sandstone Formation of the Cambrian Series 3 partially saturated with CO₂

Reservoir sandstones partially saturated with CO ₂	Initial*						Altered¶					
	Fluid saturation			V _P (m/s)	V _S (m/s)	Q _P	Q _S	ρ _{wet} (kg/m ³)	V _P (m/s)	V _S (m/s)	Q _P	Q _S
	Brine (%)	CO ₂ (%)	ρ _{wet} (kg/m ³)									
Reservoir-1	99%	1%	2340	2545	1411	127	52	2269	2443	1334	95	38
	95%	5%	2336	2262	1414	71	37	2264	2151	1337	52	27
	90%	10%	2331	2199	1412	93	51	2259	2084	1333	68	37
	85%	15%	2326	2172	1410	129	72	2253	2055	1331	94	53
	50%	50%	2291	2142	1416	>400	>400	2215	2023	1336	>400	>400
	10%	90%	2251	2152	1428	>400	>400	2171	2034	1349	>400	>400
Reservoir-2	99%	1%	2400	2581	1354	358	131	2387	2543	1286	>400	184
	95%	5%	2397	2236	1356	155	76	2384	2163	1288	219	104
	90%	10%	2393	2153	1356	187	99	2380	2069	1288	259	134
	85%	15%	2389	2116	1356	250	137	2377	2028	1288	341	184
	50%	50%	2362	2067	1361	>400	>400	2351	1972	1293	>400	>400
	10%	90%	2330	2069	1369	>400	>400	2321	1970	1301	>400	>400
Reservoir-3	99%	1%	2305	2644	1523	107	47	2187	2500	1427	102	45
	95%	5%	2300	2410	1527	61	33	2181	2266	1431	59	31
	90%	10%	2295	2356	1524	81	45	2174	2212	1429	78	43
	85%	15%	2288	2332	1523	113	65	2167	2189	1428	109	62
	50%	50%	2247	2311	1531	>400	>400	2118	2173	1439	>400	>400
	10%	90%	2200	2328	1546	>400	>400	2061	2195	1458	>400	>400

* Initial – before the alteration approach (Figs 4; 5-sc1-a-c; 5-sc3-a-c)

¶ Altered – after the alteration approach (Figs 4; 5-sc2-a-c; 5-sc4-a-c)

we estimated and analysed petrophysical, geochemical and mineralogical alterations of the reservoir rocks from the studied E6 structure caused by modelled CO₂ storage (Shogenov *et al.* 2015, submitted-accepted; Shogenov *et al.* 2015, accepted). Thus, here we consider alteration of petrophysical properties of reservoir rocks, induced by CO₂–fluid–rock geochemical and mineralogical interactions (Scenario-2 and Scenario-4). Nevertheless, for simplicity, we implemented the results of the laboratory alteration experiment equally for all CO₂ saturation seismic sections.

The interfaces defining the three units forming the reservoir in the Cambrian Deimena Formation

and the Saldus Formation of the Upper Ordovician oil reservoir (Fig. 2) were impossible to distinguish on the baseline plane-wave seismic section due to relatively low frequency of seismic source (35 Hz) we considered, resulting in a single reflection.

The ‘Difference’ and NRMS sections of the layers overlain reservoir rocks show zero amplitude for two-way travel times (TWT), which are lower than for the top of the reservoir reflection layer. In fact, the reflectors in this upper region of the seismogram are not influenced by the presence of CO₂, which varies the seismic characteristics of the occurring lower reflectors, identifying the top of the reservoir and the ones below (longer TWT).

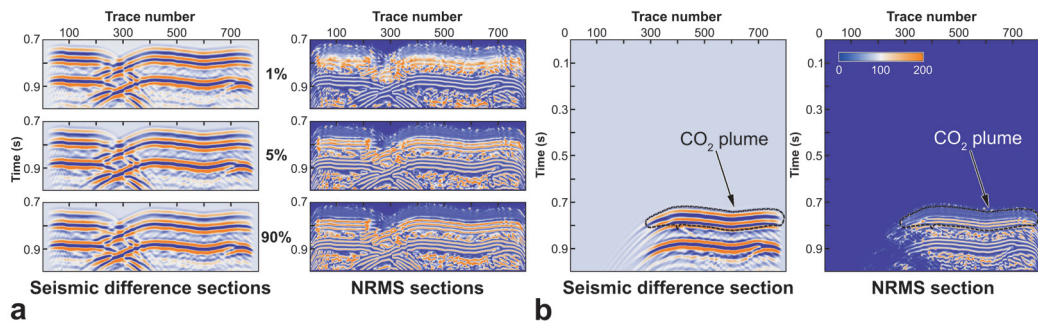


Fig. 6. Impact of the petrophysical alteration on seismic sections. (a) ‘Difference’ sections of the synthetic seismic lines of Scenario-1 (without petrophysical alteration) and Scenario-2 (with petrophysical alteration) with 1%, 5% and 90% CO₂ saturation are presented on the left part. Corresponding NRMS sections are shown on the right part. Seismic sections of the reservoir and underlying rock (b) ‘Difference’ section of the synthetic seismic lines of Scenario-3 and Scenario-4 (left part) and corresponding NRMS section (right part); arrows indicate the CO₂ plume.

This can be seen in e.g. Figure 5-sc1-b and Figure 5-sc1-c.

The decrease of P-wave velocity due to injected CO₂ causes the velocity push-down recognizable in all the synthetic seismic sections for all provided scenarios below the reservoir. This phenomenon is well known and already documented in Arts *et al.* (2000), among others.

Previously published papers based on theoretical and field experimental studies (Domenico 1977; Jain 1987; Rossi *et al.* 2008; Picotti *et al.* 2012; Vera 2012 & Arts *et al.* 2003, 2004a, b; Carcione *et al.* 2006; Chadwick *et al.* 2006, respectively) reported significant drop of the P-wave velocity values of the sandy reservoir rocks between 0 and 20% of CO₂ saturation and slow increase after 30% of CO₂ saturation. Laboratory studies of unconsolidated sands by Domenico (1974, 1976) show that the presence of gas reduces the V_{Pwet} by as much as 30%, while the V_{Swet} is marginally increased (Jain 1987). Vera (2012) reported only 7% as maximum change of the V_{Pwet} . In our study we estimated reduce of the V_{Pwet} in the range of 10–11% between 0–1% of CO₂ saturation and 20–22% of V_{Pwet} decrease in total after 5% of CO₂ saturation (Tables 1–3). The V_{Swet} did not significantly increase compared to the V_{Pwet} (0.2–3%).

The trend of the acoustic impedance, i.e. the product of the bulk density and P-wave velocity, was strongly dominated by the velocity and showed an elbow point approximately where the V_{Pwet} stops to decrease, and a constant gentle decrease for increasing saturations (Fig. 4).

The reflectors affected by the presence of CO₂ rapidly change their characteristics (i.e. amplitude and frequency content) at the beginning of the injection phase, up to 5% of gas saturation, approximately. For increasing CO₂ saturation the influence of the gas on the reflected signals fade down. This phenomenon is explained by the relatively stable V_{Pwet} values in the reservoir rocks after fluid saturation of approximately 5% (Fig. 4; Table 3).

The time-lapse ‘Difference’ and NRMS section techniques supported the visualisation of changes on the seismic datasets and allowed us to monitor possible CO₂ plume evolution within the studied storage site. The comparison of synthetic seismic sections of two corresponding scenarios (Scenario-1 and Scenario-2; Scenario-3 and Scenario-4) clearly showed expected difference in signals for all CO₂ saturation levels (Fig. 6a), proving the effectiveness of the implementation of the petrophysical alterations effect. According to these results, we can suggest the application of the

presented methodology to model the monitoring of CGS within the considered structure (E6) or extrapolation to storage sites with similar stratigraphy, lithology, geochemical and petrophysical properties of the rocks in the Baltic offshore area (Baltic sedimentary basin), as well as in other geological regions.

CONCLUSIONS

The main outcomes of this study can be summarized as follows:

1. For the first time seismic 4D time-lapse numerical modelling based on rock physics studies was applied to monitor possible CO₂ storage in the largest offshore Latvia geological structure E6 in the Baltic Sea.
2. The novelty of the applied approach was the coupling of the chemically induced petrophysical alteration effect of CO₂ hosting rocks measured in laboratory with time-lapse numerical seismic modelling.
3. Synthetic seismic sections were produced from synthetic datasets and compared with baseline section within four scenarios: (1) uniform model without alteration effect, (2) uniform model with alteration effect, (3) plume model without alteration effect and (4) plume model with alteration effect.
4. The presence of CO₂ in the Deimena Reservoir Formation of the Cambrian Series 3 in the E6 offshore structure could be indicated by direct interpretation of the synthetic plane-wave seismic sections and more efficiently with ‘Difference’ and NRMS sections, allowing to determine time-lapse differences between the baseline and CO₂ plume models.
5. The implemented petrophysical alteration effect is clearly detectable on the ‘Difference’ and NRMS sections, showing the highest difference on seismic sections with 1% of CO₂ saturation, decreasing with increase of CO₂ content. The integration of the results of the CO₂ injection-like alteration experiment increased the reliability of the seismic modelling.
6. P-wave velocity decreased for the CO₂ saturation range 0–50% with drastic drop of values between 0 and 5%. Between 50–100% of saturation minor increase of P-wave velocity was determined due to the bulk density decrease.
7. Time shift or push-down effect of reflectors below CO₂ storage area was observed.

8. This study:

- demonstrated the ability of the applied time-lapse rock physics and seismic methods to monitor the presence of the injected CO₂ within the considered E6 offshore oil-bearing structure since the beginning of the injection
- shows effectiveness of the seismic surveys to detect CO₂ injected into the deep aquifer formations even with low CO₂ saturation values according to changes in amplitude and two-way travel times in the presence of CO₂
- has significant importance for developing an optimal seismic monitoring plan in the studied area and other areas with similar geological, lithological and petrophysical parameters.

This study was funded by EU FP7 Marie Curie Research Training Network 'Quantitative Estimation of Earth's Seismic Sources and Structure' (QUEST), Contract No. 238007, hosted by OGS (Trieste, Italy), Estonian targeted funding programmes (project IUT19-22) and is a part of K. Shogenov PhD research. We would like to thank Daniel Sopher (Uppsala University) for grammar editing.

REFERENCES

Andrushenko, J., Vzosek, R., Krochka, V. *et al.* 1985. *Report on the results of drilling and geological and geophysical studies in the exploration well E6-1/84*. Unpublished exploration report of E6-1/84 offshore well. Latvian Environmental, Geology and Meteorology Centre (LEGMC). Latvia, Riga (In Russian).

Arts, R., Brevik, I., Eiken, O., Sollie, R., Causse, E., & van der Meer, B. 2000. Geophysical methods for monitoring marine aquifer CO₂ storage - Sleipner experiences. In: Williams, D., Durie, B., McMullan, P., Paulson, C., Smith, A. (eds). *Proceeding of the 5th International Conference on Greenhouse Control Technologies*, Cairns, 366–371.

Arts, R., Eiken, O., Chadwick, R.A., Zweigel, P., Van der Meer, L. & Zinszner, B. 2003. Monitoring of CO₂ injected at Sleipner using time lapse seismic data. In: Gale, J. & Kaya, Y. (eds). *Greenhouse Gas Control Technologies*, Elsevier, Oxford, 347–352.

Arts, R., Eiken, O., Chadwick, R.A., Zweigel, P., van der Meer, L. & Zinszner, B. 2004a. Monitoring of CO₂ injected at Sleipner using time-lapse seismic data. *Energy*, Elsevier Science Ltd, Oxford, **29**, 1383–1392.

Arts, R., Eiken, O., Chadwick, R.A., Zweigel, P., Van der Meer, L. & Kirby, G.A. 2004b. Seismic monitoring at the Sleipner underground CO₂ storage site (North Sea). In: Baines, S. & Worden, R.J. (eds). *Geological Storage for CO₂ Emissions Reduction*. Geological Society, London, Special Publications, **233**, 181–191.

Arts, R., Chadwick, A., Eiken, O., Thibeau, S. & Nooner, S. 2008. Ten years of experience of monitoring CO₂ injection in the Utsira Sand at Sleipner, offshore Norway. *First break*, **26**, 65–72.

Bachu, S., Bonijoly, D., Bradshaw, J., Burruss, R., Holloway, S., Christensen, N.P. & Mathiassen, O.M. 2007. CO₂ storage capacity estimation: Methodology and gaps. *International Journal of Greenhouse Gas Control*, **1(4)**, 430–443.

Bacon, M., Simm, R. & Redshaw, T. 2003. *3-D Seismic Interpretation*. Cambridge, New York, Melbourne, Cambridge University Press. ISBN 0 521 79203 7.

Batzle, M. & Wang, Z. 1992. Seismic properties of pore fluids. *Geophysics*, **57**, 1396–1408.

Bickle, M., Chadwick, A., Huppert, H.E., Hallworth, M. & Lyle, S. 2007. Modelling carbon dioxide accumulation at Sleipner: Implications for underground carbon storage. *Earth and Planetary Science Letters*, **255**, 164–176.

Brocher, T.M. 2005. Empirical relations between elastic wave speeds and density in the Earth's crust. *Bulletin of the Seismological Society of America*, **95**, 2081–2092.

Carcione, J.M., Helle, H.B. & Pham, N.H. 2003. White's model for wave propagation in partially saturated rocks: Comparison with poroelastic numerical experiments. *Geophysics*, **68**, 1389–1398.

Carcione, J.M., Picotti, S., Gei, D. & Rossi, G. 2006. Physics and seismic modeling for monitoring CO₂ storage. *Pure and applied geophysics*, **163**, 175–207.

Carcione, J.M. 2007. Wave fields in real media: wave propagation in anisotropic, anelastic, porous and electromagnetic media. 2nd edition, revised and extended. *Handbook of Geophysical Exploration*, Elsevier, Amsterdam, **38**.

Carcione, J.M., Gei, D., Picotti, S. & Michelini, A. 2012. Crosshole electromagnetic and seismic modeling for CO₂ detection and monitoring in a saline aquifer. *Journal of Petroleum Science and Engineering*,

- <http://dx.doi.org/10.1016/j.petrol.2012.03.018>, **100**, 162–172.
- Castagna, J.P., Batzle, M.L. & Eastwood, R.L. 1985. Relationships between compressional-wave and shear-wave velocities in clastic silicate rocks. *Geophysics*, **50**, 571–581.
- Castagna, J.P. Batzle, M. & Kan, T. 1993. Rock Physics - The Link Between Rock Properties and AVO Response. In: Castagna, J.P. & Backus, M. eds. *Offset-Dependent Reflectivity—Theory and Practice of AVO Analysis*, DOI:10.1190/1.9781560802624, 135–171.
- Chadwick, A., Arts, R., Eiken, O., Williamson, P. & Williams, G. 2006. Geophysical monitoring of the CO₂ plume at Sleipner, North Sea: an outline review. In: Lombardi, S., Altunina, L.K. & Beaubien, S.E. (eds.). *Advances in the geological storage of carbon dioxide: international approaches to reduce anthropogenic greenhouse gas emissions. NATO Science Series IV: Earth and Environmental Sciences*, Dordrecht, Netherlands, Springer, 303–314.
- De Waals, J.A. 1986. *On the rate type compaction behaviour of sandstone reservoir rock*. PhD thesis, Delft University of Technology, The Netherlands.
- Domenico, S.N. 1974. Effect of water saturation on seismic reflectivity of sand reservoirs encased in shale. *Geophysics*, **39**, 759–769.
- Domenico, S.N. 1976. Effect of brine-gas mixture on velocity in an unconsolidated sand reservoir. *Geophysics*, **41**, 882–894.
- Domenico, S.N. 1977. Elastic properties of unconsolidated porous sand reservoirs. *Geophysics*, **42**, 1339–1368.
- Dortman, N.B. (ed.) 1992. *Petrophysics. A Handbook*. Book 1. Rocks and Minerals. Nedra, Moscow (in Russian).
- Fornel, A. & Estublier, A. 2013. To a dynamic update of the Sleipner CO₂ storage geological model using 4D seismic data. *Energy Procedia*, Elsevier, DOI:10.1016/j.egypro.2013.06.401, **37**, 4902–4909.
- Gardner, G.H.F., Gardner, L.W. & Gregory, A.R. 1974. Formation velocity and density – The diagnostic basics for stratigraphic traps. *Geophysics*, **39**, 770–780.
- Gercek, H. 2007. Poisson's ratio values for rocks. *International Journal of Rock Mechanics and Mining Sciences*, Elsevier, **44(1)**, 1–13.
- Gregory, A.R. 1977. Fluid saturation effects on dynamic elastic properties of sedimentary rocks. *Geophysics*, **41**, 895–921.
- Grigelis, A. 2011. Research of the bedrock geology of the Central Baltic Sea. *Baltica*. http://www.gamtostyrimai.lt/uploads/publications/docs/82_0252d92099d58df467d52315b52c81c3.pdf, **24(1)**, 1–12.
- Haase, A. & Stewart, R. 2004. Attenuation estimates from vsp and log data. 74th Annual International Meeting, *SEG Expanded Abstracts*, 2497–2500.
- Holloway, S. 2002. Underground sequestration of carbon dioxide - a viable greenhouse gas mitigation option. *Proceedings of the 5th International Symposium on CO₂ Fixation and Efficient Utilization of Energy and the 4th International World Energy System Conference*, Tokyo Institute of Technology, Tokyo, Japan, 4–6 March 2002, 373–380.
- Huppert, H.E. & Woods, A.W. 1995. Gravity flows in porous layers. *Journal of Fluid Mechanics*, **292**, 55–69.
- IEA (International Energy Agency) 2004. *Prospects for CO₂ Capture and Storage*. IEA/OECD, Paris, France.
- IEA (International Energy Agency) 2013. *CO₂ Emissions from Fuel Combustion. Highlights*. IEA/OECD, Paris, France.
- IPCC (Intergovernmental Panel on Climate Change) 2005. *IPCC Special Report on Carbon Dioxide Capture and Storage. Prepared by Working Group III of the Intergovernmental Panel on Climate Change* [Metz, B., Davidson, O., de Coninck, H.C., Loos, M. & Meyer, L. A. (eds.)]. Cambridge University Press, Cambridge, United Kingdom and New York, NY, USA.
- IPCC (Intergovernmental Panel on Climate Change) 2013. Working Group I Contribution to the IPCC Fifth Assessment Report, Climate Change 2013: The Physical Science Basis, Summary for Policy Makers. Available at: www.ipcc.ch/.
- Jain, S. 1987. Amplitude-vs-offset analysis: a review with references to application in western Canada. *Canadian Society of Exploration Geophysicists Journal*, **23**, 27–36.
- Kragh, E. & Christie, P. 2002. Seismic repeatability, normalized RMS, and predictability. Society of Exploration Geophysicists, *The Leading Edge*, **21(7)**, 640–647.

- Lacombe, C.H., Campbell, S. & White, S. 2011. Improvements in 4D Seismic Processing -Foinaven 4 Years On. *Extended Abstract. 73rd EAGE Conference & Exhibition incorporating SPE EUROPEC 2011*, 23–26 May 2011, Vienna, Austria.
- Ludwig, W.J., Nafe, J.E. & Drake, C.L. 1970. Seismic refraction. *The Sea*, Maxwell, A.E. (Ed.), Wiley-Interscience, New York, **4**, 53–84.
- Lyle, S., Huppert, H.E., Hallworth, M., Bickle, M. & Chadwick, A. 2005. Axisymmetric gravity currents in a porous medium. *Journal of Fluid Mechanics*, **543**, 293–302.
- MacBeth, C., Stammeijer, J. & Omerod, M. 2006. Seismic monitoring of pressure depletion evaluated for a United Kingdom continental-shelf gas reservoir. *Geophysical Prospecting*, DOI: 10.1111/j.1365-247
- National Research Council 2010. *Ocean Acidification: A National Strategy to Meet the Challenges of a Changing Ocean*. Washington, DC. The National Academies Press.
- Pawar, R.J., Warpinski, N.R., Lorenz, J.C., Benson, R.D., Grigg, R.B., Stubbs, B.A., Stauffer, P.H., Krumhansl, J.P. & Cooper, S.P. 2006. Overview of a CO₂ sequestration field test in the West Pearl Queen reservoir, New Mexico: The American Association of Petroleum Geologists/Division of Environmental Geosciences. *Environmental Geosciences*, **13(3)**, 163–180.
- Peng, D.Y., & Robinson, D.B. 1976. A new two-constant equation of state. *Industrial & Engineering Chemistry Fundamentals*, **15(1)**, 59–64.
- Picotti, S., Carcione, J.M., Gei, D., Rossi, G. & Santos, J.E. 2012. Seismic modeling to monitor CO₂ geological storage: The Atzbach-Schwanenstadt gas field. *Journal of Geophysical Research*, B06103, DOI: 10.1029/2011JB008540, **117(6)**.
- Rossi, G., Gei, D., Picotti, S. & Carcione, J.M. 2008. CO₂ storage at the Atzbach-Schwanenstadt gas field: a seismic monitoring feasibility study. *First Break*, **26**, 45–51.
- Saxena, V. 2004. Role of associated minerals and porosity in Vp-Vs response for sandstone and limestone. The paper was prepared for presentation at the International Symposium of the Society of Core Analysts held in Abu Dhabi, UAE, 5-9 October, 2004. SCA2004-46, 1–7.
- Shogenov, K. & Gei, D. 2013. Seismic numerical modeling to monitor CO₂ storage in the Baltic Sea offshore structure. *Extended Abstract. EAGE*, ID 16848, Tu-P08-13, 10-13 June 2013, London, UK, DOI: 10.3997/2214-4609.20130631, 1–4.
- Shogenov, K., Shogenova, A. & Vizika-Kavvadias, O. 2013a. Petrophysical properties and capacity of prospective structures for geological storage of CO₂ onshore and offshore Baltic. *Energy Procedia*, Elsevier, DOI:10.1016/j.egypro.2013.06.417, **37**, 5036–5045.
- Shogenov, K., Shogenova, A. & Vizika-Kavvadias, O. 2013b. Potential structures for CO₂ geological storage in the Baltic Sea: case study offshore Latvia. *Bulletin of the Geological Society of Finland*, ISSN: 0367-5211, **85(1)**, 65–81.
- Shogenov, K., Shogenova, A., Vizika-Kavvadias, O. & Nauroy, J.F. (2015 submitted-accepted). Experimental modeling of CO₂-fluid-rock interaction: evolution of the composition and properties of host rocks in the Baltic Region. *Earth and Space Science*, AGU, XX–XX.
- Shogenov, K., Shogenova, A., Vizika-Kavvadias, O. & Nauroy, J.F. (2015 accepted). Reservoir quality and petrophysical properties of Cambrian sandstones and their changes during the experimental modelling of CO₂ storage in the Baltic Basin. *Estonian Journal of Earth Science*, **64(3)**, XX–XX.
- Shogenova, A., Sliupa, S., Vaher, R., Shogenov, K. & Pomeranceva, R. 2009a. The Baltic Basin: structure, properties of reservoir rocks and capacity for geological storage of CO₂. Tallinn: Estonian Academy Publishers. *Estonian Journal of Earth Sciences*, **58(4)**, 259–267.
- Shogenova, A., Šliupa, S., Shogenov, K., *et al.* 2009b. Possibilities for geological storage and mineral trapping of industrial CO₂ emissions in the Baltic region. *Energy Procedia*, Elsevier, **1**, 2753–2760.
- Shogenova, A., Kleesment, A., Shogenov, K., Põldvere, A. & Jõelet, A. 2010. Composition and properties of Estonian Palaeozoic and Ediacaran sedimentary rocks. 72nd EAGE Conference & Exhibition incorporating SPE EUROPEC 2010, 14-17 June 2010, Barcelona. EAGE, The Netherlands, 1–5.
- Shogenova, A., Shogenov, K., Vaher, R. *et al.* 2011a. CO₂ geological storage capacity analysis in Estonia and neighboring regions. *Energy Procedia*, **4**, 2785–2792.

- Shogenova, A., Shogenov, K., Pomeranceva, R., Nulle, I., Neele, F. & Hendriks, C. 2011b. Economic modelling of the capture–transport–sink scenario of industrial CO₂ emissions: the Estonian–Latvian cross-border case study. *Energy Procedia*, Elsevier, The Netherlands, **4**, 2385–2392.
- Sliaupa, S., Shogenova, A., Shogenov, K., Sliapiene, R., Zabele, A. & Vaher, R. 2008. Industrial carbon dioxide emissions and potential geological sinks in the Baltic States. *Oil Shale*, **25**(4), 465–484.
- Šliaupa, S., Lojka, R., Tasáryová, Z. *et al.* 2013. CO₂ Storage Potential Of Sedimentary Basins of Slovakia, The Czech Republic, Poland, And Baltic States. *Geological Quarterly*, **2**, 219–232.
- Vedanti, N., Pathak, A., Srivastava, R.P. & Dimri, V.P. 2009. Time lapse (4D) seismic: some case studies. *e-Journal Earth Science India*, <http://www.earthscienceindia.info/>, ISSN: 0974-8350, **4**, 230–248.
- Vera, C.V. 2012. *Seismic modelling of CO₂ in a sandstone aquifer*. MSc Thesis, University of Calgary, <http://hdl.handle.net/1880/48934>.
- Udias, A. 1999. *Principles of seismology*. Cambridge University Press.
- USEPA (U.S. Environmental Protection Agency) 2013. *Causes of climate change*. Washington, D.C., U.S. Environmental Protection Agency Web site, accessed February 22, 2013, at <http://www.epa.gov/climatechange/science/causes.html>.
- USGS CSRA Team (U.S. Geological Survey Geologic Carbon Dioxide Storage Resources Assessment Team) 2013. *National assessment of geologic carbon dioxide storage resources*. Results: U.S. Geological Survey Circular 1386, <http://pubs.usgs.gov/circ/1386/>.
- Waters, K. 1978. *Reflection Seismology. A tool for energy resource exploration*. John Wiley & Sons, New York, NY.
- White, J. E., 1965, Seismic waves: Radiation, transmission and attenuation: McGraw-Hill Book Co.
- White, J.E. 1975. Computed seismic speeds and attenuation in rocks with partial gas saturation. *Geophysics*, **40**, 224–232.
- Zhang, Z. & Agarwal, R. 2014. Numerical simulation and optimization of Sleipner carbon sequestration project. *International Journal of Engineering & Technology*, DOI:10.14419/ijet.v3i1.1439, **3**(1), 1–13.

**DISSERTATIONS DEFENDED AT
TALLINN UNIVERSITY OF TECHNOLOGY ON
NATURAL AND EXACT SCIENCES**

1. **Olav Kongas**. Nonlinear Dynamics in Modeling Cardiac Arrhythmias. 1998.
2. **Kalju Vanatalu**. Optimization of Processes of Microbial Biosynthesis of Isotopically Labeled Biomolecules and Their Complexes. 1999.
3. **Ahto Buldas**. An Algebraic Approach to the Structure of Graphs. 1999.
4. **Monika Drews**. A Metabolic Study of Insect Cells in Batch and Continuous Culture: Application of Chemostat and Turbidostat to the Production of Recombinant Proteins. 1999.
5. **Eola Valdre**. Endothelial-Specific Regulation of Vessel Formation: Role of Receptor Tyrosine Kinases. 2000.
6. **Kalju Lott**. Doping and Defect Thermodynamic Equilibrium in ZnS. 2000.
7. **Reet Koljak**. Novel Fatty Acid Dioxygenases from the Corals *Plexaura homomalla* and *Gersemia fruticosa*. 2001.
8. **Anne Paju**. Asymmetric oxidation of Prochiral and Racemic Ketones by Using Sharpless Catalyst. 2001.
9. **Marko Vendelin**. Cardiac Mechanoenergetics *in silico*. 2001.
10. **Pearu Peterson**. Multi-Soliton Interactions and the Inverse Problem of Wave Crest. 2001.
11. **Anne Menert**. Microcalorimetry of Anaerobic Digestion. 2001.
12. **Toomas Tiivel**. The Role of the Mitochondrial Outer Membrane in *in vivo* Regulation of Respiration in Normal Heart and Skeletal Muscle Cell. 2002.
13. **Olle Hints**. Ordovician Scolecodonts of Estonia and Neighbouring Areas: Taxonomy, Distribution, Palaeoecology, and Application. 2002.
14. **Jaak Nõlvak**. Chitinozoan Biostratigraphy in the Ordovician of Baltoscandia. 2002.
15. **Liivi Kluge**. On Algebraic Structure of Pre-Operad. 2002.
16. **Jaanus Lass**. Biosignal Interpretation: Study of Cardiac Arrhythmias and Electromagnetic Field Effects on Human Nervous System. 2002.
17. **Janek Peterson**. Synthesis, Structural Characterization and Modification of PAMAM Dendrimers. 2002.
18. **Merike Vaher**. Room Temperature Ionic Liquids as Background Electrolyte Additives in Capillary Electrophoresis. 2002.
19. **Valdek Mikli**. Electron Microscopy and Image Analysis Study of Powdered Hardmetal Materials and Optoelectronic Thin Films. 2003.
20. **Mart Viljus**. The Microstructure and Properties of Fine-Grained Cermets. 2003.

21. **Signe Kask**. Identification and Characterization of Dairy-Related *Lactobacillus*. 2003
22. **Tiiu-Mai Laht**. Influence of Microstructure of the Curd on Enzymatic and Microbiological Processes in Swiss-Type Cheese. 2003.
23. **Anne Kuusksalu**. 2–5A Synthetase in the Marine Sponge *Geodia cydonium*. 2003.
24. **Sergei Bereznev**. Solar Cells Based on Polycrystalline Copper-Indium Chalcogenides and Conductive Polymers. 2003.
25. **Kadri Kriis**. Asymmetric Synthesis of C₂-Symmetric Bimorpholines and Their Application as Chiral Ligands in the Transfer Hydrogenation of Aromatic Ketones. 2004.
26. **Jekaterina Reut**. Polypyrrole Coatings on Conducting and Insulating Substrates. 2004.
27. **Sven Nõmm**. Realization and Identification of Discrete-Time Nonlinear Systems. 2004.
28. **Olga Kijatkina**. Deposition of Copper Indium Disulphide Films by Chemical Spray Pyrolysis. 2004.
29. **Gert Tamberg**. On Sampling Operators Defined by Rogosinski, Hann and Blackman Windows. 2004.
30. **Monika Übner**. Interaction of Humic Substances with Metal Cations. 2004.
31. **Kaarel Adamberg**. Growth Characteristics of Non-Starter Lactic Acid Bacteria from Cheese. 2004.
32. **Imre Vallikivi**. Lipase-Catalysed Reactions of Prostaglandins. 2004.
33. **Merike Peld**. Substituted Apatites as Sorbents for Heavy Metals. 2005.
34. **Vitali Syritski**. Study of Synthesis and Redox Switching of Polypyrrole and Poly(3,4-ethylenedioxythiophene) by Using *in-situ* Techniques. 2004.
35. **Lee Põllumaa**. Evaluation of Ecotoxicological Effects Related to Oil Shale Industry. 2004.
36. **Riina Aav**. Synthesis of 9,11-Secosterols Intermediates. 2005.
37. **Andres Braunbrück**. Wave Interaction in Weakly Inhomogeneous Materials. 2005.
38. **Robert Kitt**. Generalised Scale-Invariance in Financial Time Series. 2005.
39. **Juss Pavelson**. Mesoscale Physical Processes and the Related Impact on the Summer Nutrient Fields and Phytoplankton Blooms in the Western Gulf of Finland. 2005.
40. **Olari Ilison**. Solitons and Solitary Waves in Media with Higher Order Dispersive and Nonlinear Effects. 2005.
41. **Maksim Säkki**. Intermittency and Long-Range Structurization of Heart Rate. 2005.
42. **Enli Kiipli**. Modelling Seawater Chemistry of the East Baltic Basin in the Late Ordovician–Early Silurian. 2005.

43. **Igor Golovtsov**. Modification of Conductive Properties and Processability of Polyparaphenylene, Polypyrrole and polyaniline. 2005.
44. **Katrin Laos**. Interaction Between Furcellaran and the Globular Proteins (Bovine Serum Albumin β -Lactoglobulin). 2005.
45. **Arvo Mere**. Structural and Electrical Properties of Spray Deposited Copper Indium Disulphide Films for Solar Cells. 2006.
46. **Sille Ehala**. Development and Application of Various On- and Off-Line Analytical Methods for the Analysis of Bioactive Compounds. 2006.
47. **Maria Kulp**. Capillary Electrophoretic Monitoring of Biochemical Reaction Kinetics. 2006.
48. **Anu Aaspõllu**. Proteinases from *Vipera lebetina* Snake Venom Affecting Hemostasis. 2006.
49. **Lyudmila Chekulayeva**. Photosensitized Inactivation of Tumor Cells by Porphyrins and Chlorins. 2006.
50. **Merle Uudsemaa**. Quantum-Chemical Modeling of Solvated First Row Transition Metal Ions. 2006.
51. **Tagli Pitsi**. Nutrition Situation of Pre-School Children in Estonia from 1995 to 2004. 2006.
52. **Angela Ivask**. Luminescent Recombinant Sensor Bacteria for the Analysis of Bioavailable Heavy Metals. 2006.
53. **Tiina Lõugas**. Study on Physico-Chemical Properties and Some Bioactive Compounds of Sea Buckthorn (*Hippophae rhamnoides* L.). 2006.
54. **Kaja Kasemets**. Effect of Changing Environmental Conditions on the Fermentative Growth of *Saccharomyces cerevisiae* S288C: Auxo-accelerostat Study. 2006.
55. **Ildar Nisamedtinov**. Application of ^{13}C and Fluorescence Labeling in Metabolic Studies of *Saccharomyces* spp. 2006.
56. **Alar Leibak**. On Additive Generalisation of Voronoï's Theory of Perfect Forms over Algebraic Number Fields. 2006.
57. **Andri Jagomägi**. Photoluminescence of Chalcopyrite Tellurides. 2006.
58. **Tõnu Martma**. Application of Carbon Isotopes to the Study of the Ordovician and Silurian of the Baltic. 2006.
59. **Marit Kauk**. Chemical Composition of CuInSe_2 Monograin Powders for Solar Cell Application. 2006.
60. **Julia Kois**. Electrochemical Deposition of CuInSe_2 Thin Films for Photovoltaic Applications. 2006.
61. **Ilona Oja Açıık**. Sol-Gel Deposition of Titanium Dioxide Films. 2007.
62. **Tiia Anmann**. Integrated and Organized Cellular Bioenergetic Systems in Heart and Brain. 2007.
63. **Katrin Trummal**. Purification, Characterization and Specificity Studies of Metalloproteinases from *Vipera lebetina* Snake Venom. 2007.

64. **Gennadi Lessin.** Biochemical Definition of Coastal Zone Using Numerical Modeling and Measurement Data. 2007.
65. **Enno Pais.** Inverse problems to determine non-homogeneous degenerate memory kernels in heat flow. 2007.
66. **Maria Borissova.** Capillary Electrophoresis on Alkylimidazolium Salts. 2007.
67. **Karin Valmsen.** Prostaglandin Synthesis in the Coral *Plexaura homomalla*: Control of Prostaglandin Stereochemistry at Carbon 15 by Cyclooxygenases. 2007.
68. **Kristjan Piirimäe.** Long-Term Changes of Nutrient Fluxes in the Drainage Basin of the Gulf of Finland – Application of the PolFlow Model. 2007.
69. **Tatjana Dedova.** Chemical Spray Pyrolysis Deposition of Zinc Sulfide Thin Films and Zinc Oxide Nanostructured Layers. 2007.
70. **Katrin Tomson.** Production of Labelled Recombinant Proteins in Fed-Batch Systems in *Escherichia coli*. 2007.
71. **Cecilia Sarmiento.** Suppressors of RNA Silencing in Plants. 2008.
72. **Vilja Mardla.** Inhibition of Platelet Aggregation with Combination of Antiplatelet Agents. 2008.
73. **Maie Bachmann.** Effect of Modulated Microwave Radiation on Human Resting Electroencephalographic Signal. 2008.
74. **Dan Hüvonen.** Terahertz Spectroscopy of Low-Dimensional Spin Systems. 2008.
75. **Ly Villo.** Stereoselective Chemoenzymatic Synthesis of Deoxy Sugar Esters Involving *Candida antarctica* Lipase B. 2008.
76. **Johan Anton.** Technology of Integrated Photoelasticity for Residual Stress Measurement in Glass Articles of Axisymmetric Shape. 2008.
77. **Olga Volobujeva.** SEM Study of Selenization of Different Thin Metallic Films. 2008.
78. **Artur Jõgi.** Synthesis of 4'-Substituted 2,3'-dideoxynucleoside Analogues. 2008.
79. **Mario Kadastik.** Doubly Charged Higgs Boson Decays and Implications on Neutrino Physics. 2008.
80. **Fernando Pérez-Caballero.** Carbon Aerogels from 5-Methylresorcinol-Formaldehyde Gels. 2008.
81. **Sirje Vaask.** The Comparability, Reproducibility and Validity of Estonian Food Consumption Surveys. 2008.
82. **Anna Menaker.** Electrosynthesized Conducting Polymers, Polypyrrole and Poly(3,4-ethylenedioxythiophene), for Molecular Imprinting. 2009.
83. **Lauri Ilison.** Solitons and Solitary Waves in Hierarchical Korteweg-de Vries Type Systems. 2009.
84. **Kaia Ernits.** Study of In₂S₃ and ZnS Thin Films Deposited by Ultrasonic Spray Pyrolysis and Chemical Deposition. 2009.

85. **Veljo Sinivee**. Portable Spectrometer for Ionizing Radiation “Gammamapper”. 2009.
86. **Jüri Virkepu**. On Lagrange Formalism for Lie Theory and Operadic Harmonic Oscillator in Low Dimensions. 2009.
87. **Marko Piirsoo**. Deciphering Molecular Basis of Schwann Cell Development. 2009.
88. **Kati Helmja**. Determination of Phenolic Compounds and Their Antioxidative Capability in Plant Extracts. 2010.
89. **Merike Sõmera**. Sobemoviruses: Genomic Organization, Potential for Recombination and Necessity of P1 in Systemic Infection. 2010.
90. **Kristjan Laes**. Preparation and Impedance Spectroscopy of Hybrid Structures Based on CuIn_3Se_5 Photoabsorber. 2010.
91. **Kristin Lippur**. Asymmetric Synthesis of 2,2'-Bimorpholine and its 5,5'-Substituted Derivatives. 2010.
92. **Merike Luman**. Dialysis Dose and Nutrition Assessment by an Optical Method. 2010.
93. **Mihhail Berezovski**. Numerical Simulation of Wave Propagation in Heterogeneous and Microstructured Materials. 2010.
94. **Tamara Aid-Pavlidis**. Structure and Regulation of BDNF Gene. 2010.
95. **Olga Bragina**. The Role of Sonic Hedgehog Pathway in Neuro- and Tumorigenesis. 2010.
96. **Merle Randrüüt**. Wave Propagation in Microstructured Solids: Solitary and Periodic Waves. 2010.
97. **Marju Laars**. Asymmetric Organocatalytic Michael and Aldol Reactions Mediated by Cyclic Amines. 2010.
98. **Maarja Grossberg**. Optical Properties of Multinary Semiconductor Compounds for Photovoltaic Applications. 2010.
99. **Alla Maloverjan**. Vertebrate Homologues of Drosophila Fused Kinase and Their Role in Sonic Hedgehog Signalling Pathway. 2010.
100. **Priit Pruunsild**. Neuronal Activity-Dependent Transcription Factors and Regulation of Human *BDNF* Gene. 2010.
101. **Tatjana Knjazeva**. New Approaches in Capillary Electrophoresis for Separation and Study of Proteins. 2011.
102. **Atanas Katerski**. Chemical Composition of Sprayed Copper Indium Disulfide Films for Nanostructured Solar Cells. 2011.
103. **Kristi Timmo**. Formation of Properties of CuInSe_2 and $\text{Cu}_2\text{ZnSn}(\text{S,Se})_4$ Monograin Powders Synthesized in Molten KI. 2011.
104. **Kert Tamm**. Wave Propagation and Interaction in Mindlin-Type Microstructured Solids: Numerical Simulation. 2011.
105. **Adrian Popp**. Ordovician Proetid Trilobites in Baltoscandia and Germany. 2011.

106. **Ove Pärn**. Sea Ice Deformation Events in the Gulf of Finland and This Impact on Shipping. 2011.
107. **Germo Väli**. Numerical Experiments on Matter Transport in the Baltic Sea. 2011.
108. **Andrus Seiman**. Point-of-Care Analyser Based on Capillary Electrophoresis. 2011.
109. **Olga Katargina**. Tick-Borne Pathogens Circulating in Estonia (Tick-Borne Encephalitis Virus, *Anaplasma phagocytophilum*, *Babesia* Species): Their Prevalence and Genetic Characterization. 2011.
110. **Ingrid Sumeri**. The Study of Probiotic Bacteria in Human Gastrointestinal Tract Simulator. 2011.
111. **Kairit Zovo**. Functional Characterization of Cellular Copper Proteome. 2011.
112. **Natalja Makarytsheva**. Analysis of Organic Species in Sediments and Soil by High Performance Separation Methods. 2011.
113. **Monika Mortimer**. Evaluation of the Biological Effects of Engineered Nanoparticles on Unicellular Pro- and Eukaryotic Organisms. 2011.
114. **Kersti Tepp**. Molecular System Bioenergetics of Cardiac Cells: Quantitative Analysis of Structure-Function Relationship. 2011.
115. **Anna-Liisa Peikolainen**. Organic Aerogels Based on 5-Methylresorcinol. 2011.
116. **Leeli Amon**. Palaeoecological Reconstruction of Late-Glacial Vegetation Dynamics in Eastern Baltic Area: A View Based on Plant Macrofossil Analysis. 2011.
117. **Tanel Peets**. Dispersion Analysis of Wave Motion in Microstructured Solids. 2011.
118. **Liina Kaupmees**. Selenization of Molybdenum as Contact Material in Solar Cells. 2011.
119. **Allan Olsper**. Properties of VPg and Coat Protein of Sobemoviruses. 2011.
120. **Kadri Koppel**. Food Category Appraisal Using Sensory Methods. 2011.
121. **Jelena Gorbatšova**. Development of Methods for CE Analysis of Plant Phenolics and Vitamins. 2011.
122. **Karin Viipsi**. Impact of EDTA and Humic Substances on the Removal of Cd and Zn from Aqueous Solutions by Apatite. 2012.
123. **David Schryer**. Metabolic Flux Analysis of Compartmentalized Systems Using Dynamic Isotopologue Modeling. 2012.
124. **Ardo Illaste**. Analysis of Molecular Movements in Cardiac Myocytes. 2012.
125. **Indrek Reile**. 3-Alkylcyclopentane-1,2-Diones in Asymmetric Oxidation and Alkylation Reactions. 2012.
126. **Tatjana Tamberg**. Some Classes of Finite 2-Groups and Their Endomorphism Semigroups. 2012.
127. **Taavi Liblik**. Variability of Thermohaline Structure in the Gulf of Finland in Summer. 2012.
128. **Priidik Lagemaa**. Operational Forecasting in Estonian Marine Waters. 2012.
129. **Andrei Errapart**. Photoelastic Tomography in Linear and Non-linear Approximation. 2012.
130. **Külliki Krabbi**. Biochemical Diagnosis of Classical Galactosemia and Mucopolysaccharidoses in Estonia. 2012.

131. **Kristel Kaseleht**. Identification of Aroma Compounds in Food using SPME-GC/MS and GC-Olfactometry. 2012.
132. **Kristel Kodar**. Immunoglobulin G Glycosylation Profiling in Patients with Gastric Cancer. 2012.
133. **Kai Rosin**. Solar Radiation and Wind as Agents of the Formation of the Radiation Regime in Water Bodies. 2012.
134. **Ann Tiiman**. Interactions of Alzheimer's Amyloid-Beta Peptides with Zn(II) and Cu(II) Ions. 2012.
135. **Olga Gavrilova**. Application and Elaboration of Accounting Approaches for Sustainable Development. 2012.
136. **Olesja Bondarenko**. Development of Bacterial Biosensors and Human Stem Cell-Based *In Vitro* Assays for the Toxicological Profiling of Synthetic Nanoparticles. 2012.
137. **Katri Muska**. Study of Composition and Thermal Treatments of Quaternary Compounds for Monograin Layer Solar Cells. 2012.
138. **Ranno Nahku**. Validation of Critical Factors for the Quantitative Characterization of Bacterial Physiology in Accelerostat Cultures. 2012.
139. **Petri-Jaan Lahtvee**. Quantitative Omics-level Analysis of Growth Rate Dependent Energy Metabolism in *Lactococcus lactis*. 2012.
140. **Kerti Orumets**. Molecular Mechanisms Controlling Intracellular Glutathione Levels in Baker's Yeast *Saccharomyces cerevisiae* and its Random Mutagenized Glutathione Over-Accumulating Isolate. 2012.
141. **Loreida Timberg**. Spice-Cured Sprats Ripening, Sensory Parameters Development, and Quality Indicators. 2012.
142. **Anna Mihhalevski**. Rye Sourdough Fermentation and Bread Stability. 2012.
143. **Liisa Arike**. Quantitative Proteomics of *Escherichia coli*: From Relative to Absolute Scale. 2012.
144. **Kairi Otto**. Deposition of In₂S₃ Thin Films by Chemical Spray Pyrolysis. 2012.
145. **Mari Sepp**. Functions of the Basic Helix-Loop-Helix Transcription Factor TCF4 in Health and Disease. 2012.
146. **Anna Suhhova**. Detection of the Effect of Weak Stressors on Human Resting Electroencephalographic Signal. 2012.
147. **Aram Kazarjan**. Development and Production of Extruded Food and Feed Products Containing Probiotic Microorganisms. 2012.
148. **Rivo Uiboupin**. Application of Remote Sensing Methods for the Investigation of Spatio-Temporal Variability of Sea Surface Temperature and Chlorophyll Fields in the Gulf of Finland. 2013.
149. **Tiina Kriščiunaite**. A Study of Milk Coagulability. 2013.
150. **Tuuli Levandi**. Comparative Study of Cereal Varieties by Analytical Separation Methods and Chemometrics. 2013.
151. **Natalja Kabanova**. Development of a Microcalorimetric Method for the Study of Fermentation Processes. 2013.
152. **Himani Khanduri**. Magnetic Properties of Functional Oxides. 2013.
153. **Julia Smirnova**. Investigation of Properties and Reaction Mechanisms of Redox-Active Proteins by ESI MS. 2013.
154. **Mervi Sepp**. Estimation of Diffusion Restrictions in Cardiomyocytes Using Kinetic Measurements. 2013.

155. **Kersti Jääger**. Differentiation and Heterogeneity of Mesenchymal Stem Cells. 2013.
156. **Victor Alari**. Multi-Scale Wind Wave Modeling in the Baltic Sea. 2013.
157. **Taavi Päll**. Studies of CD44 Hyaluronan Binding Domain as Novel Angiogenesis Inhibitor. 2013.
158. **Allan Niidu**. Synthesis of Cyclopentane and Tetrahydrofuran Derivatives. 2013.
159. **Julia Geller**. Detection and Genetic Characterization of *Borrelia* Species Circulating in Tick Population in Estonia. 2013.
160. **Irina Stulova**. The Effects of Milk Composition and Treatment on the Growth of Lactic Acid Bacteria. 2013.
161. **Jana Holmar**. Optical Method for Uric Acid Removal Assessment During Dialysis. 2013.
162. **Kerti Ausmees**. Synthesis of Heterobicyclo[3.2.0]heptane Derivatives via Multicomponent Cascade Reaction. 2013.
163. **Minna Varikmaa**. Structural and Functional Studies of Mitochondrial Respiration Regulation in Muscle Cells. 2013.
164. **Indrek Koppel**. Transcriptional Mechanisms of BDNF Gene Regulation. 2014.
165. **Kristjan Pilt**. Optical Pulse Wave Signal Analysis for Determination of Early Arterial Ageing in Diabetic Patients. 2014.
166. **Andres Anier**. Estimation of the Complexity of the Electroencephalogram for Brain Monitoring in Intensive Care. 2014.
167. **Toivo Kallaste**. Pyroclastic Sanidine in the Lower Palaeozoic Bentonites – A Tool for Regional Geological Correlations. 2014.
168. **Erki Kärber**. Properties of ZnO-nanorod/In₂S₃/CuInS₂ Solar Cell and the Constituent Layers Deposited by Chemical Spray Method. 2014.
169. **Julia Lehner**. Formation of Cu₂ZnSnS₄ and Cu₂ZnSnSe₄ by Chalcogenisation of Electrochemically Deposited Precursor Layers. 2014.
170. **Peep Pitk**. Protein- and Lipid-rich Solid Slaughterhouse Waste Anaerobic Co-digestion: Resource Analysis and Process Optimization. 2014.
171. **Kaspar Valgepea**. Absolute Quantitative Multi-omics Characterization of Specific Growth Rate-dependent Metabolism of *Escherichia coli*. 2014.
172. **Artur Noole**. Asymmetric Organocatalytic Synthesis of 3,3'-Disubstituted Oxindoles. 2014.
173. **Robert Tsanev**. Identification and Structure-Functional Characterisation of the Gene Transcriptional Repressor Domain of Human Gli Proteins. 2014.
174. **Dmitri Kartofelev**. Nonlinear Sound Generation Mechanisms in Musical Acoustic. 2014.
175. **Sigrid Hade**. GIS Applications in the Studies of the Palaeozoic Graptolite Argillite and Landscape Change. 2014.
176. **Agne Velthut-Meikas**. Ovarian Follicle as the Environment of Oocyte Maturation: The Role of Granulosa Cells and Follicular Fluid at Pre-Ovulatory Development. 2014.
177. **Kristel Hälvin**. Determination of B-group Vitamins in Food Using an LC-MS Stable Isotope Dilution Assay. 2014.
178. **Mailis Päri**. Characterization of the Oligoadenylate Synthetase Subgroup from Phylum Porifera. 2014.

179. **Jekaterina Kazantseva**. Alternative Splicing of *TAF4*: A Dynamic Switch between Distinct Cell Functions. 2014.
180. **Jaanus Suurväli**. Regulator of G Protein Signalling 16 (RGS16): Functions in Immunity and Genomic Location in an Ancient MHC-Related Evolutionarily Conserved Synteny Group. 2014.
181. **Ene Viiard**. Diversity and Stability of Lactic Acid Bacteria During Rye Sourdough Propagation. 2014.
182. **Kristella Hansen**. Prostaglandin Synthesis in Marine Arthropods and Red Algae. 2014.
183. **Helike Lõhelaid**. Allene Oxide Synthase-lipoxygenase Pathway in Coral Stress Response. 2015.
184. **Normunds Stivrīnš**. Postglacial Environmental Conditions, Vegetation Succession and Human Impact in Latvia. 2015.
185. **Mary-Liis Kütt**. Identification and Characterization of Bioactive Peptides with Antimicrobial and Immunoregulating Properties Derived from Bovine Colostrum and Milk. 2015.